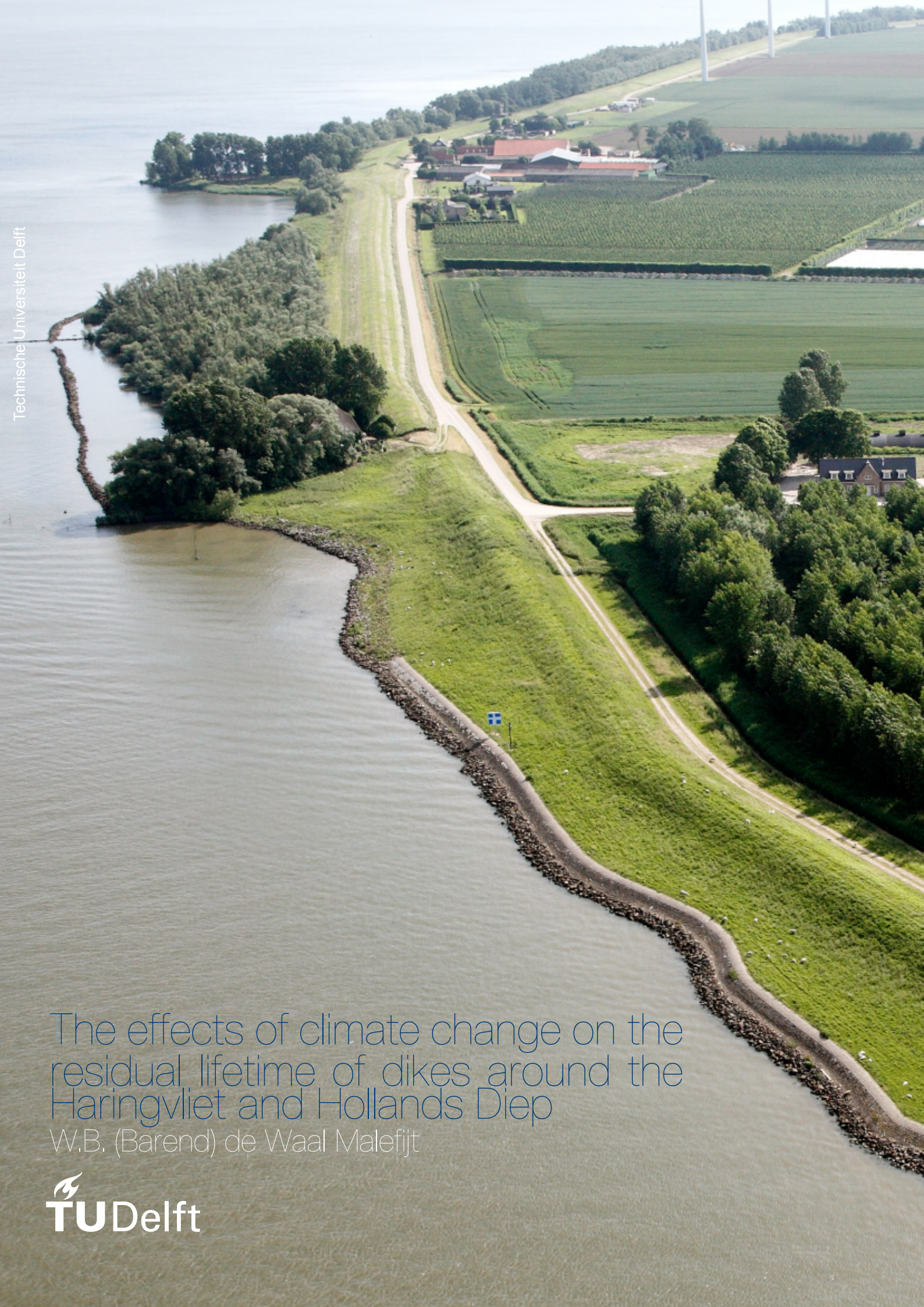

Technische Universiteit Delft

The effects of climate change on the residual lifetime of dikes around the Haringvliet and Hollands Diep

W.B. (Barend) de Waal Malefijt

TU Delft

The effects of climate change on the residual lifetime of dikes around the Haringvliet and Hollands Diep

by

W.B. (Barend) de Waal Malefijt

to obtain the degree of Master of Science

at the Delft University of Technology

to be defended publicly on Thursday August 27, 2020 at 11:00 AM.

Student number:	4206819	
Thesis committee:	Prof. dr. ir. M. Kok,	TU Delft, supervisor
	Dr. ir. W. Kanning,	TU Delft
	Dr. ir. A. P. van den Eijnden,	TU Delft
	ir. R. Slomp,	Rijkswaterstaat - WVL
	ir. D. Knops,	HKV Lijn in water

An electronic version of this thesis is available at http://repository.tudelft.nl/.
Source cover image: https://beeldbank.rws.nl/MediaObject/Details/317820.

TU Delft Delft University of Technology

Preface

This thesis is written as the final work to finish my Master of Science in Hydraulic Engineering at the Delft University of Technology. The thesis topic has been provided by Rijkswaterstaat and has been conducted in cooperation with Rijkswaterstaat, HKV Lijn in Water and the university itself. Rijkswaterstaat is the Dutch National Water Authority. HKV Lijn in Water is a Dutch consultancy agency specialized in water-related topics.

The thesis is a policy study about the use of fragility curves to calculate the effect of climate change on the residual lifetime of the dikes around the Haringvliet and Hollands Diep. This is a large estuary south of the port of Rotterdam that is closed off from the sea by the Haringvlietdam. The area is known from the big flood disaster of 1953, where multiple dikes breached, causing major flooding.

We live in a changing world. During my time as a hydraulic engineering student, climate change has become more evident than it ever has been. This was one of the reasons that hydraulic engineering and especially flood safety became more and more interesting for me. Growing up close to the beach and seeing the impact of the sea on the dunes or during a big storm made me realise how strong water can be. This made me interested in how this works and how we can protect ourselves. I feel lucky that this thesis topic made it possible to look at climate changes as well as dike safety.

I would like to thank the Delft university of Technology for all the knowledge that they have provided, enabling me to finish my Master of Science. Secondly, I would like to thank Rijkswaterstaat and HKV Lijn in Water for providing me with a nice working environment where I could work on my thesis. Special thanks to all my supervisors Robert, David, Wim, Matthijs and Bram for helping me get through this process. I really needed a lot of your support and feedback and it has taught me to ask questions and feedback whenever necessary. Especially during the global Covid-19 pandemic.

I will finish this chapter by thanking everybody around me with whom I have talked about my thesis or with whom I have had the time to relax as well. My family and the friends I have met in the past 8 years, who have helped me grow from a first year student to a Hydraulic Engineer. I would especially like to thank Clémence who has supported me through many ups and downs in the past 12 months.

W.B. (Barend) de Waal Malefijt
Delft, August 2020

Abstract

In this thesis a study is done to see if it is possible to use fragility curves for the calculation of residual lifetime. This is done by answering the following research question: What is the residual lifetime of the dikes around the Haringvliet and Hollands Diep, considering the climate scenarios G and W+ [18]?

Residual lifetime of a dike is the time until the dike is expected not to comply with the new safety standards anymore, depending on the climate scenario. For the new standards (published in 2014) that are set in the update of the Water Act [40] and the new Dutch assessment /citeDeWaal2016a and design tools [9] currently no investigation has been done of the residual lifetime of the dikes around the Haringvliet and Hollands Diep based on the various failures modes in the WBI /citeDeWaal2016a.

The residual lifetime is determined by calculating the total failure probability of a dike section (in Dutch: Dijkvak) for three reference years: 2023, 2050 and 2100. This was done by using fragility curves to calculate the conditional failure probability per failure mode (wave run-up/overtopping and piping) and combining these into an overall fragility curve for a cross section. Fragility curves are used since these allow for an easy combination of various failure modes. Since the aim of this study is to show the proof of concept, two failure mechanisms and 11 cross sections of dikes have been used.

The information of the flood defences has been provided by the local water authorities of the area. These are Waterschap Hollandse Delta and Waterschap Brabantse Delta. The hydraulic boundary conditions are provided by Rijkswaterstaat through the program Hydra-NL.

Hydra-NL is used to calculate the water level frequency statistics for each reference year. The fragility curve and water level frequency are combined by multiplying the fragility curve over the water level distribution; the area below this combined graph is the total failure probability. This is done for each reference year. The resulting failure probability for the three considered years is plotted. This graph is compared to the maximum allowable failure probability set in the Water Act. The residual lifetime is found by looking for the year where the total failure probability exceeds the maximum allowable failure probability (or bottom value). The time it takes for that year to be reached is the residual lifetime. Next, the residual lifetime is calculated for climate scenarios G and W+, to get a bandwidth of the expected residual lifetime.

For piping, the national rough subsoil SOS schematisation is used for dike stretches 21-2 and 25-2. For dike stretches 21-4 and 34-2, more detailed parameters are provided. The SOS schematization is not detailed enough for assessment in the WBI, but does give a good enough result, if more detailed information is not available, to get an overview of the residual lifetime. With the available SOS data, it is still possible to get an idea of the added value of fragility curves in calculating the residual lifetime. Piping is subdivided in the sub mechanisms: uplift, heave and backward erosion. The smallest failure probability of those three sub mechanisms was used as the governing failure probability for piping, which is an overestimation.

For wave run-up and overtopping, foreshores and dams are not considered. Both increase the dike safety, since waves lose energy on the foreshore or dams, which decreases the total load on the dike. The interaction between wind speed and water level is assumed to be independent of each other. This increases the simplicity of the calculation and makes it possible to use fragility curves to calculate the conditional failure probability.

Only the most dominant wind directions at each location is included. In most cases, this gives an overestimation of the wind load, since the probability of different wind directions occurring is not included. This is conservative to assume but good enough for an overall view of the residual lifetime.

The results of this thesis show that fragility curves can be used to get an overview of areas such as the Haringvliet and Hollands Diep. The method gives a bandwidth of the residual lifetime. For this

study area, most of the dikes have a residual lifetime that is longer than 130 years (the maximum considered). The weakest locations are found at dike stretch (in Dutch: Dijk traject) 34-2 and 20-4. Here, a residual lifetime between 25 and 90 years can be expected. These are still significant enough not to warrant immediate action. One location shows a residual lifetime of zero. This location is 20-4 0181 and this is mainly caused by piping. However, that location shows unexpected results in the total failure probability. The failure probability in 2050 is smaller than it is in 2023. This is highly unlikely. The problem is most probably caused by the numerical calculation in the FORM calculation used to create the fragility curve, since the decreasing failure probability is not found at other locations; hence it is recommended to further look into this location.

Fragility curves give a good overall view of the residual lifetime of dikes around the Haringvliet and Hollands Diep. The method can be used as a first indication of the residual lifetime. For wave run-up/overtopping, the measured dikes do all have a positive residual lifetime of more than 20 years. Only for piping there are some locations that can cause issues.

It is recommended to include other failure mechanisms in the residual lifetime calculation. Starting with inner slope instability. For an overall view of the area, more dike locations can be included. This would make it possible to also calculate the residual lifetime of a whole dike stretch. When new climate models are available, these can be used to redo the calculations. The scenarios that are used in Hydra-NL are from 2006 and use older climate models.

Contents

List of Symbols

General

Symbol	Description	Unit
Δh	steps size between water levels for the fragility curve calculation	$[m]$
γ_s	volumetric weight of sand grains	$[kN/m^3]$
γ_{sat}	saturated volumetric weight of blanket sand	$[kN/m^3]$
γ_w	saturated volumetric weight of water $\approx 10\ kN/m^3$	$[kN/m^3]$
$F(x)$	cumulative distribution function	$[-]$
$f(x)$	probability density function	$[-]$
g	gravitational accelaration $= 9.81\ m/s^2$	$[m/s^2]$
h	water level	$[m]$
H_s	specific wave height (equal to H_{m0})	$[m]$
H_{m0}	spectral wave height (equal to H_s)	$[m]$
$L_{m-1.0}$	spectral wavelength	$[m]$
n	porosity	$[-]$
$P_f(h)$	failure probability contribution per water level	$[-]$
$P_{f,dike}$	probability of failure of a dike section	$[-]$
$P_{f,standard}$	probability of failure according to the dutch standard	$[-]$
R	resistance parameters of a limit state function	$[-]$
S	load parameter of a limit state function	$[-]$
T_p	peak wave period	$[s]$
T_s	specific wave period	$[s]$
$T_{m-1.0}$	spectral wave period	$[s]$
X_i	conditonal load parameter	$[-]$
x_i	conditonal load parameter	$[-]$
Z	limit state function	$[-]$
Z_H	limit state for height (GEKB)	$[-]$
Z_M	limit state for macro instability	$[-]$
Z_P	limit state for piping	$[-]$

Grass erosion and overtopping (GEKB)

Symbol	Description	Unit
α	dike slope	$[-]$
γ_β	reduction coefficient due to wave obliqueness	$[-]$
γ_v	reduction coefficient due to crest wall	$[-]$
γ_b	reduciton coefficient due to the berm	$[-]$
γ_f	reduction coefficient due to slope roughness	$[-]$
$\xi_{m-1.0}$	spectral wave steepness	$[m/m]$
B_B	width of the berm	$[m]$
d	local water depth at the toe of the dike	$[m]$
F	fetch	$[m]$
H_b	height of the berm	$[m + NAP]$
h_b	distance between still water level and berm	$[m]$
h_c	crest level of a dike	$[m + NAP]$
L_B	length over which the berm has an effect	$[m]$
$q_{o,max}$	maximum allowable overtopping discharge	$[m^2/s]$
R_C	available freeboard	$[m]$
u_{10}	wind speed at 10 meter above the surface	$[m/s]$
z_0	average water depth	$[m + NAP]$

Piping (STPH)

Symbol	Description	Unit
$\mathrm{B}_{standard}$	reliability index of the given dike stretch	$[1/year]$
$\Delta\phi$	head difference	$[m]$
$\Delta\phi_{c,u}$	critical head difference	$[m]$
η	drag force coefficient	$[-]$
λ	damping factor	$[-]$
λ_h	leakage factor	$[m]$
ν	kinematic viscosity of water $= 1.33e^{-6}\ m^2/s$	$[m^2/s]$
Φ	standard normal distribution	$[-]$
ϕ_{exit}	potential head at exit point	$[m]$
θ	bedding angle	$[°]$
B	width dike body	$[m]$
D	thickness aquifier	$[m]$
d	thickness of hinterlands blanket layer	$[m]$
d_{70m}	reference value for d_{70} . $d_{70m} = 2.08e^{-4}m$	$[m]$
d_{70}	70% fractile of the grain size distribution	$[m]$
$F_{u,h,be}$	Factor of safety for uplift, heave and backward erosion	$[-]$
FOS_h	factor of safety for heave	$[-]$
FOS_p	factor of safety for backward erosion	$[-]$
FOS_u	factor of safety for uplift	$[-]$
g_h	function for calculating heave	$[-]$
g_p	function for calculating backward erosion	$[-]$
g_u	function for calculating uplift	$[-]$
h_p	polder water level	$[m]$
i	exit gradient	$[-]$
$i_{c,h}$	critical heave gradient	$[-]$
k	hydraulic conductivity of the aquifer	$[m/s]$
L	seepage length	$[m]$
L_f	length of the effective foreshore	$[m]$
m_p	model factor for piping	$[-]$
m_u	model factor uplift	$[-]$
$P_{f;u,h,be}$	Failure probability for each sub-mechanism	$[1/year]$
x_{exit}	distance of the exit point from the center of the footprint	$[m]$
Z_h	limit state for heave	$[-]$
Z_p	limit state for backward erosion	$[-]$
Z_u	limit state for uplift	$[-]$

Slope instabilty (STBI)

Symbol	Description	Unit
FOS_m	factor of safety for macro istability	$[-]$
M_r	resisting moment	$[kNm]$
M_s	driving moment	$[kNm]$

List of Abbreviations

List of translations and abbreviations used throughout this report

Abbreviation	Dutch	English	Description
-	Afsluitdijk	Enclosure dam	Dam that closed off the Zuiderzee from the north sea
-	Beneden rivieren	Lower Rhine and Meuse reaches	Main Rhine/Meuse delta with multiple dominant forces
-	Boven rivieren	Upper Rhine and Meuse reaches	Reaches of the Rhine with only river discharge dominance
-	Dijk doorsnede	Cross section of a dike	dimensions of a dike on one specific location.
-	Dijk ring	Dike ring	Continuous line of flood defences around a flood prone area, no longer an official definition
-	Dijk traject	Dike stretch	Part of a dike ring defined in the WBI.
-	Dijkvak	Dike section	section of a dike stretch with homogeneous dike cross sections and soil schematization
-	IJselmeer	Lake IJsel	Northern part of the former Zuiderzee
-	Kierbesluit	Haringvliet Sluice management Decision	Documentation about the management of the Haringvliet sluices to improve fish migration
-	Lek lengte	Seapage length	Combined length of foreshore and dike that reduces the chance of backward erosion by piping.
-	Markermeer	Lake Marken	Southern part of the former Zuiderzee enclose by the Houtribdijk and lake Marken
-	Middle lakes	Midden meren	Lakes in the middle of the Netherlands. The IJselmeer and Markermeer
-	Noordzee	North sea	
-	Reststerkte	Residual Strength	The strength of a dike between initial failure and actual failure
-	Volledig falen	Actual failure	Breaching of the dike
-	Waterstandfrequentielijn	Water level statistics	A cdf that gives the probability of exceedance for a given water level (x)
-	Zuiderzee	Southern sea	The water body in the middle of the Netherlands before the Afsluitdijk was created

AHN	Actual Hoogtebestand Nederland	Current Dutch national digital terrain model	Datasets that give a detailed overview of the surface level in the Netherlands
DWL	Maatgevend Hoog Water	Design water level	Water level used in semi probabilistic calculations to calculated the probability of failure
EPB	Europoort kering	Europort barrier.	Barriers in the western part of the Netherlands that close of the port of Rotterdam during severe storm condition
FC	Kwetsbaarheids curve	Fragility curve.	A statistical tool that gives the probability failure of a flood defence as a function of the water level
FOS	Veiligheidsfactor	Factor of safety	Factor that shows how save a dike is by dividing the strength of the dike by the loads.
GCM	Globaal klimaat model	Global Climate Model	Model that calculated the expected influence of a given climate scenario on global scale
GEKB	Grond Erosie Kruin en Binnen talud	Erosion of crest and inner slope	Assessment that is mainly influenced by the height of the dike.
HB	Hartelkering	Hartel barrier	barrier that closes the Hartel channel. A channel between the 2nd Maesvlakte and the hinterland.
HBN	Hydraulisch belasting niveau	Hydraulic load level	A calculation that gives the needed crest height for different return periods
HD	Hollands Diep	-	Eastern part of the study area
HV	Haringvliet	-	Western part of the study area
KNMI	Koninklijk Nederlands Meteorologisch Instituut	Royal Netherlands Meteorological Institute	The Dutch Meteorological Institute
LIR	Lokaal Individueel Risico	local individual risk	The risk an individual has on dying in a certain area. In this case because of flood risk
LWL	lokale waterstand	local water Level	Water level at a certain location. Close to a dike
MHW	Maatgevend Hoog Water	Design water level	see DWL
MLB	Maeslant kering	Maeslant barrier	Barrier that closes the Nieuwe Waterweg
MSL	Gemiddelde waterstand (NAP)	Mean Sea Level	Same as NAP.
NAP	Normaal Amsterdams Peil	Amsterdam Ordnance Datum	Shows the average high water mark. It is used in the Netherlands and parts of Western Europe as a datum for the water level
NW	Nieuwe Waterweg		Channel through the port of Rotterdam closed of with the Maeslant Barrier

pbl	Planbureau voor de leefomgeving	Netherlands Environmental Assessment Agency	Governmental Consultancy for environment, nature and space
RCM	Regionaal klimaat model	Regional Climate Model	Climate model on a much more local scale than GCMs
RLD/ RLT	Rest levensduur	Residual Lifetime	The time until the failure probability of a dike is equal to the safety standard defined in the WBI
RWS	Rijkswaterstaat	Rijkswaterstaat	National Water Authority. Responsible for the design, construction, management and maintenance of the main infrastructure facilities in the Netherlands
SLR	Zee niveau stijging	Sea level Rise	Expected amount of sea level rise due to climate change.
SOS	Stochastiche Ondergrond Schematisatie	Stochastic soil schematization	A rough national schematization of the subsoil beneath all primary flood defences (except dunes). It only gives a overall view and needs additional information to be suitable for assessments
STBI	Macrostabiliteit binnenwaards	Slope stability of the inner slope	Assessment for the failure mechanism macro stability of the inner slope.
STPH	Piping	Piping	Assessment for the failure mechanism piping which consists of: Uplift, Heave, and Backward erosion
SWL	Stilstaand water niveau	Still water level	The water level at the toe of the dike without waves
WBI	Wettelijk beoordelings instrumentarium	Formal assessment tools	Tools used in assessing all the flood defences in the Netherlands

1

Introduction

In the Netherlands, water safety always has to be considered. With 60% of the country located in flood prone areas, it is a tremendous task to ensure the protection against flooding of those areas. Each part of the 3,700 kilometres of primary flood defences has to be assessed to ensure that the flood defences do meet the set safety standards. These are set in the Water Act [40].

The flood protection system consists of dikes, dams, dunes and hydraulic structures. The failure probability of those flood defences can be linked with the effect of climate change. This can be done by calculating the residual lifetime of a dike. The residual lifetime is defined as the time until a dike section no longer complies with the safety standards set in the Water Act [40]. Knowing the residual lifetime makes it possible to better understand when and where dikes need to be reinforced. This can be assessed for different sets of hydraulic boundary conditions based on the climate scenarios from the KNMI [18].

In most cases, climate change will increase the hydraulic loads on dikes in the future. This is mainly caused by the increase in sea level rise and river discharge. The projections done by the KNMI [18] are used to find this load and the corresponding water level.

1.1. Problem Analysis

Climate change will impact the safety of all the dikes in and around the Netherlands. Coastal dikes need to withstand higher sea water levels, with possibly more extreme storm events and wind speeds, while river dikes will experience an increase in river discharge, inducing higher water levels and thus higher loads. Estuaries are influenced by both higher sea water levels and higher discharges. The increased hydraulic load will decrease the probability of failure of a dike, which will cause an increased probability of failure.

The change in climate will create a shift in the water level frequency which shows the exceedance probability of the water level at a given dike location. A shift to the right means that, in time, the exceedance probability becomes higher for higher over the full range. This can be shown as figure 1.1. This is mainly caused by the rising global temperatures which impact sea level rise and the river discharges and much more.

Most policy studies in the past have mainly focussed on the failure probability based on overtopping and overflow. Additionally, since january 1st 2017, new rules and regulations have been established. Also the requirements which determine failure for overtopping and overflow have changed. This means studies from the past have to be updated. With the new regulations, it is therefore not known how much climate change influences the residual lifetime of the dikes. This report will look for a method that can be used to evaluate the residual lifetime for the two failure mechanisms: wave run-up/overtopping and piping. The residual lifetime of the combined failure mechanisms is also calculated.

To understand the impact that climate change has on the failure probability of a dike, a link must be made between the water level frequency and the strength of a dike. The strength is dependent on a

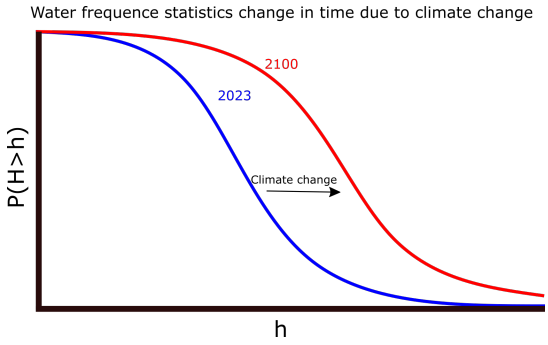

Figure 1.1: Change in water level frequency due to climate change

large amount of failure mechanisms that all affect the strength of a dike in different ways. In this thesis, the focus is on two failure mechanisms: overtopping and piping. The failure probability of both failure mechanisms can be calculated with the help of fragility curves. A fragility curve is a statistical tool that gives the probability failure of a flood defence as a function of the water level. This results in a graph that shows the failure probability of a dike at a conditional water level. For this research, the change in dike strength over time is not included. This is done since the research will focus on the effect of climate change on the residual lifetime.

Climate change influences both sea level rise and the river discharge. The melting of land ice will increase the sea water level, while extreme precipitation and snowmelt will increase the river discharges. The effects of all those events are put together in different climate scenarios (G, G+, W, W+) [18]. Of these scenarios, G is the least extreme, while W+ is the most extreme scenario. Depending on the scenario, climate change can have a big effect on the residual lifetime of a dike.

In the methods that are currently used by the Dutch water authorities, residual lifetime is not yet included. Implementing this extra step can make it possible to get a quick and general overview of the reliability of the dikes in the future.

1.2. Research Design

1.2.1. Objectives

The main objective of this research is to determine the residual lifetime of the dikes around the Haringvliet and Hollands Diep for the failure mechanisms overtopping and piping. Particularly for the influence of climate change on the residual lifetime. This is done with the help of fragility curves which makes it possible to combine multiple failure mechanisms. Calculating the residual lifetime with fragility curves should give a relatively quick, probabilistic calculation of the reliability of a dike.

The outcome of this research gives two answers. An overview of the residual lifetime of the dikes around the Haringvliet and Hollands Diep. But will also give an indication of the added value of fragility curves for calculating residual lifetime. The focus lies on the added value of fragility curves. Fragility curves make it possible to assess multiple climate scenarios and combine multiple failure mechanisms in a relatively fast way. A method is developed in which fragility curves are used to assess a dike cross section for the failure mechanisms overtopping and piping.

Overtopping concerns failure caused by the erosion of the crest and the inner slope of the dike. Wave overtopping causes a discharge over the dike crest. When a certain critical discharge is reached, the forces will be strong enough to cause significant erosion and eventually dike failure.

Piping as a failure mechanism can have a big impact on the stability and thus safety of a dike. Piping looks at instability issues of the dike due to seepage of water and regressive tunnel erosion under the dike. The composition of the subsoil plays a major role in the overall effect that piping has on the safety of the dike.

The water system in the Haringvliet and Hollands Diep will be used throughout this thesis. The area lies in the south-western part of the Netherlands. This area is a good example of a water system where

multiple events together create a design water level. An analysis for the residual lifetime with the new formal assessment tool [8] is not yet available for the Haringvliet and Hollands Diep.

1.2.2. Main Research Question

The main question is:

- **What is the residual lifetime of the dikes around the Haringvliet and Hollands Diep, taking into account the climate scenarios: Average (G) and Warm (W+). Using Fragility Curves**

The main research question is split into several sub questions which will be used to answer the main research question.

1.2.3. Sub Research Questions

The sub questions which will be answered throughout this research are summed up below:

- How can residual lifetime be calculated?
- What are the dominant aspects that contribute to the residual lifetime within the Haringvliet and Hollands Diep?
- For one cross section. What is the residual lifetime looking only at height (Hydraulic load level) using fragility curves?
- For one cross section. What is the residual lifetime with respect to piping using fragility curves?
- What is the residual lifetime of a dike section with the failure mechanisms combined?
- What is the residual lifetime of the dike stretch around the Haringvliet & Hollands Diep?

1.3. Thesis framework

This thesis will follow the steps described in figure 1.2 for each dike cross-section. For each cross-section the necessary data is gathered about sea level rise, river discharge, water levels, dike profiles, bottom schematization and dike locations. At each dike cross section, the information is used to calculate the failure probability for the failure mechanisms: wave run-up/overtopping and piping.

The dike cross-section will therefore be used for calculating the residual lifetime of one dike section. The cross-section that is used for a dike section should be at a location where the highest failure probability is expected. The calculation for the whole dike section would then be done for the weakest link in the dike section.

The result of the fragility curve will be verified using the existing models within Hydra-NL and Riskeer. Hydra-NL is used for wave run-up and overtopping, while Riskeer will be used for piping. Hydra-NL only supports calculations with respect to the water level and the hydraulic loads. Hydra-NL is therefore not able to take into account any geotechnical conditions.

When an acceptable result is found for the different failure mechanisms, a calculation will be done for the combined residual lifetime of one dike cross section. Subsequently, calculations will be expanded to find the residual lifetime of a dike section and stretch.

1.4. Reading guide

The current chapter (the introduction) is the first chapter of this thesis. In this chapter the problem analysis is described together with the main objective of this thesis. Afterwards, the main and sub research questions are also described. In chapter 2, the literature study is described. All the necessary definitions, methods, failure mechanisms and hydraulic loads that are included in this thesis will be described to give a basic understanding of each of those parts.

In the following chapter 3, the whole methodology that will be used to get to the residual lifetime will be explained in this chapter. The research design will be explained, followed by the way the data is gathered, the scope, and the method. In the following two chapters, the method will be used on two different failure mechanisms. First for the hydraulic load in chapter4 and for piping in chapter 5. The

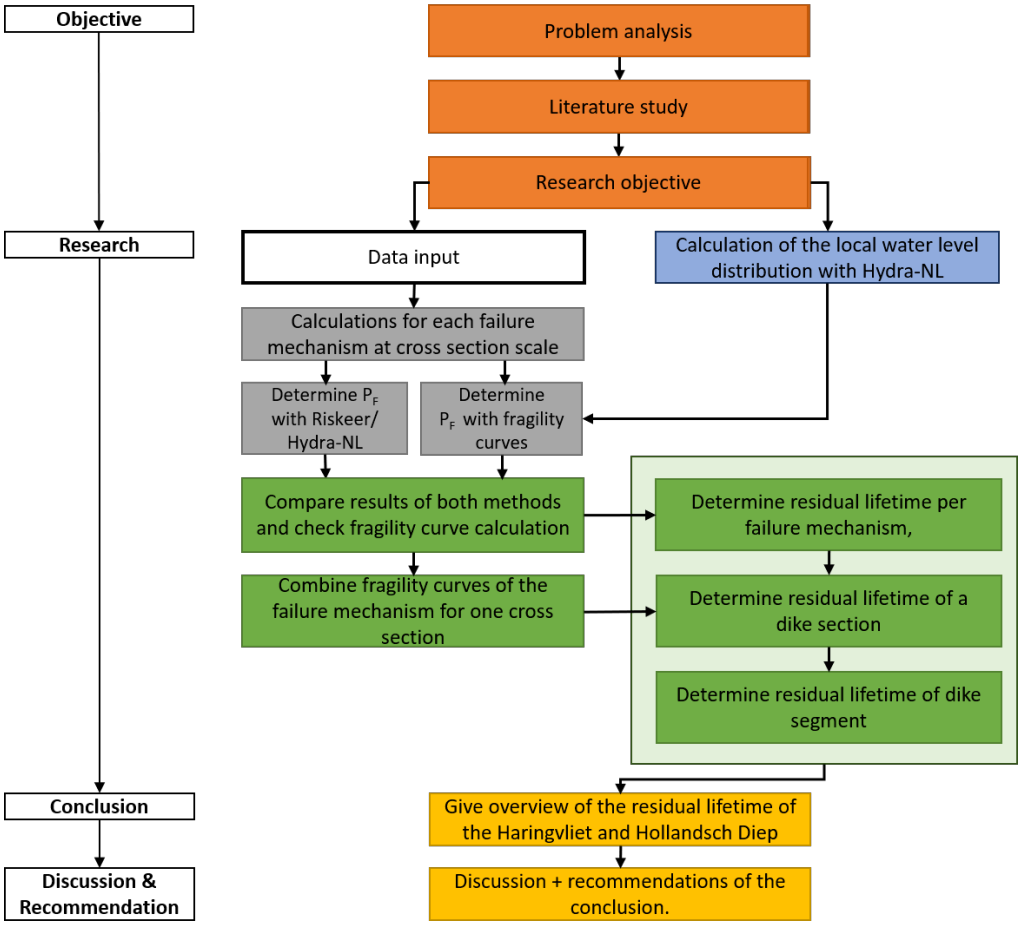

Figure 1.2: Thesis framework

results will be plotted for one individual location. In chapter 6 the results of both failure mechanisms will be combined in one fragility curve and onwards into the residual lifetime. The results for each of the used dike sections will be given at the end of this chapter.

Finally a discussion will be given in chapter 7 which will also be the final chapter of this thesis. The thesis is concluded with chapter 8 where the conclusions and recommendations will be given. After this chapter the bibliography and Appendices are given. The list of symbols and list of abbreviations are found at the beginning of the thesis.

2

Literature Study

2.1. Introduction

In this chapter, an explanation is given of the different aspects needed to conduct this research. The definitions that are used throughout the thesis will be given and it is explained how these are used. Furthermore, the influence of climate change on the different aspects of the water system are given. Afterwards the chapter will briefly go into the different failure mechanisms that are included in this thesis. Here the used limit states and equations will be given. The chapter will close with an explanation of the models used to calculate the effect of climate change on residual lifetime. The information in this chapter is used as a starting point for the calculation of the residual lifetime.

2.2. Brief history of flood defences in The Netherlands

The first signs of flood protection were built more than 2500 years ago [19]. They are mostly found in the northern part of the Netherlands. Inhabitants living in the low areas started to create small mounds, called a ”terp” in Dutch, on which they built their homes. From the 12^{th} century onward these ”terps” were connected together with long elevated hills. These structures are now known as dikes. This created new and safer land protected by ”terps” and their “dikes”.

In time, the amount of connections kept increasing, creating an ever growing plot of land which was safer from flooding. In the middle ages, the amount of dikes and their size became too complex to be maintained individually. In this period (1000-1500), due to sea level rise, thousands of acres have been lost to the sea. Those two events caused the need for Waterboards.

A waterboard is the elected regional water authority that has as one of their tasks to look after the hydraulic works and flood defences within a certain area [35]. One of their important tasks is to maintain and assess the current dikes in and around their area. The number of waterboards has decreased from more than 2500 in 1950 to 21 in 2018. The size of waterboards has increased proportionally by the merging areas managed by the waterboards.These are called the regional water authorities.

In the Netherlands, the flood hazard comes from storm surges, river discharges and combinations. Figure 2.1 shows all the areas in the Netherlands that are prone to flooding. The legend at the right side indicates which areas are prone to flooding. Dark blue areas are prone to flooding and lie below NAP (Amsterdam Ordnance Datum). Light blue areas are flood prone and lie above NAP. The orange areas show areas that are not surrounded by a dike ring. Purple shows an area of the Meuse that has no dikes.

Some big changes have been made in the water system in the previous centuries. One of the major changes happened in the 18^{th} century. To reduce the amount of water flowing through the Rhine in the direction of some major settlements, the Pannerdensche channel was constructed. This channel redirected about one third of the total discharge into the lakes in the middle of the Netherlands. This increased the flood protection around the Rhine branches called the Lek and Waal.

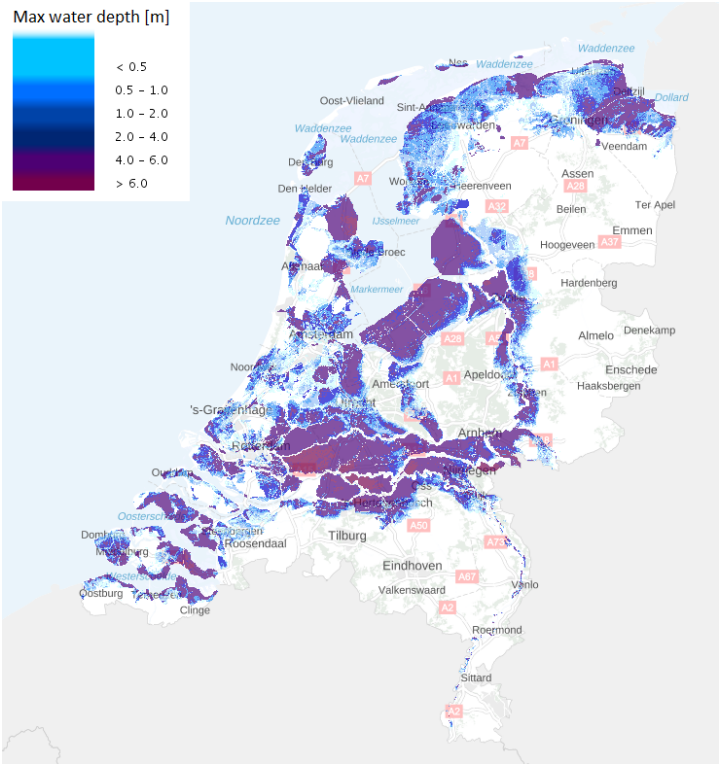

Figure 2.1: Flood prone areas in the Netherlands from [24]

The areas around the former Zuiderzee still had regular flooding. The capital city of Amsterdam was located in this area. At the end of the 19^{th} century, plans were developed to close off the Zuiderzee from the sea with the Afsluitdijk. A dike that would create lake IJssel with a 31 km long dam. This would greatly reduce the probability of flooding. The main contributor to the development of the Afsluitdijk was Cornelis Lely, minister in the Dutch cabinet and a hydraulic engineer. He was the main founder of those plans. The construction of the Afsluitdijk made it possible to retrieve land from the former Zuiderzee. This created the Wieringermeer, Flevopolder and Noordoostpolder. These polders can be seen in figure 2.2. The green areas are the reclaimed areas and were part of the former Zuiderzee before the construction of the Afsluitdijk. The Afsluitdijk was completed in 1932 and Amsterdam has not been flooded since.

The next major change in flood protection came after the big floods of 1953 in Zeeland, a province in the south-western part of the Netherlands. A storm surge together with the spring tide created a water level that breached multiple dikes throughout the whole province. figure 2.3 shows the areas where breaches occurred. More than 180,000 ha of land flooded and 1,800 inhabitants lost their lives. The Haringvliet and Hollands Diep lie in this area.

This flood disaster was the motivation for creating the Delta Commission. Their primary task was to establish safety standards against flooding in the Dutch law. Dike height calculation went from a deterministic to a more probabilistic approach. The old dike design was based on the water level found in the highest known storm plus an additional height of approximately 0.5 meter. The new design was based on the probability that the design water level was exceeded.

The last overhaul of the rules and regulations was finished in January 2017. From 1996 to 2017, the standards were primarily targeting the load side of the embankments. Water retaining structures needed to withstand a certain water level. After 2017, the standards were changed from a probability of exceeding a design water level (DWL) to a probability of dike failure. The design water level was based on a water level at return period that was specified for each dike stretch. Now the load on the dike is calculated with a probabilistic analysis that takes into account a combination of different water levels and their corresponding wave characteristics. The new standards makes it possible to take into

Figure 2.2: Polders in the former Zuiderzee [1]

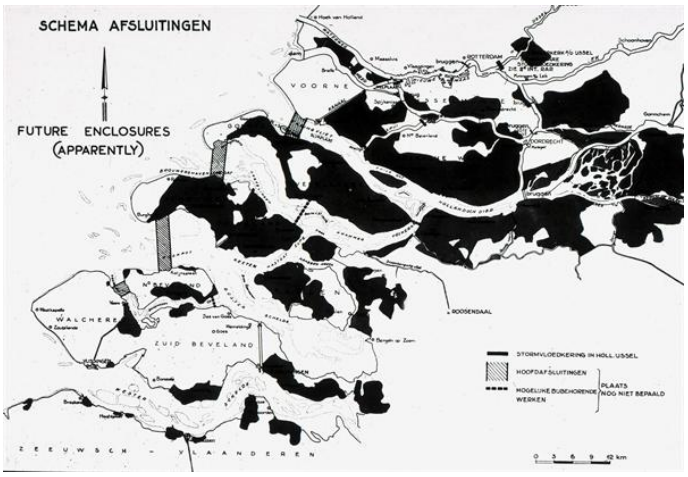

Figure 2.3: Floods of 1953 in dark & proposed dams in grey. By [26]

account both the hydraulic loads on the dike and the strength of the dike. The hydraulic load level (HBN in Dutch) is defined as the needed crest height for a dike at which the applicable wave overtopping criterion is met exactly. The HBN dates from rules and regulations from 1996 but is sometimes still used. Mainly since this concept is less complicated and therefore easier to understand. In the new assessment tools, each dike stretch is maximum failure probabilities depending on the risk of flooding. The risk is a combination of the probability of a flooding and the damages when such a flooding occurs. The situation in the hinterlands does therefore play a large role in the accepted risk. A rural hinterland will have less damage in a flood than urban areas. The population is also less in rural areas. When the risk is equal, dikes around rural areas will have bigger maximum failure probability than dikes around urban areas.

2.3. Definitions

In the sector of flood defences and hydraulic engineering, a lot of different meanings are given for the same definition. In this part of the thesis, the most important definitions that are used throughout this thesis will be explained.

Four main principles will be described: the failure definition, different definitions for the water levels, the definition of residual lifetime and an explanation of how dike cross section, sections, stretches and dike rings are related. But first, an introduction of the Dutch formal assessment tool will be given.

2.3.1. The Dutch Formal Assessment Method (WBI2017)

The current formal assessment methods are described in the WBI 2017 (in Dutch: Wettelijk BeoordelingsInstrumentarium) [8]. The assessment period is from January 1st 2017 until the end of 2022. The new rules are an accumulation of decades of experience in living and working in flood prone areas.

The rules describe the translation of the Dutch water law [40] (in Dutch: Waterwet), in methods that can be used to assess flood defences. The Dutch law gives a maximum allowable probability of failure for all the dikes and hydraulic structures in the Netherlands. Throughout the thesis, the standards in the WBI will be used as the base values.

2.3.2. Dike cross-section to dike ring

In the formal assessment method, an area that has to be protected against flooding is surrounded by a continuous line of flood defences such as dikes, dunes, hydraulic structures or high grounds. In the previous standards, before WBI2017, this was called a dike ring. In the current assessment tool such a ring is no longer used. They are now split into dike stretches. These stretches are large stretches of dike. Within one dike stretch, the effect that dike failure has on the hinterland is approximately equal

over the whole length. This means that it does not matter where dike failure occurs, the effect and damages are the same.

Each dike stretch is split into multiple dike sections. Dike sections have similar dike dimensions, hydraulic loads and soil conditions. For each dike section the probability of failure is determined for each failure mechanism, depending on the length of the section. Figure 2.4 shows how stretch 34-2 is built up of different dike sections that together form one dike stretch. Each section is given a different colour. Figure 2.5 shows the location of this stretch in the Hollands Diep.

A dike section is the smallest scale which is calculated in the WBI [8]. They are defined by one of the dike cross-sections that fall within this section. This dike cross-section has information about its dimension and can be linked to the local soil conditions. Within one dike section, multiple cross-sections are found. From these cross-sections, one cross section is used to calculate the failure probability of the dike section. To do this, the so-called length effect has to be included. The length effect takes into account the uncertainties in the dikes dimensions and subsoil over the whole length of a dikes section. The subsoil conditions are measured for each 50-100 meter. The conditions between two points are uncertain. This uncertainty is included with the length effect. The length effect is mainly important for piping since this failure mechanism is dependent on the subsoil conditions. Overtopping does not have a length effect since the height can be determined much quicker [16].

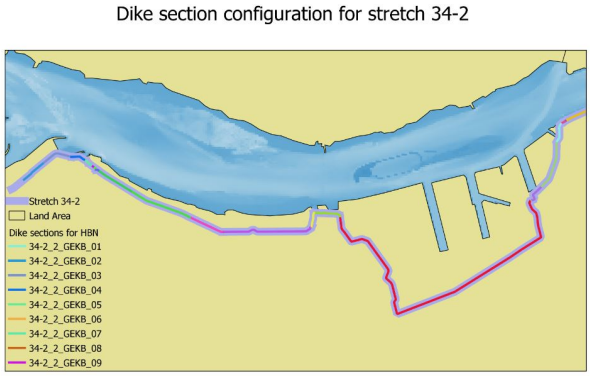

Figure 2.4: Build up from dike stretches to sections

2.3.3. Dike assessment

The WBI also makes a distinction between two values for the allowable failure probability. A signal and a bottom value. The signal value is used to indicate dike stretches for which the failure probability is becoming too big. The signal value may be exceeded for a period of time since it can take up to a decade for dike reinforcement to take place. The signal value takes this time frame into account when setting the value. The bottom value gives the maximum allowable failure probability of a dike stretch provided by the Dutch Water law [40].

Values for the signal and bottom value Table 2.1 shows the probability of failure for each of the stretches around the Haringvliet and Hollands Diep. Figure 2.5 shows the locations of each of the stretches within the Haringvliet and Hollands Diep.

The bottom and signal value in table 2.1 give the highest allowable failure probability for a whole dike stretch. The values are given in the Dutch water act [40]. The whole dike stretch cannot have a failure probability larger than the set value in the table. This means that the bottom and signal value has to be distributed over the different failure mechanisms and the dike sections. This gives the maximum failure probabilities in table 2.2. The length effect for piping creates the big difference between the values for overtopping and piping. As long as the failure probability for each dike section is within the set maximum value, the bottom value for the whole dike stretch will also be met.

Initial failure vs actual failure In the formal assessment in the Netherlands, not the whole process of dike failure is taken into account to determine the failure probability. The dike has failed the assessment

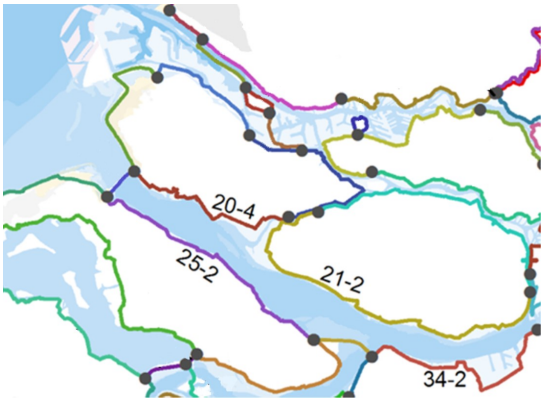

Figure 2.5: Locations of the four main dike stretches in the Haringvliet and Hollands Diep.
Source: [40]

Table 2.1: Standards set for the failure probability in the rules and regulations [40] for the different dike stretches around the Haringvliet & Hollands Diep

Dike stretch	Signal value	Bottom value
20-4	$1/1000$	$1/300$
21-2	$1/300$	$1/100$
25-2	$1/1000$	$1/300$
34-2	$1/1000$	$1/300$

Table 2.2: Failure probability per failure mechanisms of the different dike sections around the Haringvliet & Hollands Diep

Failure mechanism	Dike stretch	Signal value	Bottom value
Wave run-up and overtopping	20-4	$1/8,333$	$1/2,500$
	21-2	$1/2,500$	$1/833$
	25-2	$1/8,333$	$1/2,500$
	34-2	$1/8,333$	$1/2,500$
Piping	20-4	$1/114,055$	$1/34,216$
	21-2	$1/68,454$	$1/22,818$
	25-2	$1/153,545$	$1/46,064$
	34-2	$1/132,082$	$1/39,624$

whenever the first damage has occurred. This is called the point of initial failure. For each failure mechanism the initial failure is described by a condition. This condition is then used in the probabilistic calculations for those mechanisms.

Actual failure happens after the initial failure has occurred and follow-up processes decrease the strength of a dike. At this point, the dike can no longer perform its primary function, which is protection against flooding. Water can then flow freely over or through the dike. For revetment failure on the inner slope, the top layer, which consists of grass, has failed. This will lead to erosion of the dike core, often sand in the Haringvliet and Hollands Diep area (so with little resistance), which will eventually lead to a breach in the dike. Table 2.3 shows the conditions for run-up/overflow, piping and inner slope stability for initial and actual failure. The difference in failure probability between initial and actual failure differs between each of the mechanisms.

Table 2.3: Failure definition for the failure mechanisms wave run-up and overtopping, piping, and inner slope stability.

Failure mode	Initial failure [8]	Actual failure
Wave run-up and overtopping	$q_{o,max} > 1\ l/m/s$	Flooding/ breach of dike
Piping	$g_u < 0 \cap g_h < 0 \cap g_p < 0$	
Inner slope stability	Slip failure (see section 2.5.3)	

With: $q_{o,max}$: the critical overtopping discharge and $g_{u,h,p}$: the functions for each sub process within piping: uplift, heave and backward erosion respectively. The equations used to calculate the probability of initial failure will be further elaborated in the literature study.

The critical wave overtopping discharge is given a very small value of $q_{o,max} = 1\ l/m/s$ meaning that a small overtopping volume can already lead to dike failure according to the set standard. In reality, the overtopping discharge is a distributed value that differs for each dike section. It depends on the quality of the grass revetment and slope and the number of obstakels (e.g. houses on the dike). Urban areas are more affected by flooding than rural areas. These areas have more obstacles than rural areas.

This results in dikes around urban areas having a smaller $q_{o,max}$ than dikes around rural areas. In most cases $q_{o,max}$ is much larger than 1 l/m/s. For this thesis $q_{o,max}$ is intentionally set to a value that is smaller than the set standard in the WBI. This makes it easier to assess the dikes without looking at the hinterlands.

2.3.4. Water Level

The different water levels that will be used are: the mean sea level, design water level and local water level.

The mean sea level (MSL) is the average sea water level at a certain location. Sea level rise (SLR) is the expected increase in MSL in meters due to climate change. This is the reference water level in the assessment in the Netherlands. In the Netherlands the MSL is defined with the Amsterdam Ordnance Datum (in Dutch: NAP).

The local water level (LWL) is a range of expected water levels in the estuary close to a dike profile and is expressed in meters + NAP. This water level is calculated with the help of computer model Hydra-NL. Given the location of the dike and the boundary conditions, Hydra-NL can calculate the probability of exceeding for each water level in the given range. Hydra-NL can calculate the water level for return periods between 1/10 and 1/100,000 years. The LWL is a combination of the range of water levels with the probability of those happening. Hydra-NL includes effects on the water levels, such as wind direction, wind waves, wave run-up, sea level rise, and river discharges. How Hydra-NL works will be explained in section 2.8. This is also the water level that will be used in the model that will be explained in chapter 3.

The design water level is expressed in m + NAP. It is used as a design value of the local water level and is only available at section or cross sectional level. For a whole stretch, there is not one DWL, due to the differences the DWL can have over the length of one stretch. The DWL is used in semi-probabilistic calculations. Such a calculation does not require to calculate the failure probability on each water level within range but uses the DWL. The DWL is defined as the water level that has a certain return period. This return period is defined for each dike stretch and can be found in the Water Act.

2.3.5. Residual Lifetime

To define the residual lifetime it is important to understand how the water level is influenced in time. The current standards give a probability of failure which cannot be exceeded. (see table 2.1). For now, it is assumed that the current maximum allowable probability of failure will not change in time. This means that in the future, the dikes still need to have a probability of failure which is lower than given in the Dutch water law (in Dutch: Waterwet) [40]. In reality, they will be evaluated every 12 years. The last evaluation took place in 2016.

In the future, climate change will increase the probability of failure of a dike section due to an increase in the local water level distribution. Eventually, the probability of failure for the dike will become equal to the bottom value of that dike section which is set in Dutch assessment tools. The amount of time that is needed for the failure probability to reach that point is the residual lifetime. This can be written as:

The residual lifetime of a dike section is the time until the failure probability of a dike is equal to the safety standard defined in the WBI [8].

This can be put as an equation 2.1 and plotted in a figure 2.6.

$$P_{f,dikesection}(t) = P_{f,standard} \tag{2.1}$$

With $P_{f,standard}$ being the failure probability given in the Dutch standard and $P_{f,dikesection}$ the failure probability of the dike section taking into account climate change over time. Hence that the residual lifetime can be negative if the dike failure probability is already bigger than the standards in the water act.

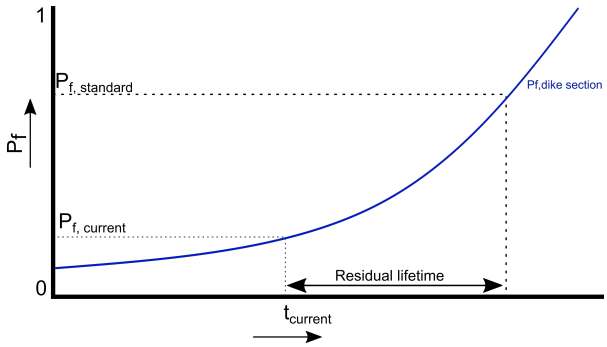

Figure 2.6: Change in failure probability of the dike in time

2.4. Area of Consideration

The area which will be used throughout the whole research is described in the next paragraphs. The reasons for choosing this area will be explained. The influences of both the upstream and downstream boundary will also be explained. With this, an overview is given about which effects of climate change will influence this area.

In the southern part of the province South-Holland, which lies in the south-western part of the Netherlands, the Rhine-Meuse delta is split in multiple channels and estuaries. The main outlet is the Nieuwe Waterweg. This channel flows from Rotterdam to the southern coastline and is the main sea entrance to the port of Rotterdam (figure 2.8). During normal circumstances, the main portion of the Rhine and Meuse river discharge is directed through this channel.

Just below the Nieuwe Waterweg lies the Haringvliet and Hollands Diep. This estuary is responsible for the remainder of the outflow. The area is shown in the red square in figure 2.7. Upstream, the Hollands Diep starts where the Nieuwe Merwede and Amer rivers come together. This is also the most downstream part of national park the Biesbosch. Downstream, the estuary is closed off by the Haringvlietdam. This dam, completed in 1970, is built of numerous gates that can be opened and closed. The gates in the dam are used to regulate the amount of water flowing through the Nieuwe Waterweg. A higher river discharge in the Nieuwe Waterweg means a smaller salt wedge flowing into the Rotterdam area. During high river discharge events, the gates in the Haringvlietdam play a major role in creating extra outflow for the Rhine-Meuse Delta into the North sea.

In the past, the gates in the Haringvlietdam have always been closed during high tide. This created a freshwater lake behind this dam. Nowadays some of the gates are opened with high tide to increase the biodiversity in the Haringvliet and Hollands Diep. One of the requirements was that in no way should the opening have any effect on the safety of inhabitants of the hinterlands. This is agreed upon by the government and provinces and put together in a report called Het Kierbesluit (in English: The Haringvliet Sluice Management Decision).

The management of the flood defences around the Haringvliet & Hollands Diep is split between two different waterboards. In the west waterboard Hollandse Delta, and in the south-east Waterboard Brabantse Delta. The largest part of the total circumference falls in the waterboard Hollandse Delta (see figure 2.7).

During the big flood disaster of 1953 in the south-west of the Netherlands (see figure 2.3) some dikes around the Haringvliet and Hollands Diep were breached [19]. Directly after the flood the dikes were repaired, in the 1960's the dikes were rebuilt a lot larger and higher. Finally, after rebuilding the dikes, the estuary was closed off with the Haringvlietdam. This lowered the influences of the tide and wind on the dikes in the estuary. This also reduced the total hydraulic load on the dikes within the new lake.

The residual lifetime of the dikes around the Haringvliet & Hollands Diep is currently unknown for the new standards and regulations [8]. Fortunately, a lot of data is available at the waterboards. This data can be used to calculate the residual lifetime. Some of the data that is collected by the waterboards consists of dike profiles and geotechnical information of the grounds subsurface. With this data it is

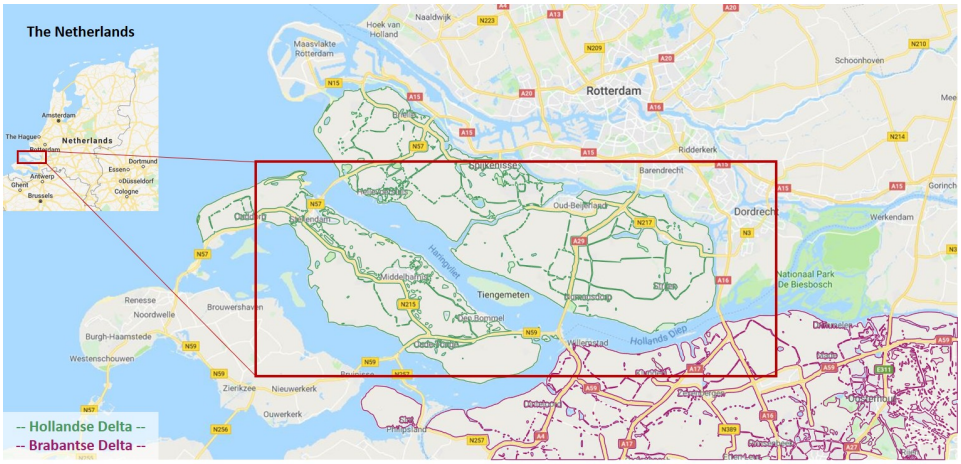

Figure 2.7: Haringvliet & Hollands Diep from Google Maps

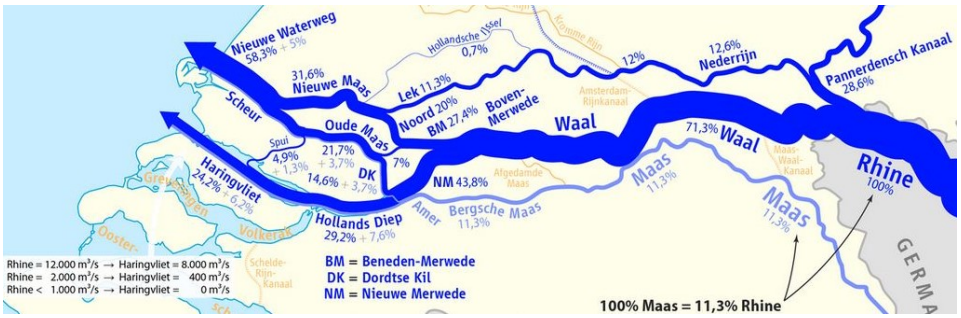

Figure 2.8: Haringvliet & Hollands Diep discharge distribution according to information from 2000-2011 [10]

possible to get a unique view of the influence that climate change has on the residual lifetime of areas like the Haringvliet and Hollands Diep. Figure 2.7 shows the location of the two waterboards within the Haringvliet and Hollands Diep. The large differentiation in dike profiles and soil types on top of multiple hydraulic factors that come into play due to climate change make this study interesting but also very complicated. It is therefore chosen to begin with an area where the countryside is mostly rural. This is the case for the areas around the Haringvliet and Hollands Diep, with the exception of some cities and the Moerdijk industrial area in the north-west. Due to this, only calculations for dikes are considered. Quay walls and hydraulic structures are uncommon in this area and are therefore not considered.

2.5. Failure Mechanisms

The WBI defines different failure mechanisms that can occur on a dike. A total of 24 different failure mechanisms are described in WBI2017 [8]. Appendix I shows all those failure mechanisms. A distinction is made between four categories in the WBI:

- Geotechnical failure (piping, inner and- outer slope stability)
- Revetment of the inner and outer slope
- Dune erosion
- Multiple failure modes for hydraulic structures

Geotechnical failure consists of all the failure mechanisms that are influenced by the soil of the dike and its subsurface. The main failure mechanisms in category are piping, slope stability of the inner and outer slope, and micro instability. Revetment of the inner and outer slope consists of all the failure mechanisms that have something to do with the protection of the slopes and crest of the dike or dam. Dune erosion will, as the name suggests, only look at dunes. The failure modes for hydraulic structures will take into account all the mechanisms that are important for the safety and stability of those

structures.

The two main failure mechanisms for this research in the group of geotechnical mechanisms are piping and inner slope stability . Both of those mechanisms are influenced by the inside and outside water levels. At the outside this is the local water level, while the inside is the polder water level. The polder water level is given by the regional water authorities [42, 43]. The other mechanisms, slope stability of the outer slope and micro instability are not considered further, since those mainly have a much smaller impact on dike failure and have a much smaller chance of creating actual dike failure.

The revetments of the dikes in the Haringvliet and Hollands Diep are very diverse. Many dikes have asfalt covers, or stone revetments on the lower parts of the slope and grass on the top of the slope. In this thesis, these mechanisms will not be discussed further. Including these mechanisms would further increase the complexity of the thesis without adding much more information towards a global view of the area.

Wave run-up/ Overtopping will be included in this report. In the WBI, this is put under the name GEKB (Dutch abbreviation for: erosion of crest and inner slope). The failure mechanism depends highly on the crest height of the dike. Climate change can therefore have a big impact on the failure probability of this mechanism. Wave run-up and overtopping causes a flow of water over the dike crest that can cause erosion of the crest and inner slope of the dike when the flow of water becomes too large. Therefore be assessed by defining a critical overtopping discharge over the dike. The assumption is made that when the critical overtopping discharge is reached, erosion of the crest or inner slope will occur and the dike will fail according to the Dutch assessment tools. It is therefore not necessary to calculate the erosion itself but only the probability of the critical overtopping discharge happening.

In the Haringvliet and Hollands Diep there are almost no dunes. Only in the northwestern part, west of Hellevoetsluis dunes can be found. This thesis will only focus on dikes and therefore this group is excluded from this thesis. The thesis will focus on sections that are not affected by hydraulic structures that lie in the near vicinity.

Eventually this gives three failure mechanisms that are of importance: wave run-up and overtopping, piping and inner slope stability . Of these three, only wave run-up/ overtopping and piping will be discussed further. slope stability is not taken into account due to time constraints.

Indirect mechanisms Indirect mechanisms are the mechanisms that need consequential damage before safety is at stake. Only when extra damage occurs before any repairs are made, these mechanisms have to be considered. These include mechanisms such as: wave, erosion of the foreland and damage against harbour dams. Since the indirect mechanisms by themselves are not capable of dealing enough damage for breaching, these will also be excluded.

2.5.1. Wave run-up and Overtopping

Wave run-up and overtopping can be described as the flow of water over a dike that erodes the protective grass layer on the crest or inner slope of the dike. When the stronger (grass) top layer is breached, the much weaker (sand) sub layer/core will be subjected to this flow as well. This will create a hole in the inner slope that often migrates upstream until the crest of the dike is reached and eroded away. At this point the dike is breached. Not all dikes have a sand core with a clay top layer. Many different dike compositions are used. For now the above mentioned composition of clay top layer with a sand core is used. This can be done since the dike internal composition will not be affected by the. A sand core does erode much faster than a core consisting mainly of clay. The top layer of a grass dike most of the time consists of a cover layer that is approximately 20 cm thick [33]. The grass takes up around 5-10 cm. The remainder of this layer is kept together by the grass roots. A more dense root area gives a stronger cover layer [33]. A lot of large scale experiments have been conducted in which numerous failure paths are described. A typical path is given and explained in figure 2.9.

The initial failure of the grass cover layer often happens at weak or damaged points. Those weak points are often places with inhomogeneous characters: transition areas, poles, benches, stairs and so on. Mainly objects that cut through the cover layer can create a weaker point in the dike. The strength of a grass cover layer lies in the bonding of the grass roots with each other and the clay layer. This bonding

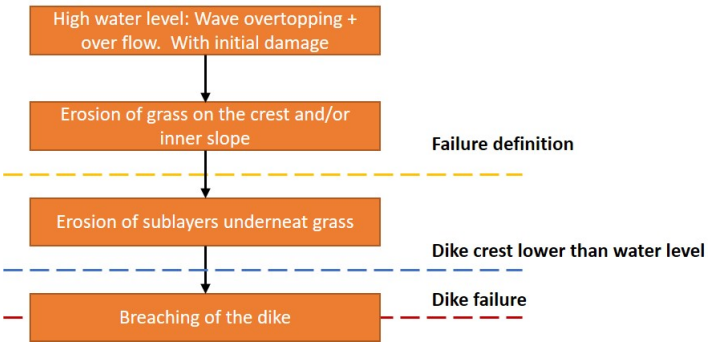

Figure 2.9: Overtopping and wave run-up failure path after [33]

does not exist between grass and structures. The transition area creates a weaker point in the dikes cover layer and is more prone to failure.

With wave run-up/overtopping, water will flow over the crest and inner slope of the dike. This creates a high flow velocity in short bursts. These turbulent flow characteristics create a water pressure that fluctuates a lot. These fluctuations will exert a force on an already weakened cover layer. This will increase the damage on that part of the dike, resulting in possible erosion. The exact point where the grass top layer fails is a completely different subject and is very complicated. A combination of turbulent flow, wave breaking, the density of grass, length of its roots and other aspects provide a certain resistance against the hydraulic load. In the WBI the resistance against the hydraulic load is put together in a maximum allowable overtopping discharge $q_{o,max}$. This parameter is also found in table 2.3.

Erosion of the crest and inner slope After initial damage, the grass layer will slowly start to erode. This will increase over time, eroding a bigger area. This erosion will first go down the slope before it goes deeper. This process will keep going until the grass cover layer is eroded enough to expose the sub layer. Within the WBI this mechanism is tested in the GEKB mechanism. In the WBI this is done by setting a certain maximum allowable discharge that may flow over the crest of a dike.

Erosion sublayer In most cases the sublayer is more prone to erosion than the cover layer. The main soil types in the layers underneath the cover layer are sand or clay. If the sublayer mainly consists of sand, the erosion will pick up in speed and move deeper at a faster pace. Eventually the erosion will move upstream, starting erosion of the crest. When the erosion has decreased the crest level of the dike below the water level, breaching will occur. If the core/sub layer consists of clay, the erosion will be much slower than for sand. However, failure will still occur over time.

Breaching After the initial breach, water can flow freely through the breached part of the dike. The big difference in water level on both sides of the dike creates a high flow velocity. The flow will greatly increase the erosion of the exposed core material, resulting in an increase in size of the breach.

Limit State

The limit state for this failure mechanism describes the erosion of grass at the crest and inner slope. In the WBI, a critical overtopping discharge $q_{o,max}$ is considered. The value changes, depending on what kind of dike is assessed. The limit state uses the same equation as is used in Hydra-NL. This will make it possible to compare the results of the fragility curve method and the HBN calculation in Hydra-NL. Hydra-NL is used instead of Riskeer since it will give a more simplified result.

The limit state for wave run-up and overtopping is written in equation 2.2. This equation is a revised version of the Van Der Meer formula [39].

$$Z_o = \frac{0.067 \cdot \gamma_b \cdot \xi_{m-1.0}}{\sqrt{tan\ \alpha}} \cdot exp\left(-\left(\frac{4.3 \cdot R_c}{\gamma_b \gamma_f \gamma_\beta \gamma_v \cdot \xi_{m-1.0} \cdot H_{m0}} \right) \right) - \frac{q_{o,max}}{\sqrt{g \cdot H_{m0}^3}} \tag{2.2}$$

With a maximum of:

$$Z_{o,max} = 0.20 \cdot exp\left(- \frac{2.3 \cdot R_C}{H_{m0} \cdot \gamma_\beta \cdot \gamma_f} \right) - \frac{q_{o,max}}{\sqrt{g \cdot H_{m0}^3}} \tag{2.3}$$

with: α = dike slope; $\xi_{m-1.0}$ = wave steepness; R_C = run up $[m]$; H_{m0} = significant wave height $[m]$; and $q_{o,max}$ = maximum allowable overtopping discharge $[m^2/s]$. The reduction coefficients $\gamma_{b,f,\beta,\nu}$ each describe different influences which reduce the load on the dike.

The main parameters in this equation are $q_{o,max}$, H_{M0}, and $\xi_{m-1.0}$. $\xi_{m-1.0}$, the iribarren number, is calculated by equation 2.4 given below.

$$\xi_{m-1.0} = \frac{tan\ \alpha}{\sqrt{\frac{H_s}{L_{m-1.0}}}} \tag{2.4}$$

With:

$$L_{m-1.0} = \frac{gT_{m-1.0}^2}{2\pi} \tag{2.5}$$

From equation 2.2 & 2.4, the only unknowns are H_{m0} and $T_{m-1.0}$. The specific wave height and spectral time period. These variables can be found with the Bretschneider equations (2.6 & 2.7) as given in [2].

The Bretschneider equations will be used instead in this thesis instead of a 2D Swan model. The Swan model is more exact but the Bretschneider equations can be calculated much quicker. However, depending on the fetch and/or wind speed, there can be significant differences in the calculated significant wave height and period. Unfortunately it is difficult to give an exact value to the difference between those two methods [32]. For the goals of this thesis it is not needed to have exact data. The Bretschneider equations are therefore accurate enough.

$$\begin{aligned} H_s &= \frac{0.283 \cdot u_{10}^2 \alpha}{g} \cdot tanh\left(\frac{0.0125}{\alpha \cdot \left(\frac{gF}{u_{10}^2}\right)^{0.142}} \right) \\ \alpha &= tanh\left(0.530 \cdot \left(\frac{gd}{u_{10}^2}\right)^{0.75} \right) \end{aligned} \tag{2.6}$$

Bretschneider gives the specific wave period T_s instead of the spectral wave period $T_{m-1.0}$ needed in equation 2.2. $T_{m-1.0}$ can be found by using: $T_p = 1.08 \cdot T_s$ and $T_{m-1.0} = \frac{T_p}{1.1}$. This leads to equation 2.7.

$$\begin{aligned} T_{m-1,0} &= \frac{1.08 \cdot T_s}{1.1} = \frac{1.08}{1.1} \cdot \frac{2.4 \cdot \pi \cdot u_{10} \cdot \beta}{g} \cdot tanh\left(\frac{0.77}{\beta} \cdot \left(\frac{gF}{u_{10}^2}\right)^{0.25} \right) \\ \beta &= tanh\left(0.833 \cdot \left(\frac{gd}{u_{10}^2}\right)^{0.375} \right) \end{aligned} \tag{2.7}$$

With: u_{10}, the wind speed in m/s, d, the local water depth and,F, the fetch. Only the wind speed u_{10} will have a distribution, the other values are all deterministic. The local water depth changes for each water level h_i that is calculated in the fragility curve. The fetch is found for each location in Hydra-NL as is mentioned above.

The berm coefficient γ_b can be found by:

$$\gamma_b = 1 - \frac{B_B}{L_B} \cdot [0.5 + 0.5cos(\pi \cdot \frac{h_B}{x})] \tag{2.8}$$

with: $x = z_{2\%}$ when the berm lies above still water level (SWL). A berm has no effect when it lies above the $z_{2\%}$ run-up level or below $2 \cdot H_S$ [17]. Figure 2.10 shows the other parameters that are needed. The berm coefficient is limited by: $0.6 < \gamma_b < 1$.

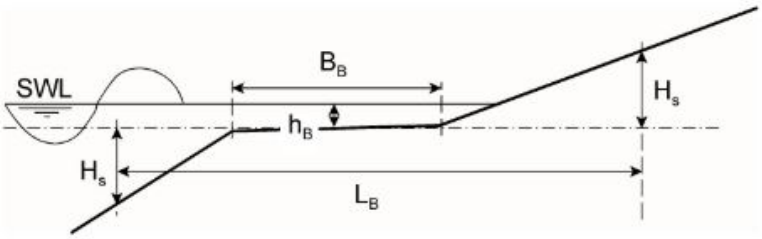

Figure 2.10: Berm reduction coefficient parameters according to [17]

The friction coefficient γ_f is found by large scale model tests. The results are given in the EurOtop Manual [25]. For grass the roughness coefficient is put on: $\gamma_f = 1.0$ The wave obliqueness has different formulas for run-up and overtopping. $\gamma_\beta = 1 - 0.0022|\beta|$ and for overtopping $\gamma_\beta = 1 - 0.0033|\beta|$ [17]. With β in degrees. The formula applies for $\beta < 80°$.

Walls on top of the crest are taken in γ_v. Such walls are rarely used anymore after 1953. Since the study area does not have such walls, the wall coefficient γ_v will not be elaborated further and is not used in this research.

The limit state will be compared with the standards set for a dike section. The standard contains the length effect and is already given in table 2.2. Foreshores are and dams are not included. This is taken into account in the locations that are chosen. Only locations with limited or no foreshores or dams are picked.

2.5.2. Piping (STPH)

Piping is a mechanism that is created by the difference in water level across the dike. A permeable (aquifer) sand layer connects the river water with the ground water on the inside of the dike. On top of this layer lies a thin non-permeable (aquitard) peat or clay layer. The hydraulic head on the outside of the dike creates a high pressure in the aquifer underneath the dike. This creates an upwards pressure. A high enough hydraulic head can result in uplift of the clay layer. The top layer ruptures and water can flow upward through the clay/peat layer, creating a well. This is called seepage. When the flow reaches a critical value, the sand particles inside the dike begin to erode. Sand will flow out of the well with water. This is called heave. The amount of flow increases and thus the erosion does too. A pipe starts to form; when the full length of the dike is eroded and a clear path between the inside and the outside of the dike is established. The width of the pipe will increase in time until the dike collapses [17].

Piping can be described by the processes below. Each of these processes happens before the dike collapses. The path is also shown in figure 2.11. The main sub-mechanisms: uplift, heave, backward erosion and the continuous pipe will be further discussed.

Uplift In storm or high discharge conditions the water level at the outside of the dike rises, increasing the hydraulic head. Due to existing sand layers in the soil, the river water is connected with the groundwater. The permeable sand layer inside the soil is covered with a non permeable clay or peat layer. This means that the water is not able to flow upwards. This creates a hydraulic pressure underneath this non-permeable layer. This layer (also called an aquitard) can only hold a certain amount of pressure, depending on the weight and thickness of this layer. During periods of high hydraulic pressure this force can be too high. This creates uplift of the aquitard, which can create ruptures in this layer.

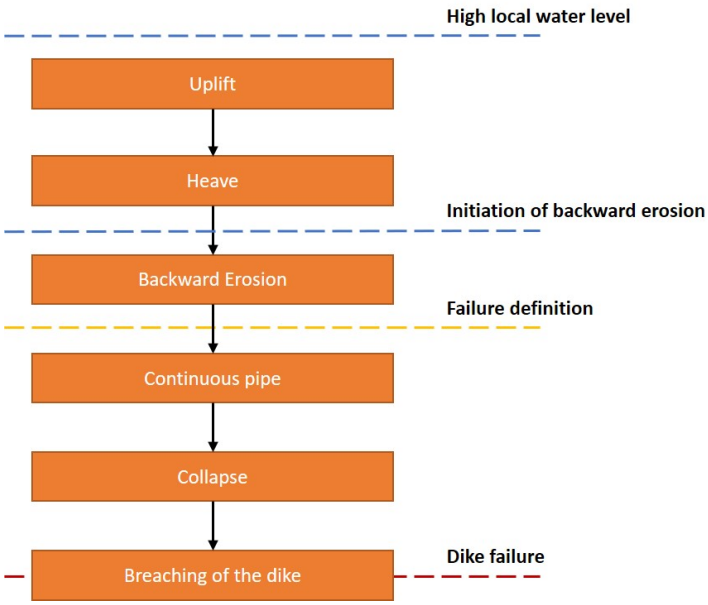

Figure 2.11: Piping instability failure path after [33]

Heave Water can flow directly out of the sand layer through the crack. This creates flow lines in the sand layer towards the exit point. High pressure areas flow towards areas with lower pressure. The channel through the clay layers creates a low pressure just underneath the entry point in the sand layer. This creates a flow towards this point, increasing the flow velocity in that direction. At the exit point, the flow velocity is largest. Having a high enough water pressure in the sand layer makes it possible to reach the critical shear stress of the sand. This creates sand transport upwards through the crack. At the exit of the crack, the flow velocity reduces and the sand will settle down. This process is called heave.

Backward Erosion If the high water event sustains for a long period, the sand transport through the crack (also called a well) will increase. From the land side of the dike, sand will slowly start to erode underneath the dike. This will create a small channel that moves upstream. This is called backward erosion. The channel is located at the top of the permeable sand layer. The clay/peat layer above forms the roof creating stability of this channel. The size of this channel starts out at not more than a couple of grain sizes high. While the channel migrates upstream, the width will slowly increase. Eventually the channel will reach the upstream side of the dike, creating a continuous pipe underneath the full dike [33].

However, there are some mechanisms that slow down backwards erosion or fully stop it. Blockages or obstacles in the soil can stop erosion. Heterogeneity of the soil can also impede soil erosion. For example, if the grain size of the sand increases at some points in the soil, the channel gets clogged. This can stop the growth of the pipe. Sand can still flow out of the well. A cause can be the erosion of a channel perpendicular to the band of bigger sand grains.

Continuous pipe When backward erosion persists long enough, a continuous pipe from the well to the water body with the higher hydraulic head is formed. Water can now flow freely underneath the dike. The pipe will deepen and widen in time. It is assumed that the amount of erosion and transportation of sand does not change over time. At the upstream end of the pipe, strong erosion starts immediately after the full pipe is formed. This sand is transported downstream through the small pipe that is formed. The diameter of this pipe is initially very small(order of magnitude millimetre) and will clog up. This blockage will slowly dissolve due to backwards erosion. These three processes will continue to circulate, increasing the size of the pipe after each circulation. This process can take over 24 hours to create a pipe of the full width of the dike. This was observed in a case study at the IJdijk in the Netherlands [33].

Collapse The final step happens much faster than the creation of the widened pipe. When the full pipe is widened, the amount of flow and erosion will increase considerably. Eventually a big tunnel is created underneath the whole dike. The dike will collapse on to the tunnel when the stability of the tunnel's roof is no longer held. The crest will be lowered considerably. Depending on the water level and overflow condition, breaching can happen soon after collapse [33].

Limit state
The limit state of piping consists of three separate limit states that all have to fail before total failure happens. The three parts in the equation define the limit state for uplift, heave and piping. Each of these parts needs to happen before piping will occur. This can be put in a fault tree 2.12.

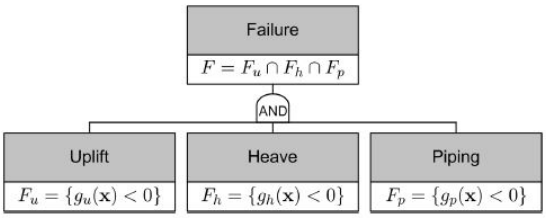

Figure 2.12: Fault tree for piping [17]

Uplift (Z_u) is calculated with the limit state in equation 2.9

$$Z_u = g_u(x) = m_u \Delta\phi_{c,u} - \Delta\phi \tag{2.9}$$

with:

$$\Delta\phi_{c,u} = d\frac{\gamma_{sat} - \gamma_w}{\gamma_w};\ \ \Delta\phi = \phi_{exit} - h_p \tag{2.10}$$

Heave can be calculated with the following limit state:

$$Z_h = i_{c,h} - i \tag{2.11}$$

$$i_{c,h} = \frac{(1-n)(\gamma_s - \gamma_w)}{\gamma_w} \approx 1.65(1-n) \tag{2.12}$$

Backward erosion is determined by the formulas given below. These formulas are a revised and improved version of the Sellmeijer [36] formulas.

$$Z_p = g_p(x) = m_p H_{c,p} - H = m_p H_{c,p} - (h - h_p - 0.3d) \tag{2.13}$$

$$H_{c,p} = F_R \cdot F_S \cdot F_G \cdot L \tag{2.14}$$

With respectively the resistance, scale, and geometrical shape factor:

$$F_R = \eta\left(\frac{\gamma_s}{\gamma_w}\right)tan\Theta;\quad F_S = \frac{d_{70m}}{\sqrt[3]{\frac{k\nu}{g}\cdot L}} \cdot \left(\frac{d_{70}}{d_{70m}}\right)^{0.4};\quad F_G = 0.91\left(\frac{D}{L}\right)^{\frac{0.28}{(\frac{D}{L})^{2.8}-1}+0.04} \tag{2.15}$$

The limit state system works in series, which means that all three mechanisms have to occur before failure happens. This means that the probability of failure can be defined as the product of the three sub mechanisms.

In practise, there are two different methods to calculate the limit state for piping. The first is described above. The second method only takes into account the smallest probability of failure of the three failure mechanisms.

The first method, where the product of the three sub mechanisms is taken, can only be justified if independence between each of the sub mechanisms is considered. This is difficult to justify, since multiple parameters are used in each of the three mechanisms. This means that the sub mechanisms are certainly not independent.

The other options, where the minimum probability of failure between the sub mechanisms is used, is more conservative. It states that if the sub mechanism with the smallest failure probability occurs, the other two sub mechanisms will already have happened. This can also be described as the sub mechanisms being fully dependent on each other. This takes into account the correlation between the sub mechanisms. In practice, the answer lies somewhere between the two described methods.

In the Dutch standards, the second approach is used: taking into account only the smallest failure probability across the three sub mechanisms. It is therefore chosen to use the same approach in this thesis. The total failure probability for piping is written as given in equation 2.16.

$$P_{f,piping} = min\Big(P(Z_U < 0), P(Z_H < 0), P(Z_{BE} < 0)\Big) \tag{2.16}$$

With the subscript (U , H, BE) giving the failure probability for Uplift, Heave and Backward Erosion. The limit state for each sub mechanism is given by equation 2.9, 2.11 and 2.13 respectively. The complete definition and description of the parameters in each of the limit states can be found in the literature under section 2.5.2. The indicator for the residual lifetime should include: uplift, heave and piping. Looking at the formulas for all sub mechanisms, it is clear that primarily the outside water level is included in all steps. In uplift, the outside water level is needed to calculate the potential head ϕ_{exit} at the exit point. For heave, the critical slope depends on the difference between polder and outside water level. For piping, the head difference is compared with the critical head difference. Here, the head difference depends on the outside water level.

Assumptions The limit state for piping will, just as overtopping, be compared to the maximum allowable probability of failure for one dike section. The length effect for piping is included in this comparison since this will greatly reduce the maximum failure probability. Foreshores are taken into account in the seepage length, up to a maximum of two times the dike width as is stated in the piping manual [27] of the Dutch assessment tools.

2.5.3. Inner slope stability (STBI)

Inner slope stability is an important failure mechanism in dike safety calculations. However, due to time constraints, the choice is made to exclude this failure mechanism in the rest of the thesis. The combination wave overtopping and piping is enough to analyse the usefulness of fragility curves in calculating the residual lifetime of a dike.

2.6. Hydraulic loads

The hydraulic loads can be derived with methods described in the second appendix [22] of the WBI. Within the appendix, the load is divided in three main components: water levels, wind waves and currents/flows. Additionally, the hydraulic loads can be increased by: wind, ice, seismic activities, shipping, and traffic. Wind increases the hydraulic load by wave set up and an increase in water level. The wind is taken into account in both Riskeer and Hydra-NL. For dike stability calculations, only the water level increase is needed, while for wave-run up and overtopping, the wind wave action is also important. Ice loads are not assessed in the Netherlands. They are, however, taken into account in the design guides [34]. Seismic activity can greatly reduce the stability of a dike. For areas where such kind of activity is possible, it is important to take this into account. For the Haringvliet and Hollands Diep this is not the case. Therefore it is not included in this study. The hydraulic load caused by shipping consists of three main properties: primary and secondary waves, and return currents. The extra hydraulic loads are mainly important in the design of smaller channels and rivers. For extreme events shipping is most

of the time not considered. Also, shipping causes a smaller additional hydraulic load than wind. This makes it possible to exclude those forces. Loads due to traffic on the dikes fall in the same category as shipping. Roads will be closed off during high water events, keeping those loads from happening. For overall stability of the dike, it is important to take into account traffic loads. Dikes are not assessed for collision damages and loads. Collision is only considered in the stability of hydraulic structures with a small width (in Dutch: sterkte en stabiliteit kunstwerk, punt constructie) [23].

The flood defences that close off the channels into the Haringvliet and Hollands Diep also influence the water level. This is especially the case for the Europort barriers. The storm surge barriers consist of the Maeslant and Hartel barrier. These barriers close off the Nieuwe Waterweg and the Hartel channel. These channels lie just north of the Haringvliet and are the main channels into the port of Rotterdam. Figure 2.8 in the introduction shows the location of the Nieuwe Waterweg and Hartel channel in one arrow just north of the Haringvliet.

In a research about the water safety of Rotterdam and the area around it [30], the closure of the Europort barriers impact the local water levels inside the Haringvliet and Hollands Diep. During big storms, the Europoort barriers are closed. The river discharge from the Rhine can no longer flow through the Nieuwe Waterweg (closed by the Maeslant barrier) and will instead flow into the Haringvliet and Hollands Diep. Since the Haringvlietdam will be closed as well, the water will build up in this estuary, resulting in an increase in water level. Both the closure of the Europoort barriers and the failure of closing have an effect on the water level in the Haringvliet and Hollands Diep.

For the calculation of residual lifetime, the future change in sea water level, river discharge and wind speed have to be taken into account . Most of those loads are influenced by climate change. This results in an increase in sea water level, river discharges and wind driven forces. A combination of these loads, together with the closing regime of the Europoort barriers, will determine the local water levels inside the Haringvliet and Hollands Diep. It is therefore important to know what the influence of climate is on the water system.

2.6.1. Sea level Rise

Sea level rise is one of the changes that happen due to climate change. It is modelled in numerous climate models. The largest organization that copes with climate changes is the IPCC (Intergovernmental panel on climate change). Both the IPCC and the KNMI have modelled possible climate scenarios in which expected SLR is calculated for the future. The IPCC publishes its findings in assessment reports (AR). The fifth edition of this report (AR5) was published in 2014 [31]. Currently, the sixth report (AR6) is being written and is expected to be finished between 2018 and 2021. The KNMI has used the IPCC findings to model climate change for the local circumstances of western Europe and the Netherlands. The KNMI has published its findings in 2006 [18] and 2014 [38].

IPCC The IPCC has modeled four projections of possible scenarios. The scenarios differ from each other in the expected net radiative forcing in 2100. A very simplified explanation of net radiative forcing is the difference in energy level over a certain period of time, measured in Watts per meter squared [W/m^2]. A positive net radiative forcing means that the earth absorbs more energy than it can emit. This causes warming of the earth and change of climate. As a result of the increasing temperature, the ice caps start melting. This will induce an increase in sea water level.

The IPCC uses four scenarios: RCP 2.6, 4.5, 6.0 and 8.5. RCP stands for Representative Concentration Pathway. The number behind RCP is the expected net radiative forcing in 2100. The four projections are the expectation dependent on the governmental policies against climate change. Big adjustments in emission and policy leads to the lowest projection RCP 2.6. Smaller adjustments lead to RCP 4.5. If no change in policy is implemented, the heavier projections are found. The expected increase in temperature and sea level are modelled and put into figures 2.13 and 2.14.

For each climate scenario, water levels are calculated and described. Table 2.4 gives a summary of the expected sea level rise in 2100. Both table 2.4 and figure 2.13 show an increase in sea level over time. How much the sea level will rise depends on the chosen scenario.

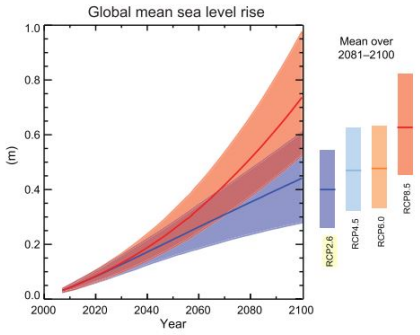

Figure 2.13: Sea level rise according to IPCC [14]

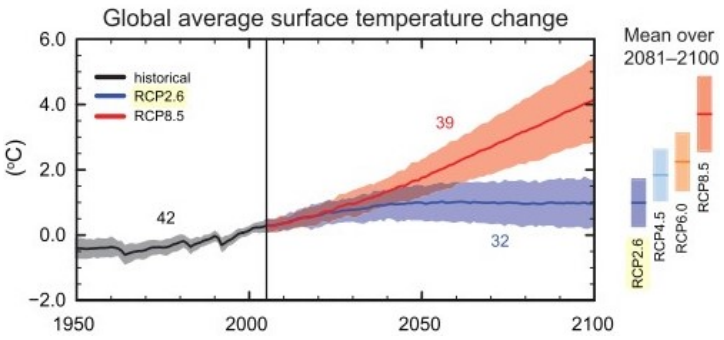

Figure 2.14: Temperature rise according to IPCC [14]

Table 2.4: Global mean sea level rise per scenario in [cm] according to IPCC [7]

	Scenarios	Quantiles		
		5%	50%	95%
Global Mean Sea level Rise[cm]	RCP 2.6	26	40	55
	RCP 4.5	32	47	63
	RCP 6.0	33	48	63
	RCP 8.5	45	63	82

KNMI'06 The KNMI'06 model is based on General Circulation Models (gcm) that are also used in preparations of the previous IPCC report AR4 [29]. The simulations of the gcm made it possible to derive different scenarios for the sea level change in the eastern North Atlantic Basin and the wind speed at the North sea. The models were also used to find the range in which changes in mean temperature and precipitation could occur in the Netherlands. It was found that the range could be related to the global mean temperature and a change in the strength of large atmospheric flow regimes in and around the Netherlands. This made it possible to use the temperature and flow changes around the Netherlands to also develop four different scenarios. Figure 2.16 shows the methodology used in [37] to find the KNMI'06 scenarios. The change in global temperature is split in an expected increase in 2050 of $1°C$ or $2°C$. Changing air flow can affect the air temperature. Instead of a flow regime moving cold air from north-east to south-west, the flow can reverse, creating a warmer airflow from the north-west, warming the area.

Table 2.5 shows the scenarios split by the global mean temperature and the flow regime. G and G+ show the scenarios where the expected temperature rise in 2050 is $1°$C. The G stands for 'Gematigd' which means 'Moderate'. W and W+ show the scenarios for a bigger increase of temperature: $2°$C. The W stands for 'Warm' and is the more extreme scenario. The plus (+) shows whether or not the flow regime changes. A plus (+) shows a change in flow and thus more warming. If no plus is given, there is no change in flow regime.

Table 2.5: KNMI06 climate scenarios based on an increase in Temperature in 2050.

Temperature / Flow regime	$1°$C	$2°$C
Changed	G+	W+
Not Changed	G	W

In figure 2.16 the expected sea level rise is given over time for the four different scenarios. Figure 2.17 shows the temperature rise. In table 2.6, a value for the SLR is given for the same scenarios.

Model and data usage In this thesis, the values for scenario G and W+ from KNMI'06 are used. The main reason for this is that those two scenarios are available in Hydra-NL. This makes it much easier to find reliable values, and eventually the residual lifetime for the dikes that are assessed. In 2014 a

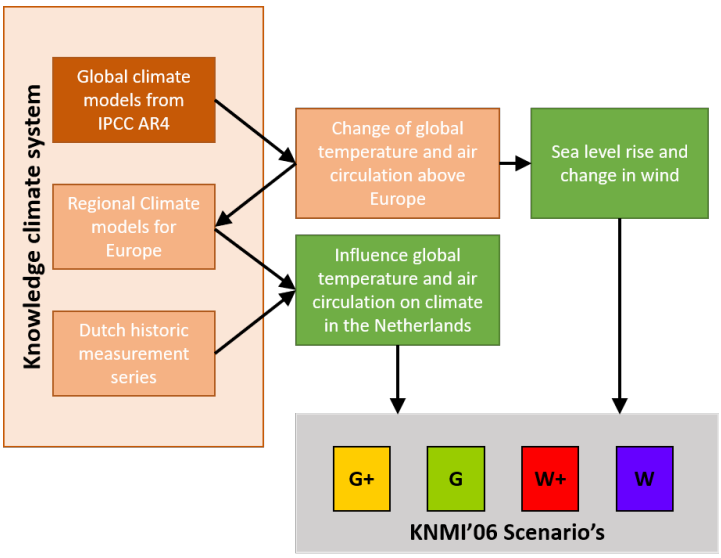

Figure 2.15: Methodology used in the KNMI models [37] to get regional climate scenarios from the gcm's in the IPCC

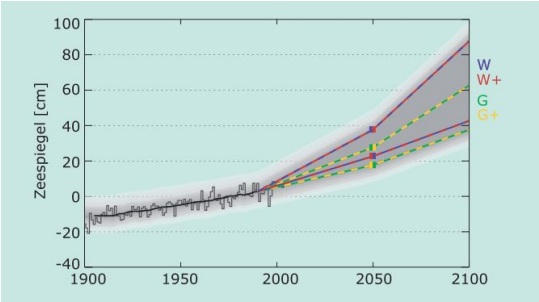

Figure 2.16: SLR according to [18]

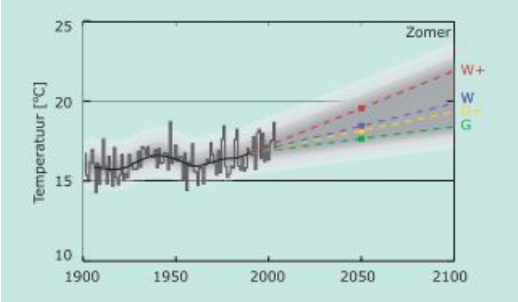

Figure 2.17: Temperature in summer according to [18]

new report was published, KNMI'14 [38]. Compared to the KNMI'06 report, it includes newly developed models and more detailed information about climate change.

For more recent results it would be better to use recent models like AR5 [15] or the upcoming assessment report AR6 from the IPCC. It is unfortunately not possible to include those models in Hydra-NL or Riskeer, since this data will only become available for the Netherlands between 2020 and 2023. For the purpose of this thesis it is however not important to have the most recent data. This thesis concerns the method used rather than merely the results. Using data from earlier models suffices to verify this method. If the method of this thesis works for the data of KNMI'06. It will also work for new, more up to date data. A big change in results can happen if the new datasets give different scenarios and boundary conditions than the data that is used now.

Table 2.6: Sea Level Rise[cm] in 2050 and 2100 according to [18]

		Year Of Occurrence	
	Scenario	2050	2100
Regional Sea Level Rise[cm]	G	15 - 25	35 - 60
	G+	15 - 25	35 - 60
	W	20 - 35	40 - 85
	W+	20 - 35	40 - 85

2.6.2. River discharges

Climate change will also influence the river discharges. This primarily happens due to the change in precipitation regime over the seasons. In winter, more precipitation will be expected, while in summer the total amount of rain will strongly decline [18]. In the winter season, the extra precipitation in both the Rhine and Meuse basin will result in a higher peak discharge. In the mountains, rain will fall instead of snow. Both of these events will increase the amount of discharge in the downstream river. This will result in a higher water level and thus higher hydraulic loads on the surrounding dikes.

In the summer season, a reduction in overall rain together with higher evaporation is expected. This will greatly reduce the discharge in the rivers. Low water levels will primarily impact shipping and water quality [18]. For the failure mechanisms wave setup/overtopping, piping and inner macro instability, low water levels are not considered. Low water levels mainly impact outer slope stability due to the instability between high water pressure in the dike body and low river water levels. Thus creating a high active pressure in the dike with low resistance with the absence of water pressure. There is also sufficient time to repair a dike after failure of the outer slope before a high discharge occurs.

2.6.3. Wind

When looking at lakes or estuaries such as the Haringvliet and Hollands Diep, the wind can also affect the hydraulic loads. The water body is wide enough for the wind to create a water setup that will increase the hydraulic load on the upwind side of the estuary. This means that the hydraulic load is dependent on the wind direction. Especially for the wind waves. Increasing the wave obliqueness will decrease the load of wave breaking/plunging on the dike. Wave obliqueness is measured in degrees from the perpendicular. The maximum angle of wind waves that influence the hydraulic load is put on $120°$. Waves with a higher angle have almost no effect on the hydraulic load since the wave obliqueness will reduce the wave height and thus the load on the dike. The angles between $80°$ and $120°$ are set to have a fixed wave coefficient ($\gamma_\beta = 0.736$) [25]. γ_β Is used in the calculation for the failure mechanism wave set up and overtopping, which will be discussed later.

Climate change influences the wind direction and wind speeds [37]. However, it is difficult to put this in a clear change in distribution. The total amount of storms seems to reduce a bit while the amount of extreme storms will increase.

For this part of the Netherlands, the important wind directions can be reduced to the range between ZW and N (see J.1). The land masses in the other direction often reduce the wind speed and its influence on the hydraulic loads. Within this range, the direction that influences the failure probability of a dike the most is NW.

To reduce the complexity of the calculation, only this direction will be used in the fragility curves. For this direction, one fixed wind speed distribution will be used for all reference years. This will most probably give an overestimation of the safety of the surrounding dikes. This has to be taken into account during the calculation of the residual lifetime.

2.6.4. Europort Barriers

The Europort barriers consist of the Maeslant barrier and the Hartel barrier. The Maeslant barrier can close off the main outlet of the Rhine-Meuse river delta. About 60% of the Rhine-Meuse basin is discharged through this channel. The remaining discharge is distributed between the Haringvlietdam and the Pannerdensch channel in the west (figure 2.8). In storm conditions with a sea level of $\approx 3.00\ m + NAP$ the Maeslant barrier is closed. This creates a barrier between the north sea and the port of Rotterdam, securing Rotterdam from possible flooding. River water which can no longer flow through the Nieuwe Waterweg will find another way towards the sea. This will create a flow towards the Haringvliet and Hollands Diep. Here, the water will build up in the estuary, since the Haringvlietdam will also be closed in storm conditions. This will create high water levels in the Haringvliet and Hollands Diep, increasing the hydraulic load. The same reasoning can also be used for extreme storms that create sea water levels just below the closure level of the Maeslant closure Barrier. The big inflow of sea water into the port of Rotterdam pushes both sea and river water in the direction of the Haringvliet and Hollands Diep, creating high water levels in the estuary.

This process is only relevant when both a high sea water level and river discharge occur simultaneously.

These events are not correlated. High sea water/storm events are created due to storm fronts on the north sea or the north Atlantic ocean. Big discharge events are created by precipitation events in the east around Bonn and Cologne so the combination of an extreme storm and extreme discharge has a very low probability.

The total hydraulic load is therefore influenced by the state of the Maeslant barrier. This provides extra safety but also makes the system more complex. High hydraulic loads can be created by extreme storm or discharge events, but can also occur due to a combination of events with a much lower return period. Different combinations of sea water level, discharge, wind speed and the state of the Barriers have to be put together to find the actual return period of different hydraulic loads inside the Haringvliet and Hollands Diep.

2.7. Residual Lifetime

Climate change will change the distribution of the local water level which is caused by a change in river discharge distribution, wind speed distribution and sea level rise.

local water level Climate change will induce a change in sea water level, river discharge distribution, and possibly a change in wind-wave interaction [18]. This will increase the probability of higher water levels occurring close to a dike. Higher water levels contribute to a higher failure probability of a dike. This means that as long as the climate keeps increasing the local water level distribution, an increase in dike failure probability will happen. Eventually, this failure probability will become larger than the maximum allowable failure probability (table 2.1) set in the Dutch assessment tools [8].

Fragility curve The probability of failure for each conditional water level is calculated with a fragility curve. Combining the fragility curve with the local water level distribution gives the failure contribution for each water level. Integrating over the water level gives the total failure probability. The fragility curve will not change with climate change. Fragility curves only look at the failure probability for a fixed water level. The occurrence probability for that specific water level is not taken into account in a fragility curve.

Failure probability Combining the fragility curve with the water level distribution will give the contribution towards the total failure probability for each water level. The area under this graph gives the total failure probability of a dike, which will increase in time.

Figure 2.18 shows what happens to the failure contribution when the local water level distribution increases towards higher water levels. The left figure shows the failure contribution. The right figure shows the results of the colored area compared to each other and to a set standard in the assessment tools. This figure given example of what happens with when the local water level distribution changes to higher water levels due to climate change

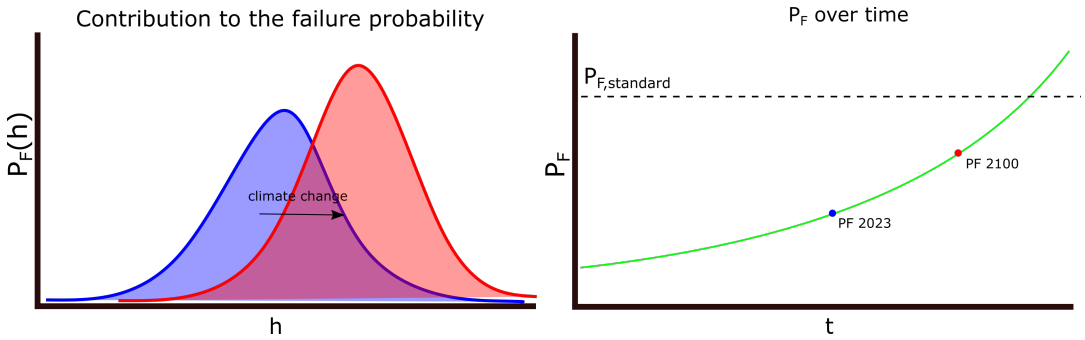

Figure 2.18: Effect of climate change on the failure probability contribution. Blue representing reference year 2023 and red 2100.

For each of the mechanisms, the residual lifetime can be calculated. This will be described for wave run-up/overtopping and piping. The DWL will be used as an indication of what happens with climate change. The DWL is a design water level and is only used in a semi probabilistic calculation where

calculations are done with design values. In a probabilistic calculation this is not the case. There the values are distributed with a mean and standard deviation. Climate change is in this case indicated with the DWL. This is only done to show the effect of climate change on a failure mechanism without the need of showing water level distributions and fragility curves.

Overtopping For wave run-up/overtopping, the water level influences the failure probability. When the critical overtopping discharge ($q_{o,max}$) is reached (probability of failing due to erosion of the crest and inner slope), the dike has failed according to the set standards. For the failure mechanism wave run-up/overtopping, the effect of climate change is given in figure 2.19.

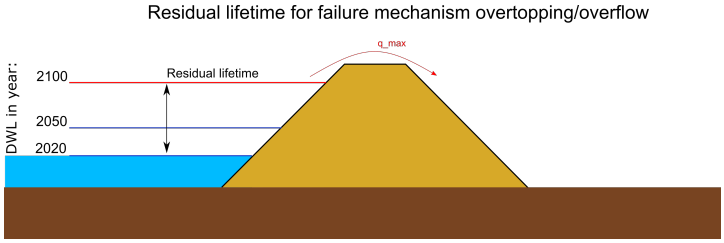

Figure 2.19: Residual lifetime for failure mechanism wave run-up/overtopping

Piping Dikes may not fail due to wave run-up/overtopping. This can be the case if the dikes are much higher than needed. In some areas of the Haringvliet and Hollands Diep this is the case, due to the raising of the dikes after the 1953 flood disaster and the closure of the Haringvlietdam afterwards. This makes it important to look at other mechanisms than wave run-up/overtopping as well. Piping is such a failure mechanism. Piping is dependent on both the water level and stability due to geotechnical conditions.

The geotechnical properties of the soil in and underneath the dike play an important role in the stability of the dike. An increase in water level will reduce the stability of the dike. However, high water levels have a short duration, while geotechnical processes need a long time to establish. The time it takes for the processes to happen will not be taken into consideration in this thesis, since time dependency will greatly increase the complexity of this thesis. For a quick overview of the study it is also not necessary to include these processes.

The influence of stability on the residual lifetime is limited by the height of the dike. For the Haringvliet and Hollands Diep this is less relevant, since the dikes are much higher than the design water level. Theoretically it is possible that the dike is stable enough to withstand a water level higher than the crest level. In practice this does not happen since the dike will already fail due to the mechanism wave run-up/overtopping.

For piping the residual lifetime is also related to the local water level. The hydraulic pressure of the water creates an upwards pressure against the inner toe of the dike. When this pressure is high enough to create uplift, heave and backwards erosion, the dike body can eventually collapse. Higher local water levels increase the head difference between the inner and outer slope of the dike, and thus create a bigger probability of failure. Figure 2.20 shows what the different local water levels do to the head in the dike. Higher local water levels will increase the head difference and will therefore increase the failure probability. The residual lifetime will be calculated to the point of the failure probability being bigger than allowed in the WBI. Hence the failure probability for piping is a combination of the mechanisms uplift, heave, and backwards erosion, all occurring together.

2.8. Models

2.8.1. Hydra-NL

Hydra-NL is a probabilistic program that can be used to calculate the hydraulic load on dikes in the Netherlands according to standards given in the Dutch assessment [8]. The input for Hydra-NL are the dikes profile and location, and boundary conditions for the water level calculations.

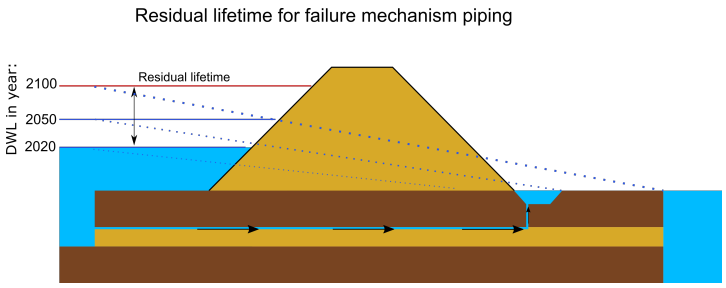

Figure 2.20: Residual lifetime for failure mechanism piping

In Hydra-NL it is possible to choose the climate scenarios G and W+. For those scenarios calculations can be done for three reference years: 2023, 2050 and 2100. For each of those reference years, different parameters can be calculated. In this thesis, this function is mainly used to calculate the local water level frequency statistics and the probability of failure of the dike cross section for validation purposes. The climate models which are used with Hydra-NL are developed by the KNMI [18]. In these models, different changes are defined, such as changes in sea water level, wind speed and river discharge distribution.

The data from the climate models are already included in Hydra-NL. Only the boundary conditions of the water system and the local dike dimensions have to be included to begin calculations. For the calculation of the local water level (in m + NAP), it is not necessary to include the dike cross sections. For the calculation of wave run-up and overtopping (in m + NAP), the dike dimensions have to be included.

To find the probability of failure and the hydraulic load level, a calculation is started in which the maximum allowable hydraulic load has to be defined. This is done with the maximum overtopping discharge($q_{o,max}[l/s/m]$) which is already mentioned earlier in this chapter. This value is set to $q_{o,max} = 1l/s/m$. When the same $q_{o,max}$ is used in Hydra-NL and the limit state function for the fragility curve, it is possible to compare the results and analyse the correctness of the fragility curve.

Hydra-NL uses a Swan model to calculate the specific wave height and period. This is different from the Bretschneider equations that will be used in the fragility curve method. The Bretschneider equation is a 1D model, while Swan is 2D. This means that Swan is more accurate but also more complex. This is no problem for Hydra-NL but is difficult to include in the fragility curve. Bretschneider is less accurate, but will give a result that should be good enough for an overall view of the study area. Mainly since the first order wave effects are correctly included in Bretschneider.

Hydra-NL will also be used in a sensitivity analysis. The fragility curve result will be compared with the result of Hydra-NL. The difference in use between Bretschneider and Swan should be considered. Hydra-NL does not include any geotechnical information. It is therefore impossible to use this for any mechanism that is dependent on geotechnical conditions. For those mechanisms, Riskeer can be used.

2.8.2. Riskeer

Riskeer (also called: Ringtoets) is an application that is used to assess dikes in the Netherlands. Riskeer can make calculations for the failure mechanisms wave run-up/overtopping with the module GEKB (grass erosion on crest and inner slope). It can calculate the failure probability and the hydraulic load level(HBN). The HBN calculations can be compared with the HBN calculations from Hydra-NL but do have some differences. For the failure probability calculation, Riskeer uses a probabilistic calculation for both the load and strength side of the equation. For the HBN calculation Riskeer uses a stochastic value for the overtopping discharge while Hydra uses a deterministic overtopping discharge. When the deterministic overtopping discharge is more or less equal to the design value, the difference in outcome between Riskeer and Hydra-NL for the HBN calculation is negligible. Riskeer also includes modules for hydraulic structures, grass erosion on the crest and inner slope, piping, slope stability and revetment damages. For piping and macro instability it does not give an exact answer, but an approximation using semi-probabilistic calculations. Riskeer needs more inputs than Hydra-NL does. Soil

information of the dike and its subsoil is needed to make calculations for the different failure mechanisms. For the hydraulic load, only the profile is needed. This profile consists of information about the geometry, dike slope, and roughness of the cover layer. For macro-instability and piping, a more detailed profile is needed in which the layers, thicknesses, soil types and their corresponding parameters have to be included. The local water level has to be connected to this information. It is therefore also important to know the location of the dike and its subsoil composition. The soil schematization is given in a stochastic subsoil schematization (SOS: Dutch abbreviation). SOS gives a chance of occurrence for different soil compositions in each dike section. The chance of occurrence represents the part of the total length of the dike that has this soil composition. The schematisation gives a global picture of the soil composition underneath the dike. For assessment the schematisation has to be supplemented with more detailed geotechnical information.

The output of Riskeer is the probability of failure of the dike given the hydraulic loads. It is possible to combine all the failure mechanisms and get an answer on the total probability of failure of that dike stretch.

3

Method to determine Residual Lifetime

3.1. Introduction

The research can be divided in five steps. Each step is needed to calculate the residual lifetime for one climate scenario. The division is done to create a structure with a clear view of the steps that have to be taken to calculate the residual lifetime. For each dike profile and each failure mechanism, the steps have to be followed.

I Data gathering
II Calculation of the water level frequencies
III Calculation of fragility curves
- Including the calculation of the reference values using Hydra-NL for HBN and Riskeer for piping.

IV Calculation of the residual lifetime
V Spatial view around the Haringvliet and Hollands Diep

In figure 3.1 an overview is given of how each step is needed to fulfil the objective of finding the residual lifetime of the dikes around the Haringvliet and Hollands Diep. This figure shows the method that will be followed in the research part of the framework. The colours between both figure 1.2 and 3.1 show the same steps. Only a small difference is found in step IV of figure 3.1, where only the calculation for a dike section is given.

In part I, the available data will be evaluated. Using the results of the literature study, a choice will be made about which dike profile and geotechnical conditions will be used. These conditions do not differ between the climate scenarios.

Part II consists of the calculation of the local water level distribution for each scenario and for the three reference years: 2023, 2050 and 2100. Before the local water level distribution can be found, the probability of exceedance has to be calculated in Hydra-NL. With this line, it is possible to calculate the local water level distribution which can also be called the probability density function of the local water level. For each reference year and each scenario, a unique distribution is calculated. The differences between those lines will already give an indication of the influence of climate change in the local water level and thus the probability of failure of that dike.

The next step is done in part III. For each failure mechanism, the probability of failure at a given local water level is calculated. This is done with fragility curves. Fragility curves make it possible to combine multiple failure mechanisms into one curve. This is used to also get the failure probability of a dike due to a combination of failure mechanisms. A fragility curve uses the conditional water level together with a limit state function to calculate the failure probability on this water level.

The method of fragility curves is shown in figure 3.2. The input consists of the necessary parameters for the chosen failure mechanism. These are dike dimensions, soil conditions, and soil parameters. The data for the chosen dike ring is selected and within this data, the location is chosen. The parameters that belong to this location will be used in the fragility curve. In the next step, a range of water levels

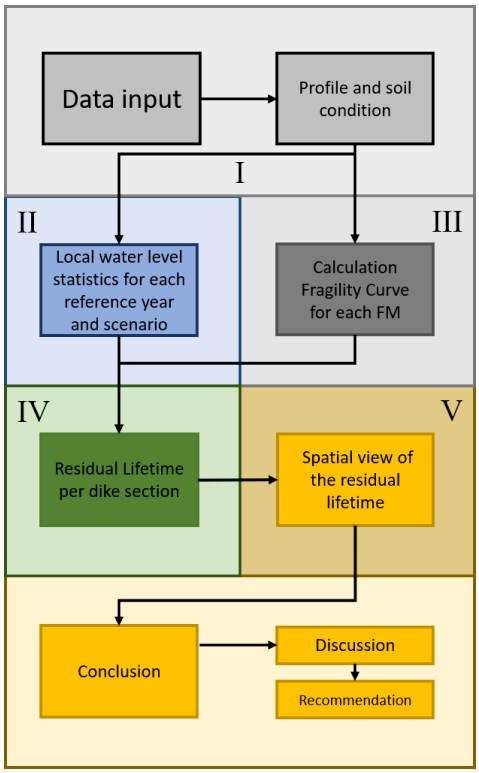

Figure 3.1: Thesis Method

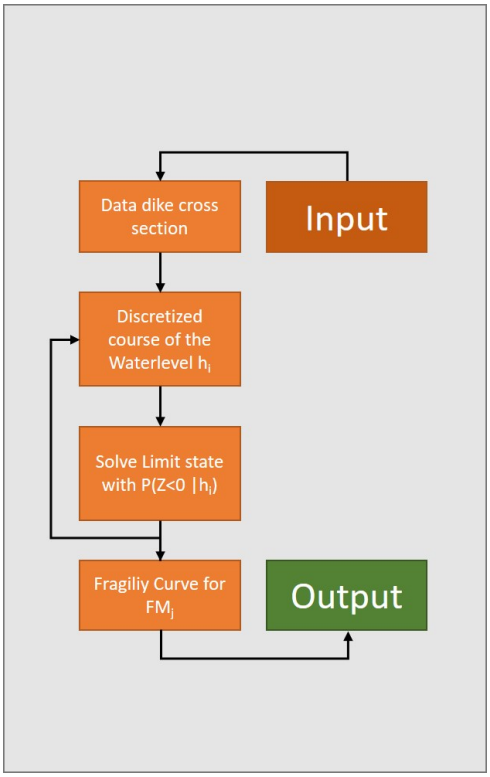

Figure 3.2: Part III: Calculation of Fragility Curves [20]

is selected for which the fragility curve will be calculated. This maximum depends on the crest height of the dike and the minimum is put on a fixed value of 1.5m + NAP. The range is then split into equal steps. Each step will be one probability calculation. Combining all the answers for each water level in one graph will give a fragility curve over the selected range of water levels. This can then be repeated for different failure mechanisms and different locations.

Fragility curves of different failure mechanisms can be combined into one overall fragility curve. This curve can be used to give an overall probability of failure for a dike section when multiple failure mechanisms are taken into account. A fragility curve can be combined with the local water level probability calculated in part II, to find the contribution to the probability of failure given that water level.

Depending on the failure mechanism, a sensitivity analysis can be done. For the hydraulic load level, Hydra-NL is used. The hydraulic load level can be calculated with Hydra-NL and will be compared with the results of the fragility curve method. For piping, Riskeer is used to verify the probability of failure. The fragility curve for piping will also be checked with the fragility curve creator tool, provided by HKV lijn in water. The analysis is done to see if the results of the fragility curve method are in line with the expected values. In part IV, the residual lifetime is calculated for a given dike cross section or dike section. Four steps have to be taken here. First, the contribution towards the total failure probability for each water level has to be calculated. This can be done with the answers given in part II and III. The failure probability contribution is found by multiplying the probability of failure from the fragility curve with the local water level probability for each water level. Secondly, the contributions have to be put together to get an overall probability of failure of one dike cross section. This is done by calculating the area under the curve of the failure probability contribution. Third, The two steps above have to be repeated for each of the reference years (2023, 2050 and 2100). For each scenario, three failure probabilities are now known. These can be plotted against the reference years to get a probability of failure over time figure. A line will be drawn through the three points that are available to extrapolate the data into the future. The standard of the WBI can be plotted in this graph as a horizontal line. The residual lifetime can then be read from this graph by subtracting the current year by the year in which the probability of failure crosses the standard. Part IV can be repeated for both scenario G and W+ to

get a bandwidth of the expected residual lifetime.

For each dike section, the parts above are repeated. These are then combined in step V. Doing this for the whole area of the Haringvliet and Hollands Diep will give a spatial view of the dikes' residual lifetime around the Haringvliet and Hollands Diep.

Parts I to V will finally be concluded with a discussion and recommendation about the obtained answers. The description of the method above is just a small overview of what happens in each part of the method. In section 3.5, a more in-depth explanation of each step is given.

3.2. Methodology

The objective of this thesis can be achieved with a literature study and modelling of the probability of failure for multiple dike cross sections. With a detailed literature study it is possible to make the right assumptions which are needed to complete the scope. For the water level distribution, existing models will be used. For the modelling of the probability of failure, fragility curves will be used.

3.2.1. Modelling

The local water levels are calculated with the help of Hydra-NL. In this program, it is possible to calculate the local water levels for each of the included reference years and for different climate scenarios. For these calculations, all the uncertainties are taken into account, to make the calculations in accordance with the assessment of the WBI.

To check the outcome of the fragility curves, Hydra-NL and Riskeer are used. Hydra-NL will be used to validate the outcome of the fragility curve for run-up and overtopping. For piping, Riskeer is used. In Hydra-NL this is done with the Hydraulic load computation taking into account the uncertainties.

For the creation of a fragility curve, probabilistic calculations have to be conducted. These can be done with different models. In this thesis, only the Crude Monte Carlo (CMC) and First Order Reliability Model (FORM) are used. For the CMC model, a python script will be created which is capable of doing this. For FORM, two different open source python packages are used. PyRe [13] and Openturns [3].

3.2.2. Case study

Case studies will be used to test the assumptions made in the calculation. Multiple cross sections spread over all stretches in the Haringvliet and Hollands Diep will be tested. Whenever the outcomes of these locations fit within the expected result, an overview is made to give an overview of the whole area.

Each dike stretch consists of multiple sections and each of those sections consist of multiple cross sections which all have to be calculated separately. Combining the failure probabilities of each section makes it possible to say something about the whole stretch. This layering is also how the current Dutch dikes are assessed. This is given in figure 3.4. Figure 3.3 shows the chosen locations which will be taken into account.

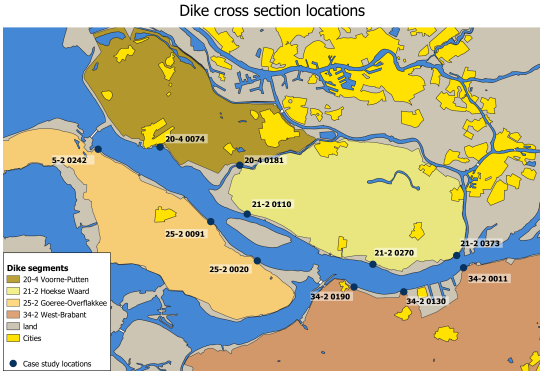

Figure 3.3: Dike cross section locations

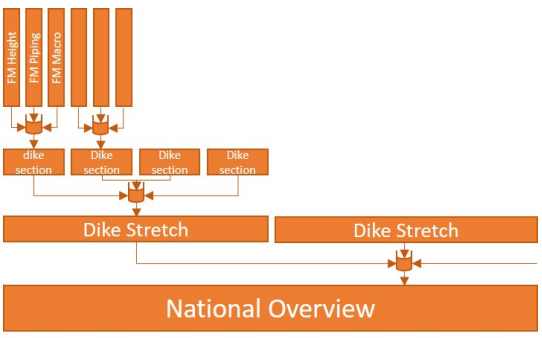

Figure 3.4: Layering in the Dutch assessment method

3.3. Data Gathering

The following data is needed in this thesis: boundary conditions, location parameters, dike schematization, hydraulic load information, stretches and soil models. This information is needed to make calculations with both Hydra-NL and Riskeer. This software is available on Helpdeskwater [28]. Hydra-NL and Riskeer are used to check the failure probability calculated with fragility curves.

For the literature study, articles and reports are provided by Rijkswaterstaat and HKV Lijn in water. Additionally, Google Scholar and the repository of TU Delft are used to find additional literature.

Helpdeskwater has a database that contains important information about each dike stretch. In these databases, information can be found for the hydraulic boundary conditions, location, hydraulic loads, and stretches. This data is freely available and usable. Most of the models that are currently used within the WBI already use the data provided by Helpdeskwater.

Dike schematization, sub soil conditions, location parameters and stretch information are provided by the local water authorities Hollandse Delta [43] and Brabantse Delta [42]. These regional water authorities which manage flood defences have provided detailed information about the flood defences in their working area.

Fragility curves cannot be created in Riskeer and Hydra for the considered area. Therefore this step will be done with the help of Python scripts and built-in functions. The outcome of the constructed fragility curves will be compared with the outcome of Riskeer or Hydra-NL to check the validity of the fragility curves. In this process, the added value of fragility curves will also be checked.

3.4. Scope

The complexity of the situation in the Haringvliet & Hollands Diep requires a well thought-out scope. This is done because it is not necessary to immediately take into account all the different aspects that will influence the water system. Since this is a first view about the added value of a method with fragility curves for the new assessment tools,some aspects will not be taken into account. As said, a lot of aspects influence the strength and lifetime of the dikes. To make it clear to the reader what is included, the current choices for the scope are explained.

Models The main models that will be used are Hydra-NL and Riskeer. Both models are developed to make assessments according to the Dutch formal assessment WBI2017. Hydra-NL will be used for the calculation of the water level frequencies and a sensitivity analysis of the wave run-up/overtopping calculations. Riskeer will be used to do the same for the piping results.

Climate Influence Two climate scenarios are taken into account and are implemented in Hydra-NL. These are scenario G and W+ from the KNMI [18]

Failure Mechanisms The two failure mechanisms that are included in this thesis are: wave run-up/overtopping and piping. Each mechanism has to be modelled individually.

Geotechnical decisions For the geotechnical parameters and dimensions the values from the stochastic subsoil schematization (SOS) will be used. SOS gives a schematized view of the subsoil compositions of most of the primary dike sections of the Netherlands. In the schematization, the thickness of the present values are given, together with its distribution. The hydraulic conductivity of aquifers are also given, together with the grain size and density of the different layers.

It has to be noted again that the SOS data gives an overview of the soil condition but is not detailed enough for an assessment in compliance with the WBI. Since this study is mainly focused on getting an overall view of the Haringvliet and Hollands Diep and testing the fragility curve method in calculating the residual lifetime, the SOS data can be used.

Seepage length The seepage length is measured using the AHN viewer [12] which contains GIS data about the height of the ground level in respect to the NAP. The seepage length is measured in the Height profile viewer tool. The seepage length is considered to be the distance between the toe of the

inner slope (exit point) and the water line. When a trench is located between the water line and outer slope, this will be used as the entree point of the seepage length. Normally an on site investigation has to be done to measure the seepage length. One of the reasons to do this is to see if the trenches are in contact with an underlying aquifer. To be safe, it is assumed that this connection exists and that the seepage length is shortened by the presence of trenches.

Critical overflow For run-up/overtopping a critical overtopping discharge of $q_{o,max} = 1.0\ l/s/m$ is used. This variable is used in both Hydra-NL and the calculation for fragility curves. Between the fragility curve model and Hydra-NL, the same value for $q_{o,max}$ should be used to make comparison between the methods possible. The maximum overtopping discharge $q_{o,max}$ is also taken as a deterministic value. This is done to make the comparison between Hydra-NL and the fragility curve method more equal. In Hydra-NL $q_{o,max}$ is also given a deterministic value. The value that is used in this study is not in compliance with the WBI. There, the maximum overtopping discharge is dependent on the location of the dike, the hinterlands, the type of grass revetment of the inner slope in combination with the hydraulic boundary condition and the slope and roughness of the outer slope of the dike.A rather small $q_{o,max}$ is used in this thesis. This makes for smaller failure probabilities for overtopping than in reality. The results will underestimate the strength of the dikes against overtopping meaning that in reality the dikes are stronger.

Failure definition The failure definition that will be used throughout this thesis is the same definition as used in the WBI [8]. This means that residual strength of the dikes will not be included. For the purpose of this thesis, the maximum allowable failure probability is set to be equal to the bottom value given in table 2.3 for each of the different dike stretches. For the dike sections, the bottom value is smaller and given in table 2.2.

An important assumption is that the Dutch safety standards do not change in the future. This can be done since the climate scenarios, that are used in this thesis, are also used in the current formal assessment and design tools.

Test Location Test locations will be selected for which the soil condition and dike profiles are easy to work with. These stretches will be used to make the model and validate the assumptions that are made. It is important that the chosen location is influenced by the failure mechanism of choice. If its influence can be neglected or is very small, a different location should be used. A total of 11 locations will be analysed in this thesis. This does not give a global overview of the whole area, but does give an indication of what to expect. Locations close to flood defence structures like sluices or dams are not included. The structures will influence the strength and load on the surrounding dikes. In most cases, those areas are much stronger than necessary. Only a small percentage of the total length of dikes does have hydraulic structures near them. These dikes will not be considered.

Time dependency Time dependency will not be taken into account. Time dependency has an effect on the duration of storms and river discharges. Wave run-up and overtopping is mainly dependent on the time of the tide and thus has a fixed time in which overtopping may happen. However, for piping and inner slope instability the duration of high water has to be much longer. The water needs time to infiltrate the dike or its subsoil. This means that there is a period of time in which the local water level does not yet influence the stability of the dike. Whenever the infiltration time is shorter than a high water event, there is no probability of failure. However, it is difficult to exactly know how fast the infiltration will go. Also, it is difficult to know how long a high water event will last, as the event is created due to multiple different events. Therefore, it is chosen to not take into account the time dependency.

Settlement and ageing The area of interest lies within the Rhine-Meuse Delta. This means that the soils underneath the dikes have high compressibility. Due to the extra weight of a dike on top of this soil, the dikes will subside. This settling can be in the order of decimetres in the lifespan of a dike. In this thesis, this settlement will not be included.

It is also assumed that the total strength of a dike will not change over time. In reality, dike strength increases in the first years after placement when maintenance is done regularly and appropriately. For older dikes, the dike strength will not change significantly.

The dikes and foreshores change very little since there is almost no erosion of the foreshore and no large settlement or soil subsidence. This effect will therefore be excluded from this report.

3.5. Method of calculating the residual lifetime

3.5.1. Fragility Curves

The failure probability of each failure mechanism is calculated using fragility curves. A fragility curve shows the probability of failure for a single conditional load. They are created by calculating the probability of failure given one conditional parameter. For flood risk calculations, this is the outside water level h. Calculating the failure probability for multiple water levels will make it possible to create a graph that shows the change in failure probability by a change in outside water level.

The probability of failure of a single failure mechanism can be found by using their limit state functions $Z = R - S$. In which Z is the limit state function for the given failure mechanism, R is the strength of the dike and S is the load on the dike. R and S are built up from multiple different variables that together determine if a dike failure happens. Z can therefore be written as a function of those parameters $Z(X_1, .., Z_n)$. Failure occurs when the load is bigger than the strength ($Z = R - S < 0$). This can be written as: $P\{Z(X_1, .., Z_n) < 0\}$. The limit state will be calculated over a range of conditional water levels.

The results of these calculations can be put into one graph to get an overview of the probability of failure per water level. Equation 3.1 shows how the limit state is put into an probabilistic calculation. h_i in this equation is the conditional water level. The upper border depends on the crest height of the dike. The bottom water level is set on 1.5 meter + NAP.

$$P_f|h_i = P(Z \leq 0|h_i) \tag{3.1}$$

A fragility curve can be constructed for each failure mechanism, showing the influence of each individual failure mechanism on the probability of failure. Since the water level is a variable that is used in both failure mechanisms, it is possible to combine the fragility curve. Fragility curves are therefore a good method for combining failure mechanisms that are dependent on the water level.

$$P_{F,total} = 1 - \prod_{n}^{i=1} \left(1 - P_{F,i}\right) \tag{3.2}$$

The two failure mechanisms are considered to happen independently of each other. However, in reality there is a dependency between each of the failure mechanisms, as both are dependent on the water level on the outside of the dike. It is however hard to model this correlation. Therefore the failure mechanisms are considered to be independent. This makes it possible to use equation 3.2 to add the outcome of the fragility curves together for each considered water level [4]. With $P_{F,i}$ being the probability of failure for the individual failure mechanisms. The equation will remove the possibility of getting a failure probability above 1.

Figure 3.5 shows how the different failure mechanisms are combined. The brown line shows the combined fragility curve. Since the failure probability for each failure mechanism is added together for each water level, the combined curve will always be higher than the highest single fragility curve. This is valid when the failure mechanisms are independent. The combined fragility curve will be used in the following steps to find the residual lifetime of the dike cross-section.

Probabilistics

The limit state function $Z_i = R - S = Z_i(X_1, ..., X_n)$ consists of multiple parameters that all have a certain distribution. To calculate the failure probability for each conditional critical water level, it is necessary to make a probabilistic calculation for each water level. This can be done with different probabilistic models. The most frequently used are Crude Monte Carlo (CMC) and FORM (First Order Reliability Model). CMC is a level III method while FORM is a level II method. The biggest difference is that CMC is a fully probabilistic numerical method. FORM gives an approximation of each of the uncertain

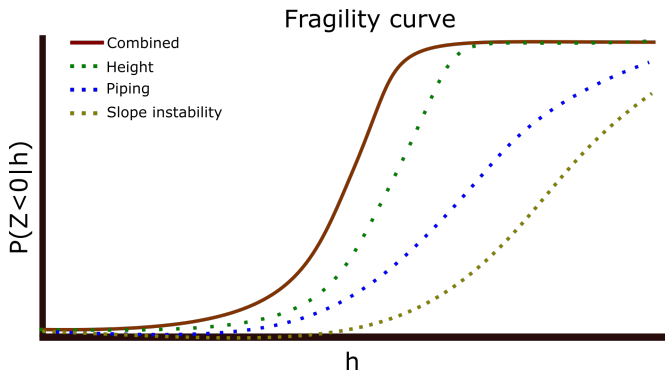

Figure 3.5: Combining Fragility curves

parameters [16]. The computation time of a CMC model is typically much longer than that of a FORM calculation.

The limit state depends on which failure mechanism is considered. The equations that are needed are described in the literature study.

3.5.2. Failure contribution

For each of the available reference years, the local water level distribution or probability density function (pdf) can be calculated. When combining a fragility curve with the pdf, the contribution to the failure probability for each water level is found. The derivative of this graph gives the dike's total failure probability. Doing this for each reference year will give the failure probabilities of each of the three reference years. These values can be used to find the residual lifetime by extrapolation. These steps can be given in four figures.

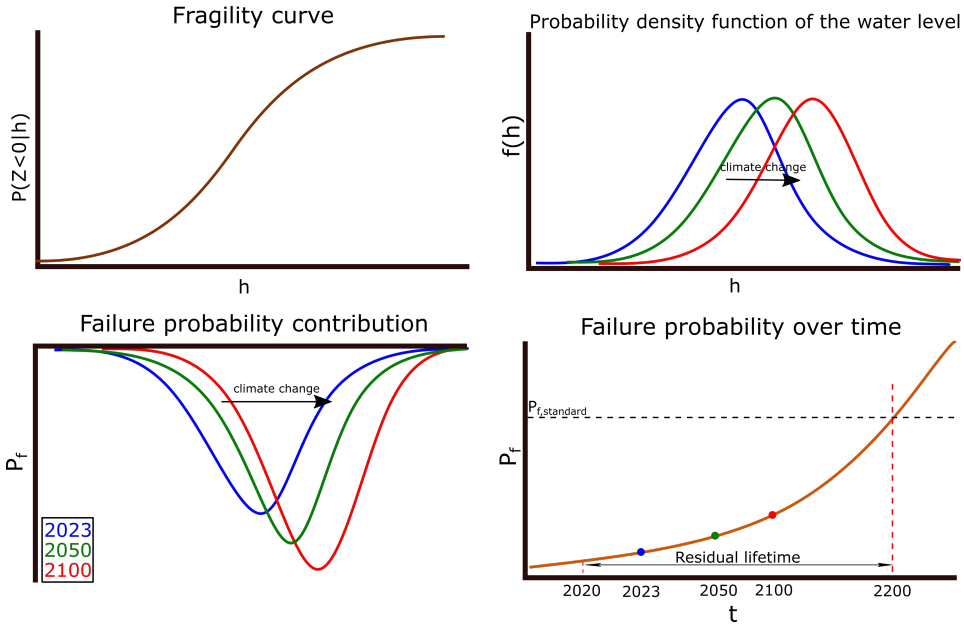

Figure 3.6: From fragility curve to residual lifetime

Figure 3.6 shows four graphs, each showing a part of equation 3.3. The top left graph shows the fragility curve $P_{f,total}|h$ with the water level as the conditional load parameter. At the top right, the probability density function for the water level $f(h)_{ref\ year\ t}$ is given for each reference year. The pdf will change for each of the three reference years. SInce this is a pdf, the area underneath the graph should be equal to 1 for each reference year. In the bottom left, the failure contribution of each water level($P(h)$) is given. This is also done for three reference years. The figure shows the product of the two top

figures. The area underneath each graph is the total failure probability of a dike section for the chosen reference year and climate scenario. This area is also the solution of equation 3.3.

The outcome of equation 3.3 is plotted in the bottom right figure as three coloured dots. Each dot represents one of the three reference years. The line in this figure is created by extrapolating over the three points. This line will be used to calculate the residual lifetime of one dike cross section.

$$P_{f,dike,ref\ year\ t} = \int_{-\infty}^{\infty} \left(P_{f,total}|h \right\} \cdot f(h)_{ref\ year\ t} dh \right) \tag{3.3}$$

In equation 3.3 the four figures in figure 3.6 are combined. $P_{f,total}|h$ is the result of the fragility curve in the top left figure, $f(h)_{ref\ year\ t}$ is the result of the probability density function at water level h. The product of the fragility curve and pdf is given in the bottom left figure. The bottom right figure gives the result of the product of the fragility curve and pdf over the water level which is the same as the area underneath the graphs in the bottom left figure.

3.6. Residual lifetime per cross section

The relation between each of the graphs from figure 3.6 can be described as in figure 3.7. The method is described to be independent of the climate scenario and failure mechanism. This means that the steps in figure 3.6 only calculate one fragility curve. These should therefore be repeated for each failure mechanism, cross-section and climate scenario. In the input, the failure mechanisms and climate scenario are chosen. Figure 3.7 gives an overview of the steps that are taken to calculate the residual lifetime with the help of fragility curves.

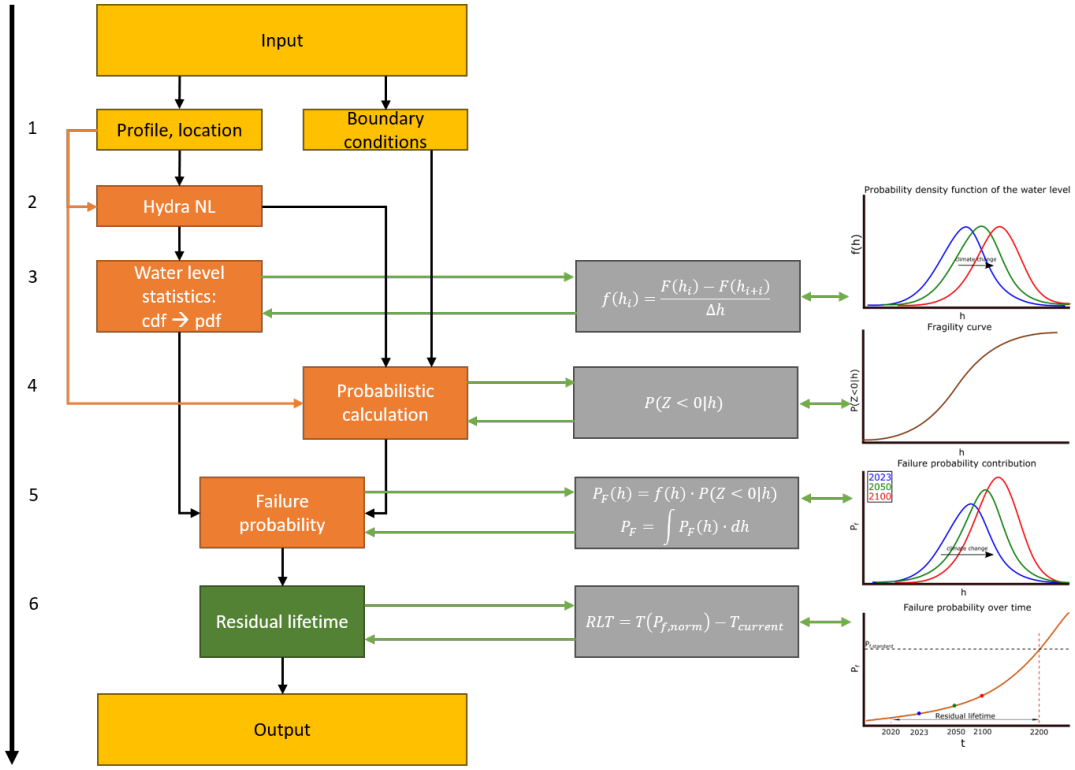

Figure 3.7: Method determining residual lifetime

The input of the model consists of the hydraulic boundary conditions, geotechnical data, dike profiles and location of the dike. This data is obtained by Rijkswaterstaat [28] and the local water authorities [42, 43]. Also, the considered failure mechanism and climate scenario will be selected. In the following steps, these inputs will be used to make the necessary calculations. In step 1, the considered location will be chosen. For this location, the right dike cross section will be chosen with its dimensions and

ground conditions. The data will be used in the following steps. Step 2 and 3 need the location and the hydraulic boundary conditions of the water system. Step 4 needs parameter distributions, limit states, soil conditions and the dike cross section.

Step 2 consists of all the calculations that have to be done in Hydra-NL. The water level frequency line will be calculated for each of the different reference years on the most extreme scenario. The water level frequency line is needed in the next step to obtain the probability density function. Step 3 is needed to change the water level frequency line (which is obtained from Hydra-NL) into the probability density function. With that distribution, it is possible to calculate the failure probability for each given water level when a fragility curve is constructed.

In step 4, the chosen failure mechanisms will be evaluated using fragility curves. For each considered failure mechanism, an individual fragility curve will be constructed. The individual fragility curves can be combined if multiple failure mechanisms are considered.

Step 5 will add the results of step 3 and 4 together. This results in a graph which will show the contribution to the failure probability per water level. Integrating this graph over the water level will give the total failure probability of the dike. This step has to be done for each of the reference years. The total failure probability will be validated against existing models to check the model and the used parameters.

Step 6 is the last step in the method. The outcomes of step 5 are all plotted in a graph that shows the probability of failure over time. For each reference year, the total probability of failure is plotted in one graph. This will result in three points in that graph. These points will be used to extrapolate the data to future years. Whenever this line crosses the bottom value given in the WBI, the year of failure can be found. The time it takes until that year is reached is the residual lifetime.

First, only the failure mechanism wave run-up and overtopping will be calculated. The failure mechanism only has a small amount of distributed parameters, making it easier to understand how the method works. Afterwards, piping will be considered. Next, the fragility curves of each failure mechanism will be combined to create one fragility curve that gives an overview of the total conditional failure probability of that dike cross section. This fragility curve will then be used to get an overview of the overall residual lifetime of the cross section.

In the final step, this method will be used on multiple locations to get an overview over the whole Haringvliet and Hollands Diep.

4

Residual lifetime for wave run-up and overtopping

4.1. Introduction

In this chapter the fragility curve method will be used to calculate the residual lifetime for wave run-up and overtopping. The steps from figure 3.7 will be worked out in separate sections. In the first section the location and associated parameters will be given. Then the water level frequency is calculated in Hydra-NL and changed into the water level probability density function. This is followed by the calculation of the fragility curve, failure contribution and total failure probability. This will eventually give the residual lifetime for wave run-up and overtopping for each location that is included.

4.2. Location and cross section

Before any calculation can be done, a location has to be chosen. Out of the dike profiles and boundary conditions that are made available by Rijkswaterstaat and the waterboards Brabantse Delta and Hollandse Delta, it is possible to find such a location.

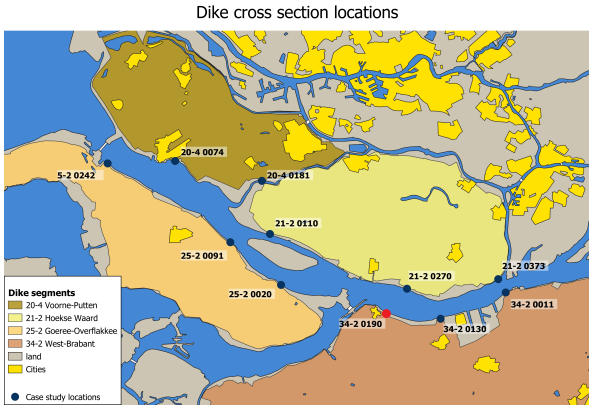

Figure 4.1: Location of profile 34-2 0190 (Willemstad)

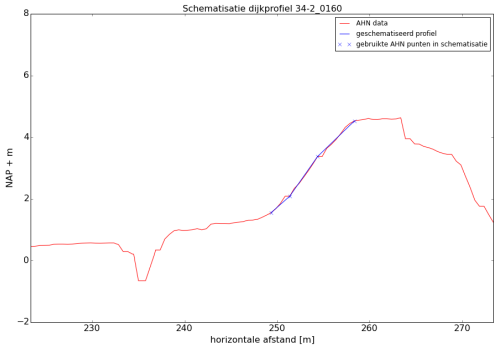

Figure 4.2: Used profile.
Source: Waterschap Brabantse Delta [42]

The first location is chosen from dike stretch 34-2. This stretch lies in the south-eastern part of the study area. Figure 4.1 shows the location as a red dot. The other dots are other locations that will be analysed later. Location 34-2 0190 near Willemstad is chosen due to the absence of any berms or forelands. This makes the calculation much simpler. In Hydra-NL, the location can be found under code '034-02-0190-9-HD-km0995'. Figure 4.2 shows the profile at this location with the left side pointing towards the river. The profile shows the outer slope of the dike. The red line gives the profile according to the AHN

(in Dutch: Actueel Hoogtebestand Nederland). The profile is used to make a schematisation which is used to calculate the slope, berm, berm height and crest. These parameters are used in the limit state of wave run-up/ overtopping.

The location of the dike cross section is needed to calculate the local water level, fetch average water depth, wind directions and wind speed. The dike profile is needed to find the slope, dike height, berm and forelands. Most of these values can be calculated in Hydra-NL or can be found in the data provided by the waterboards.

4.3. Hydra-NL

Hydra-NL is used to calculate the local water level statistics for each of the three reference years: 2023, 2050 and 2100. The boundary conditions needed for those calculations can be freely downloaded from the website of Helpdeskwater [28]. This is a website owned by Rijkswaterstaat where a lot of information is found about hydraulic structures and the used assessment tools. Hydra-NL combines forces like wind direction, wind speed, fetch, river discharge, sea water level and water depth to find the expected water level on a given location. Hydra-NL creates different scenarios, using the forces mentioned above and their probability, to calculate the water level frequency statistic for the given location. Return periods within a range of 1/10 to 1/1,000,000 years are considered [11]. Values above 1/100,000 are less reliable due to a change in the stochastic values used within Hydra-NL.

Within Hydra-NL it is possible to choose the reference years 2023, 2050 and 2100. For those years, the local water level can be calculated using two different climate scenarios: G and W+. All the reference years are selected, together with climate scenario W+. This is the most extreme scenario included in Hydra-NL. After running the program, Hydra-NL will give two output files. The first output is an html file which gives a detailed overview of all needed variables and calculations. The probability for each wind direction can be taken from this file, as well as the wind speed. Furthermore, information about the influence of each of the variables is given. This includes the river discharges of the Rhine and Meuse, The sea water level, the closure of the Europoort barriers, and the wind direction and wind speed. A combination of these variables give the local water level at the chosen location.

The second output is the water frequency line. Hydra-NL exports this information to a text file called: 'hfreq'. The water level frequency line is plotted in Hydra-NL as the water level exceedance function for different return periods. This data is plotted as the complementary cumulative density function: $\overline{F}(x)$. With this information, the probability density function $f(x)$ can be calculated which is needed to calculate the total probability of failure.

Hydra-NL will also be used to find the deterministic parameters needed to solve the limit state for wave run-up and overtopping. For each location the average water depth and the fetch are calculated for each wind direction. These values will be put into the limit state as a deterministic value. The fetch is determined using shapefiles that show the direction of the dike crest. For each wind direction, the length of unobstructed open water is calculated. This is the fetch used for the given wind direction.

4.4. Water level statistics

The output of Hydra-NL is used to obtain the probability density function of the local water level. The output of Hydra-NL is given as $h[m]$ and $ccdf$ in table 4.1. The ccdf is the complementary cdf which is the same as the exceedance probability. The column named pdf gives the probability density function. The corresponding equation for the water level frequency ($F(x)$) is given in equation 4.1,with X being a discrete random variable. In this case the water level.

$$\overline{F}(x_i) = 1 - F(x_i) = P(X \geq x_i) \tag{4.1}$$

$$f(x_i) = P(x_{i-1} \geq x_i \geq x_{i+1}) = P(x_i \geq x_{i-1}) - P(x_i \geq x_{i+1}) = \frac{\overline{F}(x_i) - \overline{F}(x_{i+1})}{\Delta x} \tag{4.2}$$

To get the pdf ($f(x)$), from $\overline{F}(x)$, equation 4.2 is used. The equation is solved for each step within table 4.1. The results are plotted in the same table. It is important to note that the step size between each

step has to be equal. Table 4.1 only shows the values for one reference year. Figure 4.3 shows the difference between the ccdf and pdf.

Table 4.1: Output of Hydra-NL & change to pdf. Reference year: 2023

h [m]	ccdf ($\overline{F}(x)$)	pdf($f(x)$)	h[m]	ccdf ($\overline{F}$(x))	pdf($f(x)$)
2.00	0.19E+00				
2.05	0.13E+00	1.05E+00	2.65	2.89E-04	4.05E-03
2.10	9.68E-02	7.51E-01	2.70	1.84E-04	2.09E-03
2.15	6.50E-02	6.36E-01	2.75	1.25E-04	1.19E-03
2.20	3.80E-02	5.41E-01	2.80	8.86E-05	7.29E-04
2.25	2.36E-02	2.89E-01	2.85	6.46E-05	4.80E-04
2.30	1.46E-02	1.79E-01	2.90	4.80E-05	3.33E-04
2.35	8.95E-03	1.14E-01	2.95	3.60E-05	2.40E-04
2.40	5.40E-03	7.09E-02	3.00	2.72E-05	1.76E-04
2.45	3.23E-03	4.35E-02	3.05	2.07E-05	1.31E-04
2.50	1.84E-03	2.77E-02	3.10	1.57E-05	9.84E-05
2.55	9.54E-04	1.77E-02	3.15	1.20E-05	7.43E-05
2.60	4.92E-04	9.25E-03	3.20	9.20E-06	5.64E-05

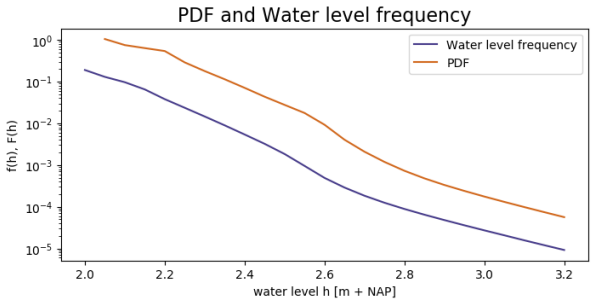

Figure 4.3: pdf and water level frequency from figure 4.1

Hydra-NL only calculates the local water level for return periods between 10 and 1E6 years. This means that a large part of daily water levels are not included in the calculation. Three options are considered: fit the data to a distribution, use the minimum values given in Hydra-NL or use the intended range of Hydra-NL. For the curve fit, a Lognormal distribution will be used. The minimum value of Hydra-NL is 1/10 year and the intended range starts at 1/100 year.

A curve fit is done with the help of python. An existing package (Scipy) is used, which can curve fit the Hydra-NL data to different distributions. This package is widely used in both companies and universities. Figure 4.4 shows the curve fitted data for each reference year (2023, 2050, 2100).

Curve fitting is done in figure 4.4. The figure shows this data for each reference year as a solid line. The water level frequency data is fitted to a Lognormal distribution. The fitted points are given as the dashed lines in figure 4.5. Equation 4.2 is then used to get the local water level distribution (pdf) from the fitted data. This is shown in figure 4.4 as the dotted lines.

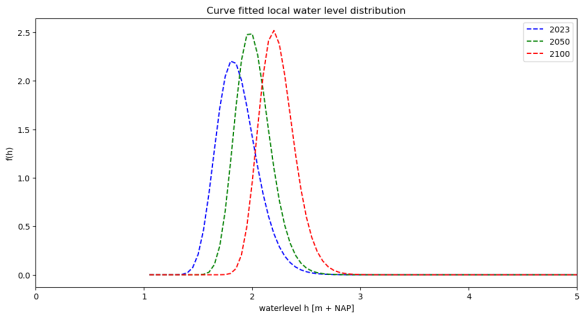

Figure 4.4: Extrapolated pdf for each reference year

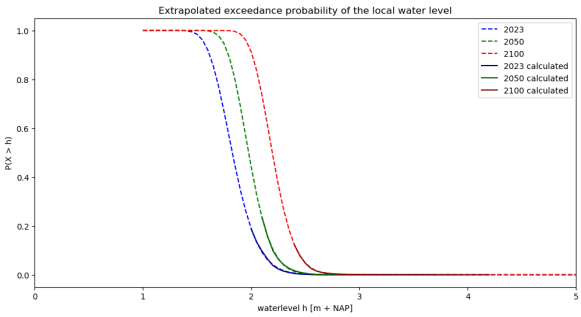

Figure 4.5: curve fitted exceedance probability of the local water level for each reference year using a Lognormal distribution

The curve fitted Lognormal distribution seems to work well for the lower water levels, but does underestimate the exceedance probability of much higher water levels. Instead of extrapolating the curve fit, the water level frequency data from Hydra-NL is extrapolated. Since the excess probability for such high water levels is still very small, it will only have a very small contribution total failure probability. To avoid negative values in the exceedance probability, the extrapolation is done by using the logarithmic values.

For the other two options, a curve fit is not needed. Only the minimum value in data from Hydra-NL has to be changed to 1/10 year or 1/100 year, depending on which data is checked. Each of the options has to be tested. The fitted local water level distribution (pdf) might give too much contribution towards the lower water levels. This is caused by the curve fit only having data for water levels with a return period between 100 and 100,000 year. Figure 4.5 shows how much of the range has to be fitted to a

distribution as a dotted line. The contribution towards the total failure probability of this area has to be checked. This will be done within a sensitivity analysis where the outcome of Hydra-NL and the fragility curve method will be compared.

This completes all the steps towards the water level statistics. The following steps will focus on the development of the fragility curve and the extraction of the failure probability and residual lifetime. The steps above only have to be done once per cross section, since they do not change for other failure mechanisms.

In the following step, the fragility curve will be drafted. This step will change for each failure mechanism, as the limit state will change.

4.5. Fragility curve calculation

With the water level as the conditional load parameter, the following equation has to be solved.

$$P_f(h_i) = P(Z < 0|h_i) \tag{4.3}$$

The right hand side of this equation 4.3 shows the probability of a function, Z being smaller than zero, given a conditional value for the local water level h_i. The Z function is called the limit state function, which can be solved with a reliability analysis. A limit state will always be in the form of: $Z = R - S$ with R the resistance and S the load parameters.

For the failure mechanism wave run-up/overtopping, the limit state function is based on the Van der Meer & Bruce formulas for overtopping [39]. This equation is already given in equation 2.2 in the literature study (Chapter 2).

For each water level in $P(Z \leq 0|h)$ a probabilistic calculation will be performed. Given this conditional water level, the probability of failure is calculated. The first model is done with a Crude Monte Carlo reliability model. A FORM reliability model will be performed afterwards.

At first, the CMC model will only take into account one wind direction. This wind direction is found in Hydra-NL as the most dominant wind direction. This is the north-west. Afterwards it is checked if multiple wind directions have to be included.

In a research conducted by Deltares [6] the main stochastic variables used in the Dutch assessment are described. For different stations around the Netherlands, the wind speed distributions are given. In the calculations in Hydra-NL, the wind speed at airport Schiphol is used. In the Deltares report, both a peak over threshold (POT) and a yearly maxima analysis is done to find the best fitted distribution. In the report, it is found that for the POT analysis an exponential distribution fits the data best. For the yearly maxima analysis a Gumbel distribution works better. Overall the report of Deltares uses the exponential distribution.

The parameters for the exponential distribution are found for each of the 12 wind directions and omni-directional. The difference between the overall wind direction and omni-directional does not give a big change in the overall distribution. Therefore the omni-directional parameters given in the Deltares report [6] will be used in this thesis. This distribution is given by:

$$u_{10} = \text{Exponential}(\lambda = 2.99; u = 16.6))$$

With λ the scale parameter and u the location parameter.

For the chosen wind direction ($315°$ or north-west), the fetch (F) and water depth (z_{avg}) are calculated with Hydra-NL. In the study, only grass dikes are considered. The roughness coefficient (γ_f) for grass is 1 and will be used throughout the whole study. Walls on top of the dike (γ_v) are not considered. The dike crest (h_c), outer slope(α) and dike direction are all provided by data from the waterboards. The value for each parameter for location 34-2 0190 is given in the table below (table 4.2).

The variables above are all deterministic. The only stochastic variable in overtopping calculation is the wind speed (u_{10}).

Table 4.2: Parameters for wave run-up/overtopping limit state for location 034-2 0190

Parameter	Mean	Unit
h_c	4.63	m
α	0.33	rad
$Dike\ direction$	30°	deg
γ_f	1	-
γ_v	1	-
F	4761	m
z_{avg}	-5.11	m
$q_{o,max}$	1	l/m/s

Over a range of water levels with a fixed step size, the failure probability is calculated. The solution for each point is then plotted in the same figure to get a fragility curve. For location '034-02-0190-9-HD-km0995' the result is given in the upper plot of figure 4.6. As mentioned above, only the NW wind direction is used in this calculation.

What is not taken into account is the correlation between the wind speed and water level. This correlation will most probably increase the total probability of failure. High local water levels are partly induced by the wind set-up. Higher wind speed creates a higher set-up and thus a higher water level. This correlation is not included in the calculation because the water level is taken as a conditional value. It can therefore not have a correlation with the stochastic values in the calculation.

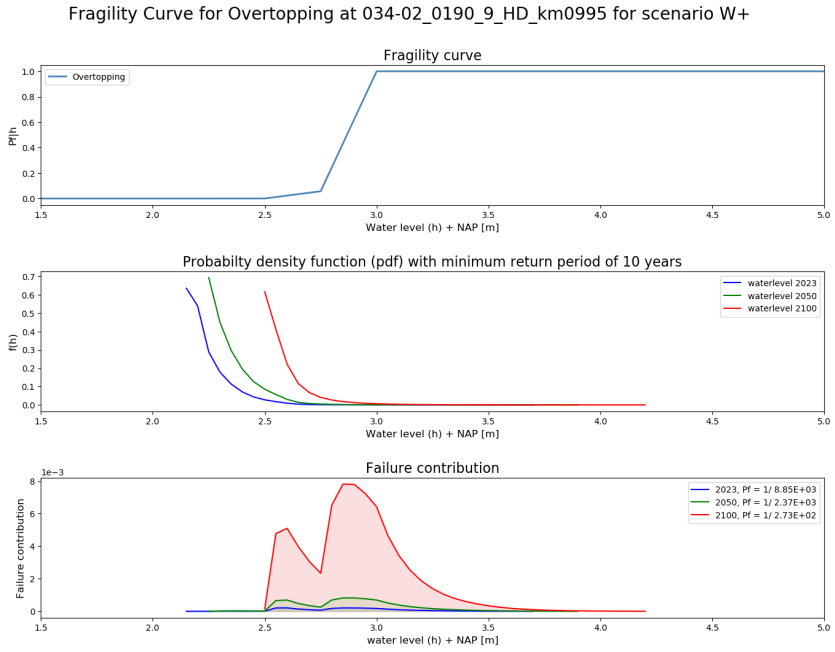

Figure 4.6: Top: Fragility curve CMC with u_{10} = E(2.99;16.6) using the parameters from 4.2 with 1E5 simulations.Middle: The probability density function of the water level. Bottom: The failure contribution

The fragility curve has a shape that is expected [41]: a steep change in failure probability from 0 to 1. The sudden change in the line around a water level of 3.0 meter can be explained by the way water levels above the crest height are modelled. In the Van der Meer and Bruce equation [39], the available freeboard (R_C) cannot be smaller than zero. Whenever this happens, the code assumes the available freeboard to be equal to 0.1 meter. Since at such a high water level, the probability of the dike failing is already very high, this can be done without impacting the failure probability much. Note that for this calculation, no extrapolation of the calculated probability density function is used. This results in the smaller range in the bottom two graphs. In the middle graph (pdf of the water level), the beginning of each line is not the same, because of Hydra-NL using a maximum return period of 10 year. For each reference year, the corresponding water level is different. The water level corresponding to a return period of 10 year increases over time, which is expected for an ever increasing climate influence on

the water level in this area.In the sensitivity analysis (section 4.8), the influence of extrapolating the water level distribution will be investigated. The bottom figure in figure 4.6 shows an unexpected drop in failure contribution at $h \approx 2.75m$. The drop has something to do with the way the fragility curve is extrapolated between two measured points. It is not totally clear why the extrapolation causes this problem. The computation time of a CMC reliability model is long. These will only become longer when multiple wind directions are included. Reducing the computation time is therefore the next point which will be looked at. This is done by implementing a FORM reliability model.

4.5.1. FORM reliability model

In the calculations done with the CMC, the computation time is a problem. CMC requires at least a 100 times the return period $\left({}^{1}/_{P_f}\right)$. This means that for a probability of failure of around ${}^{1}/_{10,000}$, already 1,000,000 calculations are needed per water level. In reality, much smaller failure probabilities are expected.

One solution is to increase the step size, which will reduce the amount of calculations needed. The area between those steps will then be extrapolated to fit the step size used in Hydra-NL ($\Delta h = 0.05m$). Using a step size of $0.25m$ already reduces the amount of probabilistic calculations by a factor five. Unfortunately, for the CMC model this will still cost a considerable amount of time.

This is the main reason to implement a FORM reliability analysis instead of CMC. Multiple open source python packages are available which can be used to make this model. The Python package Openturns [3] is eventually chosen for the modelling of fragility curves. In Openturns, all the variables are given a distribution. Stochastic values are given the corresponding distribution. Deterministic values are given a normal distribution with a very small standard deviation.

Since the computation time for a FORM model is so much shorter, it is possible to look at the added value for multiple wind directions.

Wind directions Hydra-NL gives the probability of occurrence for each wind direction. For different return periods, the wind distribution over 16 directions is given. Appendix J.2 shows the wind distribution as given by Hydra-NL. For 2023 and 2100 the wind direction distribution is given that occurs at a water level that occurs once every 300 year.

The output of Hydra-NL shows that not all wind directions induce any extra failure probability to the dikes. Only directions that contribute to the failure probability are included. Those directions are: W, WNW, NW and NNW. For each of those directions, the fetch (F), average water depth (d) and probability of this wind direction occurring (p) are taken from Hydra-NL. Table 4.3 shows the used values for each wind direction.

Table 4.3: Used parameters per wind direction

	W	WNW	NW	NNW
p [%]	13.7	28.9	35	18.5
F [m]	2219	3814	4734	4761
d [m]	0.61	0.78	-7.13	-6.12

For each direction, a separate fragility curve is computed. Afterwards, these curves are put together, using the equation 4.4. Hence that the sum of all the curves is taken instead of the multiplications. Each direction can independently force failure. The probabilities in the table are adjusted in the code to sum up to 1. Figure 4.7 shows the combined fragility curve, with the dark blue line being the sum of the four individual fragility curves. The combined fragility curve can subsequently be used to find the total failure probability for each reference year. The figure shows the outcome for scenario W+ on location 34-2 0190.

$$FC_{total} = \sum_{i \to 0}^{i=n} \left(FC_i \cdot p_i\right) \tag{4.4}$$

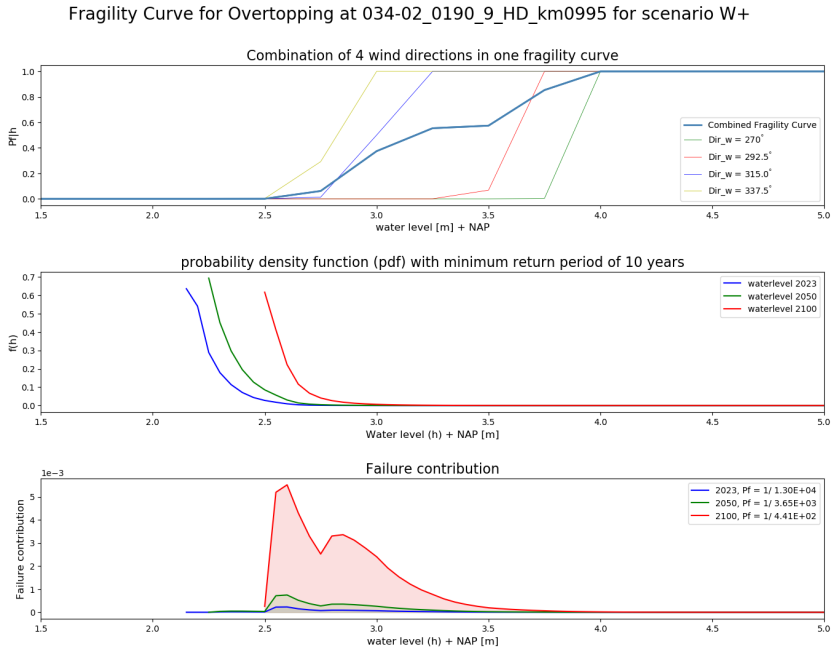

Figure 4.7: Combination of multiple wind directions in one fragility curve with omni directional wind u_{10} = E($\lambda = 2.99; u = 16.6$)

The total failure probability is reduced when multiple directions are added. For the first calculation, only the wind direction that is responsible for most of the water levels return period is taken into account. Taking into account multiple wind directions should put the model closer to reality. However, the spread in wind direction fluctuates a lot between each calculated return period. Taking into account these fluctuations makes it difficult to choose one distribution that accurately gives the wind direction distribution over the whole range of return periods. The added value does not way up against the added complexity to the system. The choice is therefore made to keep the calculation to the most dominant wind direction only.

Table 4.4: Total failure probability for scenario W+ at location 34-2 0190

	Failure probability [P_f]	
	Dominant wind	Multiple wind directions
2023	1/8.83E3	1/1.31E4
2050	1/2.37E3	1/3.66E3
2100	1/2.73E2	1/4.41E2

Table 4.4 shows the difference in failure probability between multiple wind directions or only the dominant wind direction. The difference between the two is rather small. The expected decrease in failure probability is also found in the table. More wind directions decreases the total failure probability of a dike when compared with only taking into account the most dominant wind direction.

The objective of this thesis is to get an overall view of the area. The extra wind directions do not add much to the total failure probability and are therefore not necessary. Only the wind direction that gives the highest failure probability will therefore be used in the rest of the research. For the given location that wind direction is north-west (NW). The model will therefore calculate a worse scenario than in reality will happen.

In the validation, it will be checked whether it is better to use the wind speed distribution for the dominant direction or use the omni directional wind direction. For this location, a distinction is made between the north west and the omni directional wind speed. Both distributions can be found in the Deltares report [6] and are given as:

$$u_{10,NW} = \text{Exponential}(\lambda = 1.86; u = 14.8)$$
$$u_{10,omni} = \text{Exponential}(\lambda = 2.99; u = 16.6)$$

With $u_{10,NW}$ the north-western wind speed distribution and $u_{10,OMNI}$ the omnidirectional wind speed distribution.

For each location, the governing wind direction has to be found. For now, this is done with the help of the hydraulic load level calculations in Hydra-NL. Within the output of that calculation, an overview is given of the contribution of each wind direction on the total failure probability. The wind direction with the highest contribution should be used for the fragility curve calculation. Table 5.5 in Appendix A shows the used directions for each of the different locations that will be assessed throughout the thesis.

4.6. Failure contribution and total failure probability calculation

With both $P(Z \leq 0|h)$ and $f(h)$ known, it is now possible to calculate the failure probability contribution for each conditional water level. This can be done with equation 4.5. For each h in range, the failure probability contribution can be calculated and plotted. This is done in the lower plot of figure 4.6.

$$P_F(h) = f(h) \cdot P(Z < 0|h) \tag{4.5}$$

The probability of failure for each reference year can be calculated by integrating the area underneath the graph. This is done with a function in Python, which calculates the area underneath the graph using numerical approximation. This tool is called simps and is part of the scipy package in Python.

Simps uses a numerical quadratic approximation and is therefore fourth order accurate. It divides the area underneath the line in s of which it calculates the area. Each individual column will then be added together to get an approximation of the total area underneath the line. This will give the total probability of failure per reference year. In the legend of figure 4.6 the failure probabilities for each reference year is given.

4.7. Residual lifetime calculation

The final step is to calculate the residual lifetime of the dikes cross section by extrapolating the failure probabilities over time. The total failure probability per reference year is then plotted in one figure, as can be seen by the red dots in figure 4.8. The dots are used to extrapolate the probability of failure over time. This gives the blue line. The dotted black line shows the bottom value for this stretch. It has to be noted that the extrapolated line will be very inaccurate for years that lie further in the future than 2100, mainly since it is not clearly known how climate change will impact the study area after 2100. An exponential increase is expected.

However, it is also possible that climate influence will flatten out in the future. This is mainly dependent on what happens in the coming 50 years. It is therefore difficult to already make predictions for climate change that lie so far in the future. It is therefore hard to get accurate results for the residual lifetime that is longer than 80 to 100 years. Still the choice is made to extrapolate the data to 2150. This is done to show dike sections that fail just after 2100. The extrapolation is done parabolic instead of exponentially. An exponential extrapolation gave a too fast increase in the failure probability when the failure probability increases to 1 far before the last reference year (2100). A parabolic extrapolation, in most cases, seemed to give a much better answer. It sometimes gave problems the more moderate G scenario, where the extrapolation gave a decreasing failure probability in the future. In those cases a linear extrapolation was taken. A linear extrapolation reduces the residual lifetime but gives a result that can happen in practice instead of a result that gives a reduced failure probability in the future.

4.8. Sensitivity analysis of the fragility curve method

To be sure that the results are as close as possible to the correct answer, it is necessary to analyse the results of the steps described above. The main issue is that the range of the water level frequency statistic only takes into account frequencies between 1/10 and 1/100,000 year. For location 34-2 0190, this range accounts for approximately 20 % of the total probability, which can also be seen in table 4.1. It has to be checked if the calculated range for the water level frequency is large enough or that the range has to be enlarged. This is done by checking if the largest part of the failure contribution is taken

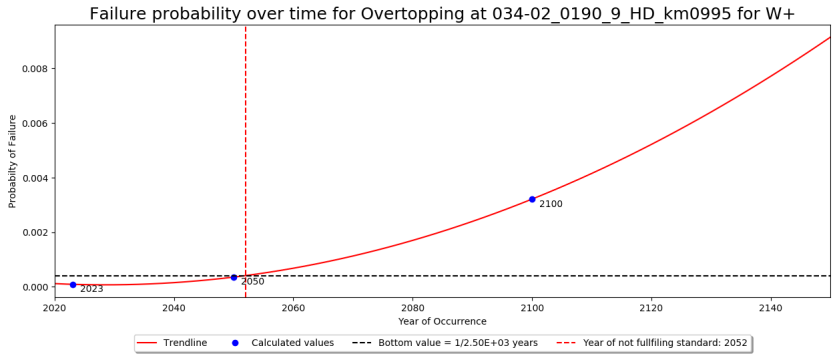

Figure 4.8: Residual lifetime calculation for location 34-2 0190 for scenario W+

into account. The enlarged range can be calculated by fitting a distribution on the known data and use this distribution to extrapolate the data.

The added value of extrapolating the data will also be checked. There are three different settings that will be compared. The extrapolated water level frequency will be compared with the water level frequency where a lower limit is introduced for the return period. This limit is set on a water level with a probability of occurring once every 10 or 100 year, which is equal to a return period of 10 or 100 years. These limits are chosen in consultation with experts in water safety.

The three different settings will be used to calculate the total failure probability of dike cross section 34-2 0190. The outcomes are compared with each other, as well as with a reference value that is calculated with Hydra-NL. In Hydra-NL, the failure probability for overtopping is calculated using the Hydraulic load level. The calculation is done with the option to include uncertainties. This is done to take into account the uncertainty in the calculations for the water level, wave height and wave period in Hydra-NL.

In figure 4.9 the result for the three different settings are plotted using the omni-directional wind speed.The top graph shows the full range, The middle figure has a limit of 1/10 year for the water level frequency and the bottom graph shows the results when a 1/100 years limit is used.The corresponding failure probabilities are given in the legend as well as in table 4.6 for each reference year. The table also gives the results for the moderate scenario (G). Table 4.5 includes the Hydra-NL reference calculation for the hydraulic load level. The same omni-directional wind speed is used here.

For both scenarios there is no substantial difference between each of the three return periods. The curve fitted data does not add much towards the total failure probability. This becomes clear when the top graph of the figure is analysed. On both sides of the bell shape, the contribution is close to zero, meaning that no extra failure probability is added at those places. The main difference between the bottom two graphs is that in the lowest graph, parts of the bell shape are cut off. A part of the failure contribution is therefore not taken into account. Note that the probability of failure in table 4.5 and 4.6 are given as the return period, which is equal to: $^1/_{P_f}$. A bigger return period gives a smaller probability of failure.

Table 4.5: Difference between the three water statistic methods using a Form analysis and using omni directional wind $u_{10} = E(2.99; 16.6)$

034-02_0190		**Water level statistic method using** $u_{10} = E(2.99; 16.6)$			
Scenario	Reference year	Full range$[1/P_F]$	1/10 year maximum $[1/P_F]$	1/100 year maximum $[1/P_F]$	Hydra-NL calculation $[1/P_F]$
W+	2023	1.09E+04	1.09E+04	1.10E+04	2.36E+03
	2050	2.82E+03	2.82E+03	2.84E+03	1.78E+03
	2100	3.09E+02	3.12E+02	3.22E+02	1.03E+03
G	2023	1.05E+03	1.05E+04	1.05E+04	2.13E+03
	2050	6.63E+03	6.68E+03	6.65E+03	1.91E+03
	2100	2.77E+03	2.79E+03	2.79E+03	1.54E+03

Table 4.6 below shows the same results but with the directional wind speed ($u_{10} = E(1.86; 14.8)$) for

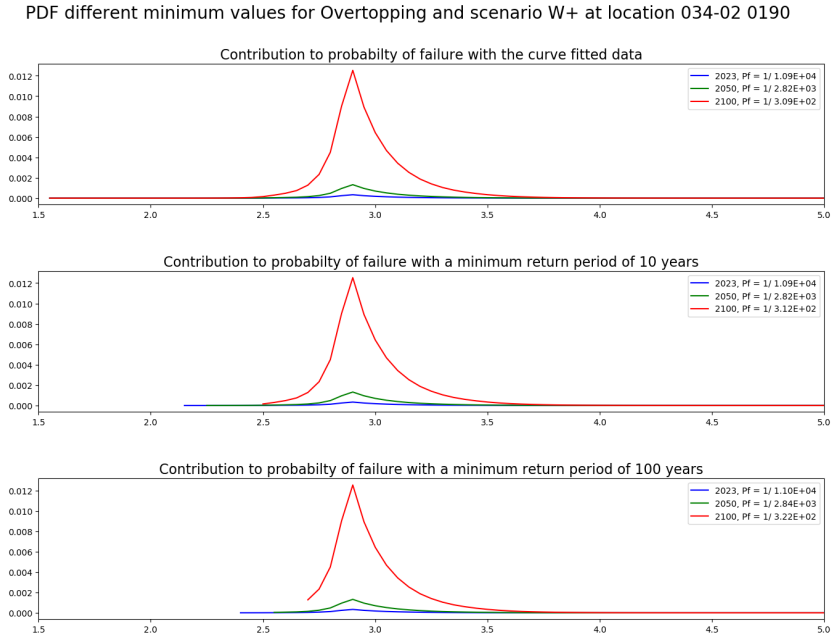

Figure 4.9: PDF analysis for location 34-2 0190 and scenario W+ with $u_{10} = E(2.99; 16.6)$

the north-western direction.

Table 4.6: Difference between the three water statistic methods using a Form analysis and using north-western wind speed: $u_{10} = E(1.86; 14.8)$

034-02_0190		**Water level statistic method using** $u_{10} = E(1.86; 14.8)$			
Scenario	Reference year	Full range$[1/P_F]$	1/10 year maximum $[1/P_F]$	1/100 year maximum $[1/P_F]$	Hydra-NL calculation $[1/P_F]$
W+	2023	3.72E+04	3.73E+04	3.78E+04	2.36E3
	2050	9.90E+03	9.94E+03	1.02E+04	1.78E3
	2100	1.16E+03	1.17E+03	1.21E+03	1.03E3
G	2023	3.55E+04	3.56E+04	3.61E+04	2.13E3
	2050	2.28E+04	2.28E+04	2.33E+04	1.91E3
	2100	9.78E+03	9.80E+03	1.01E+04	1.54E3

The calculated total failure probability for each reference year needs to be analysed before any conclusion can be drawn from this calculation. As is stated in the text and tables above, this is done with Hydra-NL. This is done with the hydraulic load level (HBN) calculation in this model.

The answers given by Hydra-NL are compared with the failure probabilities in table 4.5 and 4.6. The last column in both table 4.6 & 4.5 shows the probability of failure calculated with Hydra-NL using the hydraulic load computation for each scenario and reference year with a set critical discharge of $q_{o,max} = 1\ l/m/s$. The outcome is compared with the outcome of the fragility curve method that is used in the thesis.

What becomes clear from this comparison is that the outcome of the Hydra-NL calculation lies much closer to the calculation with the omni directional wind speed than for the north-western wind speed. This is expected since the omni directional wind speed includes the probability of the different wind directions and their corresponding wind speed distributions. This is not the case when only the dominant wind direction is included. Taking those two points together makes it clear that the omni-directional wind speed distribution should give a much better answer.

For the local water level distribution, there is not much difference between the three used methods (curve fit, 1/10 year minimum and 1/100 year minimum). The curve fitted data does give slightly smaller return periods and thus a bigger probability of failure. But it has more uncertainty due to the curve fit. Between 1/10 years and 1/100 years there is almost no noticeable difference. In figure 4.9 it is clearly

visible that a part of the bell shaped graph is cut off when looking at a minimum value of 1/100. The choice is therefore made to continue the calculations with a minimum value of 1/10 years.

The probability of failure, calculated by the fragility curve with a FORM reliability analysis, is used to find the residual lifetime. The results of this calculation are given in figure 4.10. The bottom value is shown as a black dotted line and is set at $1/2500$ year. The red dotted vertical line shows whenever the probability of failure crosses the bottom value. In this case, the dike failure probability already crosses the maximum allowable failure probability for this location in 2052, which is much faster than anticipated.

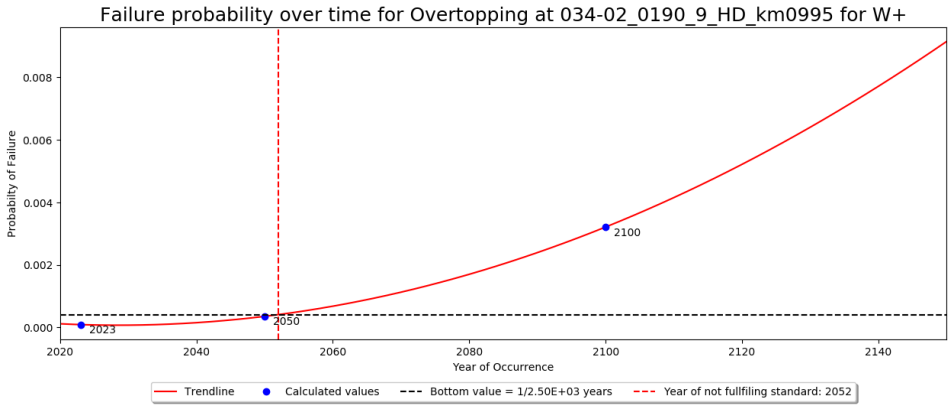

Figure 4.10: Residual lifetime calculation for wave run-up and overtopping using fragility curves for one dike section using climate scenario W+

Figure 4.10 shows the residual lifetime for scenario W+. The same is also done for the more moderate scenario G. This result is given in figure 4.11.

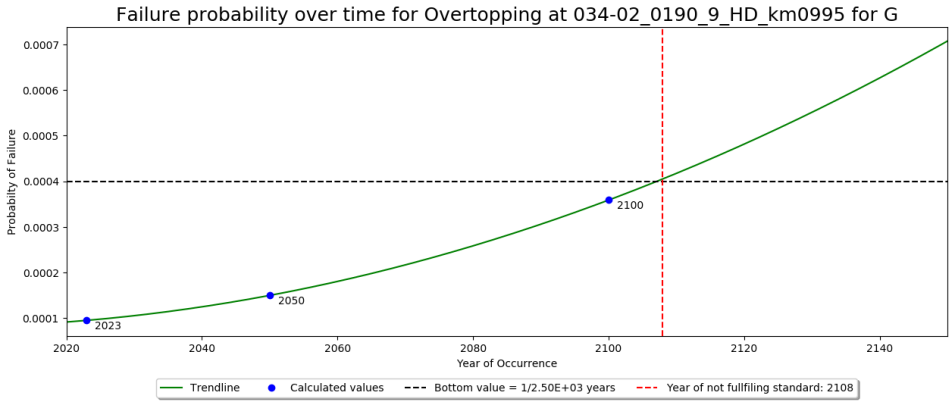

Figure 4.11: Residual lifetime calculation for wave run-up and overtopping using fragility curves for one dike section using climate scenario G

4.8.1. Importance Factors and Errors

In the probabilistic calculation for wave run-up and overtopping, the wind speed is the only stochastic value. The other parameters are all deterministic. This means that the wind speed should have the biggest influence on the failure probability. All the deterministic parameters ($h_c, F, \alpha, q_{o,max}, g$, wind and dike direction and the dike dimensions) are put into Openturns as a normal distribution with very small standard deviations. This means that these parameters can only have a very small contribution and thus have a small importance factor.

Figure 4.12 shows the importance factors of the probabilistic calculation for six different water levels that are within the range of the calculation. For each water level it is clearly visible that the wind speed is the only important factor.

The errors are put on a maximum value of $10E-6$. This value is chosen by doing multiple runs with different errors. Increase of the maximum value gave a clear change in failure probability, while a decrease did not change the probability.

In some of the graphs in figure 4.13, the error stays above the set maximum. This has to be further investigated to see how much influence this has on the correctness of the fragility curve.

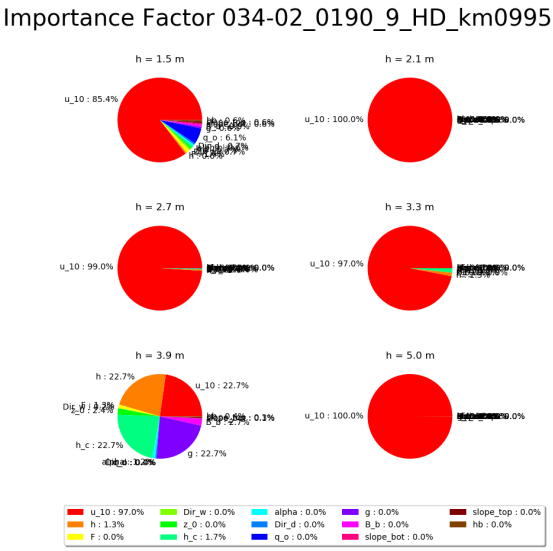

Figure 4.12: wave overtopping Importance factors for 034-2 0190

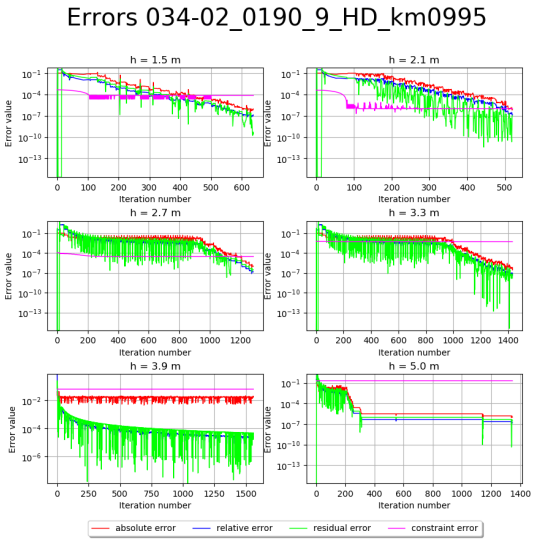

Figure 4.13: Wave overtopping Errors for 034-2 0190

4.9. Results

The probability density function can be calculated for different scenarios. These can be used to create the bandwidth in which the rise in failure probability is expected. The fragility curve itself does not change with different scenarios. Figure 4.14 shows this bandwidth. The red line shows the calculated change in failure probability for the moderate (G) scenario, while the green line shows the more extreme (W+) scenario. The bottom value is set at $1/2500$ year which is used for the assessment of a dike section.

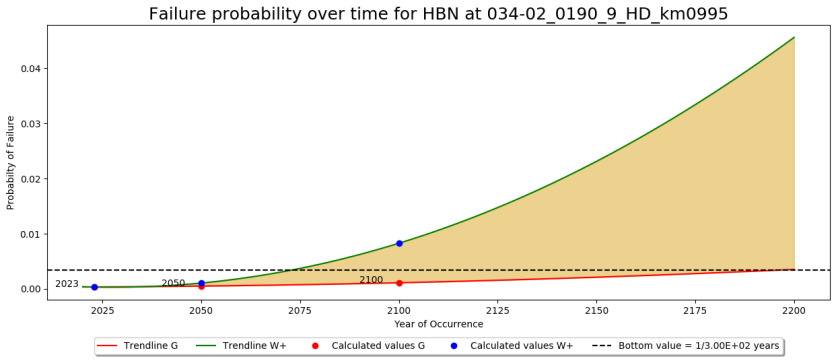

Figure 4.14: Residual lifetime bandwidth G to W+ on stretch level

Figure 4.14 shows change in failure probability for both scenarios. The residual lifetime is found whenever the black dotted line is reached. It is clearly visible that this line is crossed between 2050 and 2200, dependent on which climate scenario does happen. This outcome is not really as expected. The dikes were reinforced just before the construction of the Haringvliet Dam. This was done to withstand water levels driven by the sea without dampening from this dam. Making the dikes much higher, and thus stronger against overtopping. Also, the safety standard used for the whole dike stretch is used in this

calculation. When only looking at one dike cross-section or a dike section, the allowed bottom value is much smaller than the 1/300 years used here. Table 2.2 in the literature study shows the bottom values for a dike section. The result is shown in figure 4.15. The residual life time seems to be very small here. The residual lifetime is less than 30 years for both scenario W+, since the bottom value is met before 2050. Scenario G gives a much bigger residual lifetime of around 90 years

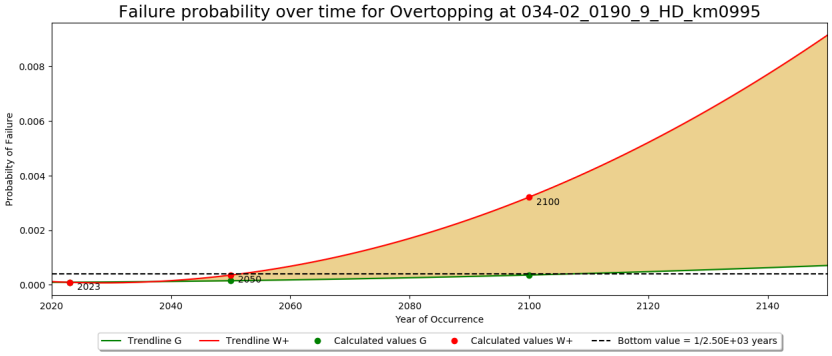

Figure 4.15: Residual lifetime bandwidth G to W+ at section level

For the eleven locations that are given in figure 4.1, the residual lifetime is calculated. The parameters that are used for each location are given in table /reftab: Used parameters AHN.

Table 4.7: Used parameter per location for the overtopping calculations

Location	**20-4**		**21-2**			**25-2**			**34-2**		
	0074	**0181**	**0110**	**0270**	**0373**	**0020**	**0091**	**0242**	**0011**	**0130**	**0190**
$h_c[m]$	4.36	4.13	4.87	4.9	5.78	5.2	5.68	5.63	6.2	4.86	4.63
$z_0[m]$	-9.72	-2.92	-10.16	-3.97	-1.95	-7.42	-6.1	-6.2	-4.95	-5.11	-6.11
F [m]	3955	3582	5319	5583	4043	5542	4358	1560	3721	6263	4761
Dike normal [°]	169	207	198	201	143	42	36	20	329.6	358.5	30.9
Wind direction [°]	247.5	247.5	270	270	225	315	315	337.5	292.5	315	337.5
$\alpha[-]$	0.24	0.33	0.36	0.27	0.33	0.25	0.36	0.42	0.29	0.38	0.33
$B_b[m]$	11.15	4.62	-	-	-	-	9.03	-	4.11	-	-
$H_b[m]$	1.92	2.09	-	-	-	-	3.21	-	2.67	-	-
$u_{10}[m/s]$	**Omni directional wind speed Exponential (2.99; 16.6)**										

With h_c: the crest level[m], z_0: the average water depth [m], F: the fetch [m], α: the average dike slope, B_b: the width of the berm [m], H_b: the average height of the berm [m]. Using these parameters the following results are found and given in table 4.8. A 0 means that the residual lifetime is negative, meaning that the bottom value of that dike section is already reached. This does not mean that the dike section can fail any second. It means that the failure probability of that dike section is lower than the bottom value given in the WBI. A →, shows when the location has a residual lifetime that exceeds the range of the calculation.

Table 4.8: Residual lifetime for each location for overtopping

		Hellevoetsluis	Spui				Den Bommel			Moerdijk	Noordschans	Willemstad
Location		**20-4**		**21-2**			**25-2**			**34-2**		
		0074	**0181**	**0110**	**0270**	**0373**	**0020**	**0091**	**0242**	**0011**	**0130**	**0190**
Overtopping	G	→	40	→	→	→	→	→	→	→	56	88
	W+	56	23	→	130	→	→	→	→	→	25	32

Looking at table 4.8 in comparison with the parameters (4.7) on each location, it becomes clear that the dike height (h_c) has the biggest influence on the safety of the dike. The highest dikes are located along

dike stretch 25-2 and at location 34-2 0011 and 21-2 0373. These are also the locations that have a residual lifetime beyond 2150 (Which is the set upper limit in the residual lifetime calculation).

The locations that have a residual lifetime before the upper limit are of more interest. Location 20-04 0180, 34-2 0130 and 0190 all have small residual lifetimes, as can be seen in table 4.8. Locations 20-4 0074 and 21-2 0270 have a much bigger residual lifetime. Both of those locations only have a value for the more extreme W+ scenario. This means that the residual lifetime for scenario G falls outside the used range in the model.

For each location the total failure probability for each reference year is also compared to the outcome of Hydra-NL. The results are given as the ratio of the Hydra-NL calculation divided by the outcome of the fragility curve calculation. A ratio close to one is preferred. When the ratio is smaller than 1, the fragility curve method makes an overestimation of the total failure probability which results in an underestimation of the residual lifetime. The real residual lifetime is longer. When the ratio is bigger than 1, the failure probability is underestimated which results in a residual lifetime that is bigger than it is in reality. Smaller ratios are therefore a bit more dangerous since the real failure probability is bigger than calculated.

Figure 4.16 shows the outcome of this analysis. In the figure, the ratio between Hydra-NL and the fragility curve method is shown as a green or red dot for climate scenario G or W+ for each reference year. The red line shows where the ratio is 1.

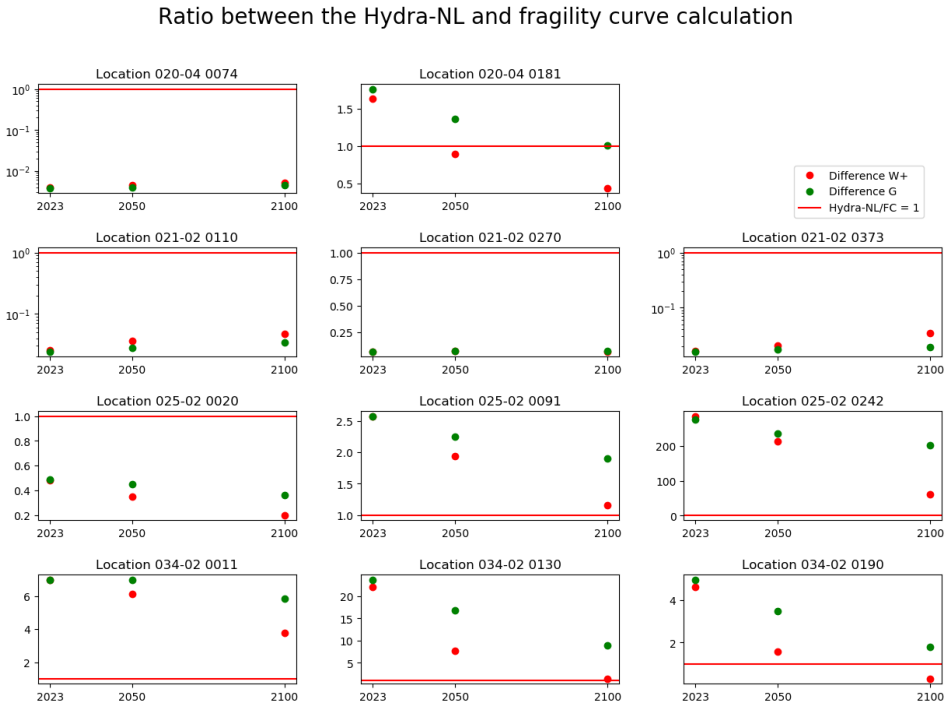

Figure 4.16: Sensitivity analysis of Hydra-NL results against the Fragility curve calculation

What becomes clear from the figure is that the calculations for dike stretches 20-4 and 21-2 do underestimate the failure probability, while the southern dike stretches 25-2 and 34-2 have a tendency to give an overestimation. It is not totally clear why there is such a clear difference between the northern dikes and the southern dikes. One explanation can be that the wave height and obliqueness coefficient in the limit state is overestimated. The northern dikes are sheltered much more from the more dominant wind directions. Together with wave obliqueness the waves should lose a lot of energy which reduces the total height of the dike and thus the failure probability. The wave angle β for most dikes at the northern shore lie close to the maximum wave angle that has any effect on the dikes [16]. One exception is the dike cross section at 20-4 0181. This section lies at the Spui river and should be affected even less by the waves and the wind speed. the method gives a better estimation when wind action is smaller.

For the southern stretches (25-2 and 34-2) the opposite is true. Here an underestimation of the failure probability is found for most cases. The real residual lifetime is smaller than calculated with fragility curves. This is mainly a problem for locations 25-2 0242 and 34-2 0130 where the difference between the methods is substantial. Both of these dike cross sections have somewhat the same surroundings, both lying on a protruding piece of land. How and if this causes the difference between Hydra-NL and the fragility curve is unknown.

Most likely it has something to do with how the wind direction and wind speed that is used in both Bretschneider and Swan. Swan uses a 2D model where the waves can change direction towards the dike. This will cause an increase as well as a decrease in wave height (typically an increase is found). This can be a cause of the higher waves at the southern shores.

4.10. Conclusion

For wave run-up and overtopping, the fragility curve method does give a good overall view of residual lifetime. Most of the analysed locations have residual lifetime that falls outside the calculated range. Which means that for those dikes the residual lifetime is longer than 130 year. The smallest residual lifetime is mostly found by dikes with lower crest heights. This is as expected since these locations have a smaller available freeboard which greatly influences the resistance against wave run-up and overtopping.

5

Residual lifetime for piping

In this chapter the fragility curve method will be applied on the failure mechanisms piping. The same steps have to be done as in the previous chapter. Starting with the limit state function for piping and the location that will be used for piping.

5.1. Limit state function

The limit state for piping consists of the three sub mechanisms uplift, heave and backward erosion as is described in the literature study (section 2.5.2). For each sub mechanism a separate fragility curve is constructed. The fragility curve with the smallest failure probability will then be used in the rest of the calculation.

5.2. Location

For piping, another location will be used than in the previous chapter. The dike cross section that is chosen for piping is location 20-2 0110 and lies at the north side of the Haringvliet. Figure 5.1 shows the exact location as a red dot. The location is different from the previous chapter. At the first location, the influence of piping can almost be neglected. This makes it difficult for that location to be used as an example for the used method. Therefore location 20-2 0110 is used.

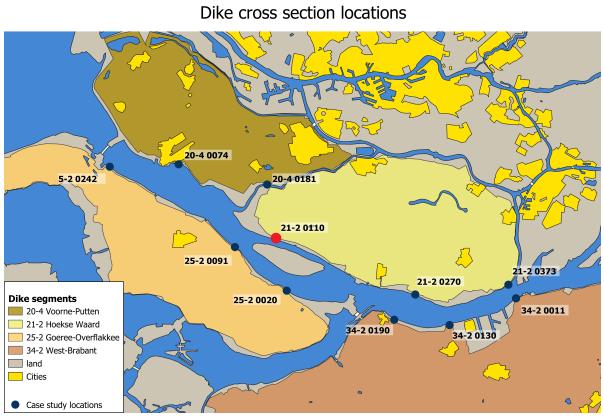

Figure 5.1: Piping Location 21-02 0110

5.3. Parameters

Piping needs a lot more parameters than wave run-up/overtopping. The distributions that are used are given in table 5.1. Together with the local water level distribution, the residual lifetime can be calculated.

Table 5.1: Distributions of the parameters for the piping limit state at location 021-02 0110

	Distribution	Mean [μ]	σ	$V = \mu/\sigma$	Location
Θ	-	$37°$	-	-	-
η	-	0.25	-	-	-
ν	-	$1.33E-06$	-	-	-
λ	Lognormal	0.7	0.1	-	-
$i_{c,h}$	-	0.3	-	-	-
h_p	Normal	-0.3	0.1	-	-
d_{70}	Lognormal	$1.45E-04$	-	0.12	-
d_{70m}	-	$2.08E-4$	-	-	-
k	Lognormal	$3.47E-04$	-	- 0.5	-
D	Lognormal	3	0.5	-	-
d	Lognormal	1.5	0.5	-	-
γ_s'	Lognormal	16.19	-	scale = 1	10
γ_w	Normal	10	0.1	-	-
L	Lognormal	70	0.1	-	-

5.3.1. Sources

The main source of finding the piping parameters are the waterboards. For dike stretch 20-4 and 34-2, a lot of information is available near each dike cross section. The data is available from the SOS (Stochastic Subsoil Schematization) and the Dutch assessment tools [8]. The SOS can be viewed in the computer program DSOIL-Model or Riskeer and consists of sub soil data which is mentioned before. In the SOS, each dike section has multiple sub soil scenarios. From these scenarios. The scenario is chosen that has the biggest failure probability. This scenario is found by mainly looking at the cover layer (d). The scenario with the smallest cover layer is chosen and used to find the needed parameters.

Note that the SOS data that is used here is not yet detailed enough to comply with the Dutch assessment. The more detailed schematization is done by the waterboard that maintains the dike stretch. For dike stretch 34-2 this data is available and used in the fragility curve calculation. For the other dike stretches this was not possible. Dike stretches 25-2 and 21-2 are currently assessed in accordance with the WBI2017, but are not yet completed. The assessment for stretch 20-4 is completed, but did not use the SOS. A detailed soil investigation was already conducted for this dike stretch [21]. That investigation is compared to the SOS with overlapping results. Since there is a large overlap, the SOS data will be used in 20-4 as well.

Summarized: For 34-2 the sub soil parameters are provided by the waterboard in their detailed soil schematisation. For the other stretches, the more general SOS is used. The distribution for each of the stochastic values given above can be found in the same way, with the exception of d_{70m}, γ_w and the deterministic parameters Θ, η, ν & d_{70m}. The leakage length L is provided for stretches 34-2 and 20-4 by the waterboards. For 21-2 and 25-2, the leakage length is measured using the AHN (Current Dutch national digital terrain model or Actueel Hoogte bestand in dutch). This data can be viewed in the AHN viewer [12]. The leakage length can be calculated using this viewer. The foreshore will be included in the leakage length.

γ_w Is assumed to be equal to the density of freshwater. The Haringvliet and Hollands Diep is mainly fresh water, which makes this assumption valid. Therefore $\gamma_w = 10.0\ kN/m^3$. For Θ, η, ν & d_{70m} the schematization manual for piping is used [27]. The manual provides standardized values for those parameters. These values will be used for all calculations with respect to piping.

5.4. Water level statistics

5.4.1. Minimum value for the return period

For piping it is also important to look at the different minimum return periods that can be used in the water level statistics. A choice has to be made between not adding a minimum value, have a minimum of 1/10 years or have a minimum of 1/100 years. Figure 5.2 shows the same three options as in the

previous chapter: Use the full range/ curve fit, a minimum return period of 10 years or a minimum return period of 100 years. The differences between each of the options are also given in table 5.2. The table also gives the result for scenario G.

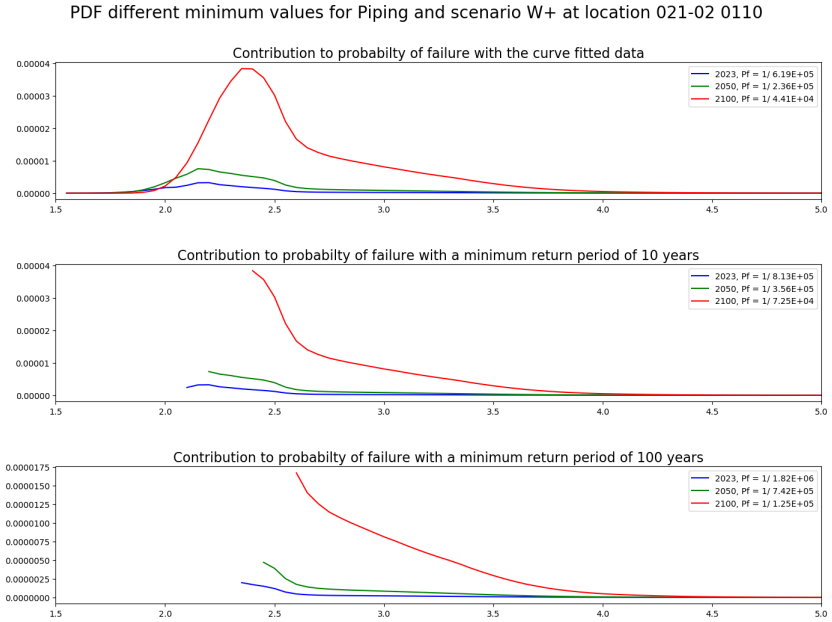

Figure 5.2: Piping sensitivity analysis for the water level distribution

In this case, the choice is also made to go for the water level statistics that have a minimum return period of 10 year ($P_f < 0.1$). Taking into account the whole range (as given in the upper figure of figure 5.2) gives a rather big failure contribution for the lower water levels.

For each reference year in figure 5.2, the failure probability mostly consists of the contribution of relatively low water levels. This is not as expected, since water levels of around 2m + NAP have happened already in the study area without any failure happening. It is highly unlikely that these water levels have such a big impact on the total failure probability of the dike on piping.

The reasoning is therefore made to not take into account the lower water levels and thus the bigger return periods,as is done for overtopping. The next step is to look at the differences between the bottom graphs in figure 5.2 which are also shown in table 5.2. Here as well, the result for scenario G is given.

Table 5.2: Total failure probability when using the three different settings for the water level frequency lines. The integrated total failure probability of the product of the fragility curve and water level pdf is calculated and compared

021-02 0110		Minimum return period [yr]		
Scenario	Reference year	Curve fit	1/10 year	1/100 year
W+	2023	6.19E+05	8.13E+05	1.82E+06
	2050	2.36E+05	3.56E+05	7.42E+05
	2100	4.41E+04	7.25E+04	1.25E+05
G	2023	5.57E+05	8.29E+05	1.72E+06
	2050	4.29E+05	6.12E+05	1.18E+06
	2100	2.08E+05	3.74E+05	7.16E+05

There is only a small difference between each of the three methods. The change in failure probability between the methods can be explained. A high bottom value for the return period will give a smaller failure probability than a lower value or no value. This is noticeable in the table as well where, for each scenario and reference year, the failure probability is biggest for the curve fitted data. However, since it is already stated that it is unlikely that the failure contributions for 'low' water levels are accurate, the

choice is made not to use the curve fitted water level statistics, but the values with a minimum return period of 10 years.

5.5. Fragility curve, failure probability and residual lifetime

5.5.1. Failure probability contribution

The failure contribution is found by finding the product of the combined fragility curve and the probability density function for each water level within the range of possible water levels, as is also done in the previous chapter. Figure 5.3 shows the fragility curve for each sub mechanism and the combined outcome. The combined fragility curve is then used in the calculations towards the residual lifetime with respect to piping. Figure 5.4 shows the fragility curve, pdf and failure contribution, which are used to calculate the residual lifetime.

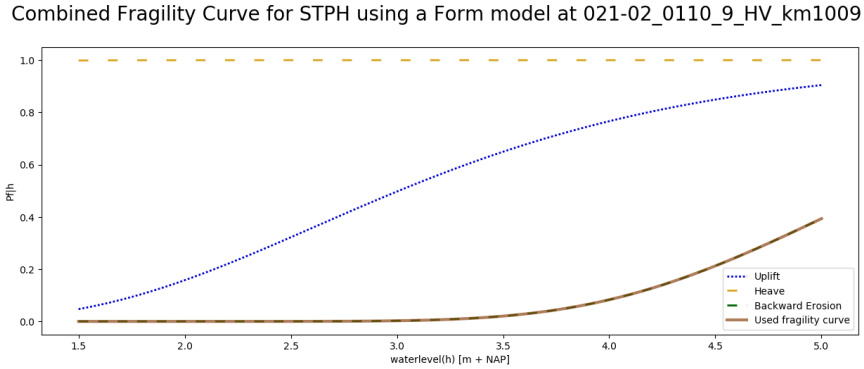

Figure 5.3: Fragility curve Piping

Note that the combined fragility curve always overlaps the fragility curve of the sub mechanism with the smallest failure probability. This makes it sometimes difficult to see one of the sub mechanisms in the figure.

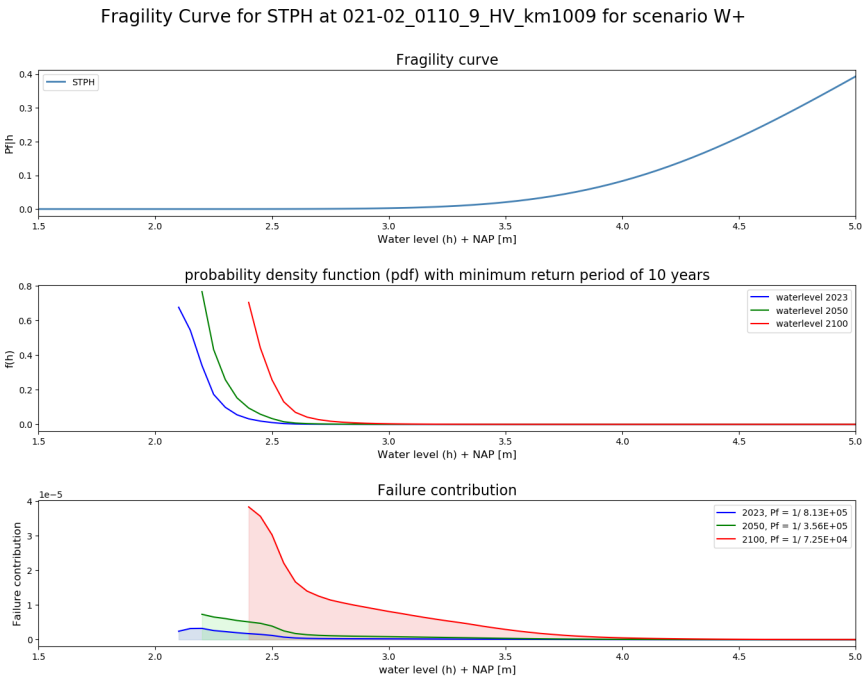

Figure 5.4: Combined Fragility Curve STPH

The same steps are taken here as they are in the previous chapter where the residual lifetime for wave run-up and overtopping is calculated. In short this means:

- Gather the geotechnical and hydraulic parameters needed in the piping calculation
- Calculate FC with the limit states for uplift, heave and backward erosion
- Calculate water level statistics with the help of the water level frequency statistics from Hydra-NL
- Analyse the difference between the settings for the lower limit of water level frequency (extrapolation versus a 1/10 year or 1/100 year lower limit for the water level frequency).
- Calculate the product of the FC and local water level distribution to get the contributions of each water level towards the total failure contribution for each reference year
- Calculate the area underneath each graph to get the total failure probability for each reference year

The results from these steps will be analysed and compared before the residual lifetime is calculated. This will be described in the next section where an analysis is to verify the results of the fragility curve method.

Finally, the residual lifetime will be calculated with the following steps as is also done for wave run-up and overtopping.

- Plot the total probability of failure against the corresponding reference years
- Extrapolate over those three points to get an estimation of the future failure probability.
- Add the bottom value of the calculated location in the same figure
- Find the point where the bottom value becomes smaller than the total failure probability and read the year of occurrence from the x axis.
- Subtract the current year from the year of occurrence to find the estimated residual lifetime of the given location.

5.6. Sensitivity analysis

The results of the fragility curve analysis will be checked with two methods. The used limit states are checked with Riskeer and the probabilistic analysis is checked using a model that is provided by the company 'HKV lijn in water'. First the limit states will be checked with the help of the factor of safety that can be calculated in Riskeer and the used fragility curve script.

5.6.1. Analysis of the limit states using Riskeer

As written above, the limit states for uplift, heave and backward erosion can be checked by calculating the factor of safety (FOS) both in Riskeer and the fragility curve method. The FOS is calculated in both Riskeer and the model using fragility curves. This approach only checks the used equation and does not yet check the probabilistic analysis itself. This is done in the next section where the method, used in this thesis, is checked with the help of a model provided by 'HKV lijn in water' that calculates the failure probability for backward erosion only using fragility curves.

The FOS can be defined by rewriting the limit states given in the literature study (chapter 2.5.2 in a form where the resistance is divided by the load $FOS = \frac{Resistance}{Load}$. This will give the following three equations with the subscripts U, H and BE defining the sub mechanisms uplift, heave and backwater erosion respectively.

$$FOS_U = \frac{m_u \Delta\phi_{c,u}}{\Delta\phi};\ \ FOS_H = \frac{i_{c,h}}{i};\ \ FOS_{BE} = \frac{m_p \cdot H_{c,p}}{h - h_p 0.3d}; \tag{5.1}$$

In Riskeer the limit state is used in a semi-probabilistic calculation. This means that each stochastic value is given a design value depending on its expected value (mean) and standard deviation. These values are then used to calculate the FOS. The design values are set as the 5 or 95 % quantile of each distribution, depending on the stochastic value. The parameters h_p, L, d, d_{70} and γ_s are using the 5 % quantile. D and k will use the 95 % quantile. The model factors m_u and m_p are both set to 1 for this calculation.

The second difference between the calculation in Riskeer and a fragility curve is that Riskeer only calculates the FOS for the design water level instead of over a whole range of water levels. To get from the FOS to a failure probability, Riskeer uses an equation which is calibrated for each single mechanism. Appendix iii [23] of WBI2017 gives this equation.

For dike stretch 21-2, there is unfortunately no Riskeer data available to calculate the factor of safety. It is therefore not possible to directly analyse this data. Fortunately, it is possible to do this for dike stretch 34-2. The outcome of both Riskeer and the used limit state equations are given in table 5.3 below, where U, H and BE stand for the sub-mechanisms uplift, heave and backward erosion respectively.

Table 5.3: Sensitivity analysis for dike locations at stretch 34-2

Location		Riskeer FOS	Fragilty Curve method FOS
34-2 0011	U	0.594	0.546
	H	0.583	0.583
	BE	1.370	1.355
34-2 0130	U	0.995	0.904
	H	0.551	0.552
	BE	0.970	0.948
34-2 0190	U	1.130	1.048
	H	0.966	0.967
	BE	2.926	2.926

Table 5.3 shows that the FOS between Riskeer and the script is almost equal. This means that the limit states used in the fragility curves are correct and can be used for further calculations. In the table, two more dike cross sections are calculated to be sure that the used equations are correct.

5.6.2. Analysis of the probabilistic model using the Fragility Curve Creator tool by HKV lijn in water

With the method mentioned above, only the limit state equations for the piping sub mechanisms are validated and approved. It is also important to validate the full probabilistic calculation within the fragility curve. This is done with a the Fragility Curve Creator provided by the company HKV Lijn in water. The python code consists of a fragility curve calculation that is used within the company. The Fragility Curve Creator is used to check the fragility curve calculation. It will only be used to validate the code, not for the calculation itself. This is done since the Fragility Curve Creator only includes backward erosion. To be able to compare the two methods, only the outcome for backward erosion will be compared. This will give the results given in table 5.4. Note that the given values for the failure probability are for backward erosion only. Also the probability of failure is given as: $1/P_f$ which is the same as the return period.

Table 5.4: Analysis between the probabilistic calculation used in this thesis and the Fragility curve creator for backward erosion at location 21-2 0110

Reference year	Scenario	Backward erosion $[1/P_f]$	HKV Fragility Curve Creator $[1/P_f]$
2023	G	8.29E+05	9.90E+05
2050	G	6.12E+05	7.50E+05
2100	G	3.74E+05	2.22E+05
2023	W+	8.13E+05	1.08E+06
2050	W+	3.56E+05	2.83E+05
2100	W+	7.25E+04	4.63E+04

Some differences are found between the two methods. This difference seems to be the biggest for the reference year 2100 and become close for the later reference years 2050 and 2100. Why the code seems to favour 2100 is not completely clear. An explanation can be that the reliability method favours bigger failure definitions, meaning that whenever a higher failure probability is found, the FORM reliability model in the Fragility curve is more accurate. The Fragility Curve Creator does also cut the failure probability when it becomes smaller than 1E-20. This should however, hardly be visible in the calculation.

5.6.3. Importance Factor and Error

For each of the sub mechanisms, the importance factors and errors are given for the probabilistic calculation in the fragility curves. These are given at six different water levels spread over the range of the fragility curve. In Appendix G the error and importance factor for each sub mechanism are given. Figure 5.5 and 5.6 show these values for backwards erosion only. The maximum errors are put on 1E-2 for all but the residual error, which is put on 1e-5. The calculated errors are below the maximums. As can be found in figure 5.6.

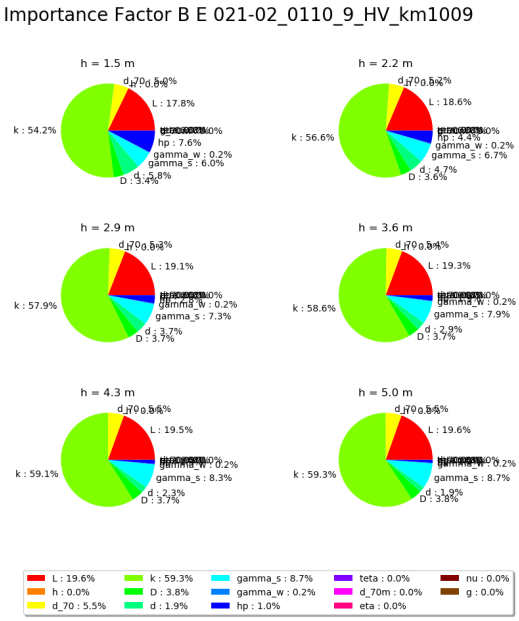

Figure 5.5: Piping Importance Factor 21-2 0110

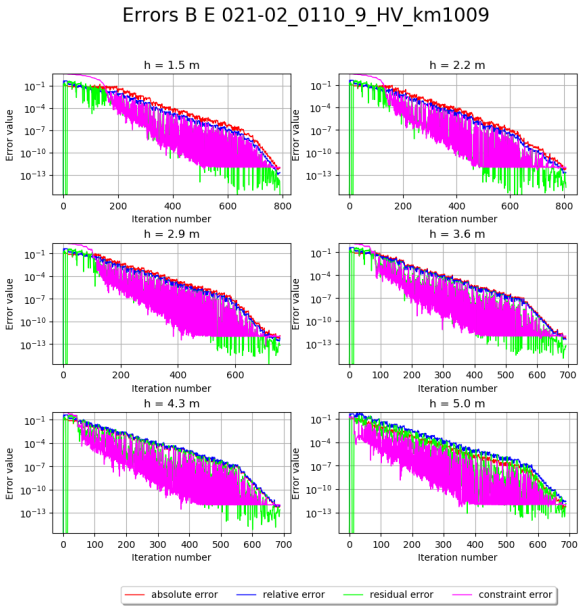

Figure 5.6: Piping Errors 21-2 0110

The Importance factors show which variables have the highest impact on the limit state. The figure clearly shows that the cover layer (d) and the hydraulic conductivity (k) have the highest impact. This can be explained as a higher value for k increasing the flow in the aquifer and thus increasing the failure probability. For d the opposite is true. A bigger cover layer means a longer channel that has to be travelled, thus increasing the strength against the sub mechanism. Looking at the limit state for backward erosion, d directly reduces the load on the dike when increasing and thus has a big effect on its strength. k is found in the variable F_s shown in equation 2.15.

5.7. Results

After creating the fragility curve, the pdf and calculating the probability contribution, the final step is to find the residual life time. The figure below shows the change in probability of failure over time. For this dike cross section, the bottom value is not reached within the range of the graph. The further the line is extrapolated in the future, the less accurate it becomes. Therefore it is not necessary to extrapolate further than done already. The main point, which is visible from figure 5.7, is that there is no danger of reaching the bottom value in the near future.

What does stand out from the bottom graph in figure 5.7 is that the failure contribution is cut off for the lower water levels. This means that in calculating the total failure probability a part of the failure contribution is not considered. However, in the results of the sensitivity analysis in table 5.2, the total failure probability is calculated without cutting the lower water levels (the top graph of figure 5.3). In the legend the total failure probability is given, and there is only a small difference between the top figure, where the full range is used, and the middle figure, which is used in the study. It is therefore possible to cut off the lower water levels without any risk of underestimating the failure probability of the dike.

In the above fragility curve, only the extreme W+ scenario is calculated. Adding the moderate scenario (G) to the calculations will make it possible to get a bandwidth of the change in failure probability over

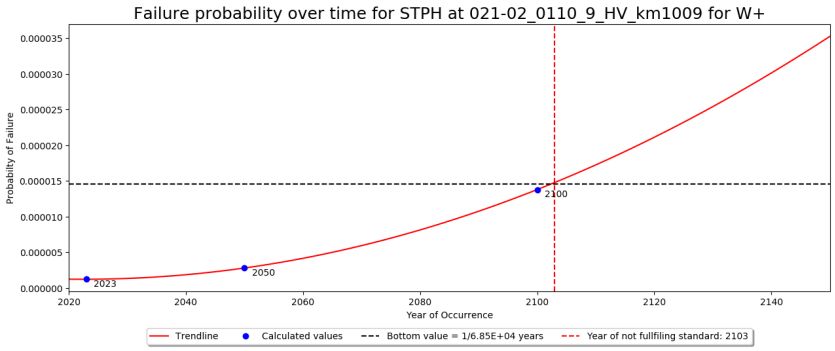

Figure 5.7: Residual lifetime at 21-2 0110 for scenario W+

time. This is shown in figure 5.8. In this figure, the residual lifetime for the dike section is given. With the green line being the moderate scenario and red line the most extreme scenario. For this particular dike cross section, the maximum allowable failure probability will be reached around 2100 for scenario W+ and falls outside the maximum range of the figure for scenario G. This means that the residual lifetime for this dike section is around 80 years. Since the residual for scenario G falls outside the range it is not possible to give a residual lifetime for this scenario. The safest option is to say that, in this case, the residual lifetime for scenario G is 130 years. Since this residual lifetime is that large, it is not a real problem that the exact residual lifetime is not known.

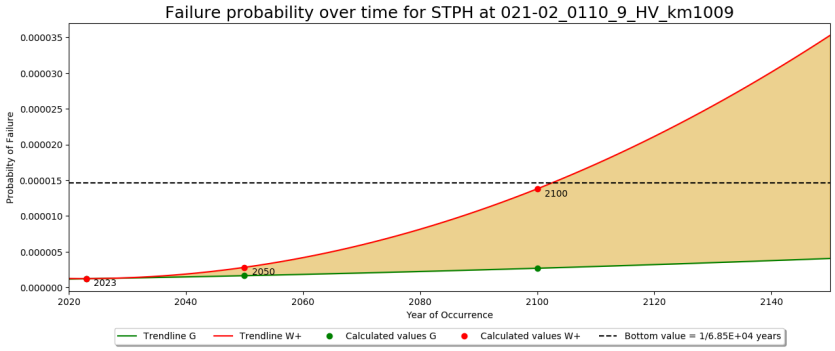

Figure 5.8: Residual lifetime at 21-2 0110

Table 5.5 shows the parameters that are used for the calculations of the residual lifetime at the other locations.

The results for the residual lifetime for piping are given in table 5.6. Again, a 0 means that the dike has already failed. An arrow means that the residual lifetime is longer than the calculated range. A number gives the residual lifetime in years with 2020 as the base.This is done for scenario G and W+.

The main observation is that for almost all locations the residual lifetime falls outside the calculated range. The only two exceptions are 20-4 0181 and 21-2 0110. Looking at the parameters in table 5.5 this can be explained by the very small cover layer at both of those locations. The small seepage length for location 20-4 0181 creates an even smaller failure probability for this location and thus a very small residual lifetime. At location 20-4 0181 the polder level (h_p) is also very low. This creates a large head difference which will affect the failure probability.

Location 20-04 0181 has a residual lifetime of 0. This means that this location already has a failure probability that is larger than allowed in the WBI. Figure 5.9 shows the bandwidth of the residual lifetime for scenario G and W+ and figure 5.10 shows the combined fragility curve. What becomes clear from this figure is that the dike section has a very high fail probability for both heave and backward erosion. Already on very low water levels, these two sub mechanisms occur. Only uplift has a much smaller failure probability. Heave has a high probability of occurrence, due to the shallow inner water level. The polder that is protected by this dike has a depth of ($h_p = -2m + NAP$). This influences the

Table 5.5: Used parameter per location for piping calculations

Location		**20-4**		**21-2**				
	Distribution	**0074**	**0181**	**0110**	**0270**	**0373**	**V**	σ
$L_{f,in}$[m]	**D**	9	9	100	100	5	-	-
$L_{f,uit}$[m]	**D**	64	60	170	170	60	-	-
L[m]	**LN**	55	51	70	70	55	0.1	-
h_p[m]	**N**	-1.05	-2	-0.3	-0.35	-0.8	-	0.1
d_{70}[m]	**LN**	125	120	145	150	150	0.12	-
k[m/s]	**LN**	40	30	30	23	23	0.50	-
D[m]	**LN**	11.5	14	3	3	25	-	0.5
d[m]	**LN**	7.75	3.5	1.5	2.5	9	-	0.5
γ_s[kN/m³]	**LN**	16.19	14.09	16.19	16.19	16.19	loc = 10	scale = 1
Location		**25-2**			**34-2**			
		0020	**0091**	**0242**	**0011**	**0130**	**0190**	**V**	σ
$L_{f,in}$[m]	**D**	13	65	200	170.64	181.56	141	-	-
$L_{f,uit}$[m]	**D**	70	115	340	251	219.5	225.12	-	-
L[m]	**LN**	57	50	140	80.36	38.44	84.13	0.1	-
h_p[m]	**N**	-1.1	-0.8	-0.6	-2.2	-0.8	-1.8	-	0.1
d_{70}[m]	**LN**	145	145	145	210	110	110	0.12	-
k[m/s]	**LN**	10	25	25	25	10	15	0.50	-
D[m]	**LN**	25	20	21	6.8	5	30.5	-	0.5
d[m]	**LN**	15	15	1.75	6	5.8	9.5	-	0.5
γ_s[kN/m³]	**LN**	14	14	16.9	14.09	15.9	13.8	loc = 10	scale = 1

Table 5.6: Piping Residual lifetime for each location

Location		Hellevoetsluis	Spui				Den Bommel			Moerdijk	Noordschans	Willemstad
		20-4		**21-2**			**25-2**			**34-2**		
		0074	**0181**	**0110**	**0270**	**0373**	**0020**	**0091**	**0242**	**0011**	**0130**	**0190**
Piping	**G**	→	0	→	→	→	→	→	→	→	→	→
	W+	→	0	83	→	→	→	→	→	→	→	→

exit gradient(i) for heave and increases the head difference between the inner and outer dike, which influences backward erosion. There is also no foreshore at this location, which reduces the leakage length (L_f). This also increases the chance of failure. Uplift has a smaller failure probability but is still much too big to pass the assessment.

Figure 5.9 shows that for reference year 2023, the failure probability for scenario G is bigger than for scenario W+. This is unexpected, since scenario G gives the more moderate climate scenario in comparison with scenario W+. A more extreme climate scenario should give a larger failure probability.

What also stands out from figure 5.9 is that the trend lines for scenario G and W+ (green and red line in the figure) intersect each other around 2030. This is unexpected, since both lines should increase in time, with scenario G increasing more slowly than scenario W+. This shows that a Form calculation is not always reliable and can cause numerical issues.

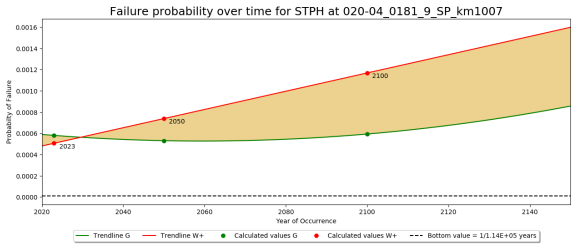

Figure 5.9: Piping residual life time bandwidth 20-4 0181. The graph shows an error in the failure probability where it reduces over time. This is unexpected and will not happen in reality

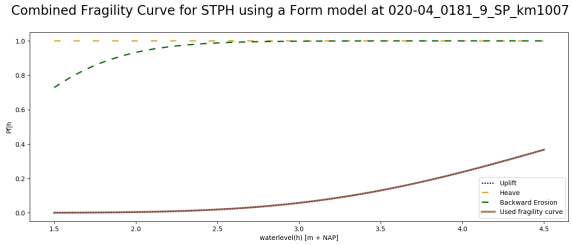

Figure 5.10: Fragility curve of piping for the combined sub mechanisms for location 025-2 0020

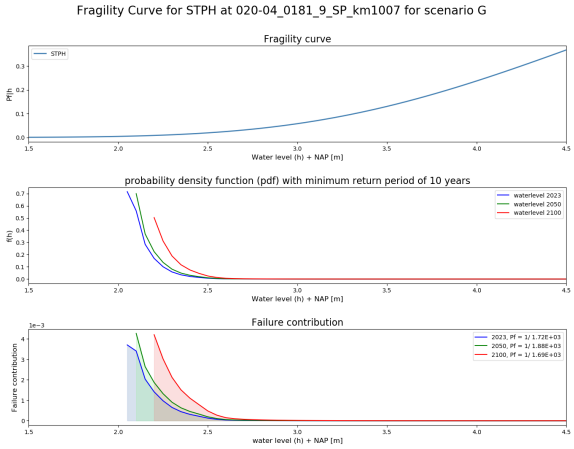

Figure 5.11: Fragility curve calculation for piping and scenario G at location 25-2 0020

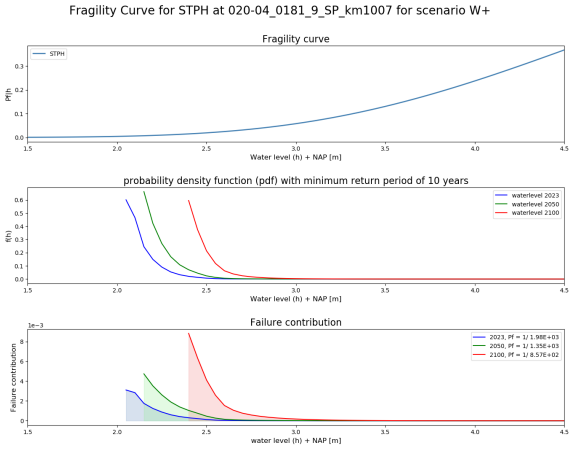

Figure 5.12: Fragility curve calculation for piping and scenario W+ at location 25-2 0020

The problem lies in the calculated total failure probability (P_f) between each of the reference years. For scenario G (figure 5.11), $P_{f,2050}$ is smaller than $P_{f,2023}$. This is unexpected. The failure probabilities also lie very close to each other. This is caused by the water level statistic that is given in the middle graph in the same figure. There is almost no difference in the pdf for reference year 2023 and 2050. The location of this dike cross section is probably the cause of this. The dike lies in the opening of the channel between dike stretch 20-4 and 21-2 named the Spui (see figure E.1). It is possible that for moderate scenarios climate change has less impact on this location. The location is sheltered from waves. This can explain that, in time, there is not much change in the water level for this location.

The main reason for the other locations having a very small failure probability is most likely the existing cover layer (d) for each of those locations. All of the locations have a thick cover layer which will reduce the probability of piping. The exception is 21-2 0270 with only a cover layer of 2.5 m. However, the aquifer thickness (D) is very wide here, reducing the pressure in this layer.

5.8. Conclusion

The residual lifetime for piping is large for most of the locations around the Haringvliet and Hollands Diep. There is one clear exception found at location 20-4 0181, where the residual lifetime is zero, meaning that the dikes do not meet the set standards in the WBI2017. However, the shape of the failure probability over time shows an unusual shape as is already mentioned in figure 5.9. This is most definitely caused by numerical issues in the form reliability calculation in the fragility curve.

Overall the fragility curve method does give an overview of the residual lifetime of the dikes against piping. For a detailed residual lifetime, the SOS data has to be increased in detail and the parameters for the damping factor λ, seepage length L and critical gradient i_{ch} have to be looked at. These are the parameters that influence the dike safety the most after accurate SOS data.

6

Dike section Residual Lifetime

6.1. Introduction

In this chapter the fragility curves for both failure mechanisms will be combined in one fragility curve. This combined fragility curve will be used to calculate the residual lifetime that takes into account both failure mechanisms. This will be done as is described in the method (chapter 3).

As the method states, the fragility curve for piping and overtopping are combined by using the following equation:

$$P_{F,total} = 1 - \prod_{n}^{i=1} \left(1 - P_{F,i}\right) \tag{6.1}$$

The outcome is used to calculate the failure contribution using per water level, which will be used to calculate the total failure probability and the residual lifetime. For each of the selected locations, a combined bandwidth for the residual lifetime is calculated.

6.2. Results

Figure 6.1 shows the results for location 21-2 0110 with the combined fragility curve at the top, the water level probability density function in the middle and the failure contribution in the bottom graph. The figure shows the results for scenario W+. The same is also done for scenario G, to make it possible to calculate the residual lifetime for both scenarios. The total failure probability for both scenarios is plotted in figure 6.2 where a bandwidth of the residual lifetime, depending on the climate scenario G and W+, is given. The parameters used for the fragility curves are previously given in table 4.7 and 5.5 for the wave run-up/overtopping and piping respectively.

Summarized: For overtopping, the governing wind direction with the omni-directional wind speed distribution is used in the calculation. The foreshore and wind/wave statistic is not taken into consideration. For piping, the sub mechanism with the smallest failure probability is used in the residual lifetime calculation. In the sub mechanism the soil schematisation with the biggest failure probability is used. This means that only one sub soil schematisation is used per location.

The total failure probability for each scenario is combined in figure 6.2 to calculate the residual lifetime. It is clear that the difference between the expected failure probability for both scenarios increases over time. This also means that the uncertainty increases as well. For the near future (from now until 2050), the calculation (as given in figure 6.2) gives a great visual overview of the effect of climate change on the safety of this dike cross section when multiple failure mechanisms are included. The figure shows the increase in failure probability in time and when they are no longer in compliance with the Dutch standard.

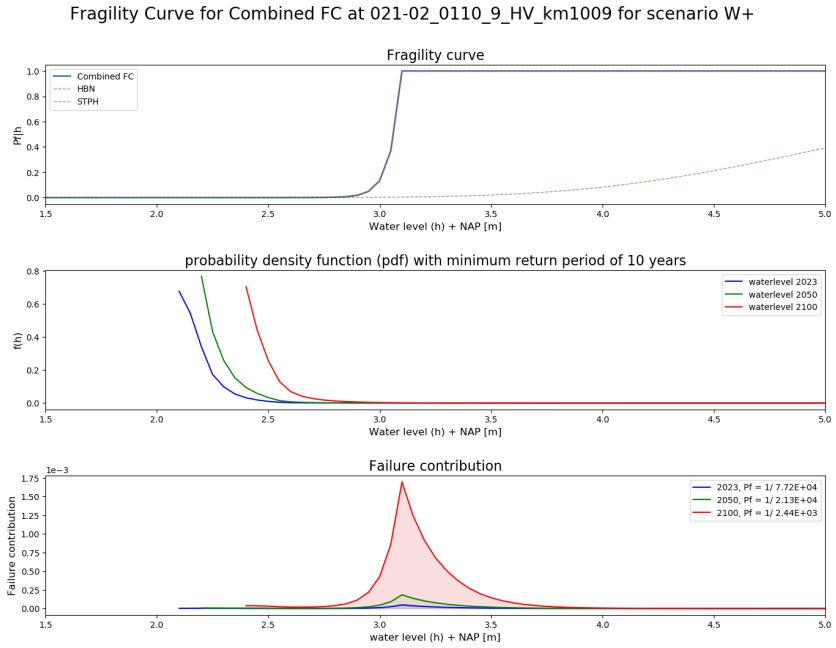

Figure 6.1: Probability of failure for Backward Erosion and Overtopping

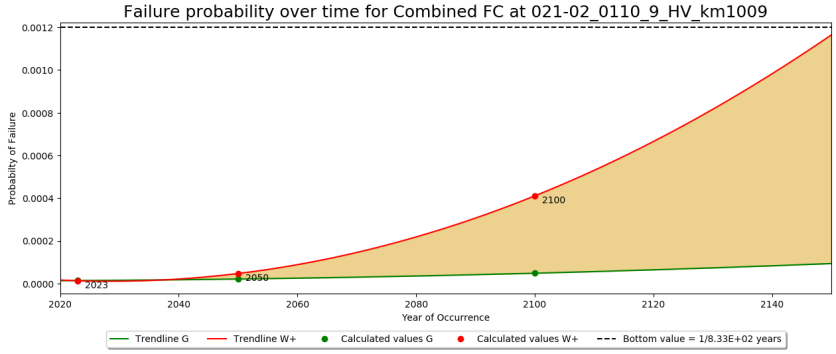

Figure 6.2: Residual lifetime at 21-2 0110

In the WBI, there is a different maximum failure probability for overtopping and piping. There is an overall bottom limit for a whole dike stretch as given in table 2.1 in the literature study, but there is no overall bottom limit for a dike section.

In the Dutch assessment, the failure probability is calculated for each single failure mechanism at each dike section. These values are then put together and are assembled to give an indication of the overall safety of the dike sections.

To calculate the residual lifetime for a combination of failure mechanisms, a combined bottom value is needed that takes into account the maximum failure probability of both included failure mechanisms. This is solved by adding the maximum allowable failure probability of both piping and wave run-up/ overtopping together. The resulting failure probability will be used as the combined maximum failure probability (or bottom value) where both wave run-up and overtopping are included.

The method above does not take into account the difference in bottom value between the two failure mechanisms. It is therefore difficult to note when a failure mechanism is more dominant. The difference in bottom value between overtopping and piping is found due to a combination of a different length effect and a difference in assigned failure space. This is a percentage of the bottom value of the dike stretch, that is assigned to each failure mechanism. This is done in the WBI and is included in the length effect calculation. In the WBI both overtopping and piping have an assigned failure space of 24 %. However,

piping has a much bigger length effect, which is responsible for the large difference in bottom value between piping and overtopping.

In figure 6.3 the failure probability of each failure mechanism is given for each location. At the x-axis, the three reference years (2023, 2050, 2100) and scenario G and W+ are given. The y-axis gives the total failure probability. Note that the y-axis has a logarithmic scale. A bigger bar in the sub figures means a larger failure probability. Here the difference between the values for wave run-up/ overtopping and piping becomes visible. In most cases does piping have a much smaller failure probability than wave run-up/ overtopping has.

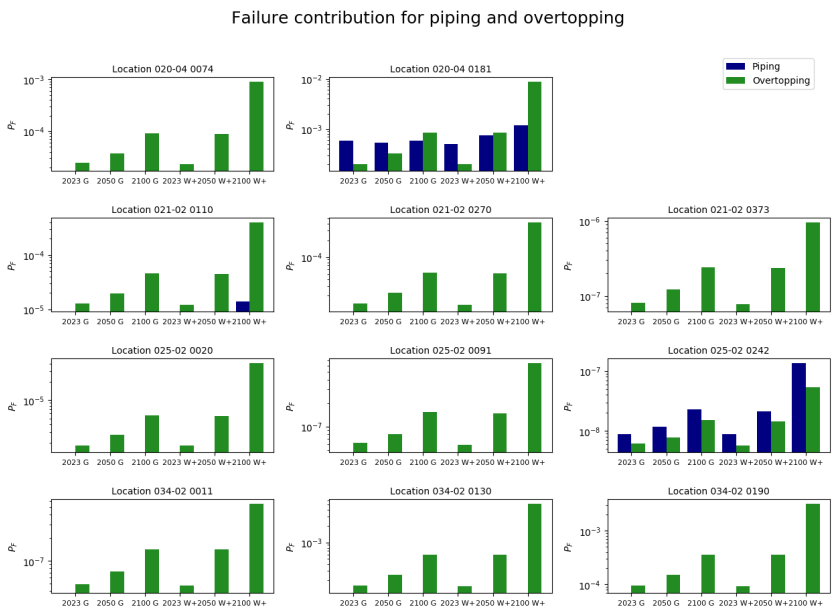

Figure 6.3: Failure probability for each location

Figure 6.3 only gives a view of the total failure probability of each failure mechanism per location, but does not say anything about the residual lifetime of that dike section. Table 6.1 shows the outcome for each of the locations. The residual lifetime is calculated for each scenario and for the single and combined failure mechanisms. Here as well, a zero means that the residual lifetime is negative, meaning that the bottom value of that dike section is already reached. This does not mean that the dike section can fail any second but that the failure probability of that dike section is lower than the bottom value given in the WBI. A →, shows when the location has a residual lifetime that exceeds the range of the calculation. In appendix B, figures are given for each location, that show failure probability change over time for the combined fragility curve for both scenario G and W+. The first two rows in the table give the same results as tables 4.8 and 5.6. The last row shows the combined residual lifetime.

Table 6.1: Residual lifetime in years for each location. With: → meaning a residual lifetime of more than 130 year (happens after 2150)

Location		Hellevoetsluis	Spui				Den Bommel			Moerdijk	Noordschans	Willemstad
Failure Mechanism	**Dike stretch**	**20-04 0074**	**0181**	**21-02 0110**	**0270**	**0373**	**25-02 0020**	**0091**	**0242**	**34-02 0011**	**0130**	**0190**
Combined	**G**	→	0	→	→	→	→	→	→	→	56	88
	W+	56	0	→	130	→	→	→	→	→	25	32
Overtopping	**G**	→	40	→	→	→	→	→	→	→	56	88
	W+	56	23	→	130	→	→	→	→	→	25	32
Piping	**G**	→	0	→	→	→	→	→	→	→	→	→
	W+	→	0	83	→	→	→	→	→	→	→	→

The table shows that for large parts of the Haringvliet and Hollands Diep, there is no real threat of dike

failure in the coming years when the guidelines of the Dutch formal assessment tool (WBI2017 [8]) are used. The exception is location 20-4 0181, where the residual lifetime is 0.

6.3. Conclusion

Combining the failure mechanism with fragility curves give a good overall view over the residual lifetime in the Haringvliet and Hollands Diep. The maximum failure probability that is used as a bottom value for the combined failure mechanisms is the bottom value for wave run-up/overtopping and piping added together.

The result is most of the time equal to the residual lifetime of the failure mechanisms that shows the smallest residual lifetime. This is mainly caused by wave run-up/overtopping have a much bigger failure probability than piping. Most of the locations are very safe with a residual lifetime of over 130 years. The one exception is also found in the fragility curve for piping. This is location 20-4 0181 which has a much to big failure probability when compared to the Dutch standards. However this is most likely caused by an anomaly in the piping probabilistic calculation.

7

Discussion

7.1. Discussion

The result from the fragility curve calculations indicate that climate change mainly influences the residual lifetime due to the contribution of the failure mechanism wave run-up and overtopping. Piping has a much smaller effect. This means that mainly the dike height is important when looking at the residual lifetime for this area. For dike stretch 25-2 there is a difference. Piping plays a much bigger part in the total residual lifetime for those locations. This is mainly caused by the shallow cover layers that can be found in this dike stretch. There are a few points of discussion: The used method, the two failure mechanisms wave run-up/overtopping and piping, the overall results, and the usefulness of the method.

Method In the fragility curve calculation, the choice is made to use a FORM model instead of a Crude Monte Carlo model. This choice is made to reduce the computation time, as discussed in the thesis. It also makes it possible to use a much smaller time step, since the computation time for a FORM model is shorter. This can increase the accuracy of the calculation. The expected failure probability can sometimes be smaller than 1E-6, the amount of simulations in a Crude Monte Carlo model should than at least be $1/(100 \cdot P_f) = 1E8$ simulation. Doing this for multiple water levels per location would easily result in more than 1E9 simulations, which would take a considerable amount of time. FORM is faster and makes it possible to use smaller time steps but it has to said that CMC is a much more accurate model than Form, since Form works with a design point for each variable while CMC is a fully probabilistic model which is much more precise when enough simulations are done. Since in this study looks for a model that can quickly given an overall view of the residual lifetime, some accuracy losses are accepted. This makes it possible to use the FORM model instead of the more accurate but much slower CMC model.

The fragility curve will take into account water levels from 1.5 m + NAP up to the dike crest. Lower water levels are not taken into account since those do not have any effect on the safety of the dike. Such water levels occur on a daily basis and have never led to any serious safety issues. This is approved when looking at the failure probability at a conditional water level of 1.5 m + NAP. The failure probability is negligible for both wave run-up/overtopping and piping. Only the sub mechanism heave shows a failure probability that is significant. Fortunately this is not a big problem, since both uplift and backward erosion have a much smaller failure probability than heave. As long as those two sub mechanisms have a much smaller failure mechanism, there is no safety risk for those lower water levels.

What is discussed above is also used to approve a set maximum occurrence probability of 1/10 years for the water level frequency that is found with Hydra-NL. Even when 80 % of the water level frequency density lies on water levels below 1.5 m + NAP. Luckily this is no issue since the failure probability is negligible.

The calculated water level statistics from Hydra-NL is known to overestimate the probability of occurrence. Water levels with an occurrence of 1/100 year in reality have an occurrence which lies closer to 1/1000 per year. This means that, in the calculation of the failure contribution, the real contribution can be overestimated up to a factor 10. Since this is an overestimation, the real resistance/strength of a dike is higher than calculated. This means that in reality the dike is much stronger than calculated. Since the thesis is only after an overall view of the dike safety, this is no big problem. The method still gives an indication of the safety of the dike and it is still possible to compare the residual lifetime with the surrounding dikes. This means that the weakest dikes are still recognized. An extra, and more detailed, calculation can then be made to calculate the dike failure probability more accurate.

There are only three reference years (2023, 2050 and 2100) for which the total failure probability can be calculated. These three years are used to extrapolate the failure probability over time which is needed to calculate the residual lifetime of a dike. This means that the uncertainty of the residual lifetime increases quickly when the residual lifetime is found beyond the last reference year. This thesis is mainly focused on the near future (the coming 50 to 100 year) since policy changes will happen between now and 2100 that will directly affect the residual lifetime. Changes in the Dutch policy towards dike safety will most likely also change the maximum allowable failure probability and will therefore affect the residual lifetime.

The addition of two scenarios increases the usefulness of the found results, since the bandwidth gives a clear range in which the residual lifetime falls. The diverging lines in those graphs clearly show the increase in uncertainty, since the bandwidths range increases over time. The most extreme scenario is plotted together with the least extreme scenario. These are seen as the two limits of the expected influence of climate change on the different dike sections. The real answer will therefore lie somewhere between those two limits.

The wave run-up and overtopping calculation The dike schematisations were all provided by the two waterboards that are responsible for the dike stretches around the Haringvliet and Hollands Diep (waterboard Hollandse Delta and Brabantse Delta). The hydraulic boundary conditions are provided by Rijkswaterstaat WVL. Both of these sources are also used for the real dike assessments in the Netherlands. The data is widely used throughout the Netherlands.

The main two assumptions for this failure mechanism in the given study area are that the water level and wind speed are considered independent of each other and that only the most dominant wind direction is taken into account. The most dominant wind direction will introduce an overestimation in the load on the dike. No correlations between the wind speed and water level gives an underestimation of the load, especially for high water levels.

Only using the most dominant wind direction does not take into account the probability of all the other wind directions from happening. The dominant wind direction is not always the wind direction that has the biggest probability, but the wind direction that has the biggest impact on the failure probability of the dike. This means that the dominant wind direction can have a small probability occurring which results in a smaller failure probability than actually occurs. This will give an underestimation of the actual residual lifetime, the method gives a safe result and can be used to give an overview of the residual lifetime of the Haringvliet and Hollands Diep.

In the fragility curve, it is difficult to take into account the correlation between wind speed and water level, since the water level is taken conditionally and the wind speed is the only stochastic value in the calculation. Changing the wind speed distribution for each water level changes the whole principle of a fragility curve, since only one parameter (in this case the water level) should change. The rest of the values should be constant or have a fixed distribution. Therefore the wind speed distribution is not changed.

Piping The three sub mechanisms for piping are separately used in a fragility curve. With the combined fragility curve being equal to the fragility curve of the sub mechanism with the lowest failure probability. This will give a bigger failure probability than in reality. Mainly due to the correlation that is not included in the fragility curves but does happen in practise. It is not exactly known how much the

sub mechanisms are correlated but since all the sub mechanisms are all dependent on the water level it there has to be some degree of correlation.

For piping, the difficulty lies in finding the correct values for each of the parameters needed for the three sub mechanisms in the piping calculation. In these calculations there were also a number of deterministic values that were assumed according to the WBI. These were the values for: $\theta, \mu, \lambda, i_{c,h}$ and d_{70m}.

The damping factor λ for uplift and the critical heave gradient $i_{c,h}$ for heave are both assumed in compliance with the WBI. For almost all the locations uplift has the smallest failure probability and heave has the largest, with backwater erosion in the middle. From the importance factors, it becomes clear that both λ and $i_{c,h}$ influence the failure probability of their respective sub mechanisms the most. After that, in most cases, the cover layer has the biggest importance factor. It is difficult to justify the calculation for both uplift and heave since they have such a dependency on λ and $i_{c,h}$. Both these values are also taken quite conservatively and do therefore give bigger failure probabilities than in practice. For heave, it is clear that the conditions in the dike allow heave to happen at rather low water levels. Uplift and backwater erosion have a much bigger failure probability and ensure a safer dike.

The seepage length is calculated using AHN viewer [12] instead of on site investigation. This is done since the data from AHN is freely on their website. In most cases, the foreshore is not taken into account for the seepage length when a trench was found close to the outer slope of the dike. This will give shorter seepage length and thus a bigger failure probability. For the soil schematisation, the SOS schematisation is used when no other data was available. This was the case for dike stretches 21-2 and 25-2. The SOS data is not detailed enough for assessment according to the Dutch regulations. For the purpose of getting an overview of the residual lifetime it gives a good enough representation.

The sensitivity analysis for piping is more intricate. The three sub mechanisms that form piping have to be validated separately. For backward erosion, this is possible with the help of a model provided by HKV. For heave and uplift, this is unfortunately not the case. It is possible to verify the equations for all the sub mechanisms with Riskeer, but the total failure probability is calculated differently. Riskeer uses a semi probabilistic approach with the critical water level as the fixed water level, while the fragility curve takes into account the full range of local water levels. The outcome of the semi probabilistic sum is then put in a calibration function to get a failure probability. This gives two different methods that both give a different answer. It can therefore not be said with certainty when the difference in results is due to the difference in approach or due to an error in the fragility curve probabilistic analysis. The analysis for heave and uplift should therefore be further developed.

Results The results show that mainly wave run-up/overtopping is responsible for the safety of the dike. In [5] this can also be found for dike stretch 34-2. Piping does have a much smaller failure probability, mainly due to the big cover layers that are found below most of the dikes around the study area. Only at the northern shore line there are two locations where the cover layer is much smaller. Location 20-4 0181 and 21-2 0110. This is immediately seen in the failure probability for piping as well. The calculated values for location 20-4 0181 are also available in the report about the dike safety of dike stretch 20-04 conducted by the waterboard Hollandse Delta[21]. Both the fragility curve method and the computations done by the waterboard find a failure probability at that location that is much too large and does therefore not meet the requirements set by the WBI.

Overall, the results of this method seem to have, in most cases, a much bigger failure probability than in reality. This means that, in reality, the calculated residual lifetime will be smaller. Which is conservative, but acceptable when only looking for an overall view of the influence of climate change on the residual lifetime of the dikes.

Usefulness of the method The Fragility curve method does give a good overall view of the residual lifetime of a dike. The method can be useful when the correct geotechnical and hydraulic data is available. The residual lifetime is an easy to understand value that clearly indicates the state of a dike section. By itself, this method gives an indication of the status of the dike, rather than detailed results. A more detailed view requires more research in the assumptions and should also include effects such as time dependency, ageing of the dike and residual strength

One of the reasons for using fragility curves is the easy way of combining multiple failure mechanisms together. This combined fragility curve can then be used to calculate the residual lifetime. It becomes more intricate when looking at the residual lifetime for combined failure mechanisms. For that, a maximum failure probability is needed which cannot be crossed by the total failure probability. This value is different for each failure mechanism due to different length effects and possible difference in failure space. The maximum probability of failure that is set for each failure mechanism is a part of the bottom value of a dike stretch that can be occupied by that failure mechanism at one dike section. These parts of the bottom value can be added together to get a combined failure space for piping and wave run-up/overtopping. The combined maximum failure probability can therefore be used to calculate the residual lifetime of a dike section for combined failure mechanisms.

8

Conclusions and Recommendations

8.1. Research questions

Before the main research question of the thesis can be given, the sub questions have to be answered first. Afterwards the main question will be answered.

How can residual lifetime be calculated? The residual lifetime of a dike is the time from now to the moment in the future where the dike no longer is approved by the minimum failure probability for that dike section. The residual lifetime can be calculated with the help of fragility curves. Fragility curves are an easy tool that can make a swift probabilistic calculation that can give a quick overview of the residual lifetime. This makes fragility curves a helpful tool. It is also very easy to combine multiple fragility curves together. This makes it possible to calculate the total failure probability of multiple failure mechanisms together.

The water level distribution can be calculated in Hydra-NL for multiple reference years. For each of the selected reference years(2023, 2050 and 2100) it is possible to calculate the total failure probability. By extrapolating the values for each of the reference years, a line is produced that gives the change in failure probability in time. Whenever the failure probability intersects the allowable failure probability, the residual lifetime is found.

What are the dominant aspects that contribute to the residual lifetime within the Haringvliet and Hollands Diep? The biggest contributor to the residual lifetime is the change in local water level distribution due to climate change. The aspects that influence this change include: wind set up, waves, river discharge, and sea level rise. The local water level is therefore a very complicated variable. There are many different aspects that can all influence the water level. Depending on the scenario each of those aspects can be the dominant force. The local water level distribution (or water level frequency) is calculated using Hydra-NL which includes most of the aspects that influence the local water level and thus the residual lifetime.

For one cross section. What is the residual lifetime looking only at wave run-up/overtopping using fragility curves? For this failure mechanism, the added value of fragility curves is small. Hydraulic models such as Hydra-NL can already calculate the failure probability of a dike. These models can more easily take into account correlations between the wind speed, wave height, and water level. In a fragility curve the water level is taken conditionally which makes it hard to take into account any correlation towards this parameter. The calculation using fragility curves takes more time than doing the calculation with Hydra-NL only. However, it is needed when fragility curves of multiple failure mechanisms are combined.

The fragility curve calculation results in most of the locations having a residual lifetime that is longer than 130 years which is the maximum residual lifetime that can be calculated with the fragility curve method as used in this thesis. This is concluded from chapter 4 and table 4.8.

The only locations that have a shorter residual lifetime are 20-4 0181, 34-2 130 and 34-2 0190 which have a residual lifetime between 25 and 88 years depending on the scenario.

For one cross section. What is the residual lifetime with respect to piping using fragility curves? The result of most of the locations with respect to piping gave very small failure probabilities and thus a large residual lifetime. This is also shown in table 5.6. The table shows that location 20-4 0181 and 21-2 0110 have a much smaller residual lifetime. For location 20-4 0181, the low residual lifetime is explained by a short leakage length and a deep polder. This leads to a very high probability of failure for both heave and backward erosions. A small cover layer increases the change on uplift and is the dominant sub mechanism for this location.

Location 21-2 0110 is discussed in detail in chapter 5. In this case backward erosion is the dominant sub mechanism. This is mainly caused by the hydraulic conductivity(k) and the leakage length(L).

It is not necessary to know the exact residual lifetime if these happen far in the future. For example after 100. Far before that time is reached, the dikes will be reassessed and strengthened where needed. For the sake of getting an overview of the residual lifetime, the fragility curve method gives a good indication of the state of dikes. The calculation for piping is fast and immediately gives an answer towards the residual lifetime.

What is the residual lifetime of a dike section with the failure mechanisms combined? For a dike section there is no combined maximum failure probability given by the WBI. Therefore the maximum failure probability of wave run-up/overtopping and piping are added together to get a combined maximum failure probability which include the failure space of both mechanisms and there length effects. The combined residual lifetime is, in most cases, equal to the residual lifetime of wave run-up and overtopping. Mainly since the maximum failure probability for wave run-up/overtopping is much larger than for piping. The information that is lost by combining the residual lifetime is whenever piping or wave run-up/overtopping is accountable for the residual lifetime. It is therefore not directly known for what failure mechanism the dike has to be strengthened. However, for an overall view of the dike sections safety this is no problem. The fragility curve method will give an indication of the residual lifetime. Locations with a small residual lifetime can then be analysed in detail to see which failure mechanism is causing the low residual lifetime.

What is the residual lifetime of the dike stretch around the Haringvliet & Hollands Diep? Looking at a whole dike stretch it is not yet possible to give a concluding answer on the residual lifetime. For a stretch the bottom value is known that includes multiple failure mechanisms. It is however needed to calculate the fragility curve and water level distribution at each dike section within one stretch. After that, the total failure probabilities of each of the sections have to be added together for each reference year to find the residual lifetime of a dike stretch. For time sake this is not done, but should be recommended in further studies.

The method of using fragility curves is a good way of calculating the residual lifetime of a dike stretch. The calculations are fast to do for each dike section and can easily be added together.

The added value of knowing the residual lifetime of a dike stretch should be discussed. A stretch can be multiple kilometres long. Knowing the residual lifetime of such a length of dikes does not say anything about the weak points within such a stretch. Knowing the residual life time of the single dike sections does therefore give a much better idea of where the weakest links are located.

8.1.1. Main Research question

What is the residual lifetime of the dikes around the Haringvliet and Hollands Diep, taking into account the climate scenarios: Average (G) and Warm (W+) using Fragility Curves. When looking at the separate and combined results for the residual lifetime in the Haringvliet and Hollands Diep, the residual lifetime is mainly caused by wave run-up and overtopping. As is expected, locations with lower dike crest heights also have a shorter residual lifetime than higher dikes. Dike stretch 25-2 has the highest dikes and therefore also the biggest residual lifetime. Stretches 20-4 and 34-2 have much smaller dike heights and do also see a shorter residual lifetime.

It has also become clear that the climate scenarios do impact the residual lifetime as expected. With the extreme scenarios having a much bigger impact than the more moderate climate scenarios. The difference between the scenarios depends on the location of the dike section. For example for location 34-2 0190 there is only a small difference between the both scenarios, while location 20-4 0074 shows a much larger difference between the two scenarios (See table 6.1).

The method of using fragility curves to calculate the residual lifetime of a dike section is a good way to get a fast view of the state of a certain area. There are however some limitations in the calculation of the limit state of each of the failure mechanisms. For wave run-up/overtopping multiple wind directions could increase the accuracy of the probability calculation. This could be implemented but will increase the amount of calculations significantly.

For piping the calculation exists of the three sub mechanisms. The calculations are fast and easy to do, the problem lies in finding the right soil conditions underneath a dike. Especially the cover layer (d) and leakage length (L) can have a major impact on the total failure probability of each reference year and thus the residual lifetime.

The combined calculation has more issues. Mainly finding the right maximum failure probability. Without a correct maximum failure probability, it is impossible to get a good result for the residual lifetime. In this case this is solve by simply adding the maximum failure probability of piping and wave run-up/overtopping together. This value can than be used to calculate the residual lifetime for multiple failure mechanisms together.

In conclusion, fragility curves can be used to get an overall view of the residual lifetime of the dike around an area like the Haringvliet and Hollands Diep. However, the overall view does not give any information about what failure mechanism is responsible for the main portion of the residual lifetime. It is therefore useful to include the residual lifetime of the failure mechanisms separately. For a better overview of the area, more dike sections should be included to make a better calculation of the residual lifetime per dike stretch. This can be done when the data for those locations is available.

8.2. Recommendations

First, the recommendations will be given for the overall study. Afterwards, the recommendations on the method and failure mechanism will be given separately to give the recommendations that are more focussed on those categories.

Overall recommendations Overall there are two recommendations that should be looked into in further studies. To get a better overview, more locations should be included. The hydraulic boundary conditions and soil compositions of those locations should be known.

The failure mechanism inner slope stability is not taken into account. This failure mechanism should be the next failure mechanism that is included in the fragility curve model. This mechanism can have a big effect on the dike safety. To do this correctly, the dike schematisation has to be extended to include the composition of the dike body as well.

Method In the method, two principles that increase the dike safety are not taken into account. These are the time dependency and residual strength of the dike. Adding those aspects will give a much more accurate view of the dike's residual lifetime but will increase the complexity of the system.

Climate change is added in the method via the calculated scenarios in [18]. This data is more than 14 years old. In this time, the climate models have improved a lot. This can create totally different results of the impact of climate change. At the time of writing this thesis, more recent data was not yet available in Hydra-NL and is therefore not used. This is no problem for checking the viability of the used method, but if the results will be used in practice, the data about climate change should be improved. In the report of the KNMI'14 [38], no big changes are found that can lead to results that differ much from the results that we have now. However it can be possible that upcoming reports such as KNMI'21 will lead to different scenarios.

Wave run-up/overtopping For the failure mechanism wave run-up and overtopping, the interaction between the wind speed and water level is taken to be independent. It should be investigated if this is has a big effect on the accuracy of the wave run-up/overtopping calculations. Mainly because, in practise, there most definitely is some interference between the two parameters.

The second point is to look into multiple wind directions. This is briefly discussed in this thesis but could be improved and enlarged. The addition of foreshore calculations makes it possible to take into account more locations around the Haringvliet and Holland Diep. For a more detailed view of the whole study area, this can be included.

Before that is done a good investigation should be done to the usefulness of fragility curves for wave run-up/overtopping. There are already other models available that do give accurate results. In this thesis wave run-up/overtopping is mainly used to get an understanding of how fragility curves can be used to calculate the residual lifetime. It is better to focus on extending the frailty curve towards other failure mechanisms

Piping At some locations, the failure probability for piping is mainly influenced by variables that are set in the WBI, such as the damping factor λ and the critical heave gradient $i_{c,h}$. In this thesis, these two values are equal for all the different locations. A more detailed value for those two variables can increase the accuracy of the piping failure probability and could be looked at.

Bibliography

[1] Zuiderzeewerken, 2005. URL https://nl.wikipedia.org/wiki/Markermeer{#}/media/Bestand:Zuiderzeewerken-NL.png.

[2] Technische adviescommissie voor de waterkeringen. *Leidraad voor het ontwerpen van rivierdijken*. Uitgeverij Waltman, Delft, 1989. ISBN 9021231689.

[3] Michaël Baudin, Anne Dutfoy, Bertrand Iooss, and Anne-Laure Popelin. OpenTURNS: An industrial software for uncertainty quantification in simulation. 2015.

[4] K. Bischiniotis, W. Kanning, S. N. Jonkman, and M. Kok. Cost-optimal design of river dikes using probabilistic methods. *Journal of Flood Risk Management*, 11:S1002–S1014, feb 2018. ISSN 1753318X. doi: 10.1111/jfr3.12277. URL http://doi.wiley.com/10.1111/jfr3.12277.

[5] D Božić, C Bus, R Hobbelen, and M Pouw. Eerste Beoordeling Primaire Keringen Overstromingkans Colofon. (september), 2019.

[6] Houcine Chbab. Basisstochasten WBI-2017. 2017.

[7] John A Church, Jonathan M. Gregory, Anny Cazenave, Jonathan M Gregory, Svetlana Jevrejeva, Anders Levermann, Glenn A Milne, Antony Payne, Detlef Stammer, Jason E Box, Mark Carson, William Roland Gehrels Collins, Piers Forster, Alex Gardner, and Peter Good. IPCC 2014, Ch. 13: Sea Level Change. *Climate Change 2013: The Physical Science Basis. Contribution of Working Group I to the Fifth Assessment Report of the Intergovernmental Panel on Climate Change*, pages 1–8, 2013. doi: 10.1017/CBO9781107415324.026. URL https://www.cambridge.org/core/product/identifier/CBO9781107415324A034/type/book{_}part.

[8] J. P. De Waal. Basisrapport WBI 2017. 2016.

[9] Deltares, VNK2, and RWS WVL. Achtergrondrapport Ontwerpinstrumentarium 2014. (december 2013), 2014.

[10] Maximilian Dörrbecker. Map of the annual average discharge of Rhine and Maas 2000-2011, 2016. URL https://commons.wikimedia.org/wiki/File:Map{_}of{_}the{_}annual{_}average{_}discharge{_}of{_}Rhine{_}and{_}Maas{_}2000-2011{_}.png{#}metadata.

[11] Matthijs Duits. Gebruikershandleiding Hydra-NL. (2.4):212, 2018.

[12] Esri Nederland. AHN viewer. URL https://www.ahn.nl/ahn-viewer.

[13] Jürgen Hackl. PyRe documentation — PyRe 5.0.3 documentation, 2018. URL https://hackl.science/pyre/.

[14] IPCC. Summary for Policymakers: The Physical Science Basis. Contribution of Working Group I to the Fifth Assessment Report of the IPCC. 2013.

[15] IPCC. *CLIMATE CHANGE 2013 - AR5*. 2014. ISBN 9781107415324. doi: 10.1017/CBO9781107415324.Summary.

[16] S. N. Jonkman, A C W M Vrouwenvelder, R D J M Steenbergen, O Morales-nápoles, and J K Vrijling. Probabilistic Design: Risk and Reliability Analysis in Civil Engineering. page 271, 2016.

[17] S.N. Jonkman, T. Schweckendiek, R.E. Jorissen, and J.P. van den Bos. Flood Defences. page 141, 2017. ISSN 02613131.

[18] KNMI. *Klimaat in de 21e eeuw Vier scenario's voor Nederland*. Koninklijk Nederlands Meteorologisch Instituut, De Bilt, 2006.

[19] M. Kok, R. Jongejan, M. Nieuwjaar, and I. Tanczos. Grondslagen voor hoogwaterbescherming. *ISBN/EAN: 978-90-8902-151-9*, 2016. URL https://repository.tudelft.nl/islandora/object/uuid:2c3abd19-7a30-40af-b537-f491a33ba66fhttps://repository.tudelft.nl/islandora/object/uuid{%}3A2c3abd19-7a30-40af-b537-f491a33ba66f.

[20] Otto Levelt and Nathalie Asselman. Uitwerking methode voor bepaling kostenreductie rivierverruiming. (November 2017):70, 2016. doi: 10.13140/RG.2.2.16817.89448.

[21] B Los. Achtergrondrapport dijken Stabiliteit en piping. 2019.

[22] Ministerie van Infrastructuur en Milieu. Regeling veiligheid primaire waterkeringen 2017 Bijlage II Voorschriften bepaling hydraulische belasting primaire waterkeringen. 2017.

[23] Ministerie van Infrastructuur en Milieu. Regeling veiligheid primaire waterkeringen 2017 Bijlage III Sterkte en veiligheid. Technical report, 2017.

[24] Ministerie van Infrastructuur en Waterstaat. Atlas voor de Leefomgeving, 2020. URL https://www.atlasleefomgeving.nl/kaarten?config=3ef897de-127f-471a-959b-93b7597de188{&}gm-x=311468.8{&}gm-y=274198.3999999999{&}gm-z=2{&}gm-b=1544180834512,true,1;1553245383594,true,0.8;.

[25] T. Pullen, N.W.H. Allsop, T. Bruce, A. Kortenhaus, H. Schüttrumpf, and J.W. Van der Meer. EurOtop, European Overtopping Manual - Wave overtopping of sea defences and related structures: Assessment manual. *also published as Special Volume of Die Küste*, 2007. URL https://repository.tudelft.nl/islandora/object/uuid{%}3Ab1ba09c3-39ba-4705-8ae3-f3892b0f2410.

[26] RWS. https://beeldbank.rws.nl, Rijkswaterstaat / Afdeling Multimedia Rijkswaterstaat, 1953.

[27] RWS. Schematiseringshandleiding piping. (available at Ministerie van Infrastructuur en Milieu), 2017.

[28] RWS WVL. Helpdesk Water, 2019. URL https://www.helpdeskwater.nl/onderwerpen/waterveiligheid/primaire/beoordelen/.

[29] S Solomon, M Manning, M Marquis, and D Qin. Climate change 2007-the physical science basis: Working group I contribution to the fourth assessment report of the IPCC. 2007. URL https://books.google.com/books?hl=nl{&}lr={&}id=8-m8nXB8GB4C{&}oi=fnd{&}pg=PA339{&}dq=climate+change+2007+the+scientific+basis{&}ots=hAlrA4pdG2{&}sig=VjRXnBERRoLYiK5ZDe6zpp5hMcA.

[30] Jan Stijnen and Nadine Slootjes. Eerste verkenning Waterveiligheid Rijnmond-Drechtsteden. Technical report, 2010. URL http://afsluitbaaropenrijnmond.tudelft.nl/fileadmin/UD/MenC/Support/Internet/TU{_}Website/TU{_}Delft{_}portal/Onderzoek/Infrastructure/Engineering{_}challenges/open{_}en{_}afsluitbaar{_}Rijnmond/doc/AOR{_}{_}Waterveiligheid{_}Rijnmond-Drechsteden{_}{_}JStijnen{_}NSlootjes,{_}TUD{_}RCP.

[31] Thomas F. Stocker, Dahe Qin, Gian Kasper Plattner, Melinda M.B. Tignor, Simon K. Allen, Judith Boschung, Alexander Nauels, Yu Xia, Vincent Bex, and Pauline M. Midgley. *Climate change 2013 the physical science basis: Working Group I contribution to the fifth assessment report of the intergovernmental panel on climate change*, volume 9781107057. Cambridge University Press, Cambridge, 2013. ISBN 9781107415324. doi: 10.1017/CBO9781107415324. URL http://ebooks.cambridge.org/ref/id/CBO9781107415324.

[32] Svasek Hydraluics and HKV lijn in Water. Vergelijking van SWAN en Bretschneider berekeningen ten behoeve van WTI2011. pages 1–19, 2011.

[33] R. 't Hart, H. de Bruijn, and G. de Vries. Fenomenologische beschrijving. page 208, 2016.

[34] TAW. Leidraad kunstwerken. Technical report, 2003.

[35] Unie van Waterschappen. Dutch water authorities, 2020. URL https://dutchwaterauthorities.com/.

[36] V.M. van Beek and G J C M Hoffmans. Evaluation of Dutch backward erosion piping models and a future perspective Evaluation of Dutch backward erosion piping models and a future. *Ewgie*, pages 97–113, 2017.

[37] Bart van den Hurk, Albert Klein Tank, Geert Lenderink, Aad van Ulden, Geert Jan van Oldenborgh, Caroline Katsman, Henk van den Brink, Franziska Keller, Janette Bessembinder, Gerrit Burgers, Gerbrand Komen, Wilco Hazeleger, and Sybren Driffhout. KNMI Climate Change Scenarios 2006 for the Netherlands. *KNMI Scientific Report WR 2006-01*, (May):1–82, 2006.

[38] Bart Van den Hurk, Peter Siegmund, Albert Klein, Tank Eds, Jisk Attema, Alexander Bakker, Jules Beersma, Janette Bessembinder, Reinout Boers, Theo Brandsma, Henk Van Den Brink, Sybren Drijfhout, Henk Eskes, Rein Haarsma, Wilco Hazeleger, Rudmer Jilderda, Caroline Katsman, Geert Lenderink, Jessica Loriaux, Erik Van Meijgaard, Twan Van Noije, Geert Jan Van Oldenborgh, Frank Selten, Pier Siebesma, Andreas Sterl, and Hylke De Vries. *KNMI ' 14 : Climate Change scenarios for the 21st Century*. Number May. 2014. doi: 10.1007/s00382-009-0721-6. URL http://www.climatescenarios.nl/images/KNMI{_}WR{_}2014-01{_}version26May2014.pdfhttp://www.klimaatscenarios.nl/brochures/index.html.

[39] Jentsje W. van der Meer. Technical report wave run-up and wave overtopping at dikes. *Technical Advisory Committee on Flood Defence, Delft, The Netherlands*, page 43, 2002. ISSN 0923-9022 ;. URL https://repository.tudelft.nl/islandora/object/uuid:d3cb82f1-8e0b-4d85-ae06-542651472f49.

[40] Waterwet. Artikel 2.2 Waterwet. URL https://wetten.overheid.nl/jci1.3:c:BWBR0025458{&}hoofdstuk=2{&}paragraaf=2{&}artikel=2.2{&}z=2018-07-01{&}g=2018-07-01.

[41] K. Wojciechowska, G. Pleijter, M. Zethof, F.J. Havinga, D.H. Van Haaren, and W.L.A. Ter Horst. Application of Fragility Curves in Operational Flood Risk Assessment. *Geotechnical Safety and Risk V*, pages 524–529, 2015. doi: 10.3233/978-1-61499-580-7-524.

[42] WSBD. Waterschap Brabantse Delta, 2019.

[43] WSHD. Waterschap Hollandse Delta, 2019.

Appendices

A

Fragility curves and Residual lifetime for scenarios G and W+

This appendix shows the results of the fragility curve method towards residual lifetime. The residual lifetime is given separate for wave run-up/overtopping and piping.

A.1. Dike stretch 20-4

A.1.1. 20-04-0074

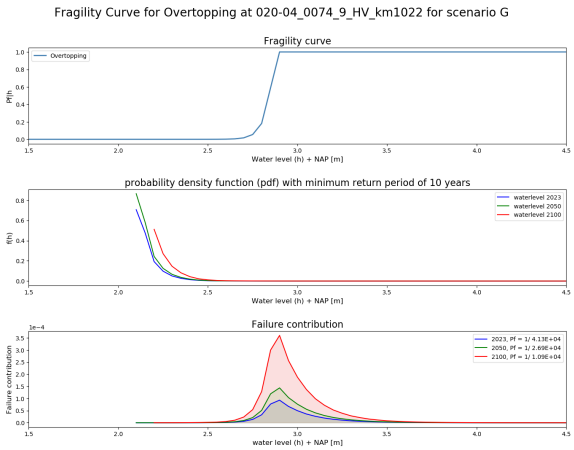

Figure A.1: GEKB FC G

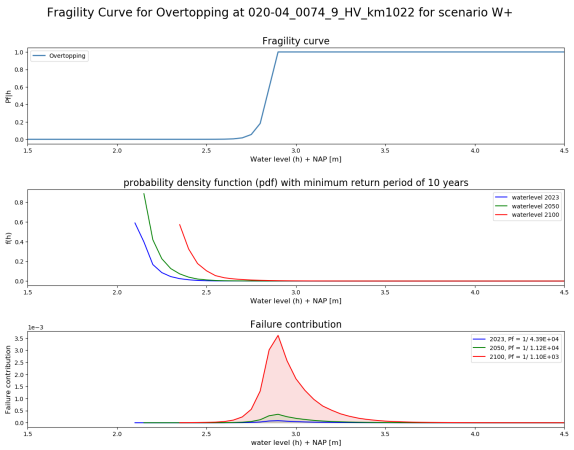

Figure A.2: GEKB FC W+

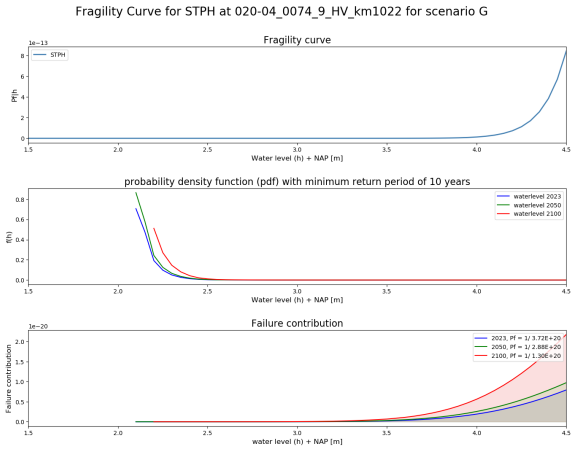

Figure A.3: STPH FC G

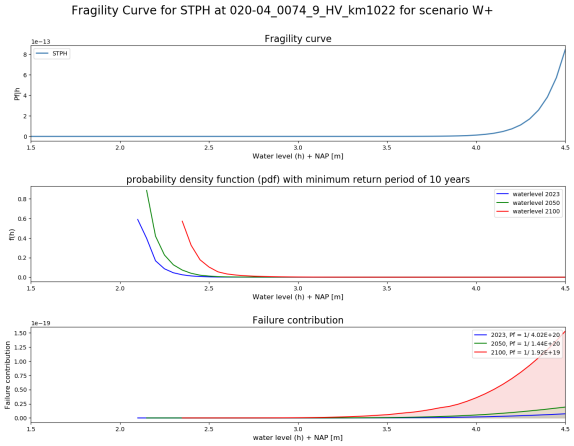

Figure A.4: STPH FC W+

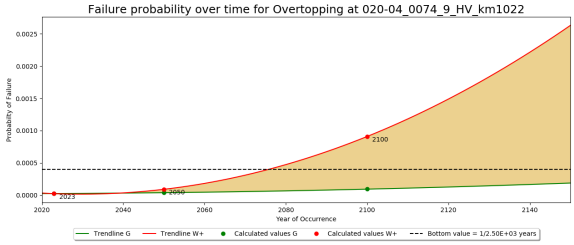

Figure A.5: Wave run-up/overtoppingResidual lifetime

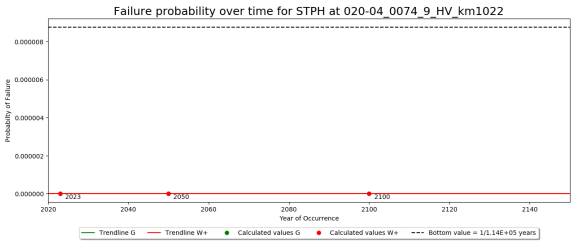

Figure A.6: Piping Residual lifetime

A.1.2. 20-04-0181

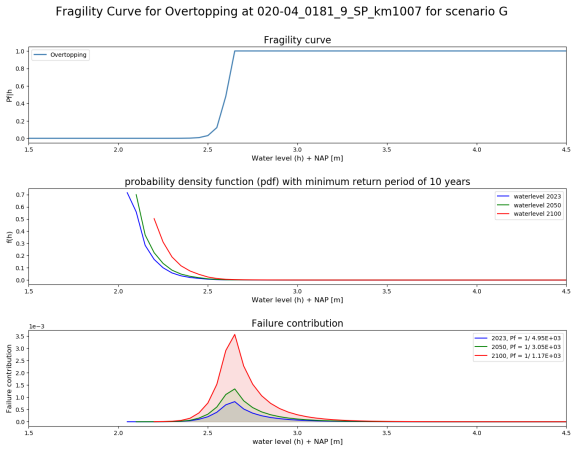

Figure A.7: GEKB FC G

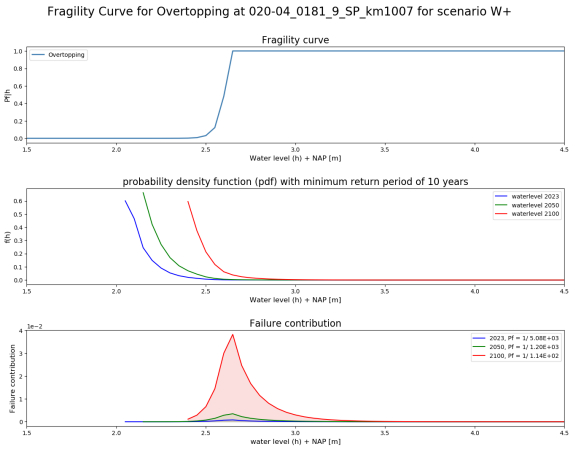

Figure A.8: GEKB FC W+

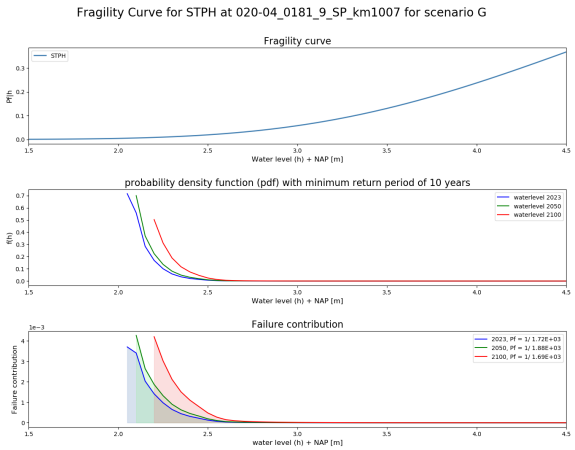

Figure A.9: STPH FC G

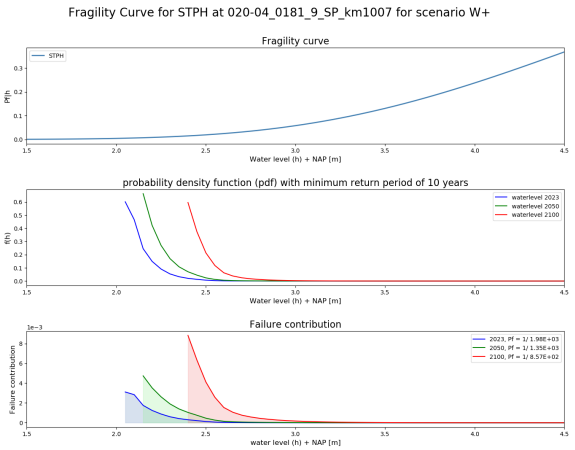

Figure A.10: STPH FC W+

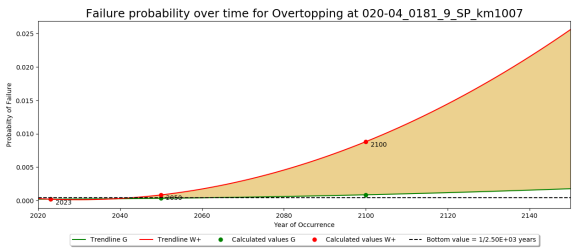

Figure A.11: Wave run-up/overtoppingResidual lifetime

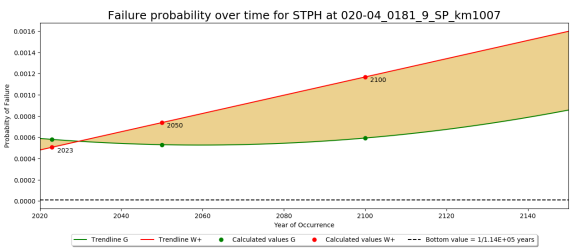

Figure A.12: Piping Residual lifetime

A.2. Dike stretch 21-2

A.2.1. 21-02-0110

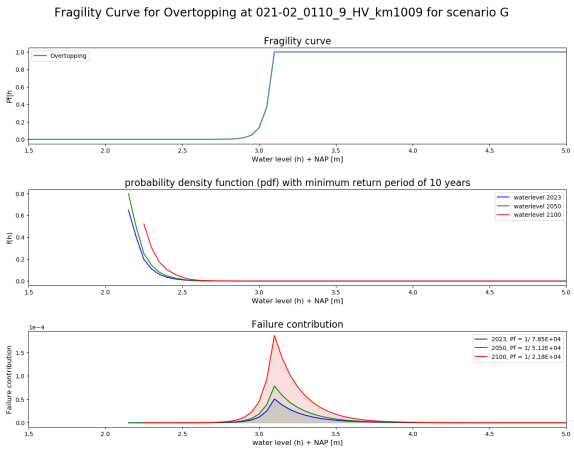

Figure A.13: GEKB FC G

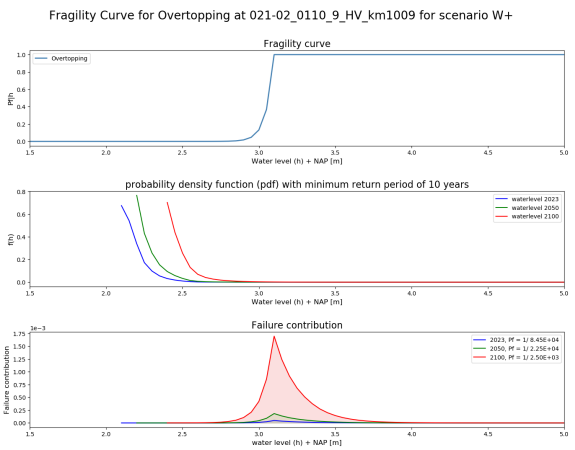

Figure A.14: GEKB FC W+

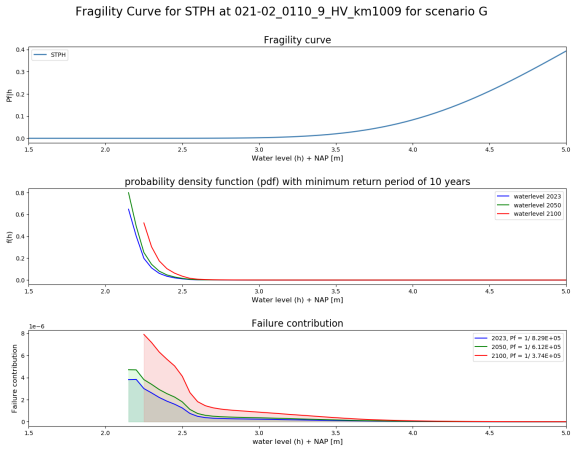

Figure A.15: STPH FC G

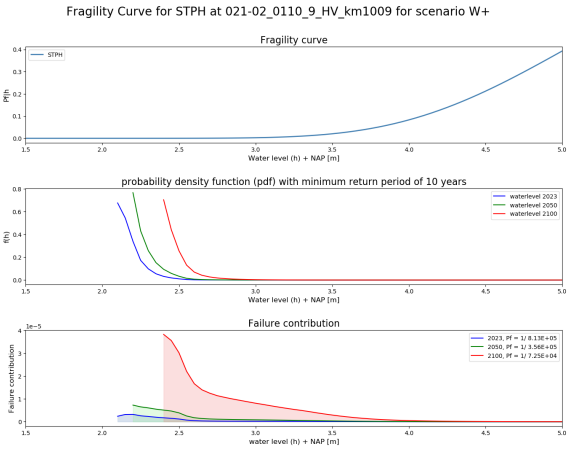

Figure A.16: STPH FC W+

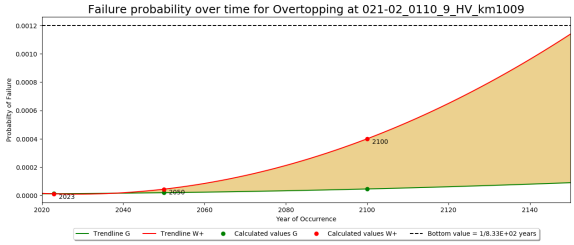

Figure A.17: Wave run-up/overtoppingResidual lifetime

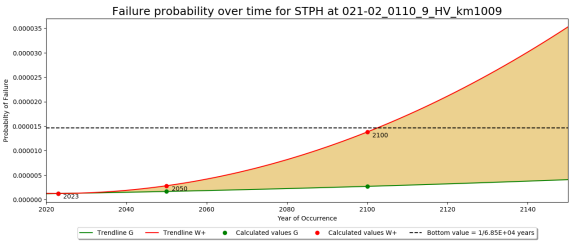

Figure A.18: Piping Residual lifetime

A.2.2. 21-02-0270

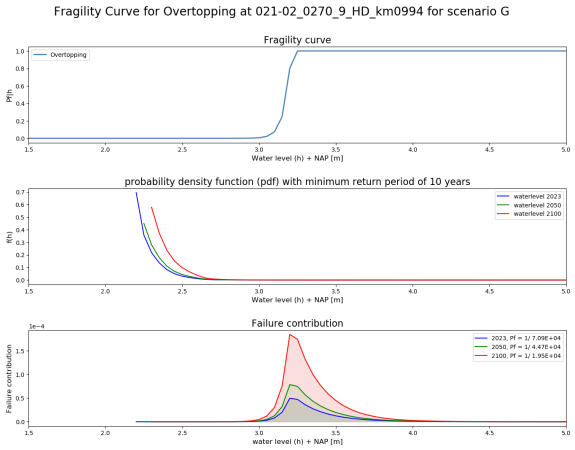

Figure A.19: GEKB FC G

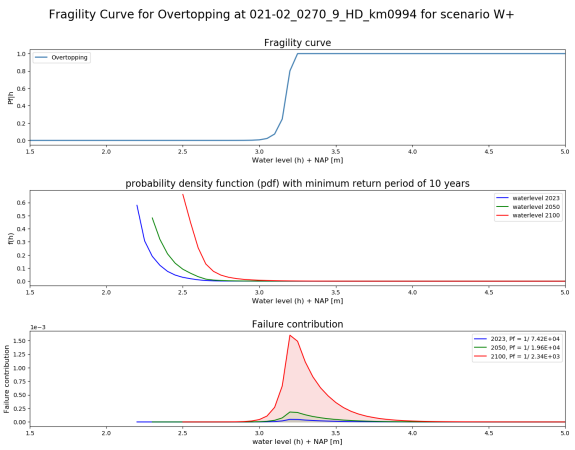

Figure A.20: GEKB FC W+

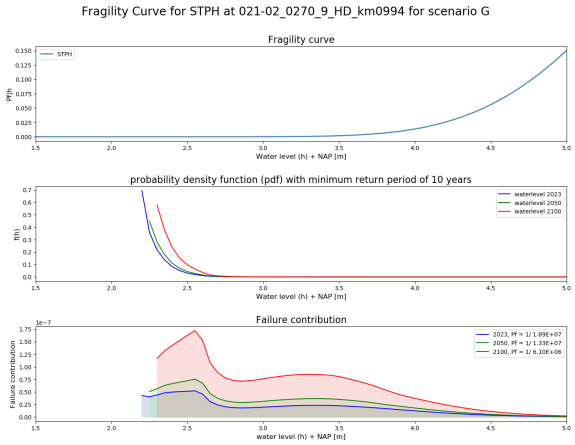

Figure A.21: STPH FC G

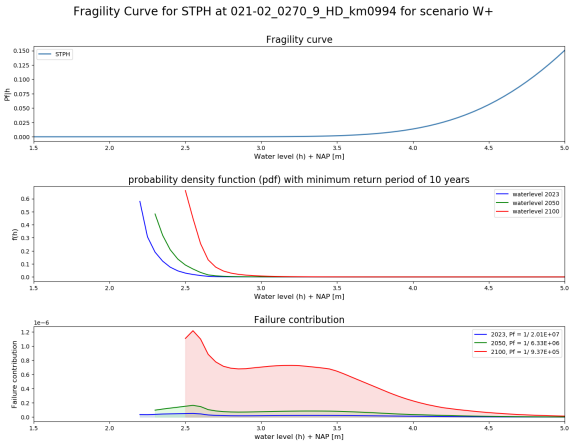

Figure A.22: STPH FC W+

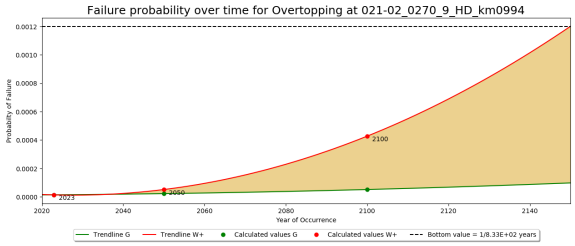

Figure A.23: Wave run-up/overtoppingResidual lifetime

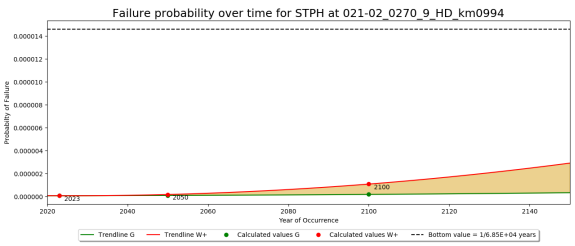

Figure A.24: Piping Residual lifetime

A.2.3. 21-02-0373

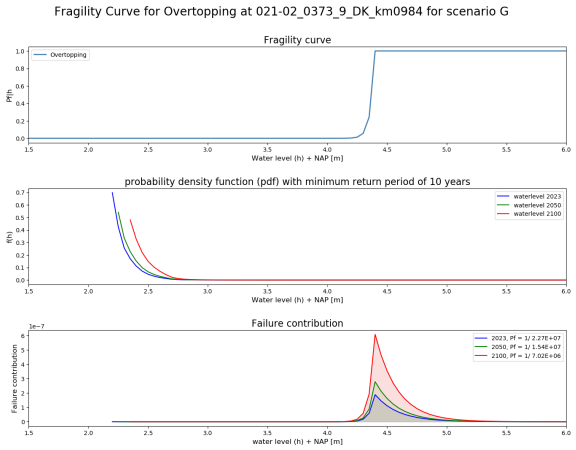

Figure A.25: GEKB FC G

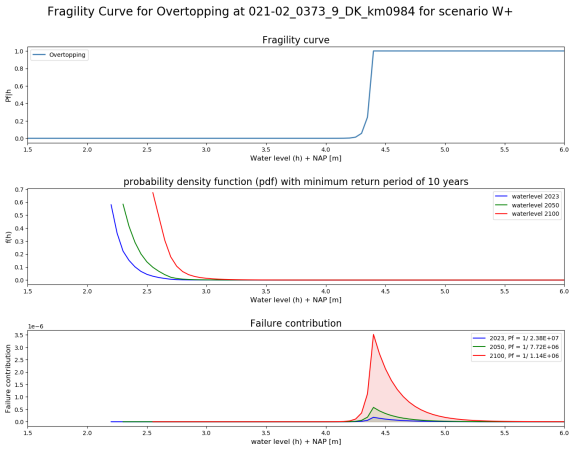

Figure A.26: GEKB FC W+

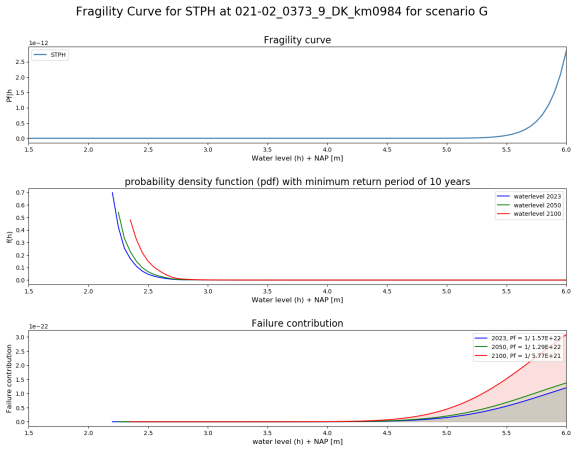

Figure A.27: STPH FC G

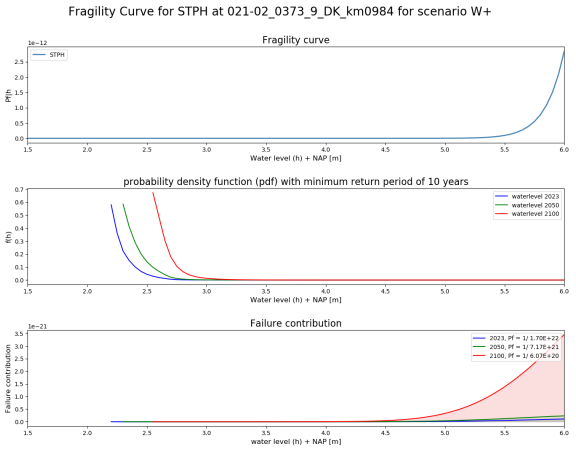

Figure A.28: STPH FC W+

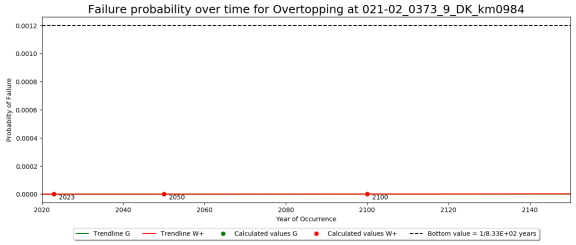

Figure A.29: Wave run-up/overtoppingResidual lifetime

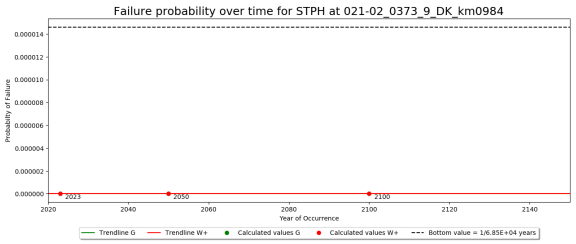

Figure A.30: Piping Residual lifetime

A.3. Dike stretch 25-2

A.3.1. 25-02-0020

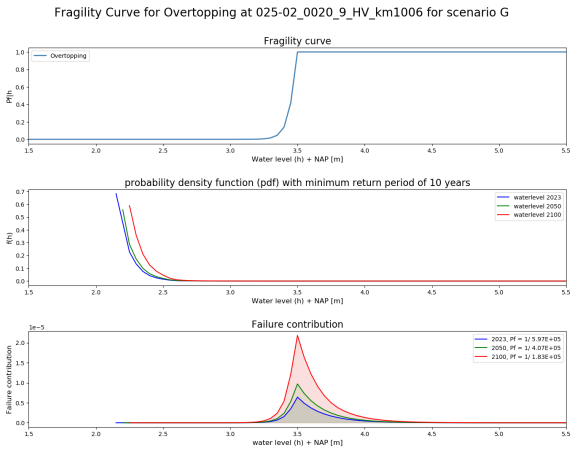

Figure A.31: GEKB FC G

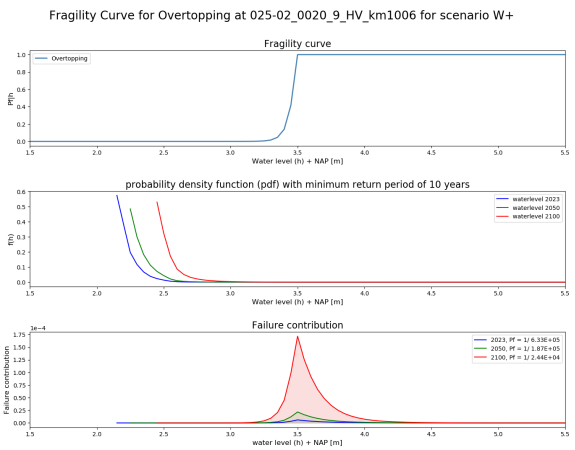

Figure A.32: GEKB FC W+

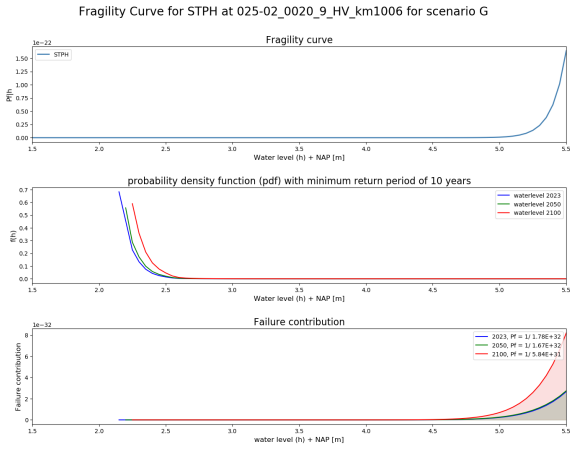

Figure A.33: STPH FC G

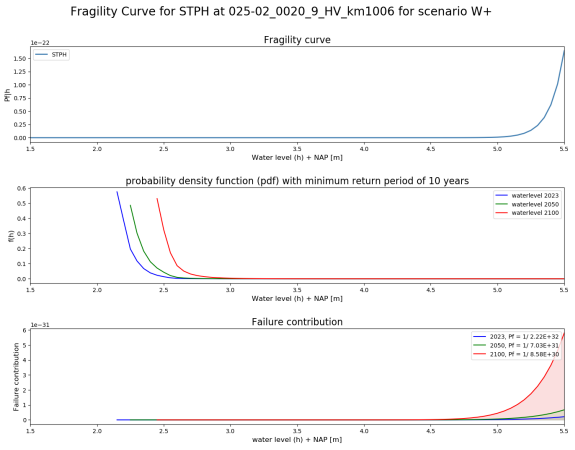

Figure A.34: STPH FC W+

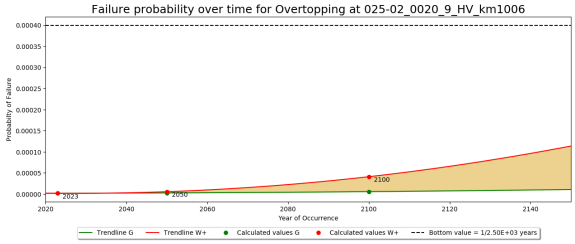

Figure A.35: Wave run-up/overtoppingResidual lifetime

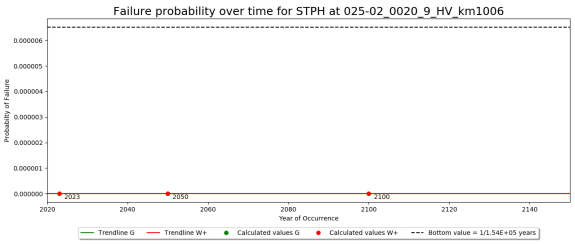

Figure A.36: Piping Residual lifetime

A.3.2. 25-02-0091

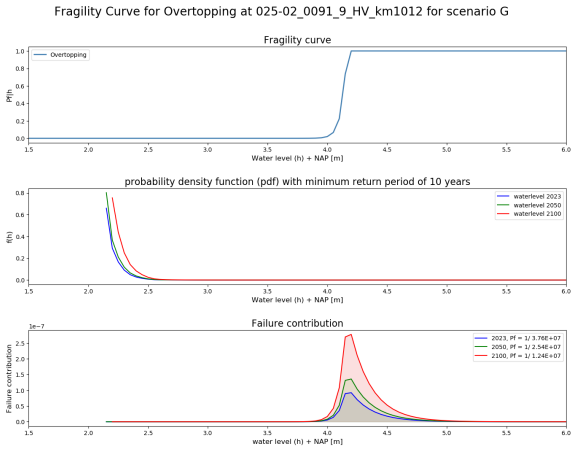

Figure A.37: GEKB FC G

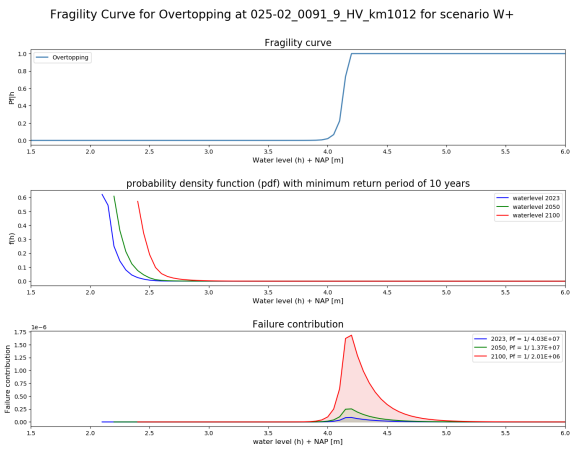

Figure A.38: GEKB FC W+

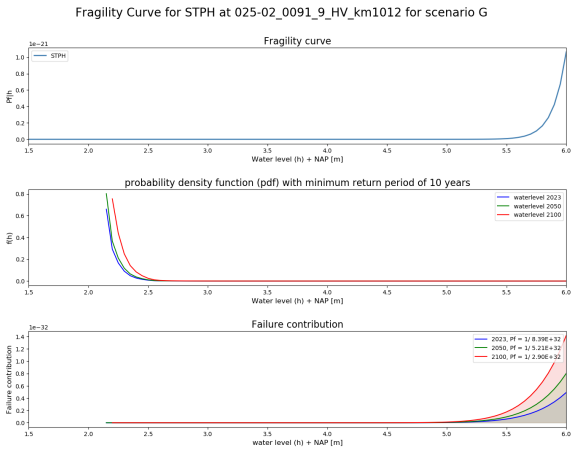

Figure A.39: STPH FC G

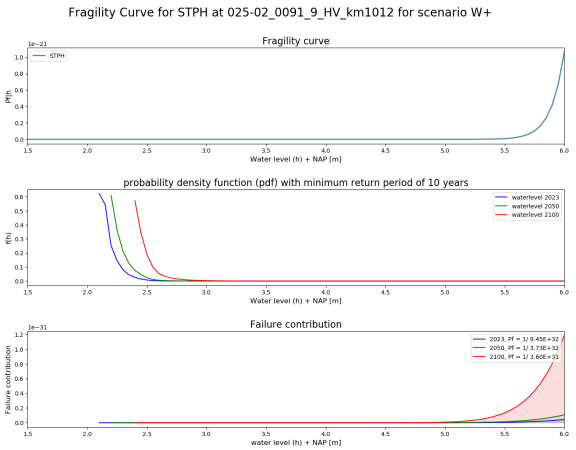

Figure A.40: STPH FC W+

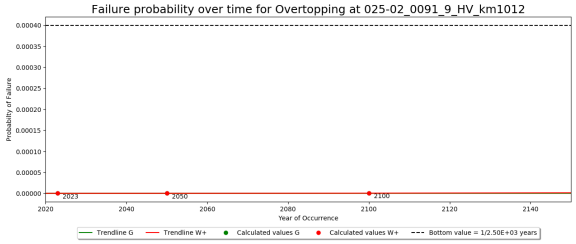

Figure A.41: Wave run-up/overtoppingResidual lifetime

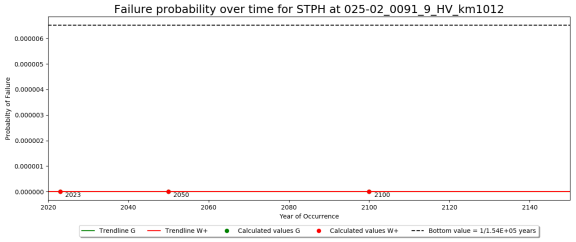

Figure A.42: Piping Residual lifetime

A.3.3. 25-02-0242

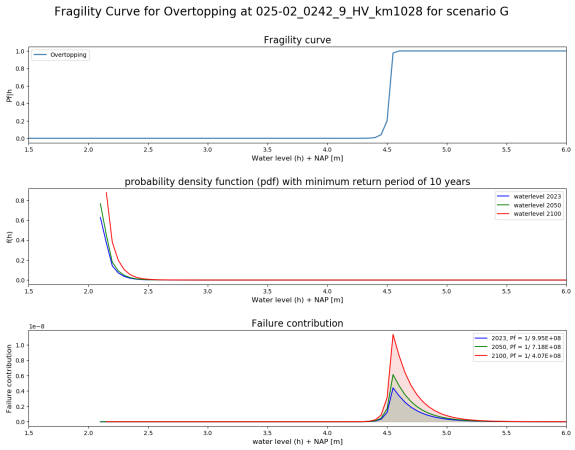

Figure A.43: GEKB FC G

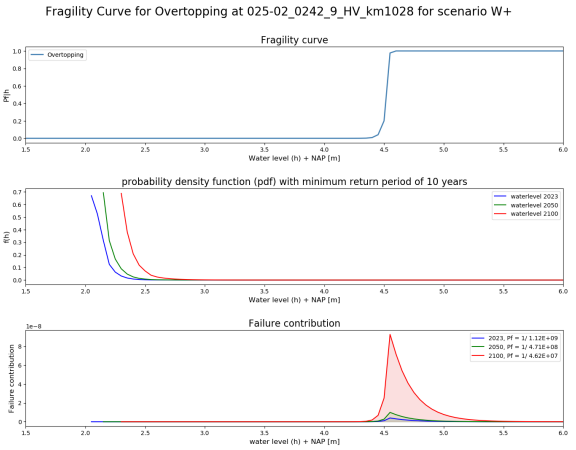

Figure A.44: GEKB FC W+

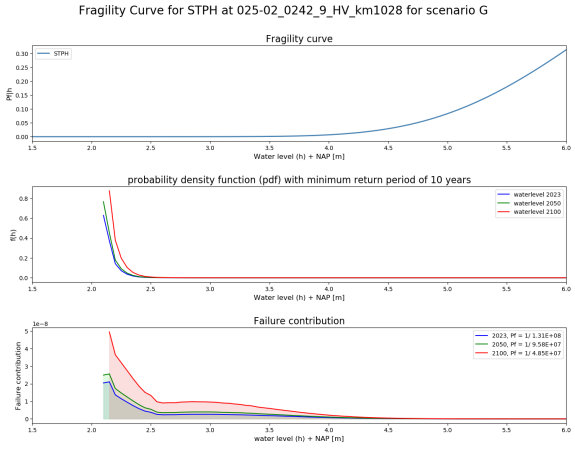

Figure A.45: STPH FC G

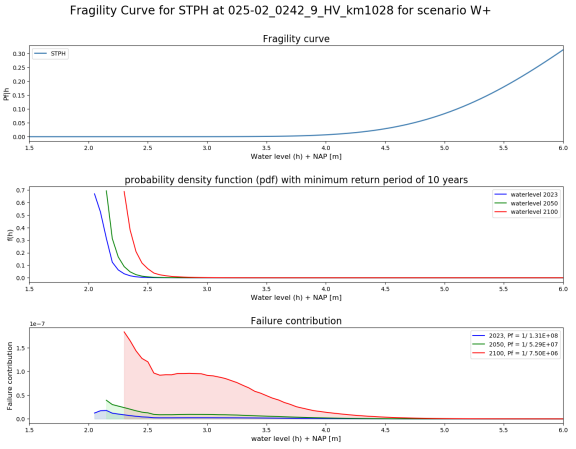

Figure A.46: STPH FC W+

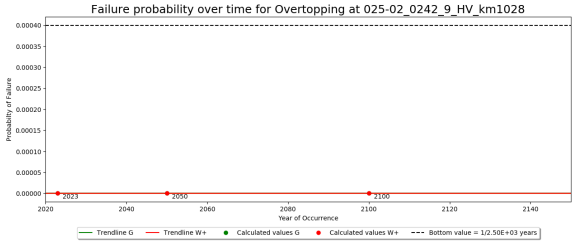

Figure A.47: Wave run-up/overtoppingResidual lifetime

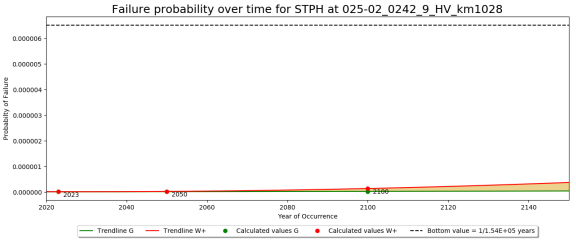

Figure A.48: Piping Residual lifetime

A.4. Dike stretch 34-2

A.4.1. 34-02-0011

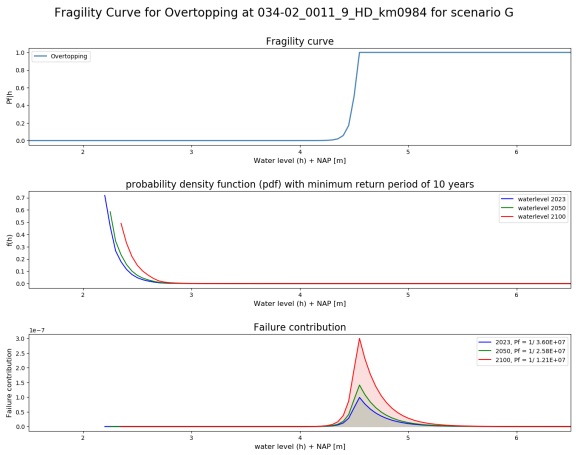

Figure A.49: GEKB FC G

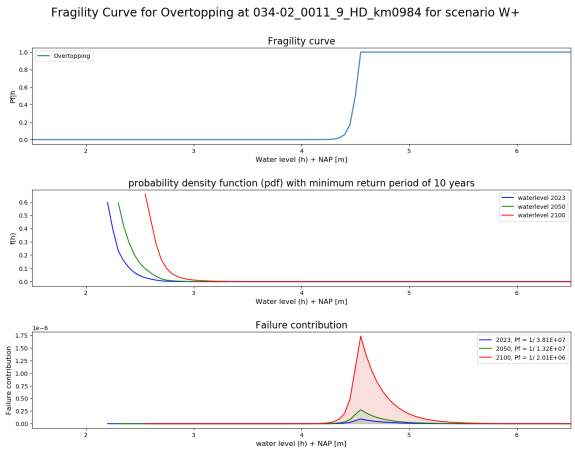

Figure A.50: GEKB FC W+

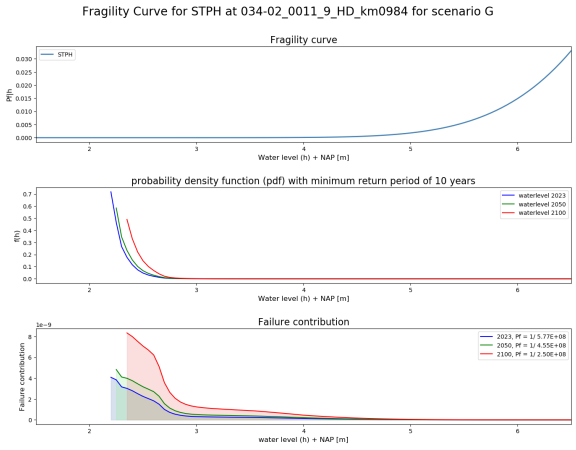

Figure A.51: STPH FC G

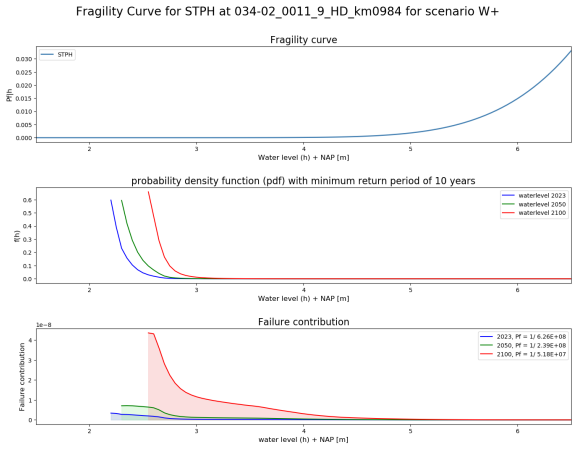

Figure A.52: STPH FC W+

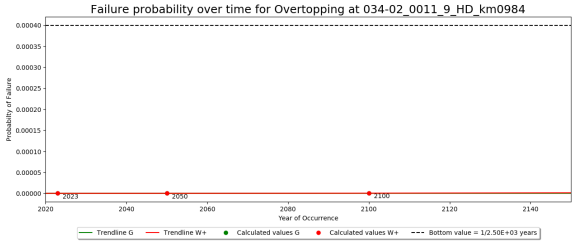

Figure A.53: Wave run-up/overtoppingResidual lifetime

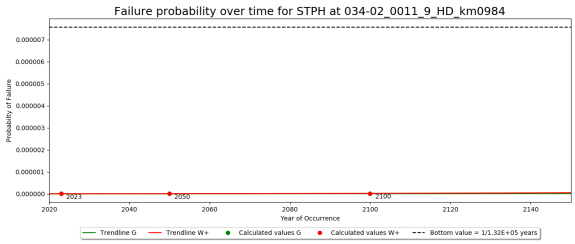

Figure A.54: Piping Residual lifetime

A.4.2. 34-02-0130

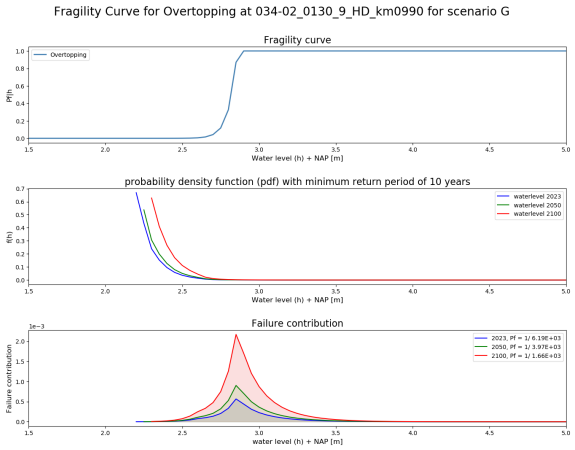

Figure A.55: GEKB FC G

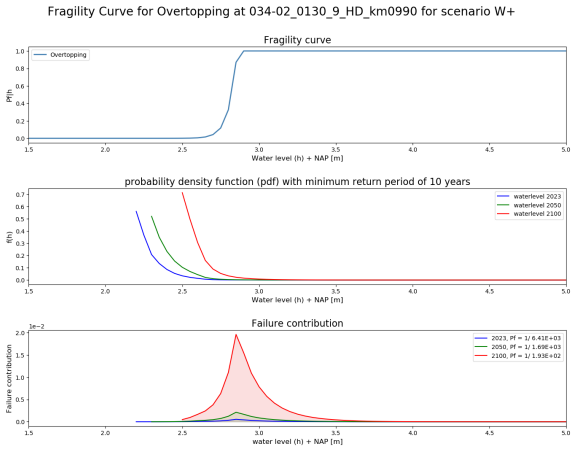

Figure A.56: GEKB FC W+

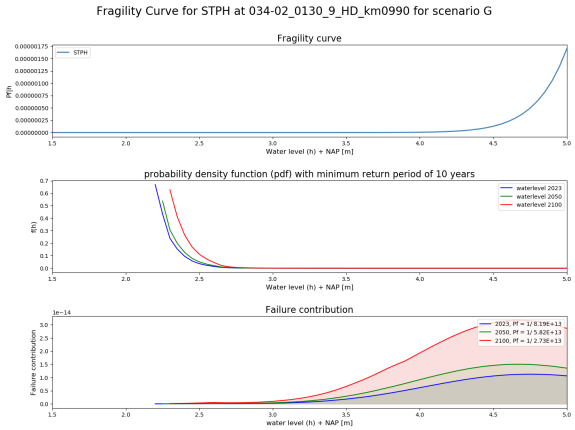

Figure A.57: STPH FC G

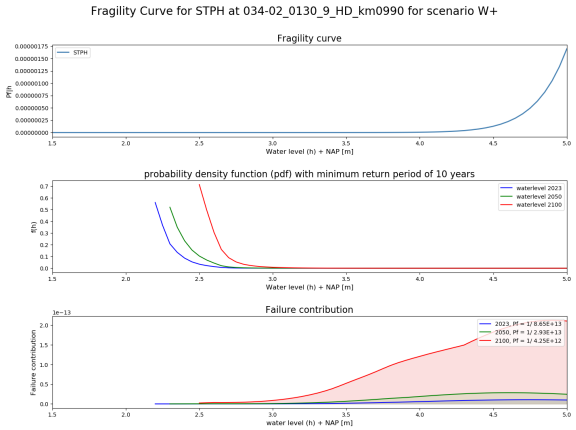

Figure A.58: STPH FC W+

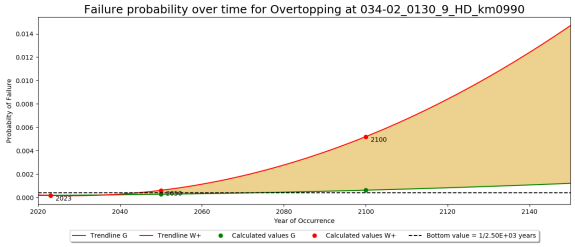

Figure A.59: Wave run-up/overtoppingResidual lifetime

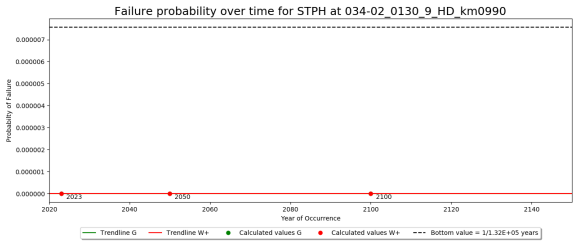

Figure A.60: Piping Residual lifetime

A.4.3. 34-02-0190

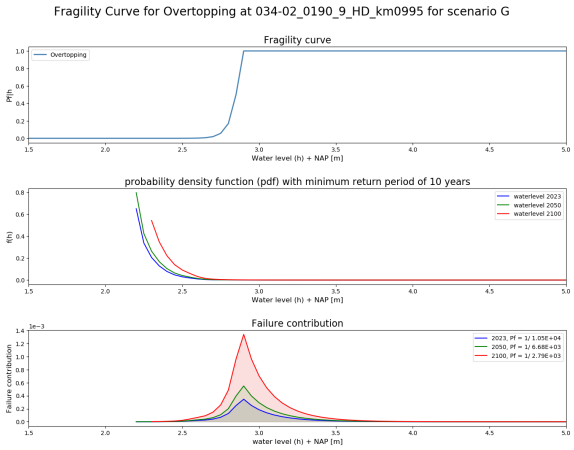

Figure A.61: GEKB FC G

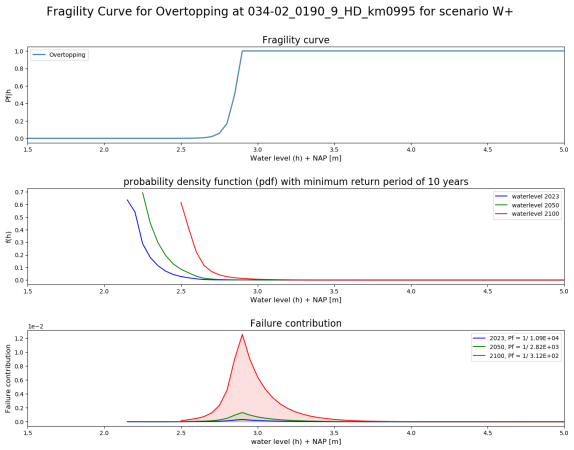

Figure A.62: GEKB FC W+

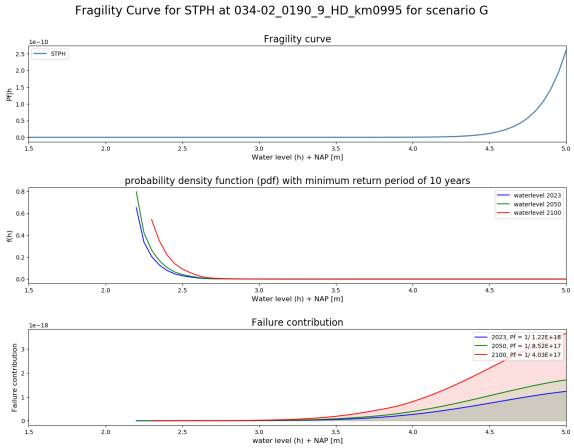

Figure A.63: STPH FC G

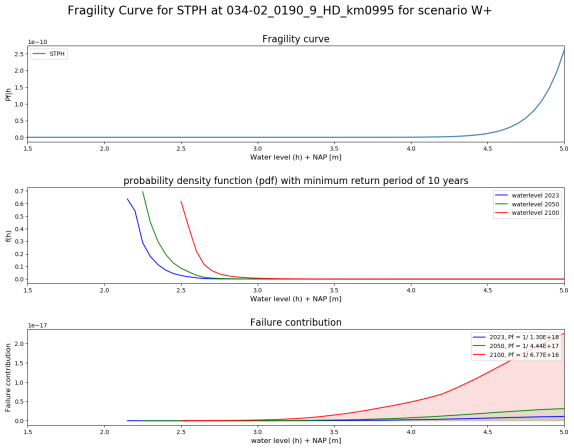

Figure A.64: STPH FC W+

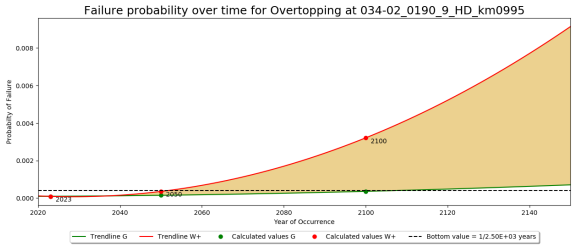

Figure A.65: Wave run-up/overtoppingResidual lifetime

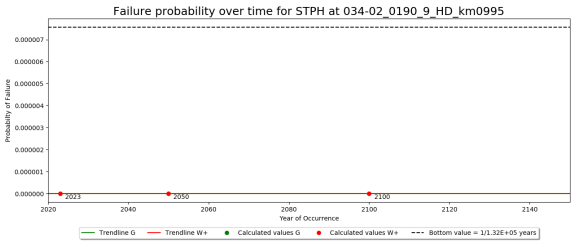

Figure A.66: Piping Residual lifetime

B

Combined Fragility curves for a dike section

B.1. Dike stretch 20-4

B.1.1. 20-04-0074

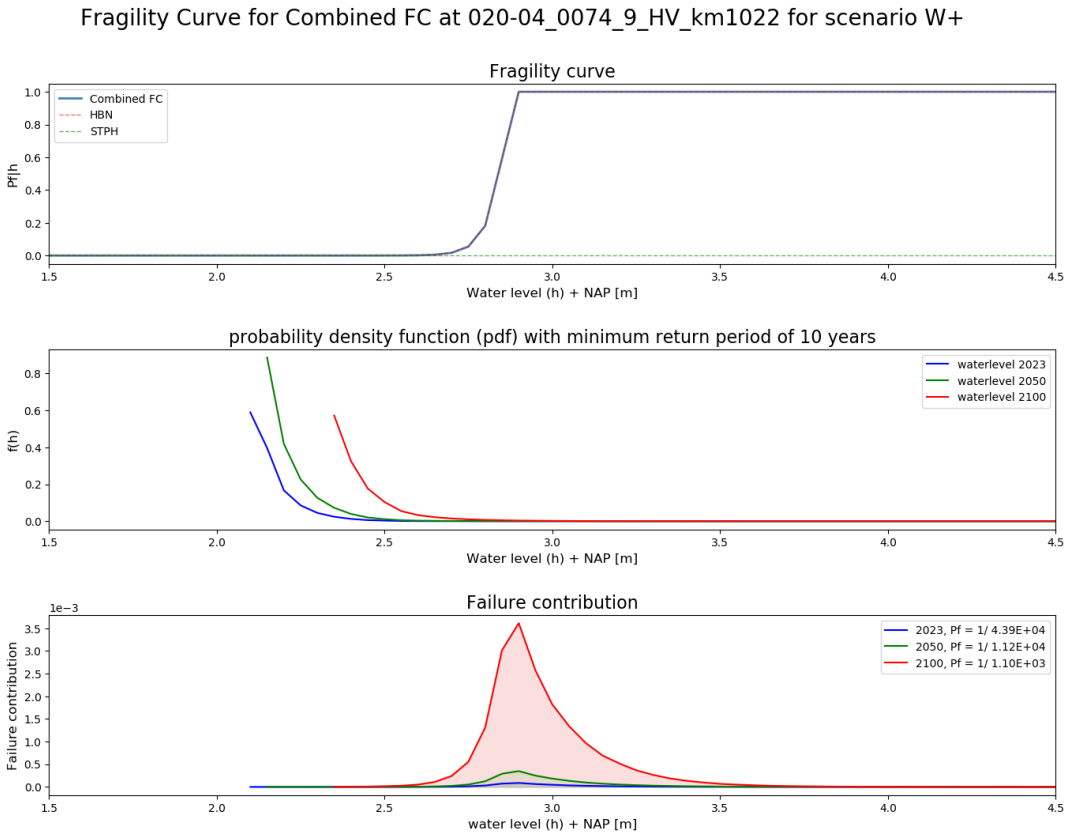

Figure B.1: Fragility Curve Combined 20-4 0074

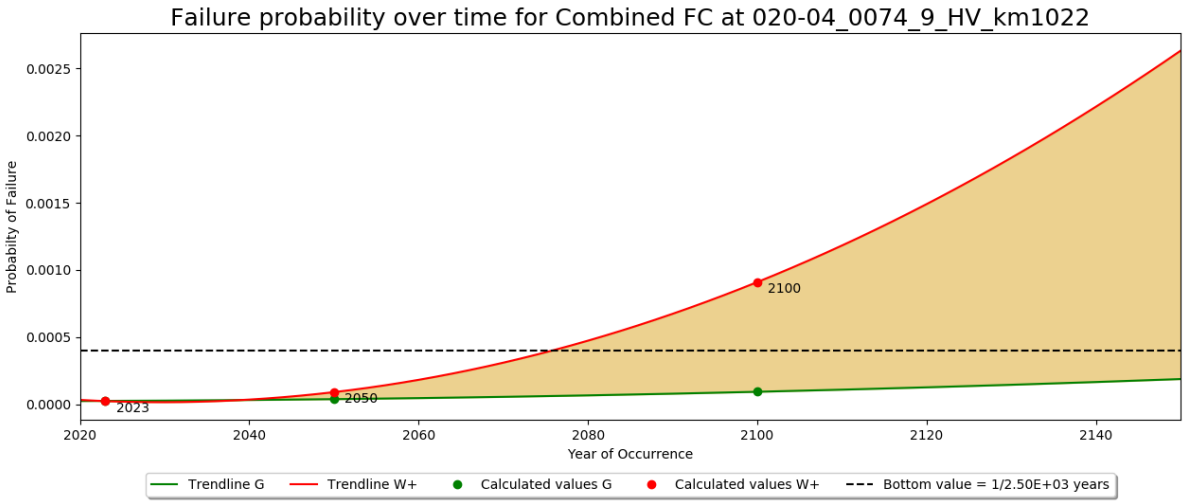

Figure B.2: Residual Lifetime for cross section 20-4 0074

B.1.2. 20-04-0181

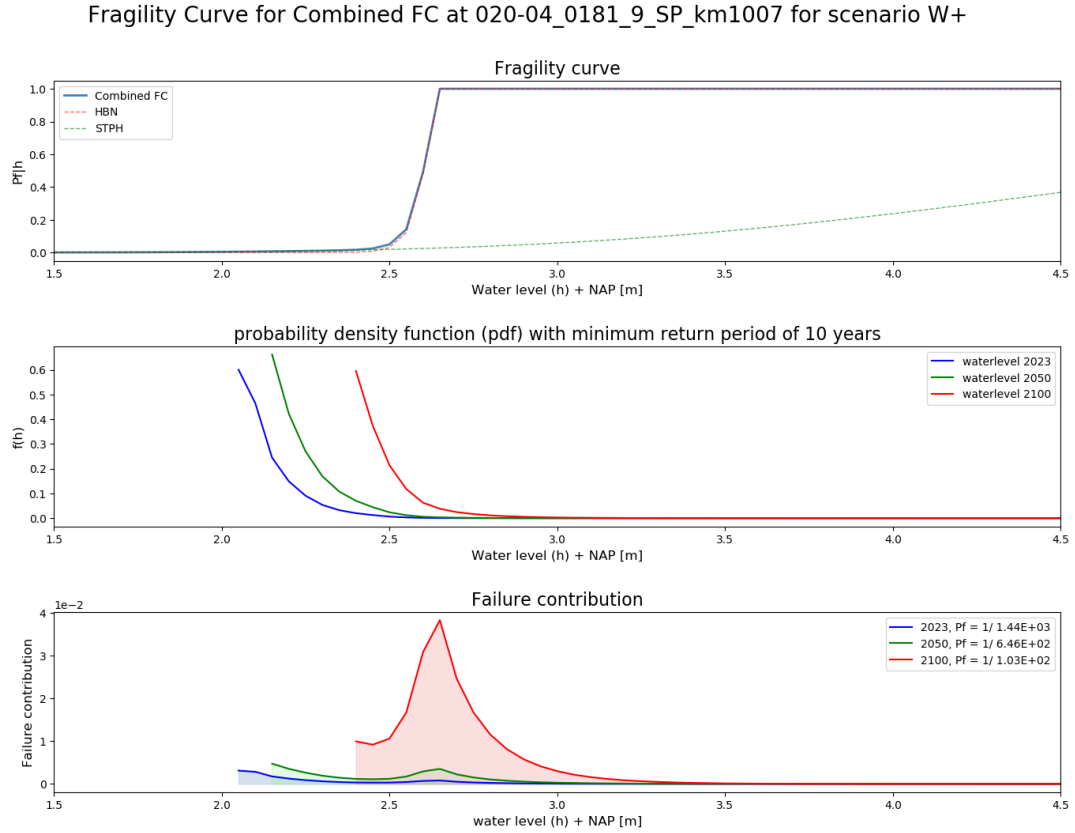

Figure B.3: Fragility Curve Combined 20-4 0181

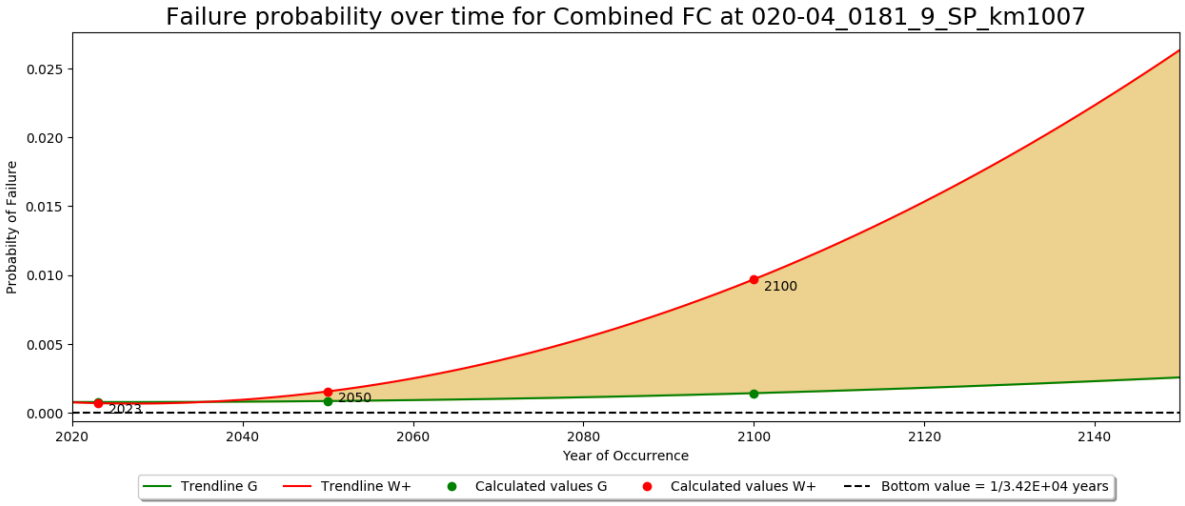

Figure B.4: Residual Lifetime for cross section 20-4 0181

B.2. Dike stretch 21-2

B.2.1. 21-02-0110

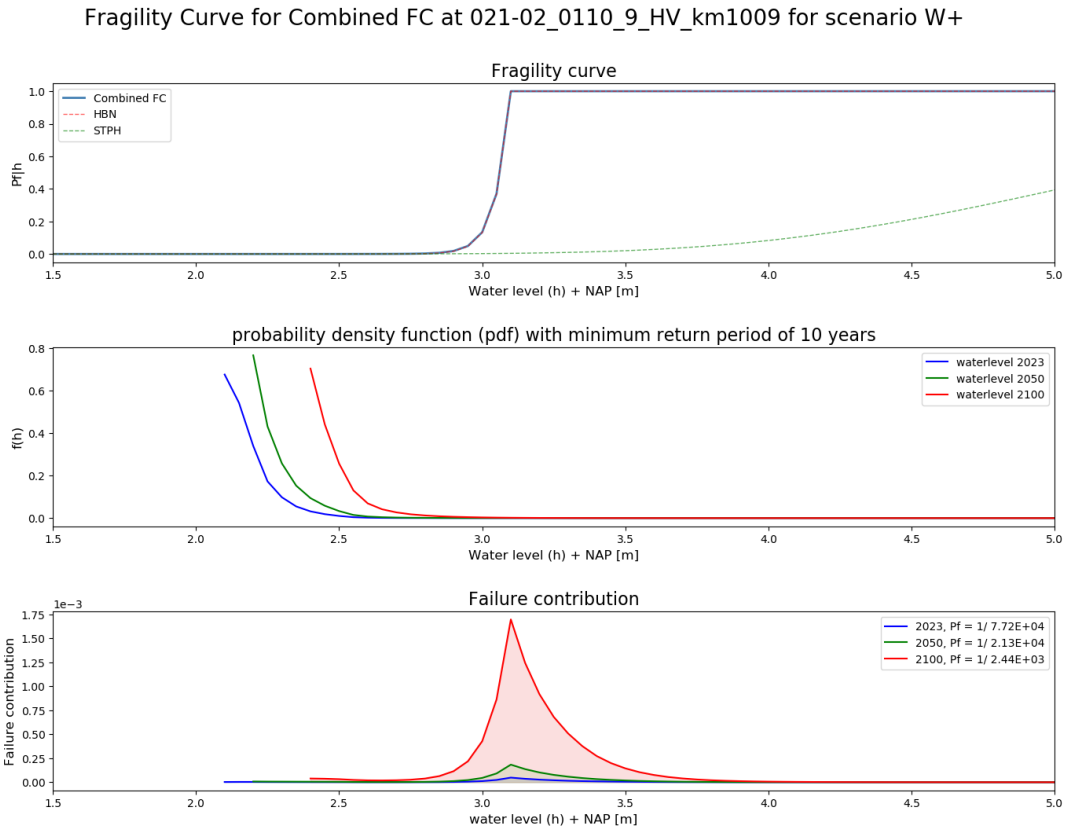

Figure B.5: Fragility Curve Combined 21-2 0110

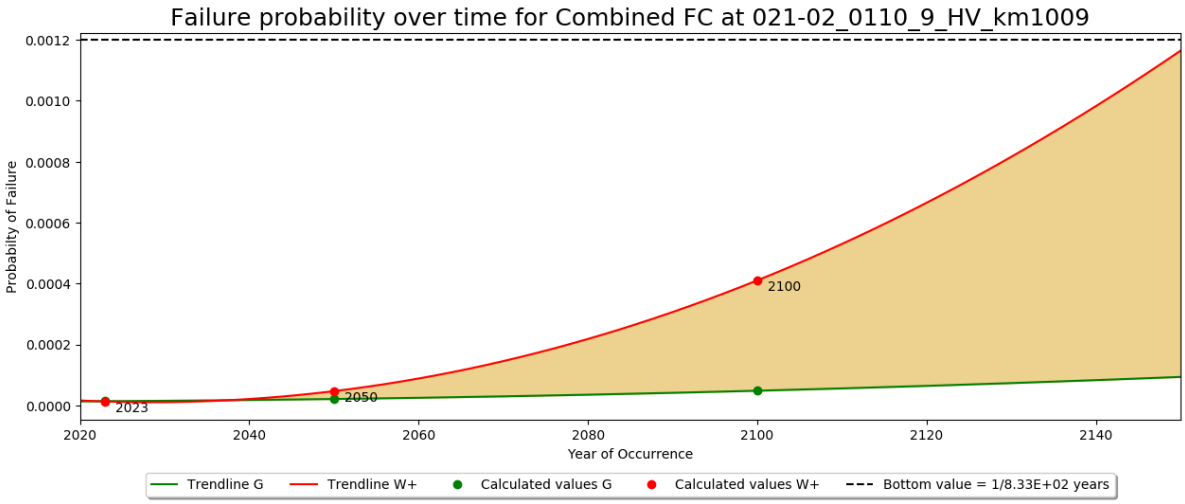

Figure B.6: Residual Lifetime for cross section 21-2 0110

B.2.2. 21-02-0270

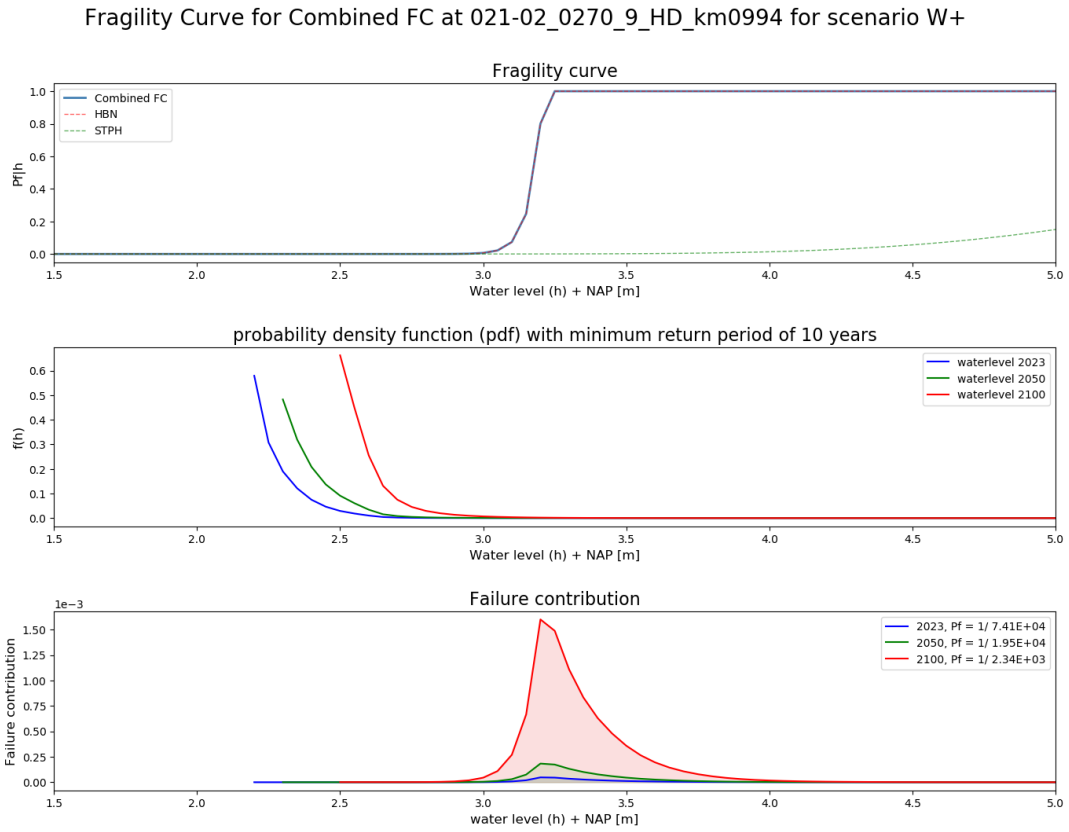

Figure B.7: Fragility Curve Combined 21-2 0270

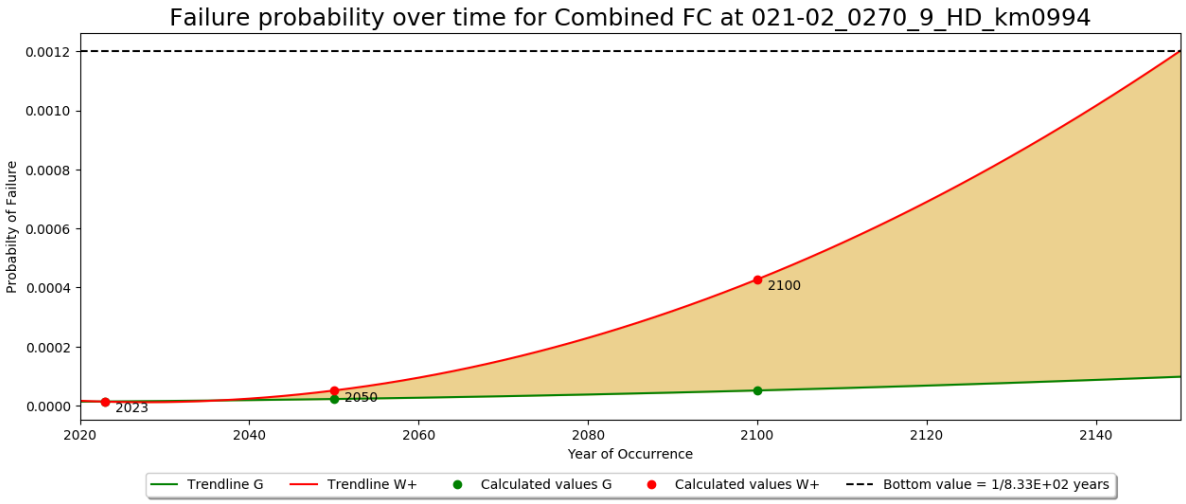

Figure B.8: Residual Lifetime for cross section 21-2 0270

B.2.3. 21-02-0373

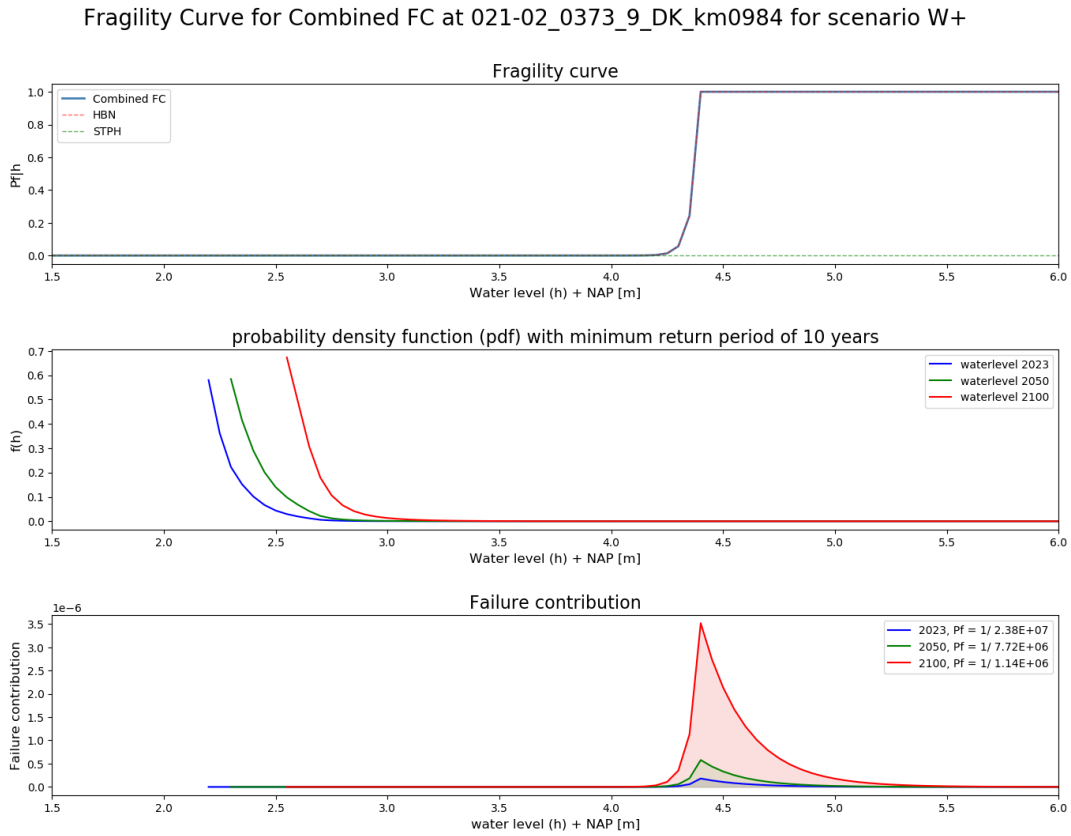

Figure B.9: Fragility Curve Combined 21-2 0373

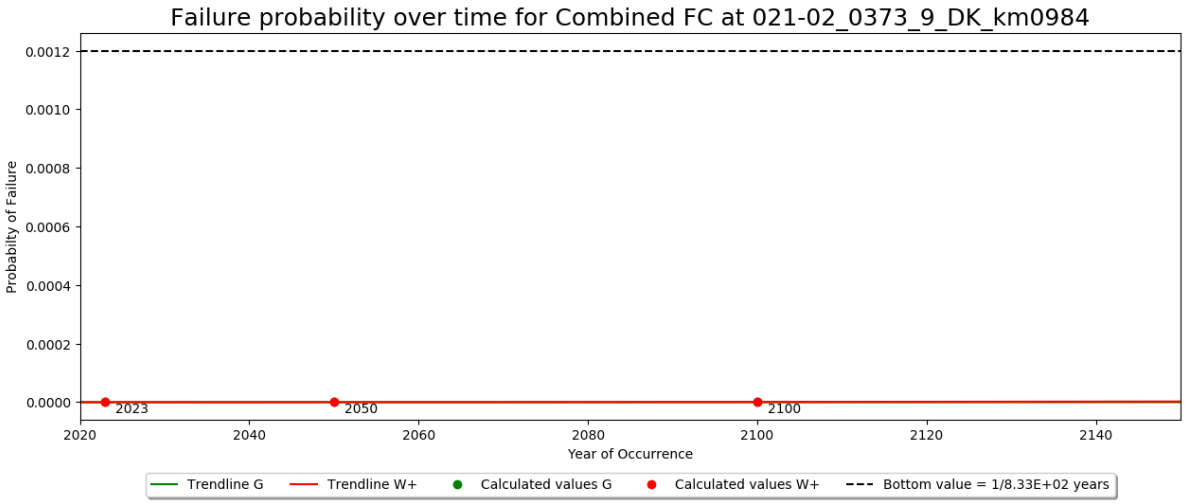

Figure B.10: Residual Lifetime for cross section 21-2 0373

B.3. Dike stretch 25-2

B.3.1. 25-02-0020

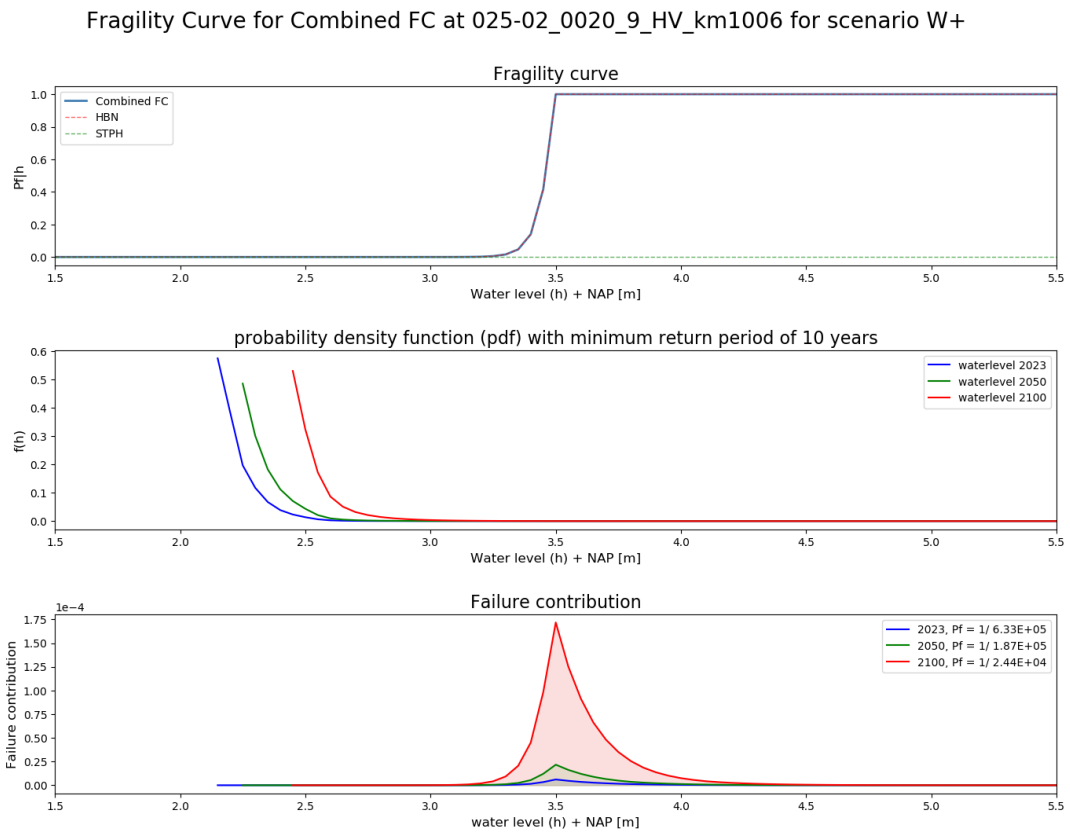

Figure B.11: Fragility Curve Combined 25-2 0020

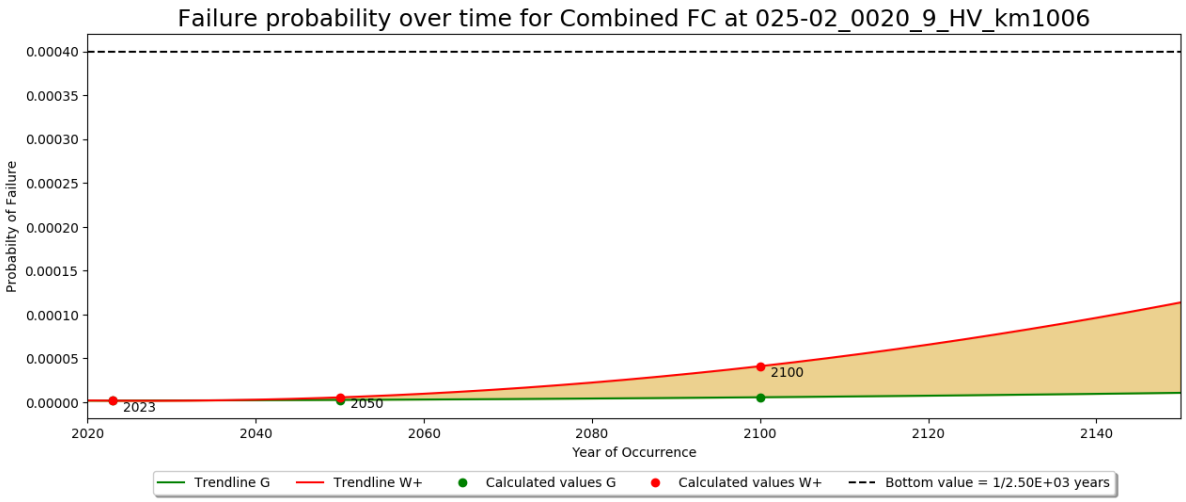

Figure B.12: Residual Lifetime for cross section 25-2 0020

B.3.2. 25-02-0091

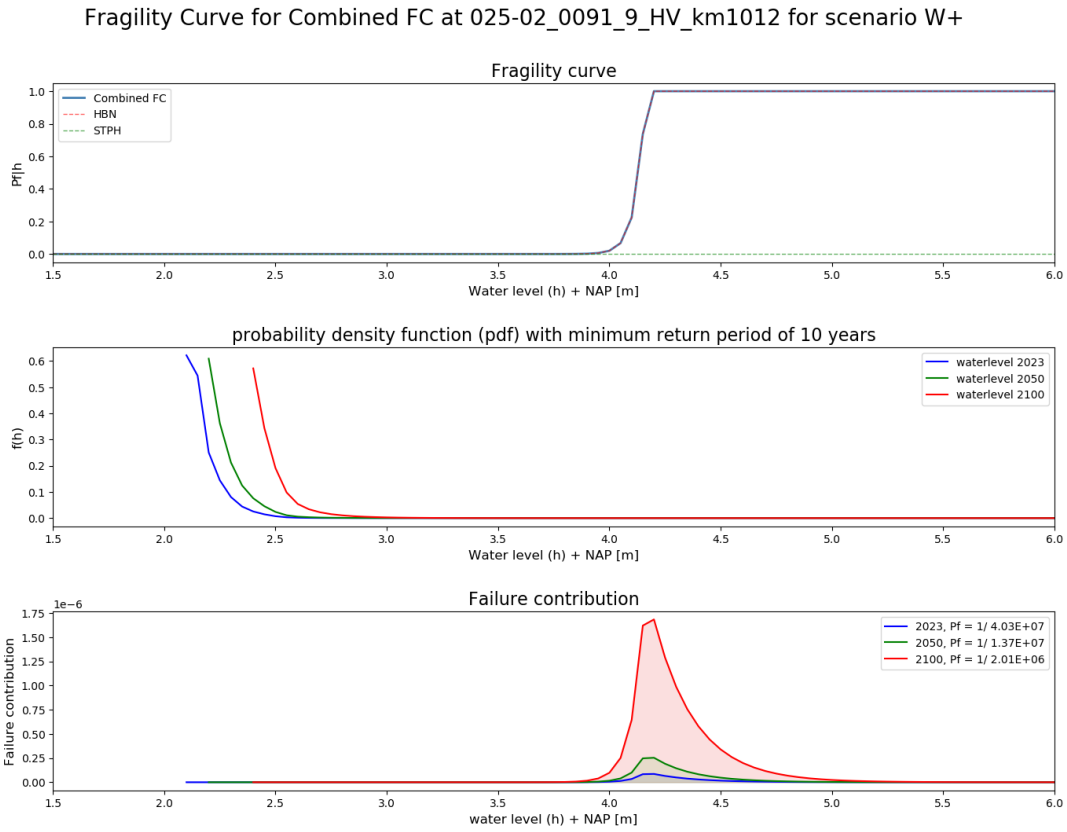

Figure B.13: Fragility Curve Combined 25-2 0091

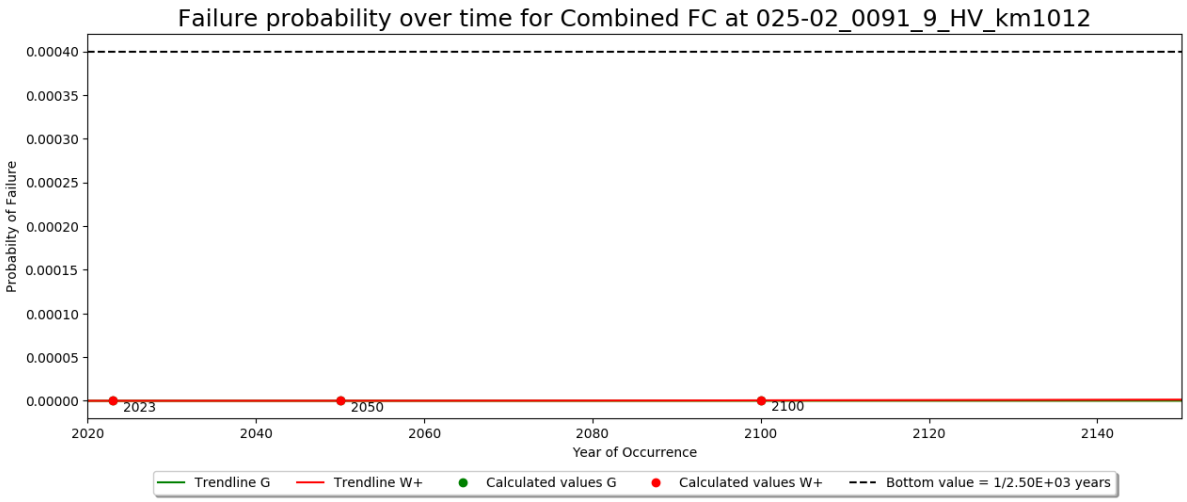

Figure B.14: Residual Lifetime for cross section 25-2 0091

B.3.3. 25-02-0242

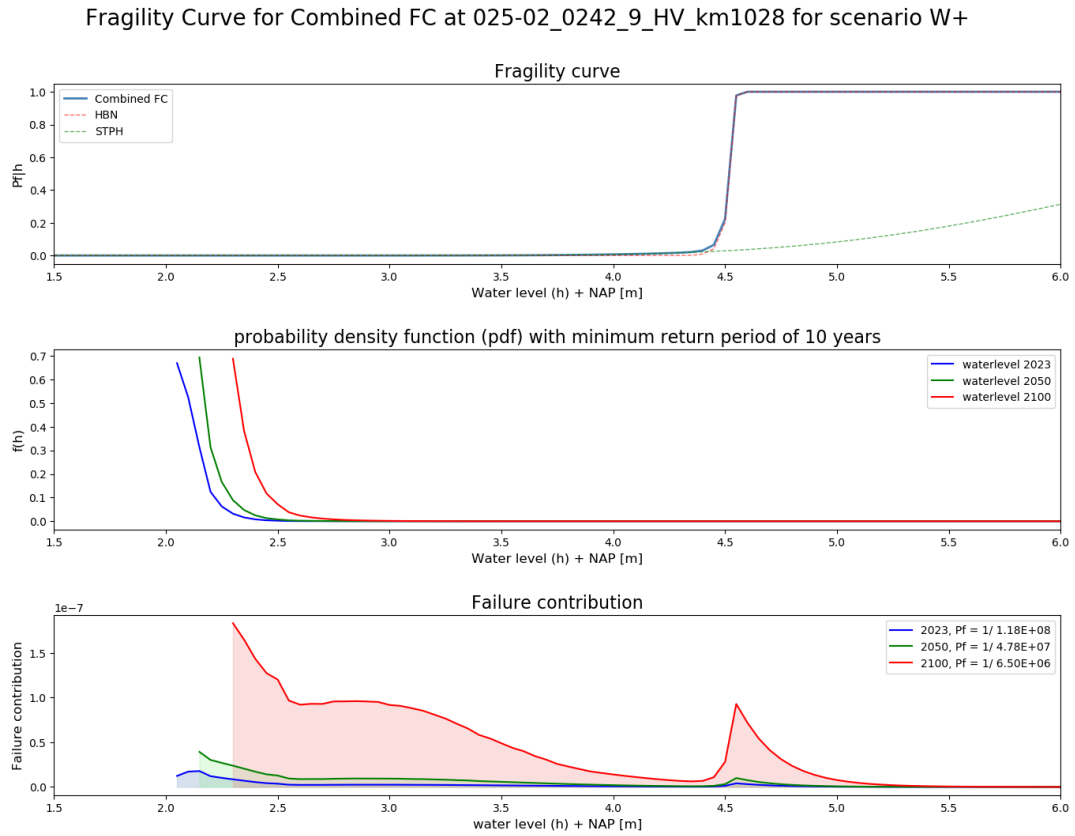

Figure B.15: Fragility Curve Combined 25-2 0242

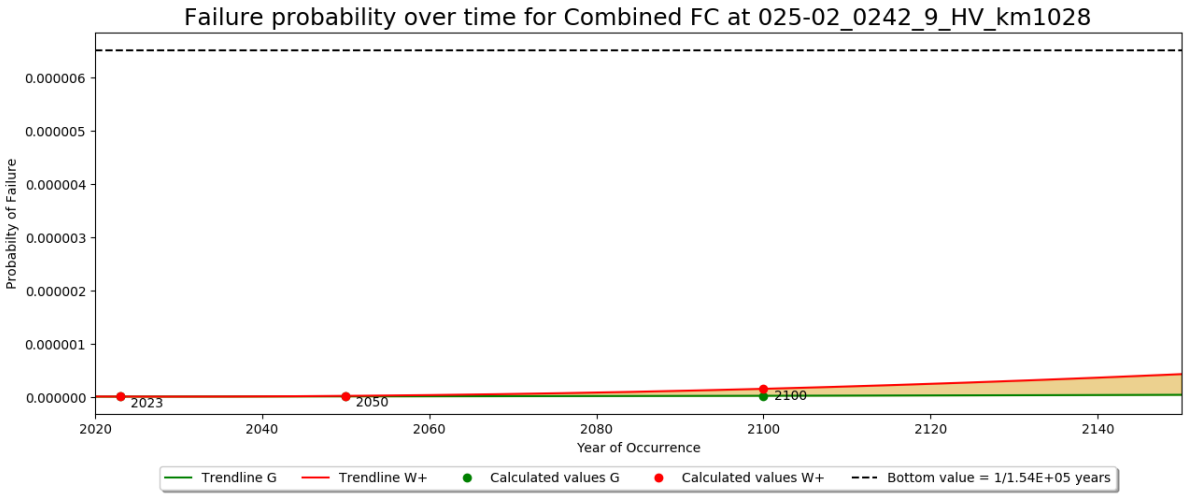

Figure B.16: Residual Lifetime for cross section 25-2 0242

B.4. Dike stretch 34-2

B.4.1. 34-02-0011

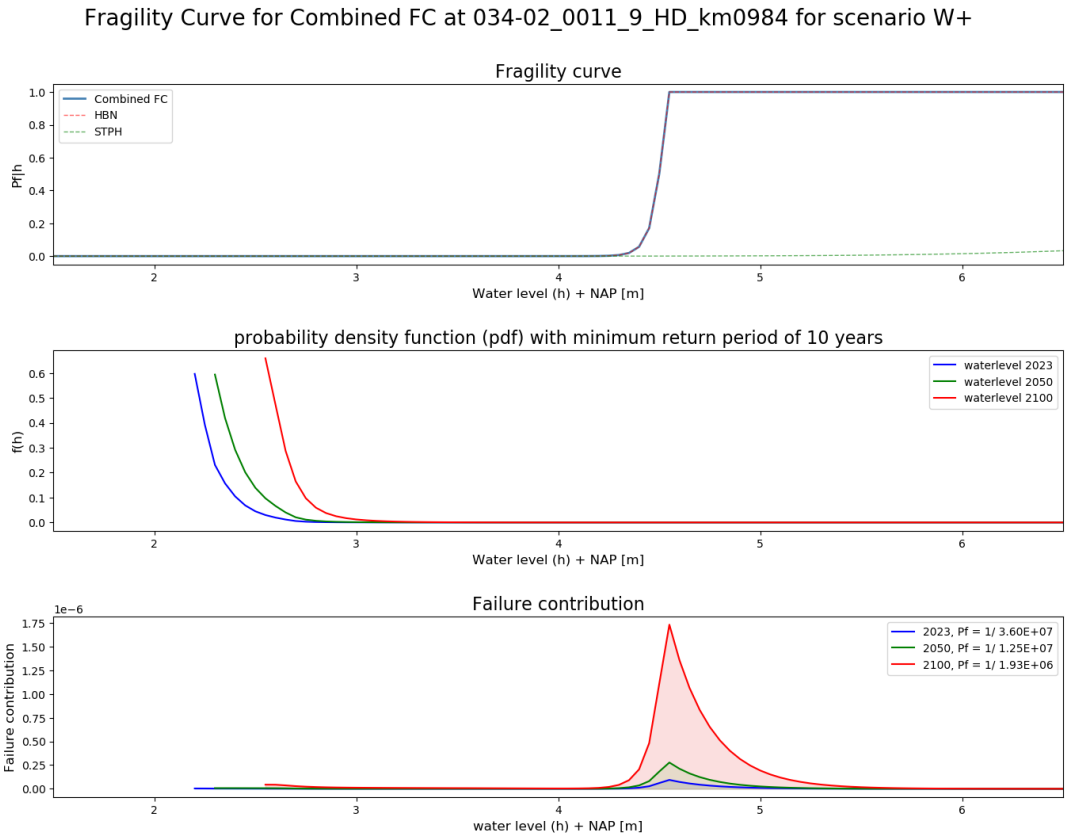

Figure B.17: Fragility Curve Combined 34-2 0011

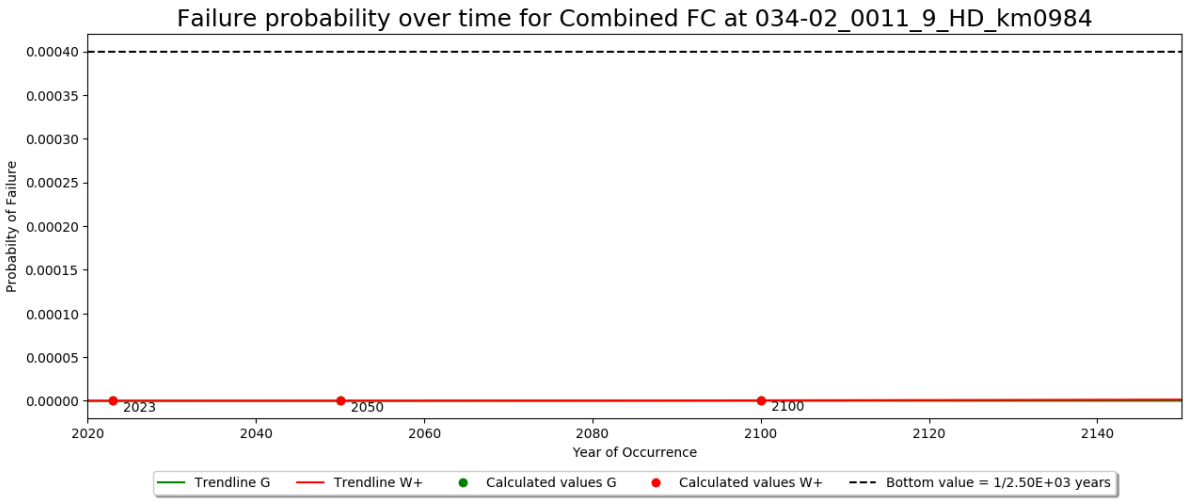

Figure B.18: Residual Lifetime for cross section 34-2 0011

B.4.2. 34-02-0130

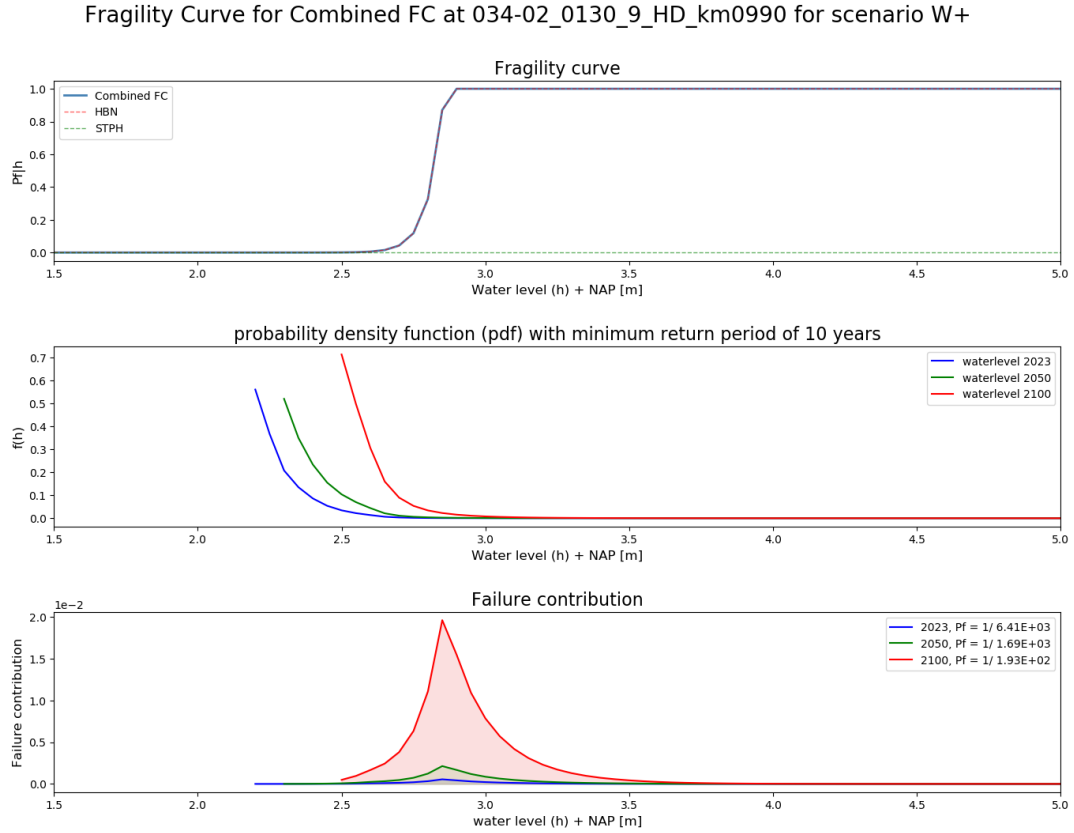

Figure B.19: Fragility Curve Combined 34-2 0130

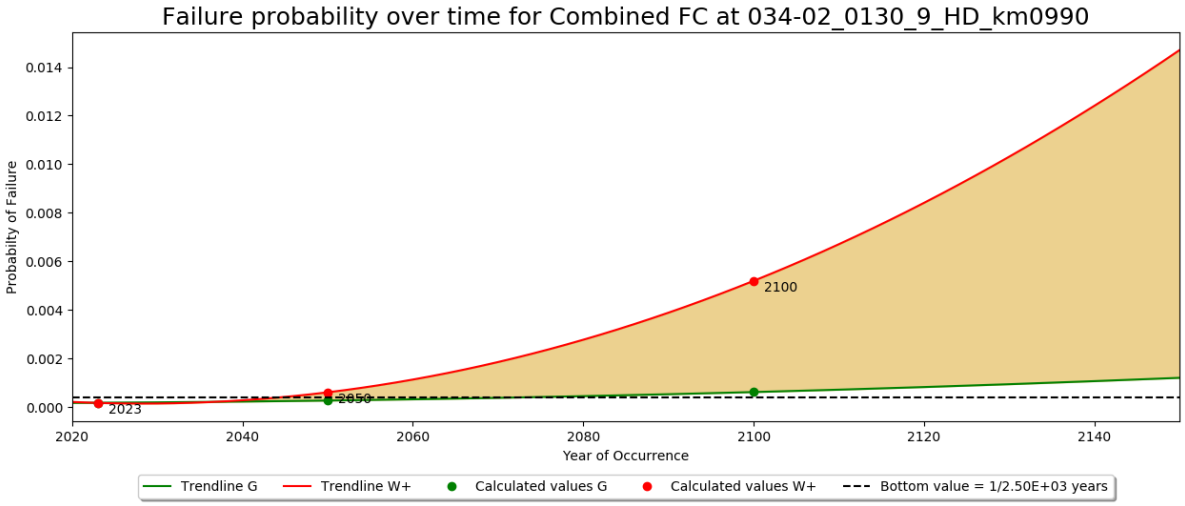

Figure B.20: Residual Lifetime for each section 34-2 0130

B.4.3. 34-02-0190

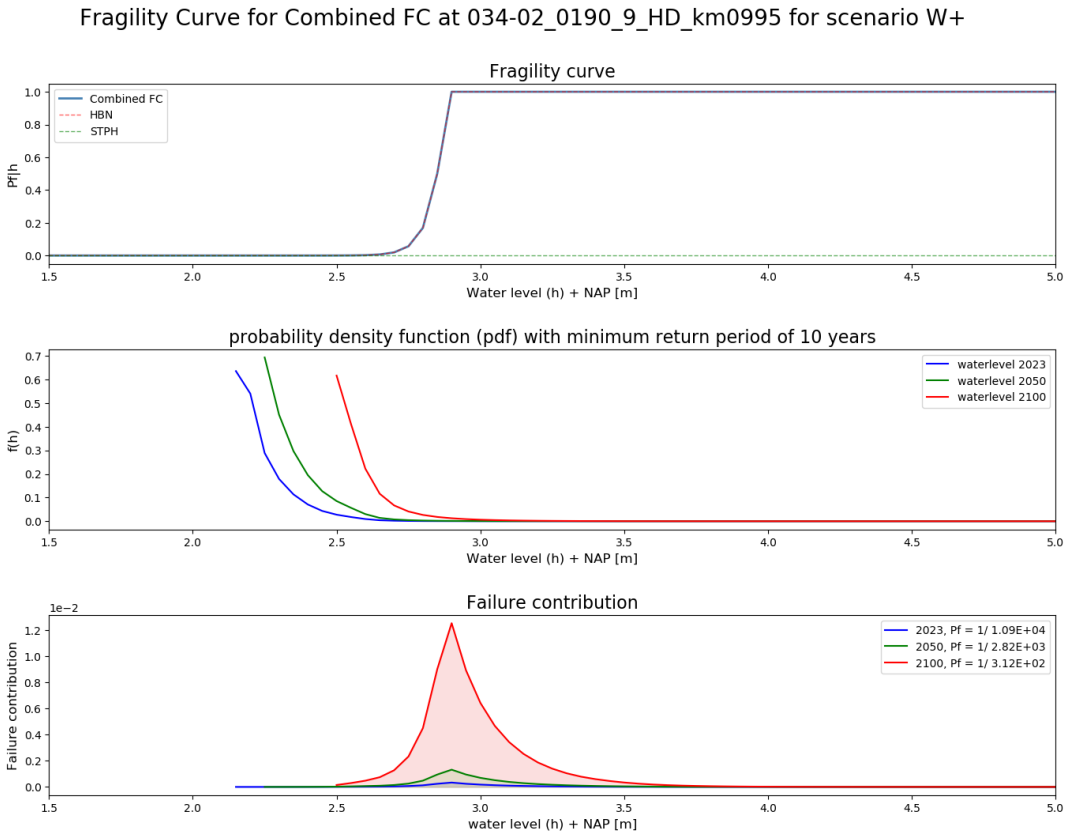

Figure B.21: Fragility Curve Combined 34-2 0190

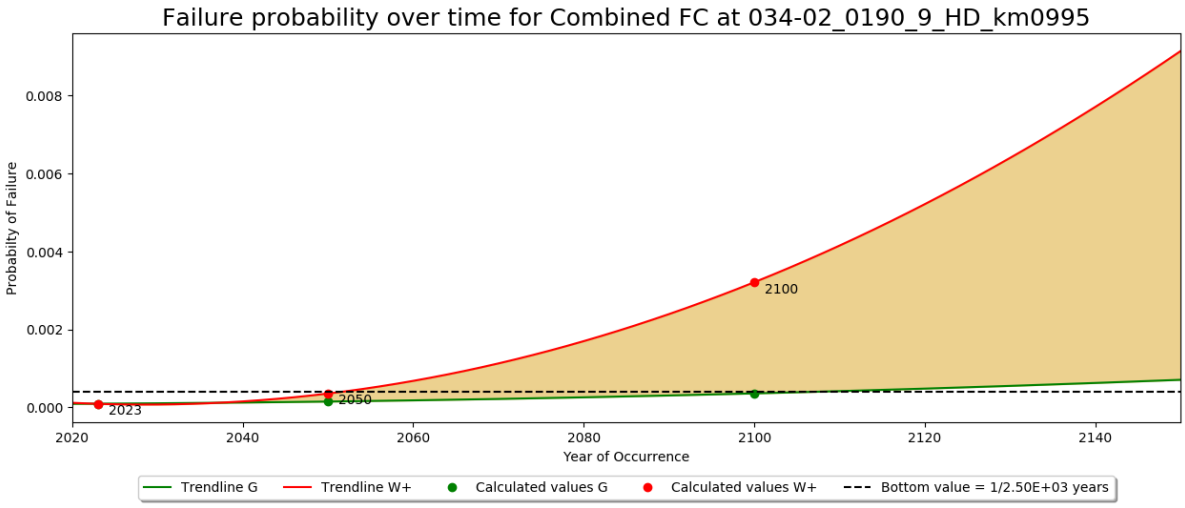

Figure B.22: Residual Lifetime for cross section 34-2 0190

C

Failure probabilities

The failure probability of a dike can be given in two ways: Giving the failure probability of a dike per year P_F or by showing the return period which is equal to $1/P_F$. The failure probability is a value between 0 and 1. The return period is a value bigger than 0.

Probability of failure for each dike location tested in the thesis

Table C.1: Probability of failure for each location given the separated or combined failure mechanisms

	Wave run-up/Overtopping					
	Scenario G			Scenario W+		
Location	2023	2050	2100	2023	2050	2100
020-04 0074	2.42E-05	3.72E-05	9.21E-05	2.28E-05	8.95E-05	9.08E-04
020-04 0181	2.02E-04	3.28E-04	8.55E-04	1.97E-04	8.36E-04	8.81E-03
021-02 0110	1.27E-05	1.95E-05	4.59E-05	1.18E-05	4.44E-05	4.00E-04
021-02 0270	1.41E-05	2.24E-05	5.13E-05	1.35E-05	5.12E-05	4.27E-04
021-02 0373	4.40E-08	6.51E-08	1.42E-07	4.19E-08	1.30E-07	8.80E-07
025-02 0020	1.68E-06	2.45E-06	5.47E-06	1.58E-06	5.36E-06	4.09E-05
025-02 0091	2.66E-08	3.94E-08	8.04E-08	2.48E-08	7.27E-08	4.97E-07
025-02 0242	1.01E-09	1.39E-09	2.46E-09	8.90E-10	2.12E-09	2.16E-08
034-02 0011	2.78E-08	3.87E-08	8.24E-08	2.62E-08	7.56E-08	4.98E-07
034-02 0130	1.61E-04	2.52E-04	6.02E-04	1.56E-04	5.93E-04	5.19E-03
034-02 0190	9.50E-05	1.50E-04	3.59E-04	9.17E-05	3.55E-04	3.21E-03

	Piping					
	Scenario G			Scenario W+		
Location	2023	2050	2100	2023	2050	2100
020-04 0074	2.69E-21	3.48E-21	7.70E-21	2.49E-21	6.96E-21	5.21E-20
020-04 0181	5.80E-04	5.31E-04	5.93E-04	5.06E-04	7.40E-04	1.17E-03
021-02 0110	1.21E-06	1.63E-06	2.68E-06	1.23E-06	2.81E-06	1.38E-05
021-02 0270	5.29E-08	7.53E-08	1.64E-07	4.98E-08	1.58E-07	1.07E-06
021-02 0373	6.36E-23	7.77E-23	1.73E-22	5.90E-23	1.39E-22	1.65E-21
025-02 0020	5.60E-33	5.99E-33	1.71E-32	4.51E-33	1.42E-32	1.17E-31
025-02 0091	1.19E-33	1.92E-33	3.45E-33	1.06E-33	2.68E-33	2.78E-32
025-02 0242	7.63E-09	1.04E-08	2.06E-08	7.61E-09	1.89E-08	1.33E-07
034-02 0011	1.73E-09	2.20E-09	4.00E-09	1.60E-09	4.18E-09	1.93E-08
034-02 0130	1.22E-14	1.72E-14	3.66E-14	1.16E-14	3.41E-14	2.35E-13
034-02 0190	8.23E-19	1.17E-18	2.48E-18	7.69E-19	2.25E-18	1.48E-17

	Combined					
	Scenario G			Scenario W+		
Location	2023	2050	2100	2023	2050	2100
020-04 0074	2.42E-05	3.72E-05	9.21E-05	2.28E-05	8.95E-05	9.08E-04
020-04 0181	7.76E-04	8.48E-04	1.42E-03	6.96E-04	1.55E-03	9.68E-03
021-02 0110	1.38E-05	2.10E-05	4.82E-05	1.30E-05	4.69E-05	4.10E-04
021-02 0270	1.41E-05	2.24E-05	5.14E-05	1.35E-05	5.12E-05	4.28E-04
021-02 0373	4.40E-08	6.51E-08	1.42E-07	4.19E-08	1.30E-07	8.80E-07
025-02 0020	1.68E-06	2.45E-06	5.47E-06	1.58E-06	5.36E-06	4.09E-05
025-02 0091	2.66E-08	3.94E-08	8.04E-08	2.48E-08	7.27E-08	4.97E-07
025-02 0242	8.59E-09	1.18E-08	2.30E-08	8.46E-09	2.09E-08	1.54E-07
034-02 0011	2.95E-08	4.09E-08	8.63E-08	2.78E-08	7.97E-08	5.17E-07
034-02 0130	1.61E-04	2.52E-04	6.02E-04	1.56E-04	5.93E-04	5.19E-03
034-02 0190	9.50E-05	1.50E-04	3.59E-04	9.17E-05	3.55E-04	3.21E-03

Return period for each dike location tested in the thesis

Table C.2: Return period in years for each location given the separated or combined failure mechanisms

	Wave run-up/Overtopping					
	Scenario G			Scenario W+		
Location	2023	2050	2100	2023	2050	2100
020-04 0074	4.13E+04	2.69E+04	1.09E+04	4.39E+04	1.12E+04	2.38E+04
020-04 0181	4.95E+03	3.05E+03	1.17E+03	5.08E+03	1.20E+03	1.83E+03
021-02 0110	7.85E+04	5.12E+04	2.18E+04	8.45E+04	2.25E+04	4.35E+04
021-02 0270	7.09E+04	4.47E+04	1.95E+04	7.42E+04	1.95E+04	6.02E+04
021-02 0373	2.27E+07	1.54E+07	7.02E+06	2.38E+07	7.72E+06	9.30E+11
025-02 0020	5.97E+05	4.07E+05	1.83E+05	6.33E+05	1.87E+05	7.99E+05
025-02 0091	3.76E+07	2.54E+07	1.24E+07	4.03E+07	1.37E+07	5.44E+11
025-02 0242	9.95E+08	7.18E+08	4.07E+08	1.12E+09	4.71E+08	5.44E+11
034-02 0011	3.60E+07	2.58E+07	1.21E+07	3.81E+07	1.32E+07	5.24E+11
034-02 0130	6.19E+03	3.97E+03	1.66E+03	6.41E+03	1.69E+03	1.43E+03
034-02 0190	1.05E+04	6.68E+03	2.79E+03	1.09E+04	2.82E+03	3.26E+03

	Piping					
	Scenario G			Scenario W+		
Location	2023	2050	2100	2023	2050	2100
020-04 0074	3.72E+20	2.88E+20	1.30E+20	4.02E+20	1.44E+20	1.92E+19
020-04 0181	1.72E+03	1.88E+03	1.69E+03	1.98E+03	1.35E+03	8.57E+02
021-02 0110	8.29E+05	6.12E+05	3.74E+05	8.13E+05	3.56E+05	7.25E+04
021-02 0270	1.89E+07	1.33E+07	6.10E+06	2.01E+07	6.33E+06	9.37E+05
021-02 0373	1.57E+22	1.29E+22	5.77E+21	1.70E+22	7.17E+21	6.07E+20
025-02 0020	1.78E+32	1.67E+32	5.84E+31	2.22E+32	7.03E+31	8.58E+30
025-02 0091	8.39E+32	5.21E+32	2.90E+32	9.45E+32	3.73E+32	3.60E+31
025-02 0242	1.31E+08	9.58E+07	4.85E+07	1.31E+08	5.29E+07	7.50E+06
034-02 0011	5.77E+08	4.55E+08	2.50E+08	6.26E+08	2.39E+08	5.18E+07
034-02 0130	8.19E+13	5.82E+13	2.73E+13	8.65E+13	2.93E+13	4.25E+12
034-02 0190	1.22E+18	8.52E+17	4.03E+17	1.30E+18	4.44E+17	6.77E+16

	Combined					
	Scenario G			Scenario W+		
Location	2023	2050	2100	2023	2050	2100
020-04 0074	4.13E+04	2.69E+04	1.09E+04	4.39E+04	1.12E+04	1.10E+03
020-04 0181	1.29E+03	1.18E+03	7.04E+02	1.44E+03	6.46E+02	1.03E+02
021-02 0110	7.23E+04	4.77E+04	2.08E+04	7.72E+04	2.13E+04	2.44E+03
021-02 0270	7.07E+04	4.46E+04	1.95E+04	7.41E+04	1.95E+04	2.34E+03
021-02 0373	2.27E+07	1.54E+07	7.02E+06	2.38E+07	7.72E+06	1.14E+06
025-02 0020	5.97E+05	4.07E+05	1.83E+05	6.33E+05	1.87E+05	2.44E+04
025-02 0091	3.76E+07	2.54E+07	1.24E+07	4.03E+07	1.37E+07	2.01E+06
025-02 0242	1.16E+08	8.50E+07	4.36E+07	1.18E+08	4.78E+07	6.50E+06
034-02 0011	3.39E+07	2.45E+07	1.16E+07	3.60E+07	1.25E+07	1.93E+06
034-02 0130	6.19E+03	3.97E+03	1.66E+03	6.41E+03	1.69E+03	1.93E+02
034-02 0190	1.05E+04	6.68E+03	2.79E+03	1.09E+04	2.82E+03	3.12E+02

D

Hydra NL hydraulic load level calculations

Hydraulic load level calculations outcome. The calculations are done with a maximum overtopping discharge of 1 l/m/s and uncertainty enabled

Table D.1: Hydraulic load level calculations using Hydra NL

Hydraulic load level calculations using Hydra with $q_{o,max} = 1 l/m/s$ NL								
			Scenario G			Scenario W+		
Location			2023	2050	2100	2023	2050	2100
20-4	0071	7.40E+01	1.09E+07	6.70E+06	2.43E+06	1.13E+07	2.46E+06	2.16E+05
	0181	1.81E+02	2.80E+03	2.23E+03	1.16E+03	3.11E+03	1.34E+03	2.61E+02
21-2	0110	1.10E+02	3.26E+06	1.84E+06	6.34E+05	3.33E+06	6.22E+05	5.36E+04
	0270	2.70E+02	1.08E+06	6.45E+05	2.71E+05	1.10E+06	2.67E+05	3.58E+04
	0373	3.73E+02	1.44E+09	8.86E+08	3.72E+08	1.49E+09	3.72E+08	3.34E+07
25-2	0020	2.00E+01	1.22E+06	9.09E+05	5.04E+05	1.32E+06	5.33E+05	1.23E+05
	0091	9.10E+01	1.46E+07	1.13E+07	6.54E+06	1.57E+07	7.09E+06	1.73E+06
	0242	2.42E+02	3.62E+06	3.05E+06	2.03E+06	3.94E+06	2.22E+06	7.45E+05
34-2	0011	1.10E+01	5.15E+06	3.69E+06	2.08E+06	5.45E+06	2.16E+06	5.34E+05
	0130	1.30E+02	2.61E+02	2.36E+02	1.86E+02	2.90E+02	2.17E+02	1.36E+02
	0190	1.90E+02	2.13E+03	1.91E+03	1.54E+03	2.36E+03	1.78E+03	1.03E+03

E

Dike cross section locations

The residual lifetime will be calculated for 11 different locations throughout the Haringvliet and Hollands Diep. The locations are chosen to be spread out over the whole area. Figure E.1 shows each of the locations and its name. The name is taken from Hydra-NL. Hence that this is not the same name as given to the dike profile or soil schematization. The location of the hydraulic calculation in Hydra-NL is coupled with the right dike schematization using Riskeer and/or shape files for GIS provided by the waterboards.

Dike cross section locations

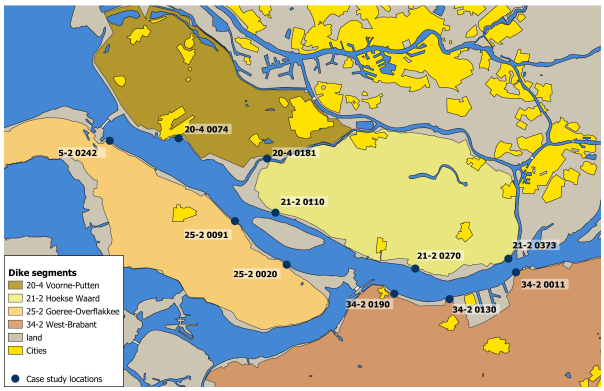

Figure E.1: Location of dike cross sections

Each dike cross section will shortly be described. The north western coast is part of dike stretch 20-4 and is called Voorne-Putten. In this stretch, two dike cross sections are analysed.

20-4 0074 (Hellevoetsluis) lies on the east border of the city Hellevoetsluis. The dike is around 4.4 meter high and has a berm at around 2 meter + NAP. There is no foreshore present at this location. The dike is covered with grass and at the inner toe a small trench is located. The berm will be taken into account for the calculation of wave run-up and overtopping. The seepage length will be equal to the width of the dike, since the trench lies just after the inner slope. Wave run-up will not have much effect on the hydraulic load. The dike lies sheltered from storms from NW. Only diffraction of the waves around the harbour of Hellevoetsluis will give some wave run-up.

20-4 0181 (Spui) is the second cross section that will be taken into account. This cross section is chosen due to the failure probability at this site calculated by the waterboards [43]. The cross section lies a little more inwards at the river Spui. The crest height is comparable with the previous cross section at 4.13m + NAP. Here as well, a berm is present on the outer slope. No foreshore is located

at this location, but there is a small trench at the outer slope of the dike. Waves will have low impact at this location, since it is so far inland. River discharges should however have a bigger impact on this location since it lies in a river entry where the water level can be higher. This cross section is also sheltered against north-western storm events.

21-2 0110 is one of three locations chosen on dike stretch 21-2, which is called Hoeksche Waard. The dike stretch is rather long and has dikes that are mainly directed between the south south-west and south-east. This partially shelters the dike against storm events. The dike cross section lies on a location with the smallest foreshore of the eastern part of this dike stretch. It will therefore have the highest waves. The grass dike does not have a berm but does have a trench at both sides of the dike. For piping, this means that the seepage length is the same length as the dike's width.

21-2 0270 lies more to the east. The dike is around a meter higher than the previous dike, at around 4.9 meter + NAP. On this location, the slopes are also covered with grass. There is no berm at this location.

21-2 0373 is the southernmost location on this dike stretch. The dike is located in the mouth towards the river Dordtse Kil, which is one of the connections between the Hollands Diep and the harbours in Rotterdam city centre and Dordrecht. The dike is much higher than the previous dikes, with 5.77 meter + NAP. It has no berm and fore shore, but does have a trench at the toe of the inner slope. Dike stretch 21-2 is the only dike stretch around the Haringvliet and Hollands diep with a bottom value of $1/100\ year$ instead of $1/300\ year$.

25-2 0242 is the easternmost cross section that will be analysed on stretch 25-2, which is called Goeree-Overflakkee. The dike lies at the southern tip of the Haringvlietdam, just east of a harbour. This dike is the first location that will feel the full force of a north-western storm. This is immediately seen in the crest height of 5.6 m + NAP. The dike does not have a berm but does have a lot of wave breaking shallows in front of the dike. These will not help against piping, but will probably reduce the wave height.

25-2 0091 (Den Bommel) is the next cross section in 25-2, which lies about 12 km more inland, towards the south. The crest height is still high at 5.7 meter + NAP. The location is chosen because almost no foreshore is located here. The dike is covered in grass, has a berm at the outer slope and a trench at the toe of the inner slope of the dike.

25-2 0020 lies a little more to the east at the same dike stretch. The cross section lies close to where two dikes meet. The dike height is a little lower at 5.2 meter + NAP, with no berms. There are foreshores present at this location.

34-2 0130 (Noordschans) is the second location at dike stretch 34-2 West-Brabant. The first location is 34-2 0190 and is used in chapter 4. 34-2 will be fully impacted by a north-western storm. However, the length of the whole Haringvliet will have dampened the waves a bit. Additionally, the available foreshores will probably reduce the wave heights. This can be seen in the crest height of the dike, which is 4.86 m +NAP. Cross section 0130 lies just east of a small harbour. In front of this dike, there is a lot of vegetation.

34-2 0011 (Moerdijk) is the last location that is analysed. This location lies at the other side of the mount towards the Dordtse Kil and is both the start of the Hollands Diep and beginning of the Nieuwe Merwede. Additionally, the highest dike is measured at this point, at 6.20 m + NAP. At this location, there is no foreshore, but a small berm is found at the outer slope. At the toe of the inner slope, a trench is found. Overall: All the dikes have some sort of trench at the inner toe. Since the subsoil conditions underneath the available foreshores are not known, they can not be used to increase any seepage length. The base for each calculation will therefore be to only use the width of the dike as the leakage length for piping. This means that in reality the residual lifetime should be longer than calculated in

this thesis. After the first calculations it is checked where it is possible to take into account a bigger seepage length and/or the foreshore.

F

Wave set-up and Overtopping: Errors and Importance factors

F.1. Dike stretch 20-4

F.1.1. 20-04-0074

Dike profile

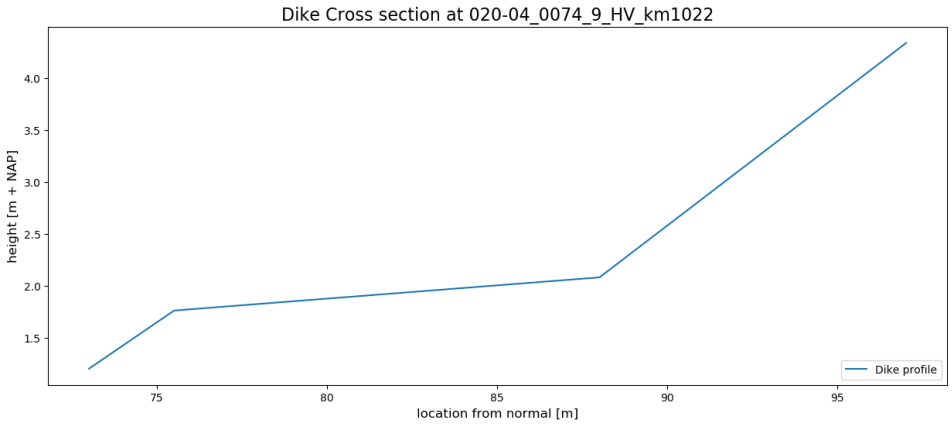

Figure F.1: Dike profile 20-4 0074

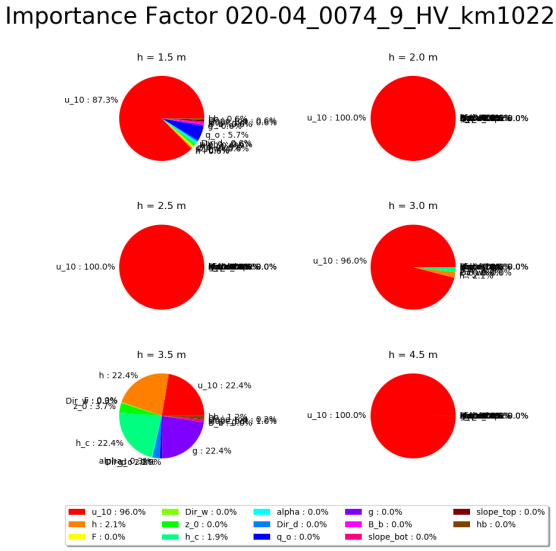

Figure F.2: Importance Factor 20-4 0074

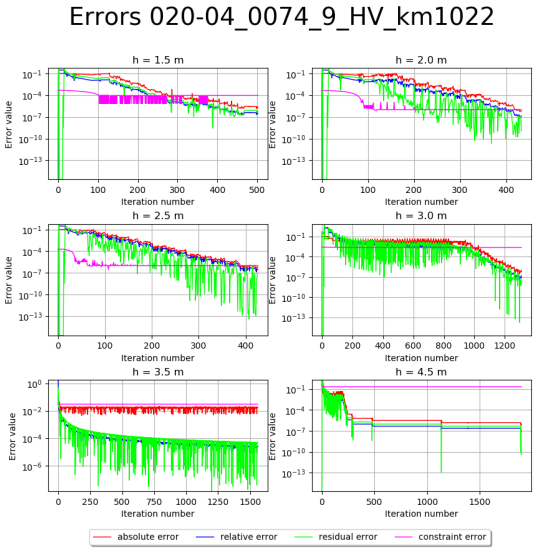

Figure F.3: Error 20-4 0074

F.1.2. 20-04-0181
Dike profile

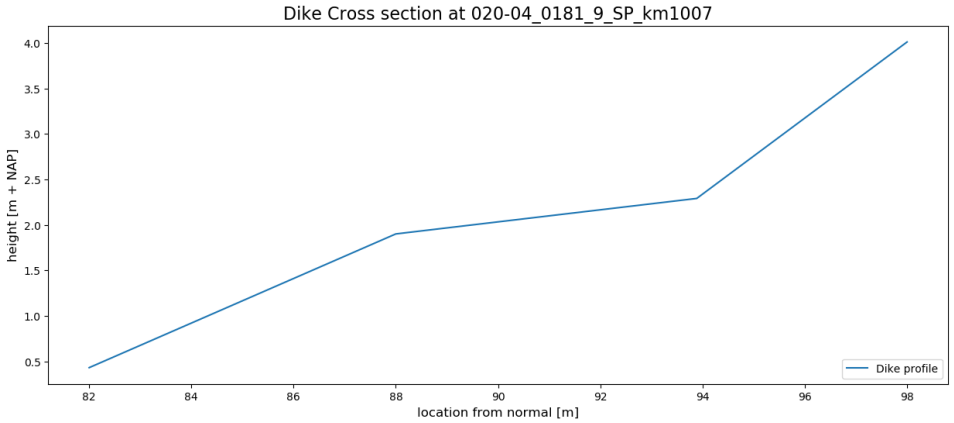

Figure F.4: Dike profile 20-4 0181

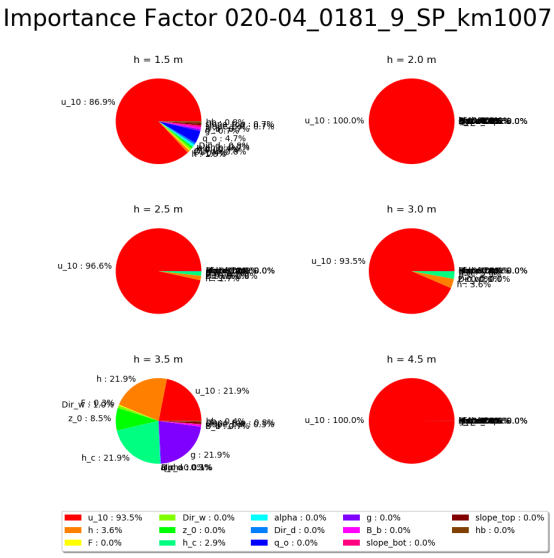

Figure F.5: Importance Factor 20-4 0181

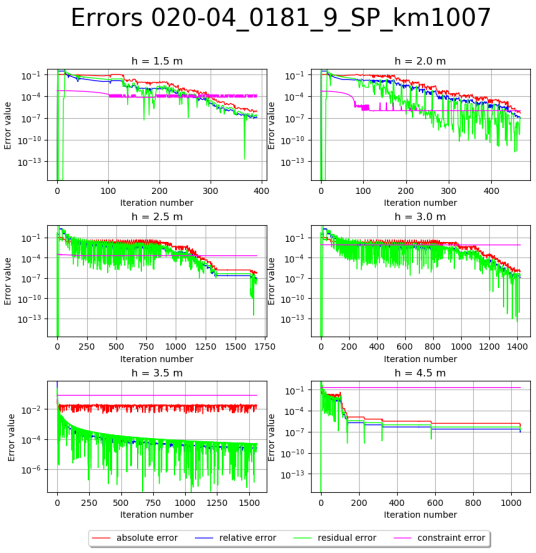

Figure F.6: Error 20-4 0181

F.2. Dike stretch 21-2

F.2.1. 21-02-0110

Dike profile

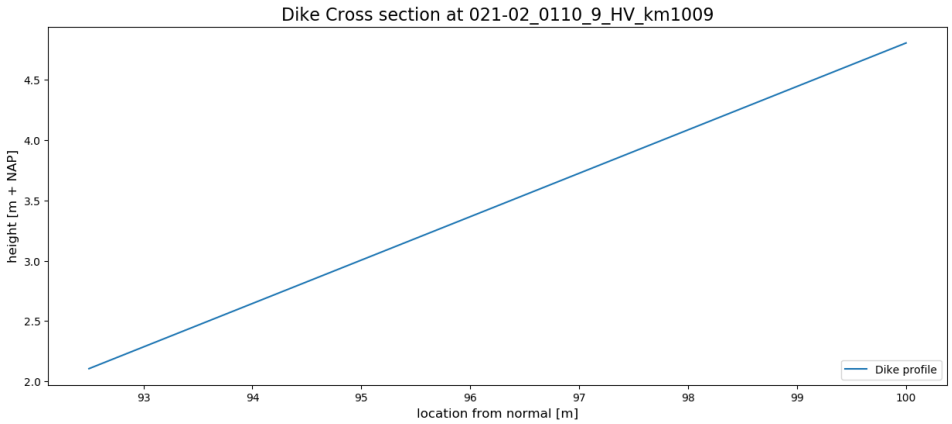

Figure F.7: Dike profile 21-2 0110

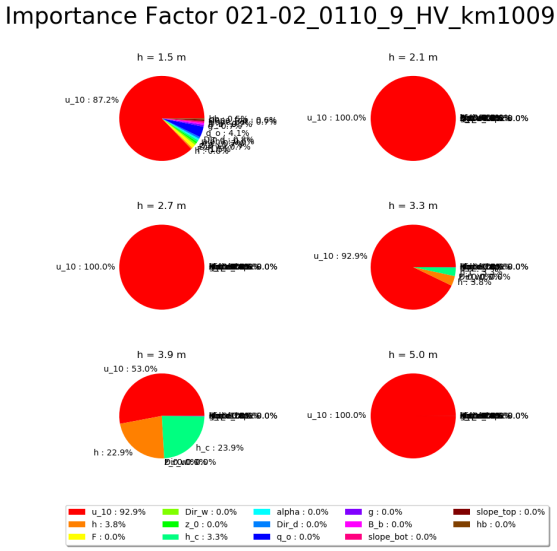

Figure F.8: Importance Factor 21-2 0110

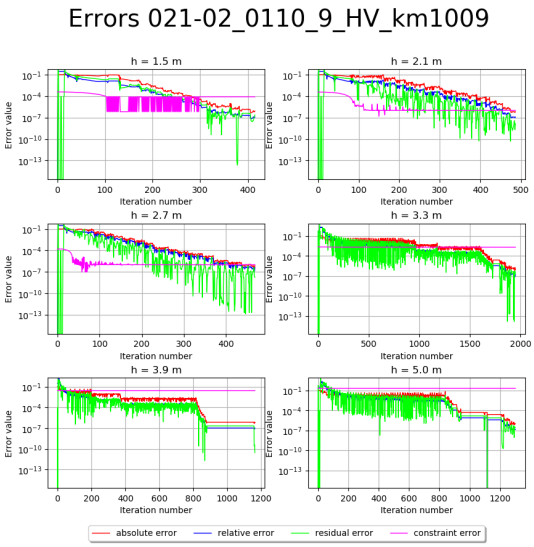

Figure F.9: Error 21-2 0110

F.2.2. 21-02-0270
Dike profile

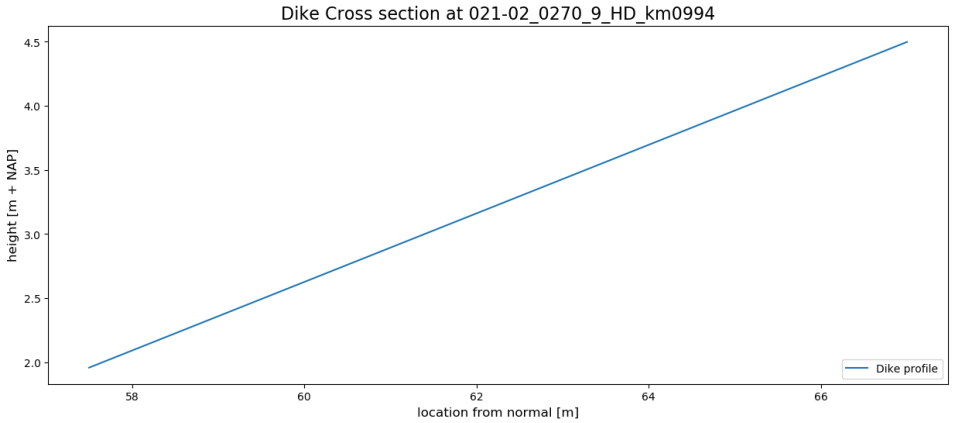

Figure F.10: Dike profile 21-4 0270

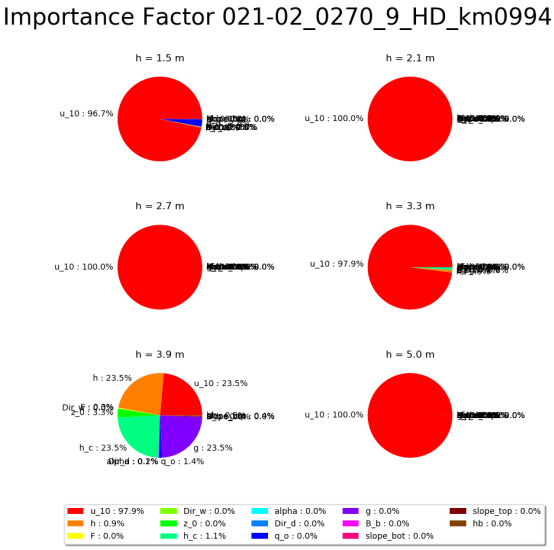

Figure F.11: Importance Factor 21-2 0270

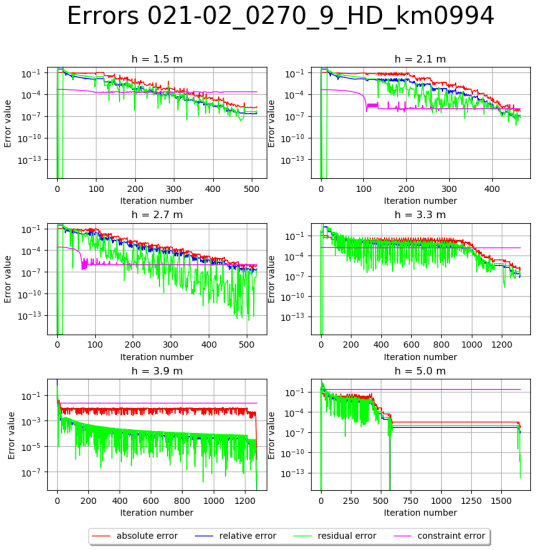

Figure F.12: Error 21-2 0270

F.2.3. 21-02-0373
Dike profile

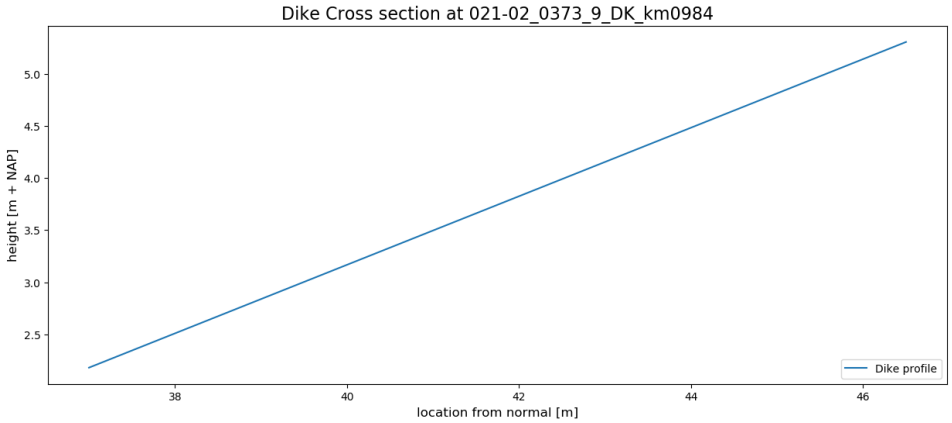

Figure F.13: Dike profile 21-2 0373

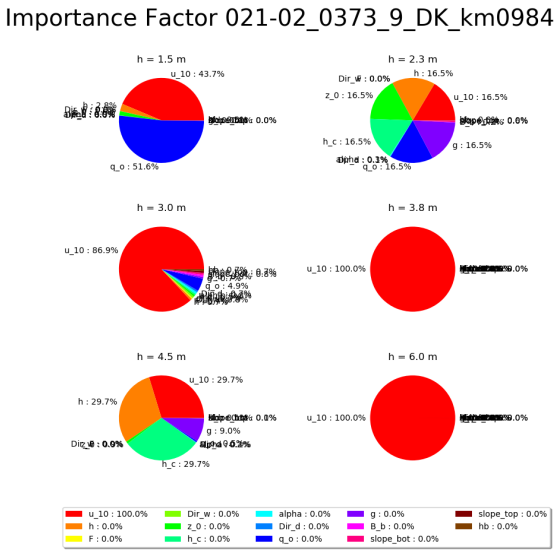

Figure F.14: Importance Factor 21-2 0373

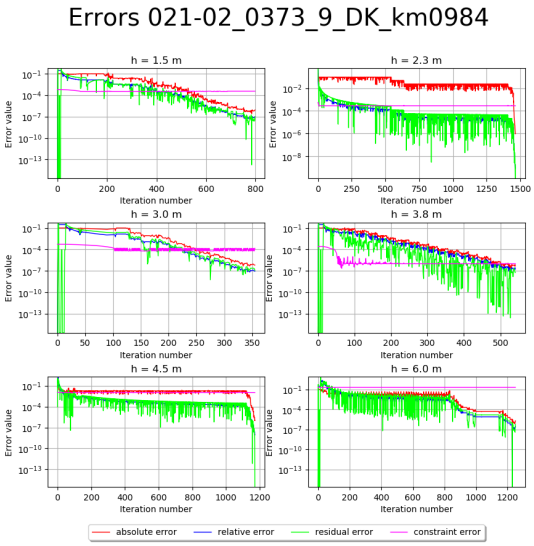

Figure F.15: Error 21-2 0373

F.3. Dike stretch 25-2

F.3.1. 25-02-0020

Dike profile

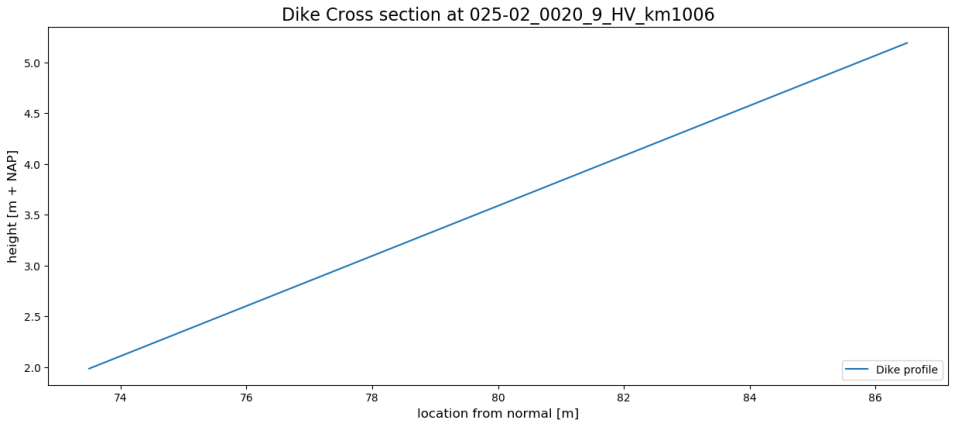

Figure F.16: Dike profile 25-2 0020

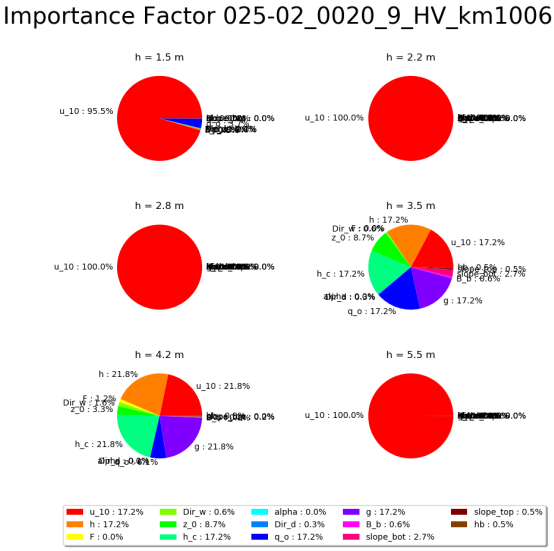

Figure F.17: Importance Factor 25-2 0020

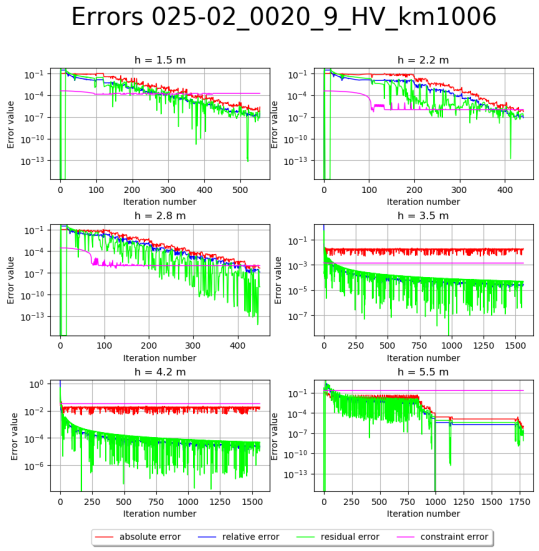

Figure F.18: Error 25-2 0020

F.3.2. 25-02-0091
Dike profile

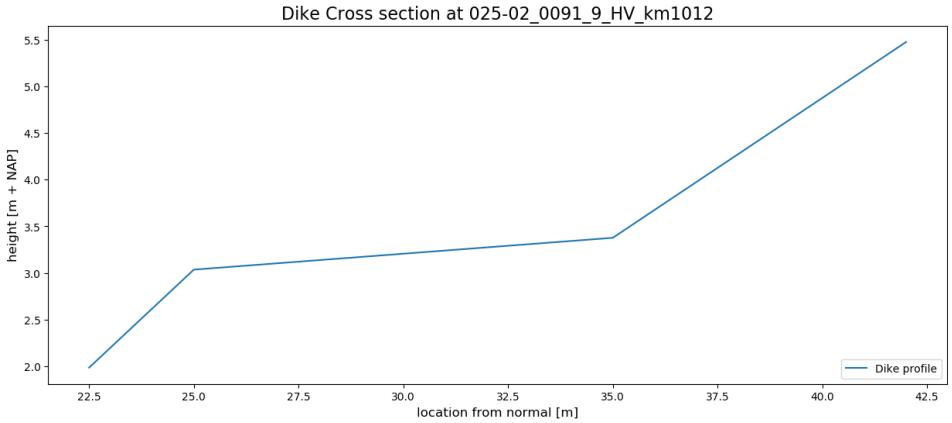

Figure F.19: Dike profile 25-2 0091

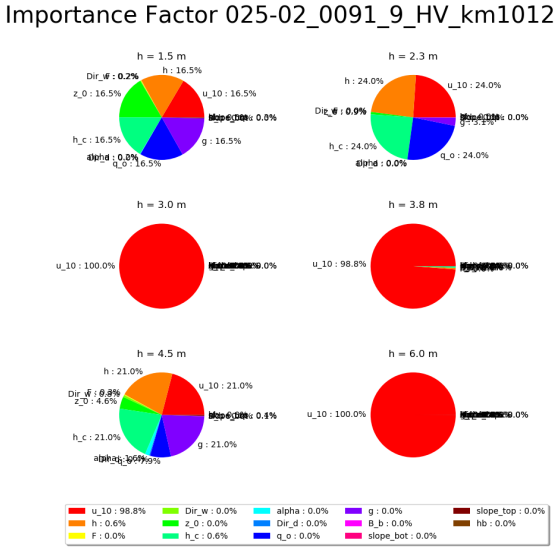

Figure F.20: Importance Factor 25-2 0091

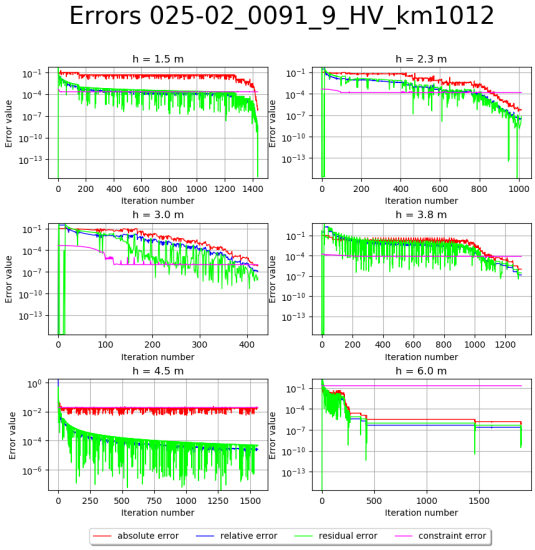

Figure F.21: Error 25-2 0091

F.3.3. 25-02-0242
Dike profile

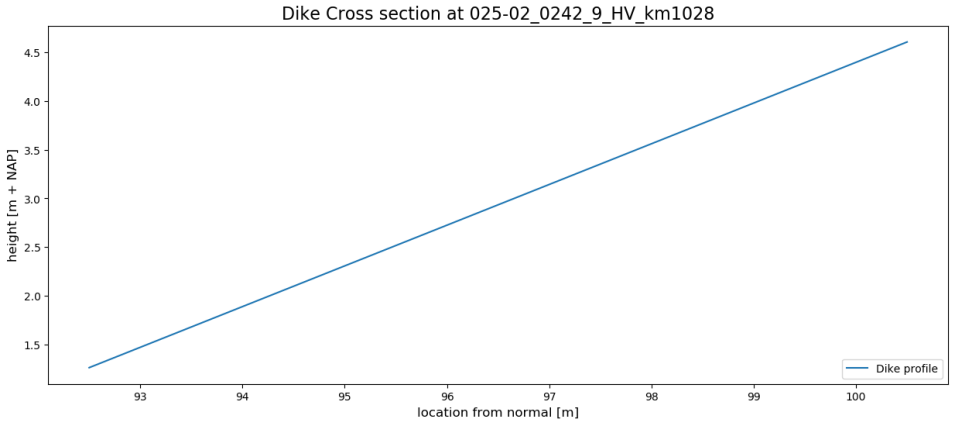

Figure F.22: Dike profile 25-2 0242

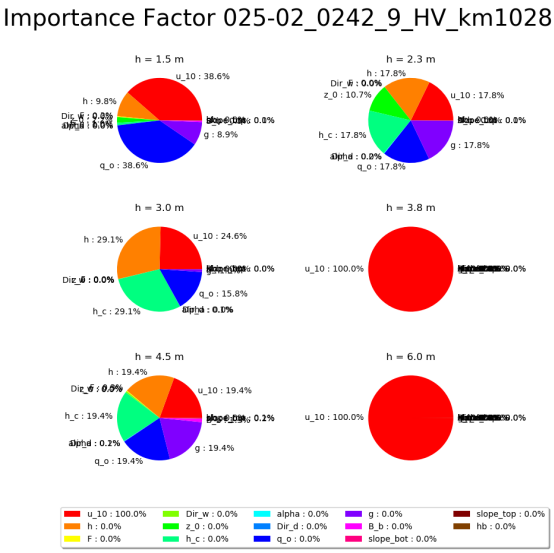

Figure F.23: Importance Factor 25-2 0242

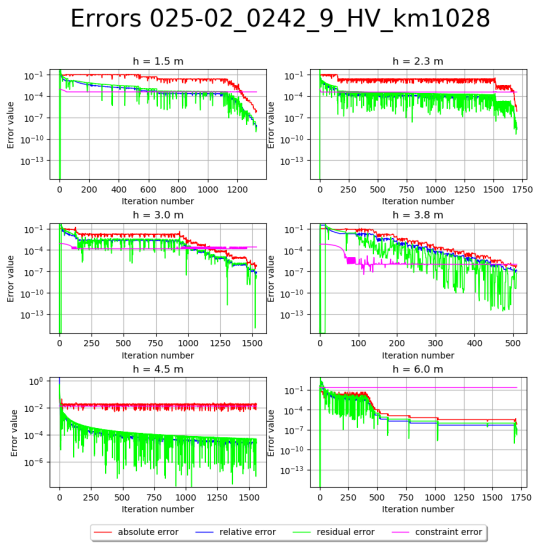

Figure F.24: Error 25-2 0242

F.4. Dike stretch 34-2

F.4.1. 34-02-0011

Dike profile

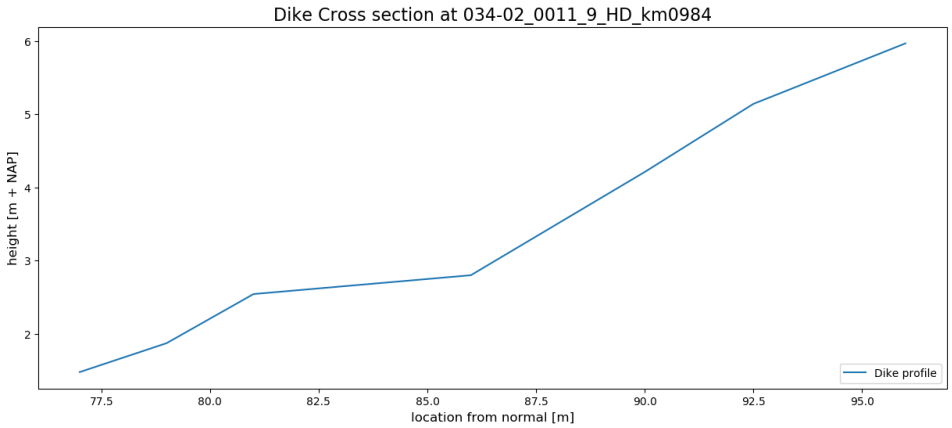

Figure F.25: Dike profile 34-2 0011

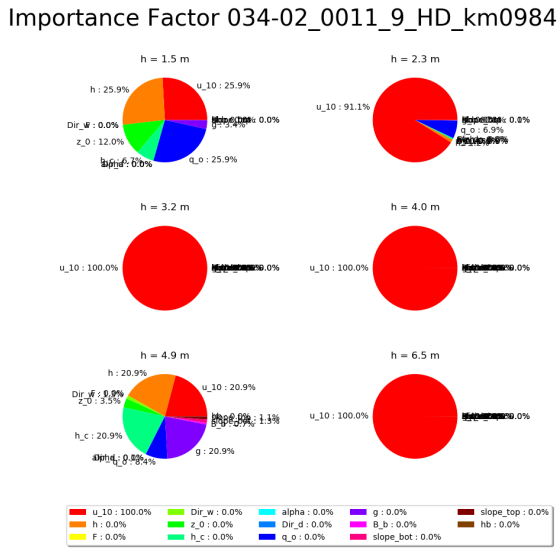

Figure F.26: Importance Factor 34-2 0011

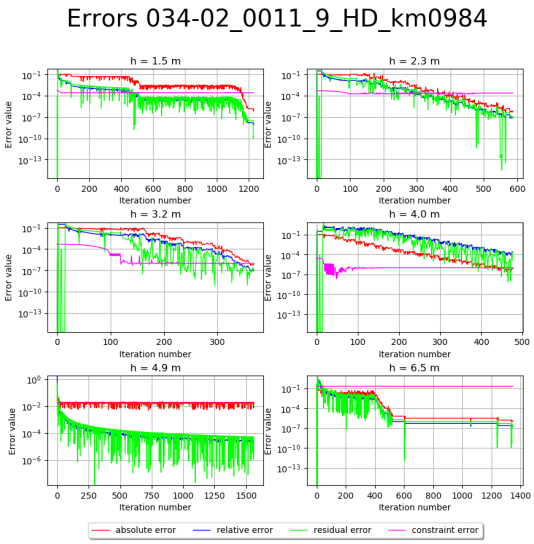

Figure F.27: Error 34-2 0011

F.4.2. 34-02-0130
Dike profile

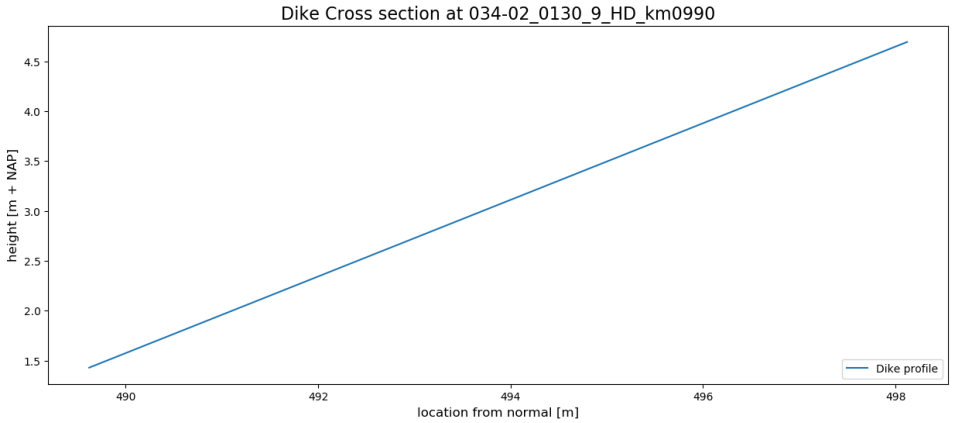

Figure F.28: Dike profile 34-2 0130

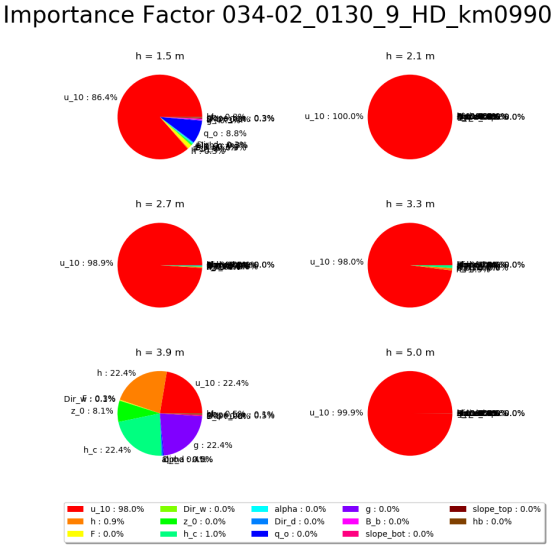

Figure F.29: Importance Factor 34-2 0130

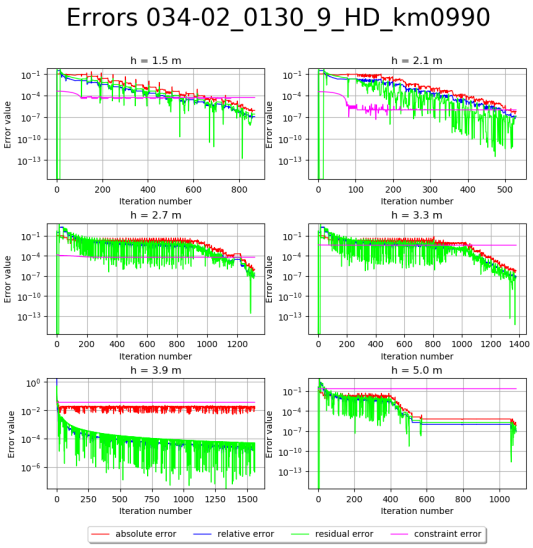

Figure F.30: Error 34-2 0130

F.4.3. 34-02-0190
Dike profile

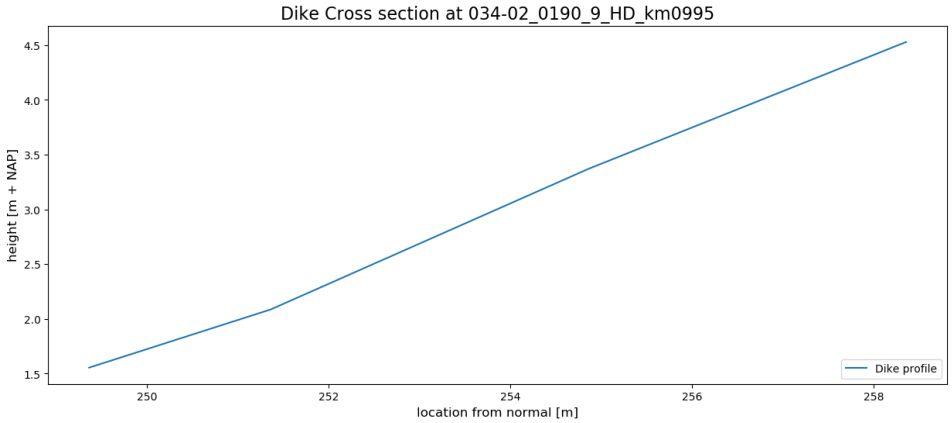

Figure F.31: Dike profile 34-2 0190

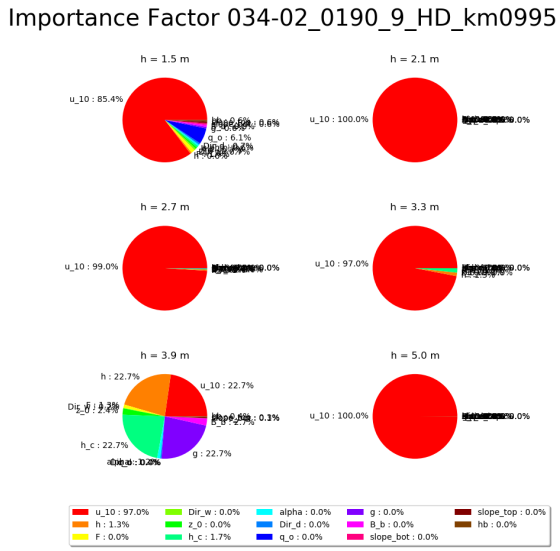

Figure F.32: Importance Factor 34-2 0190

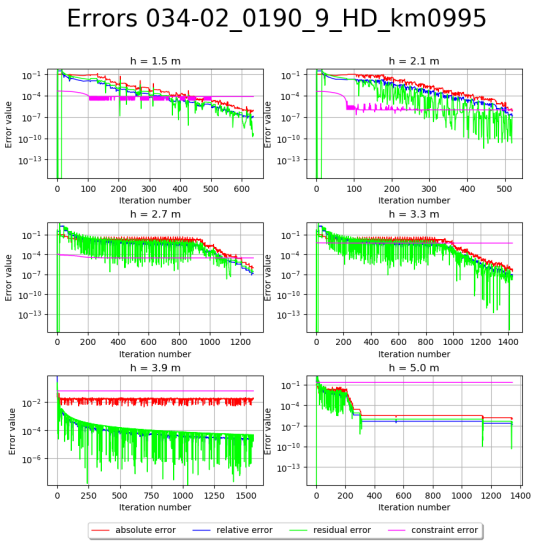

Figure F.33: Error 34-2 0190

G

Piping: Fragility curve, Errors and Importance Factor

G.1. Dike stretch 20-4

G.1.1. 20-04-0074

Fragility curve for each sub mechanism

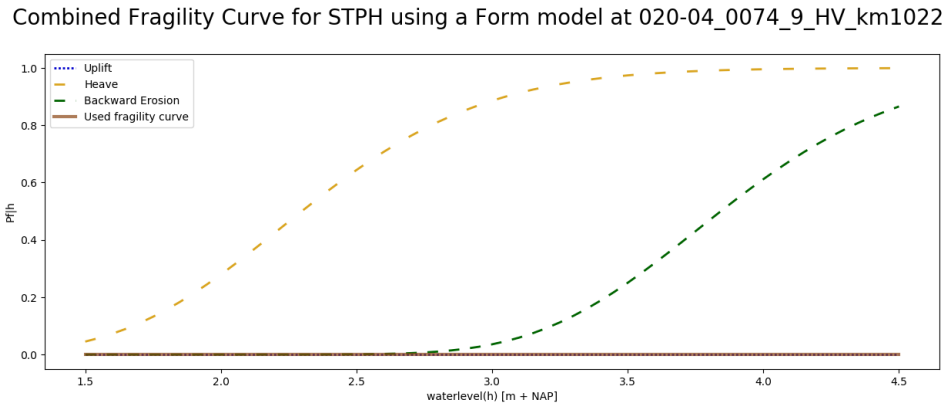

Figure G.1: Combined FC 20-4 0074

Uplift

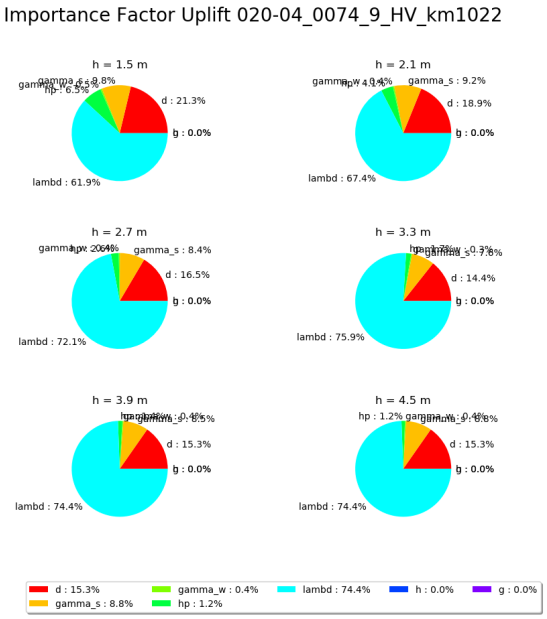

Figure G.2: Importance Factor Uplift 20-4 0074

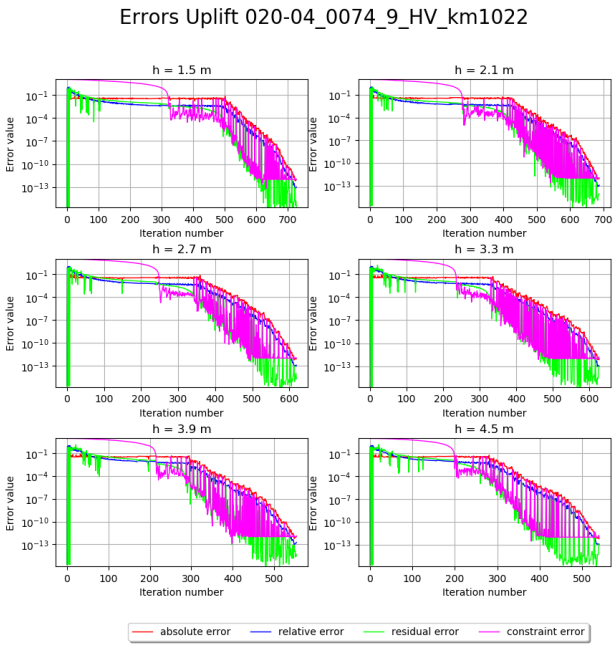

Figure G.3: Error 20-4 0074

Heave

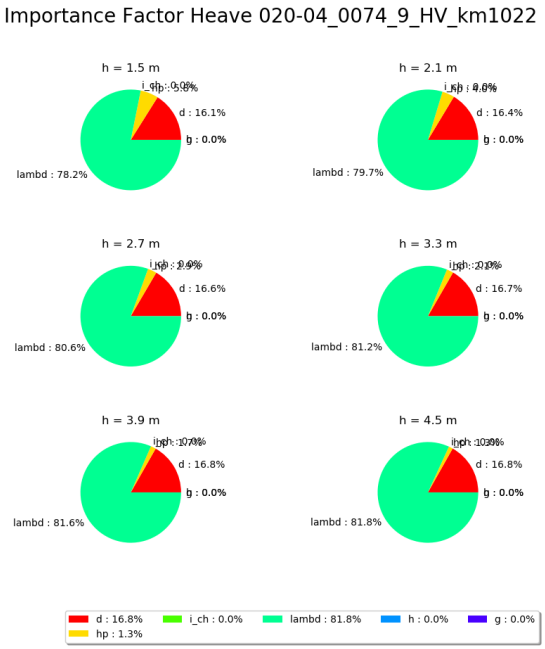

Figure G.4: Importance Factor Heave 20-4 0074

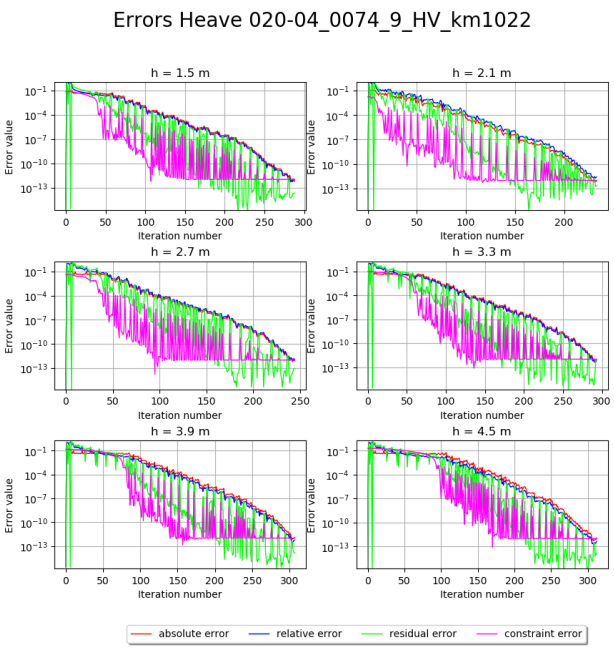

Figure G.5: Error 20-4 0074

Backward Erosion

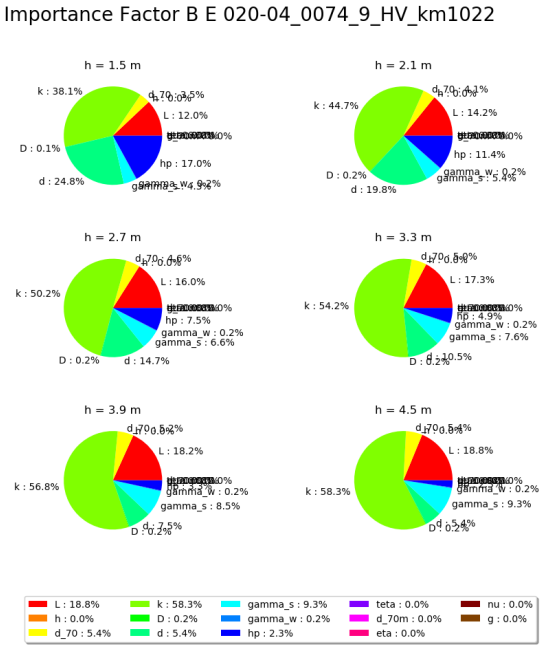

Figure G.6: Importance Factor Backward Erosion 20-4 0074

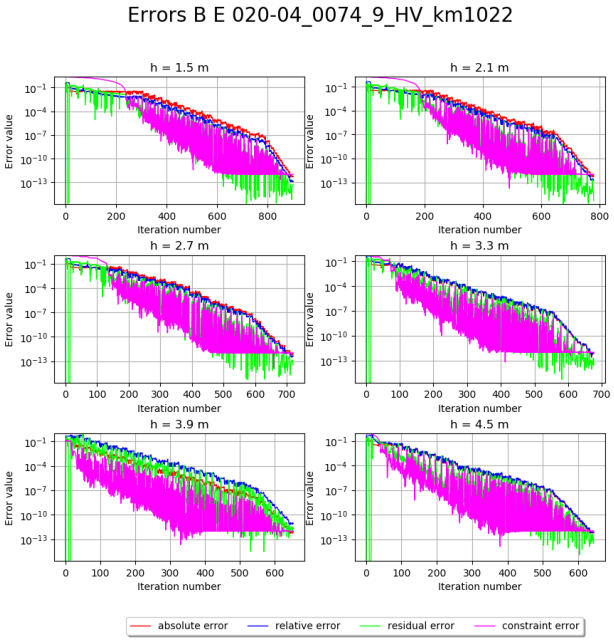

Figure G.7: Error 20-4 0074

G.1.2. 20-04-0181
Fragility curve for each sub mechanism

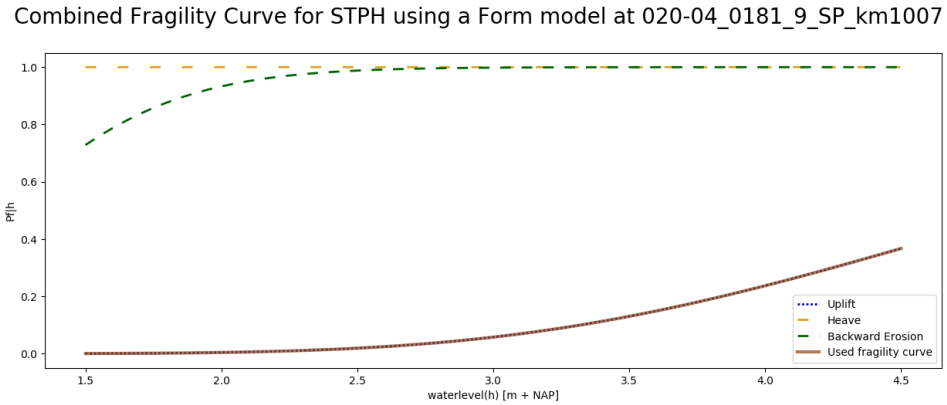

Figure G.8: Combined FC 20-4 0074

Uplift

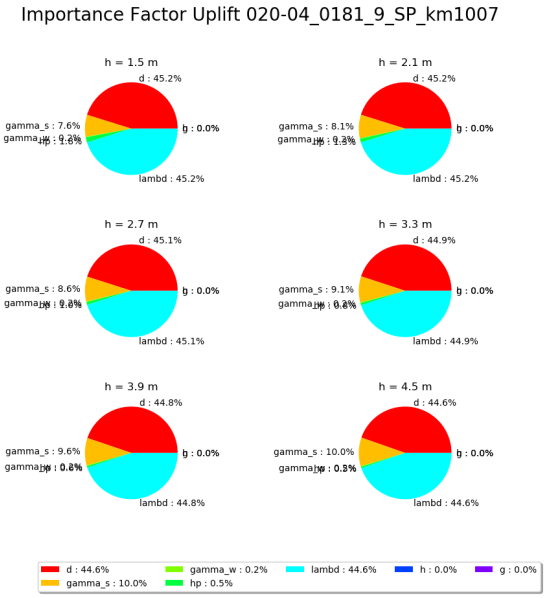

Figure G.9: Importance Factor Uplift 20-4 0181

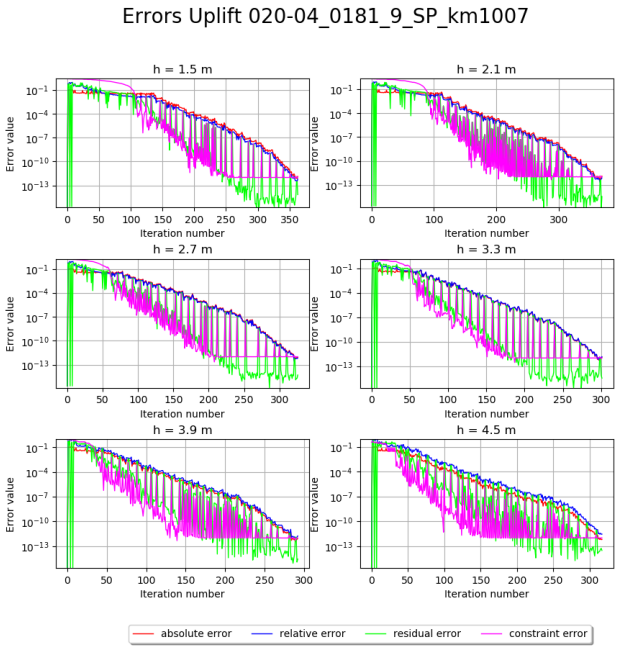

Figure G.10: Error 20-4 0181

Heave

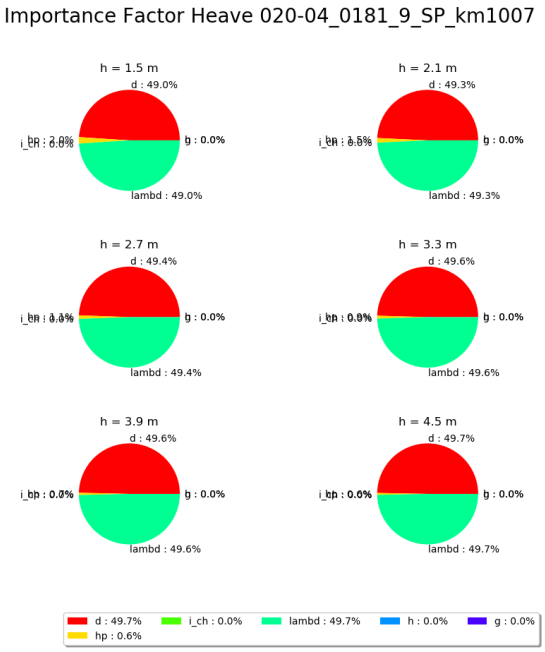

Figure G.11: Importance Factor Heave 20-4 0181

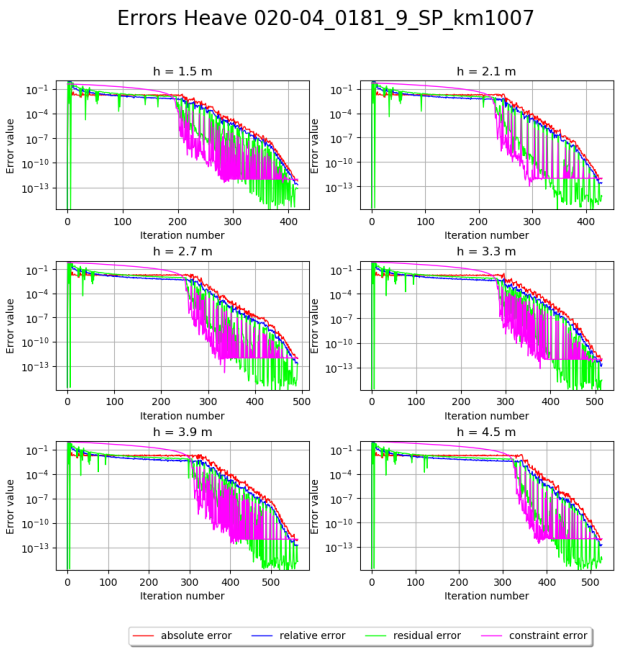

Figure G.12: Error 20-4 0181

Backward Erosion

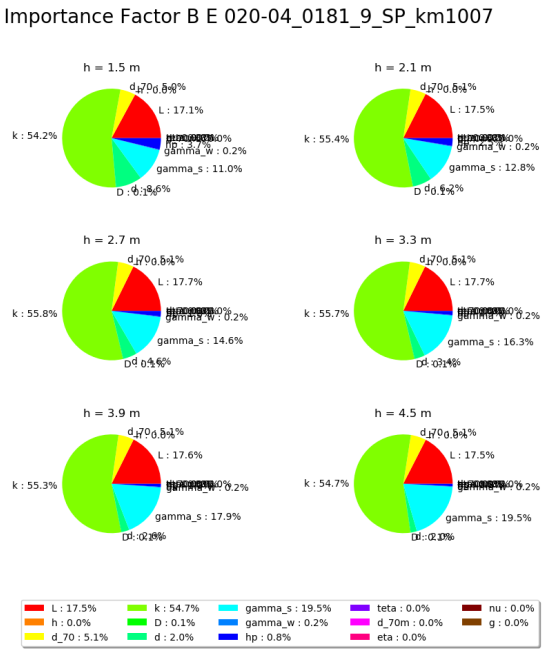

Figure G.13: Importance Factor Backward Erosion 20-4 0181

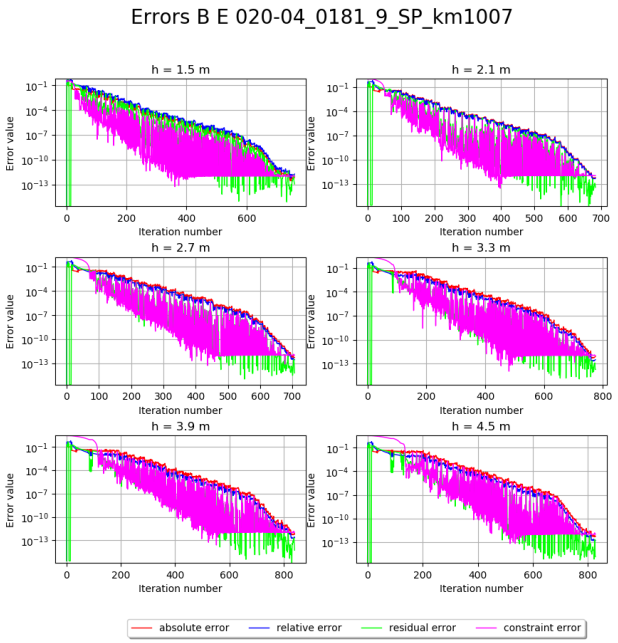

Figure G.14: Error 20-4 0181

G.2. Dike stretch 21-2

G.2.1. 21-02-0110

Fragility curve for each sub mechanism

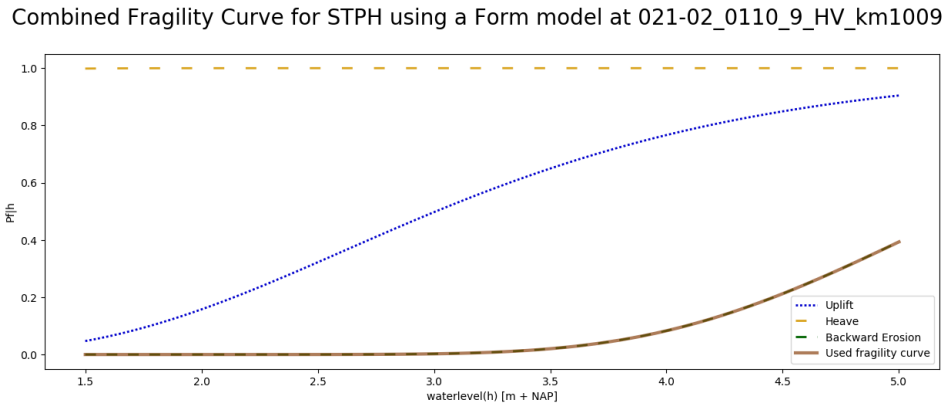

Figure G.15: Combined FC 21-2 0110

Uplift

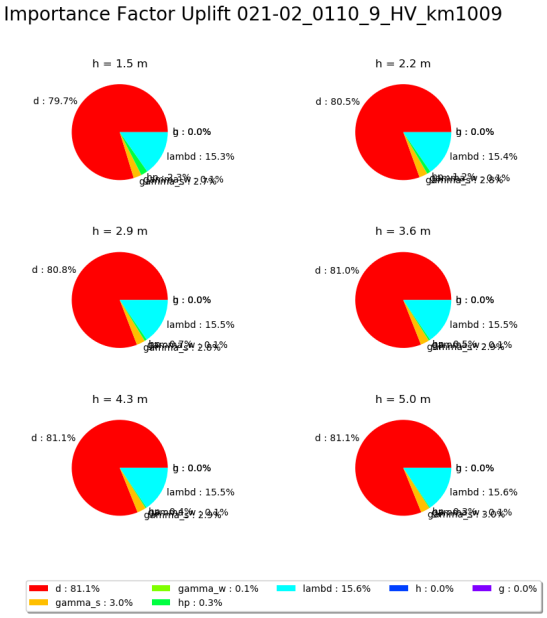

Figure G.16: Importance Factor Uplift 21-2 0110

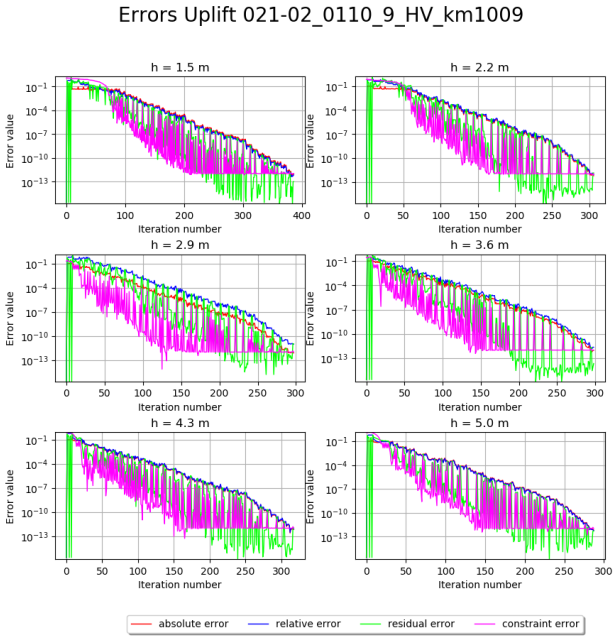

Figure G.17: Error 21-2 0110

Heave

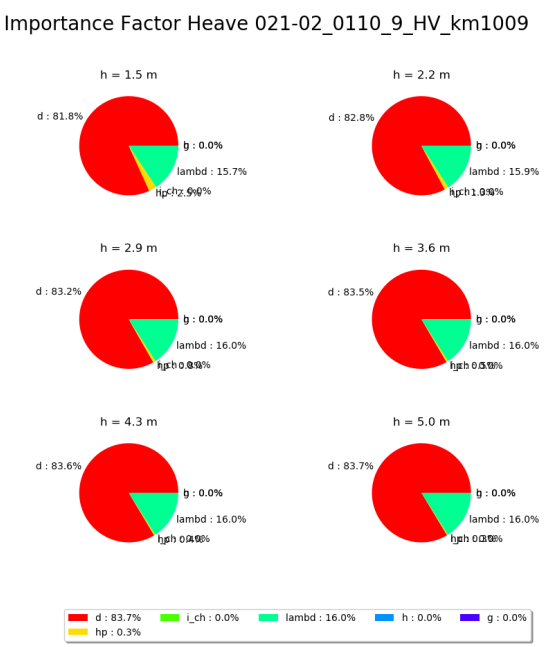

Figure G.18: Importance Factor Heave 21-2 0110

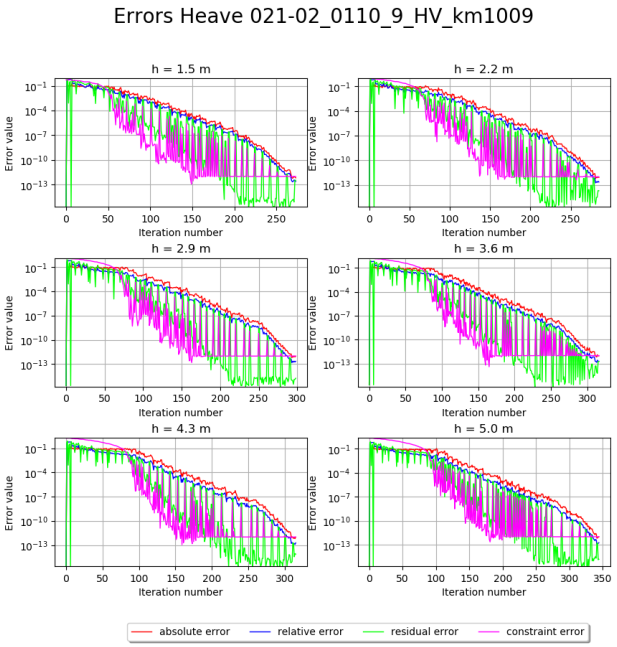

Figure G.19: Error 21-2 0110

Backward Erosion

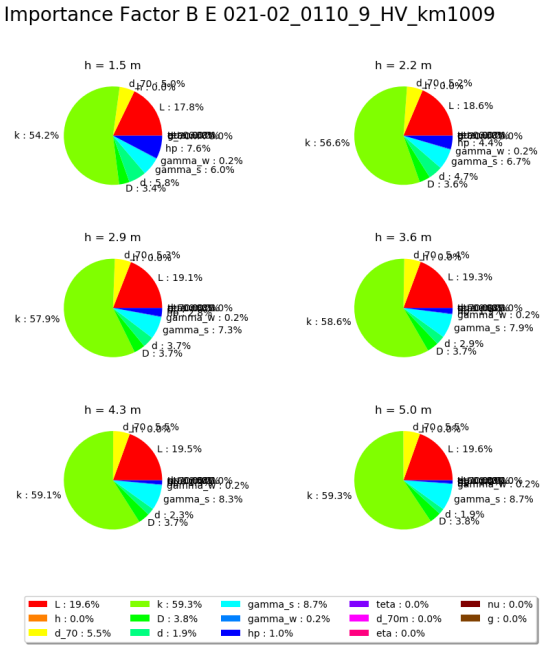

Figure G.20: Importance Factor Backward Erosion 21-2 0110

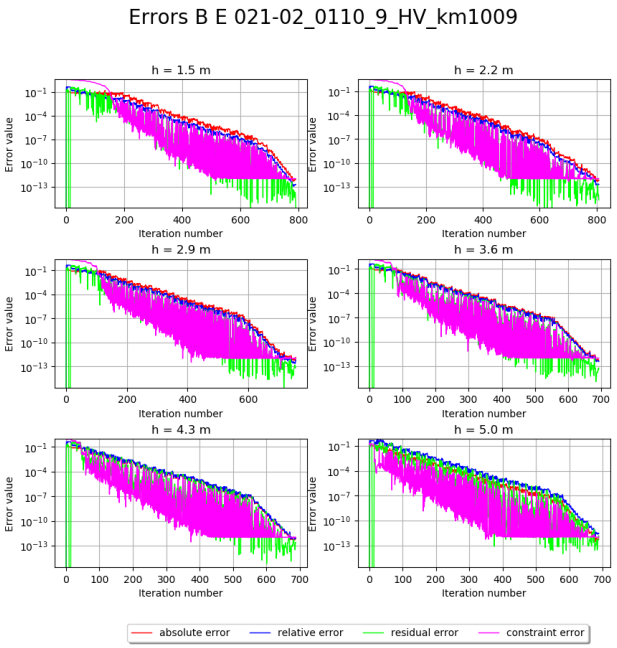

Figure G.21: Error 21-2 0110

G.2.2. 21-02-0270

Fragility curve for each sub mechanism

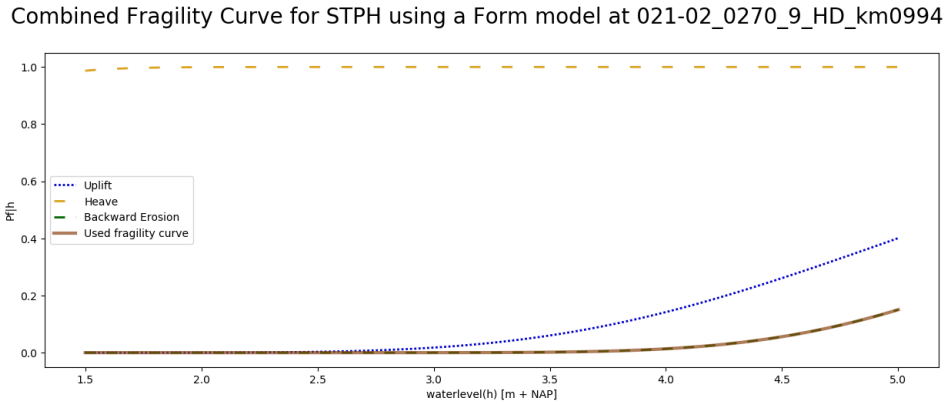

Figure G.22: Combined FC 21-2 0270

Uplift

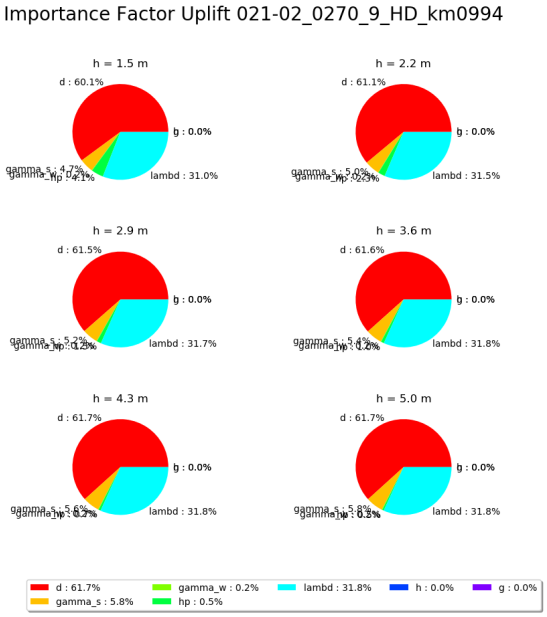

Figure G.23: Importance Factor Uplift 21-2 0270

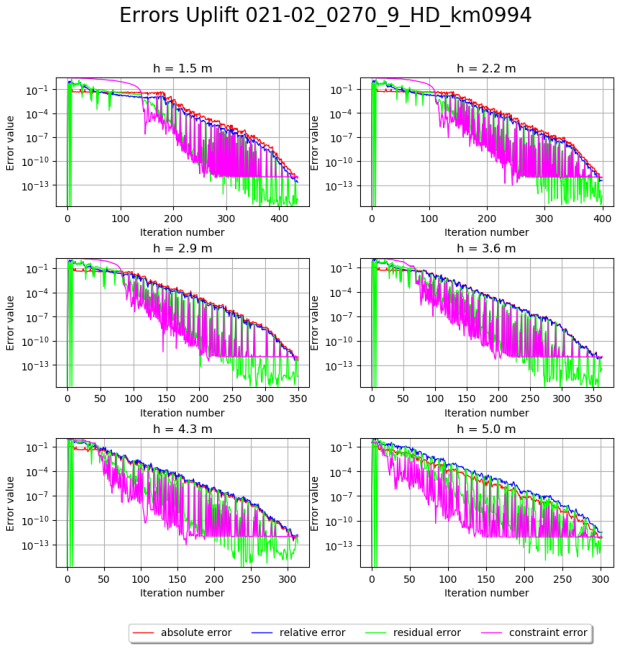

Figure G.24: Error 21-2 0270

Heave

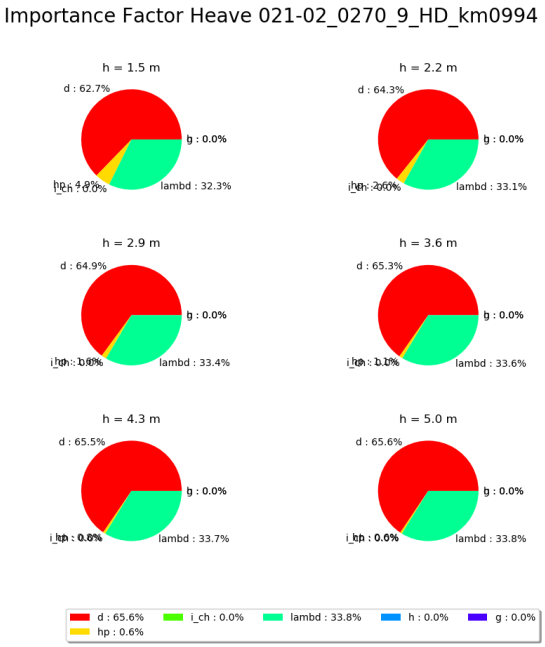

Figure G.25: Importance Factor Heave 21-2 0270

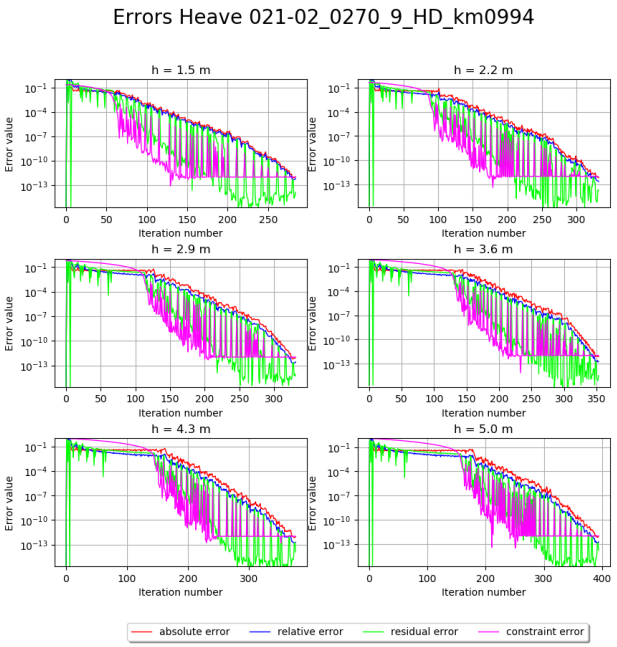

Figure G.26: Error 21-2 0270

Backward Erosion

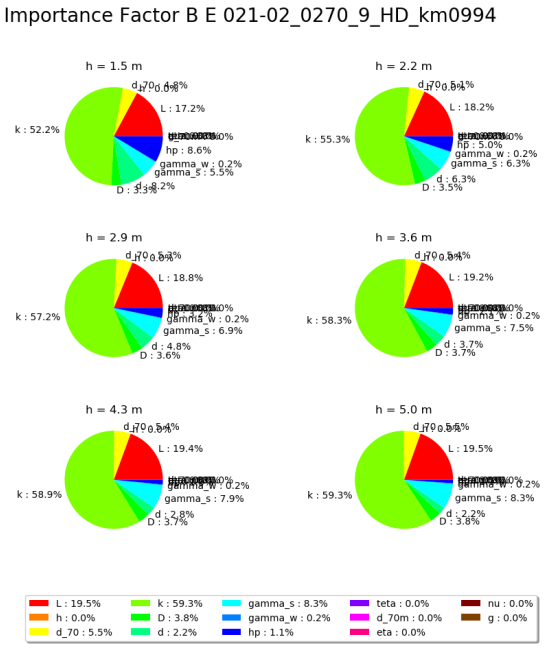

Figure G.27: Importance Factor Backward Erosion 21-2 0270

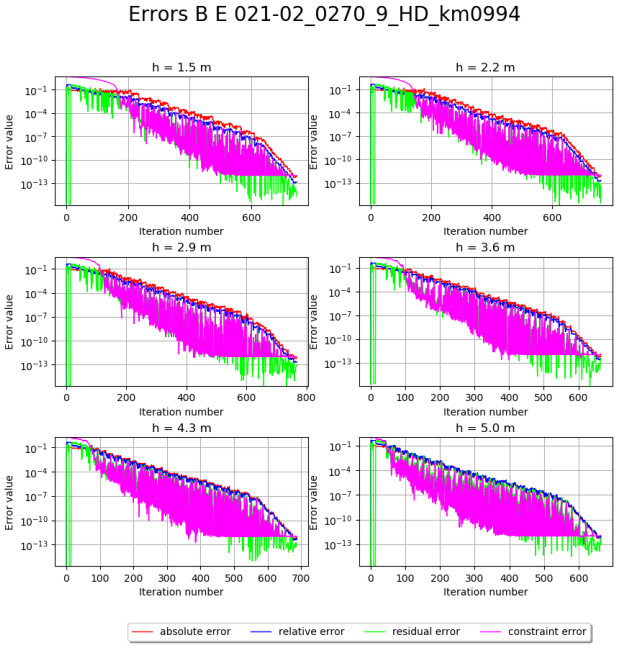

Figure G.28: Error 21-2 0270

G.2.3. 21-02-0373
Fragility curve for each sub mechanism

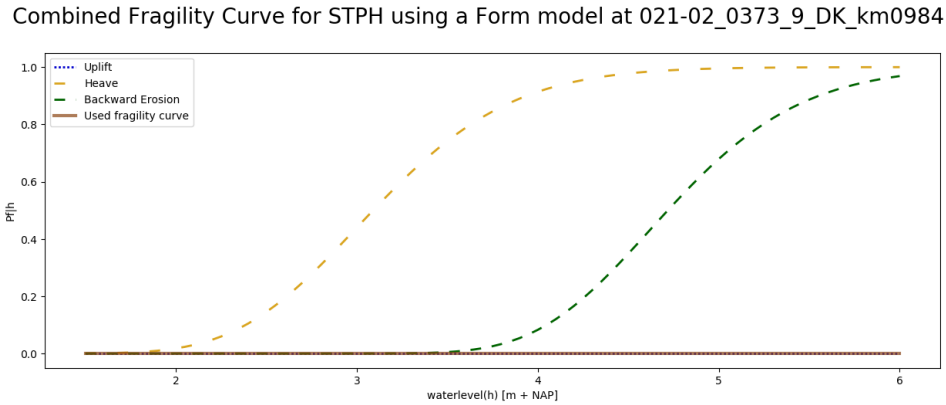

Figure G.29: Combined FC 212 0373

Uplift

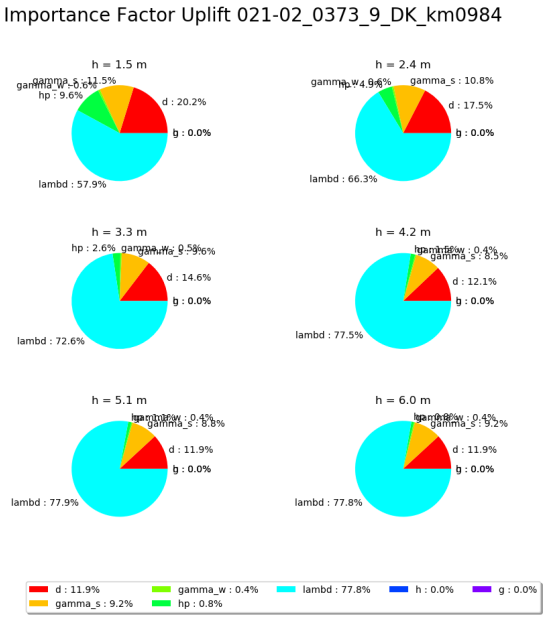

Figure G.30: Importance Factor Uplift 21-2 0373

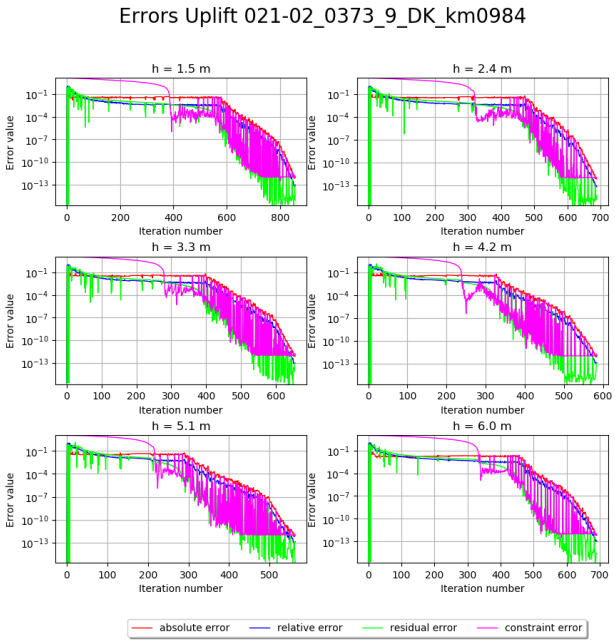

Figure G.31: Error 21-2 0373

Heave

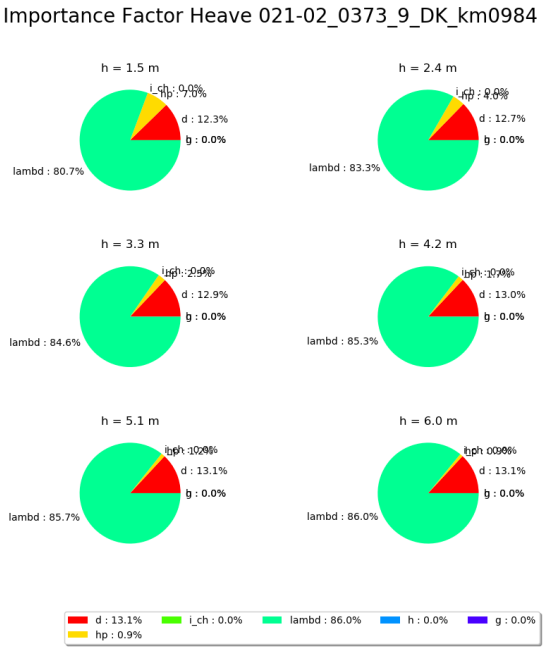

Figure G.32: Importance Factor Heave 21-2 0373

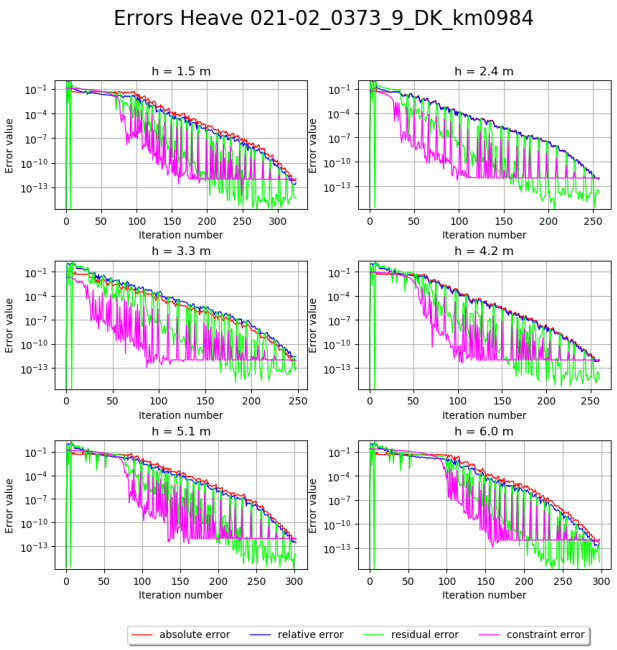

Figure G.33: Error 21-2 0373

Backward Erosion

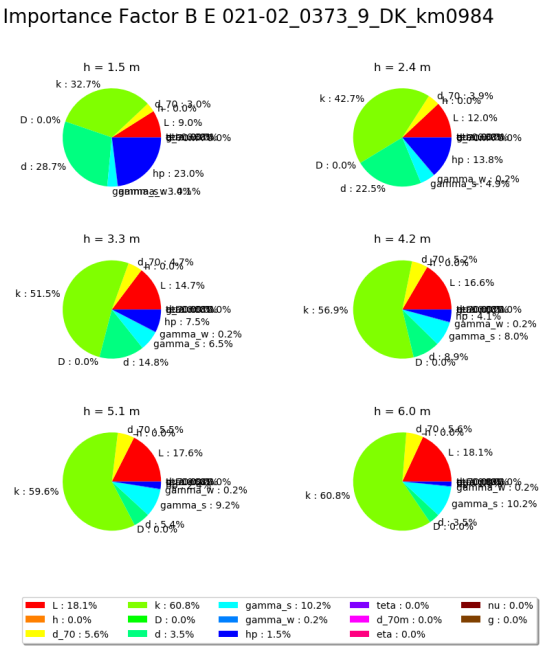

Figure G.34: Importance Factor Backward Erosion 21-2 0373

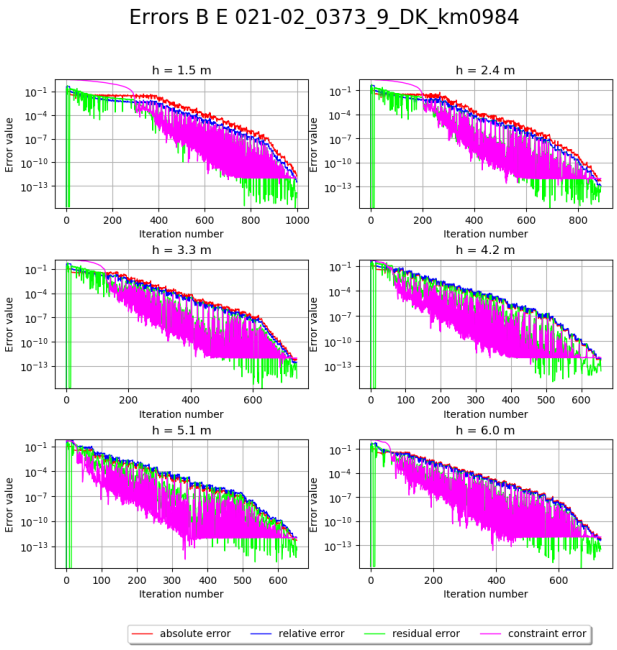

Figure G.35: Error 21-2 0373

G.3. Dike stretch 25-2

G.3.1. 25-02-0020

Fragility curve for each sub mechanism

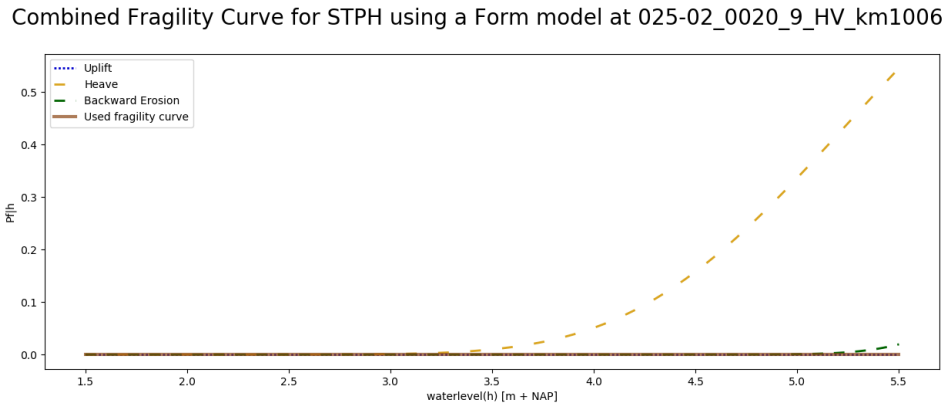

Figure G.36: Combined FC 25-2 0020

Uplift

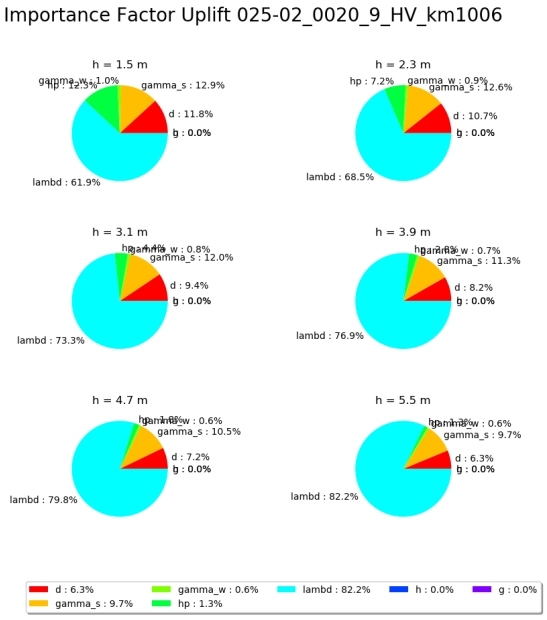

Figure G.37: Importance Factor Uplift 25-2 0020

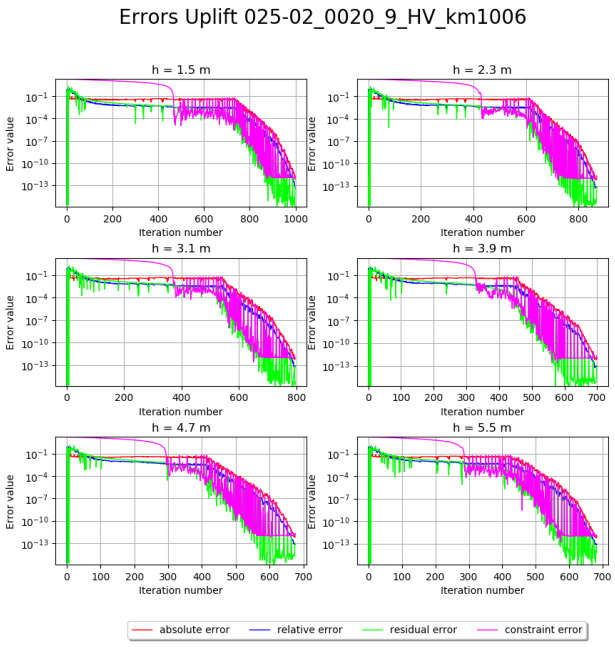

Figure G.38: Error 25-2 0020

Heave

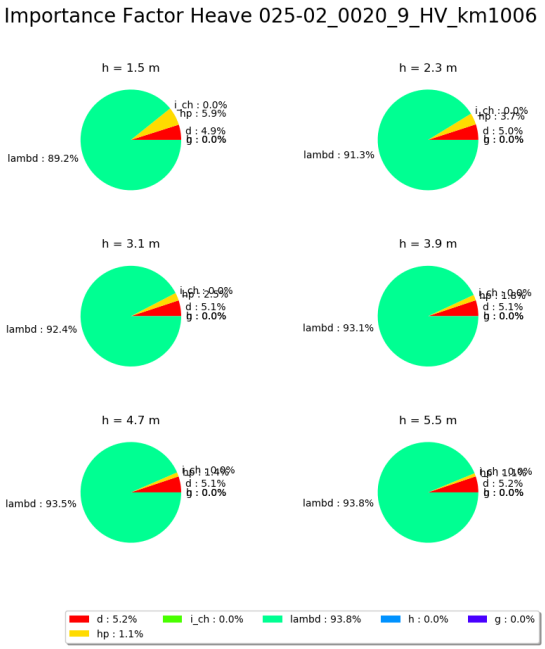

Figure G.39: Importance Factor Heave 25-2 0020

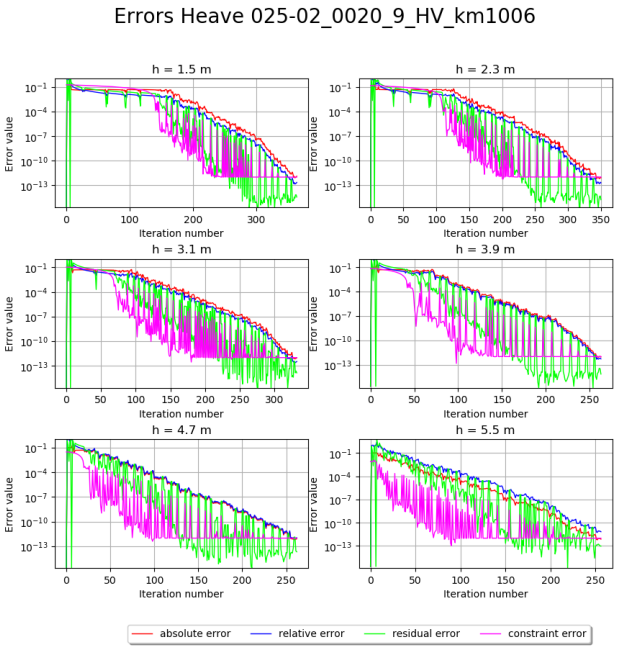

Figure G.40: Error 25-2 0020

Backward Erosion

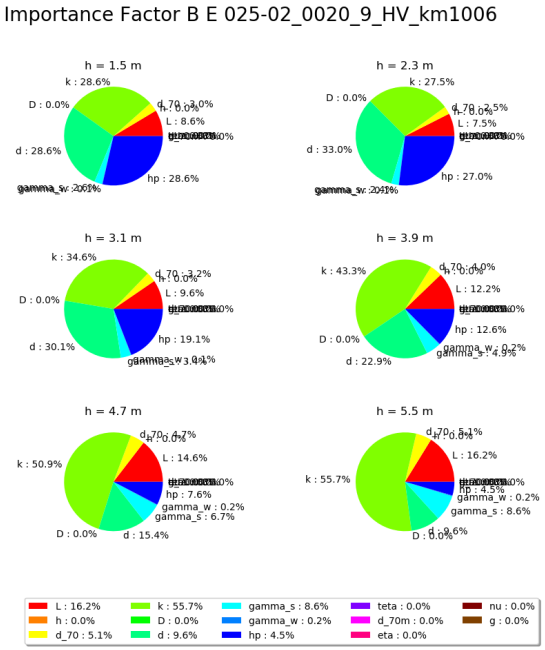

Figure G.41: Importance Factor Backward Erosion 25-2 0020

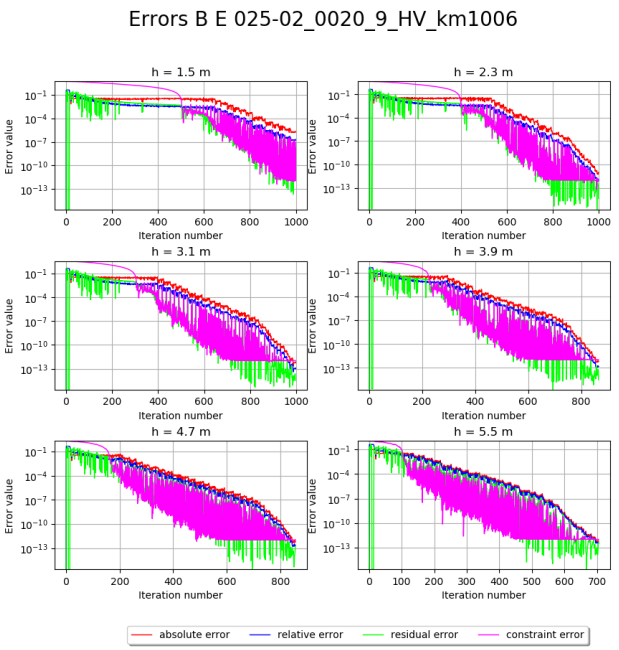

Figure G.42: Error 25-2 0020

G.3.2. 25-02-0091

Fragility curve for each sub mechanism

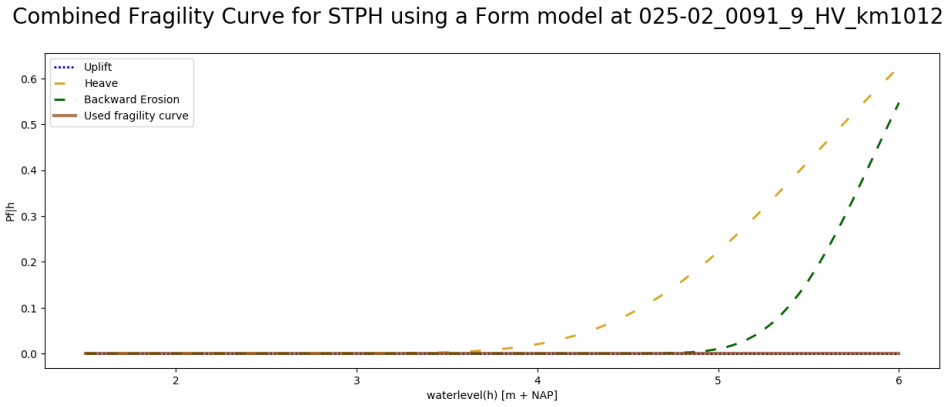

Figure G.43: Combined FC 25-2 0091

Uplift

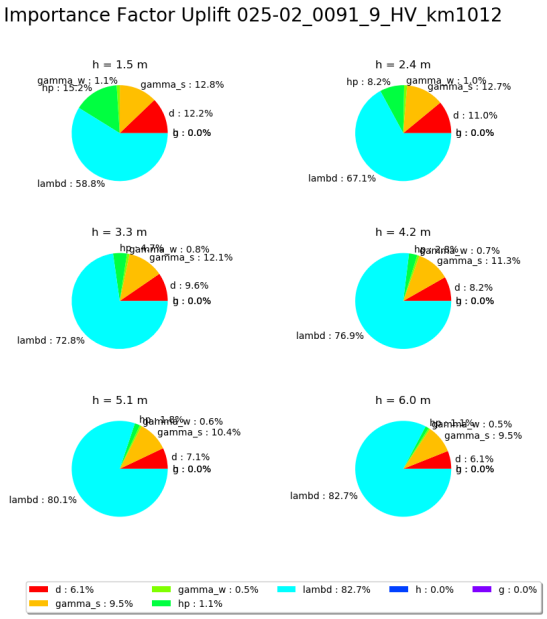

Figure G.44: Importance Factor Uplift 25-2 0091

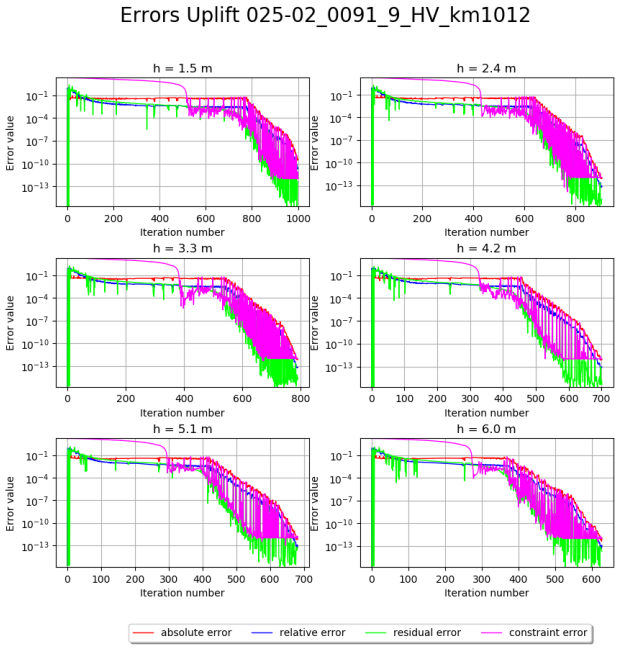

Figure G.45: Error 25-2 0091

Heave

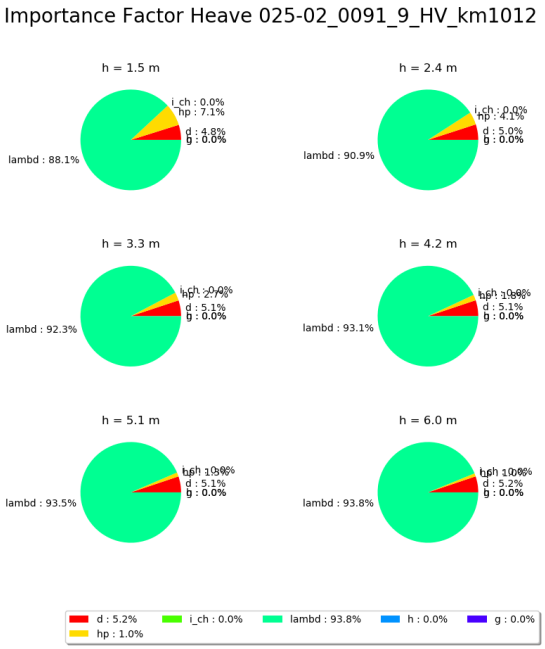

Figure G.46: Importance Factor Heave 25-2 0091

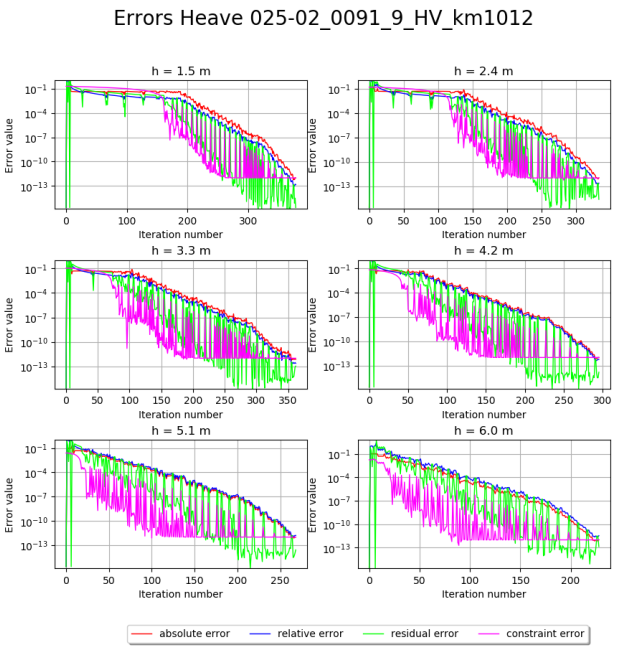

Figure G.47: Error 25-2 0091

Backward Erosion

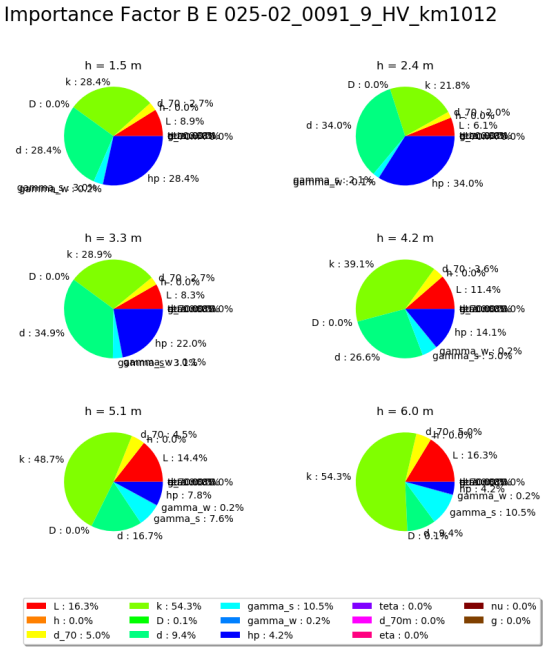

Figure G.48: Importance Factor Backward Erosion 25-2 0091

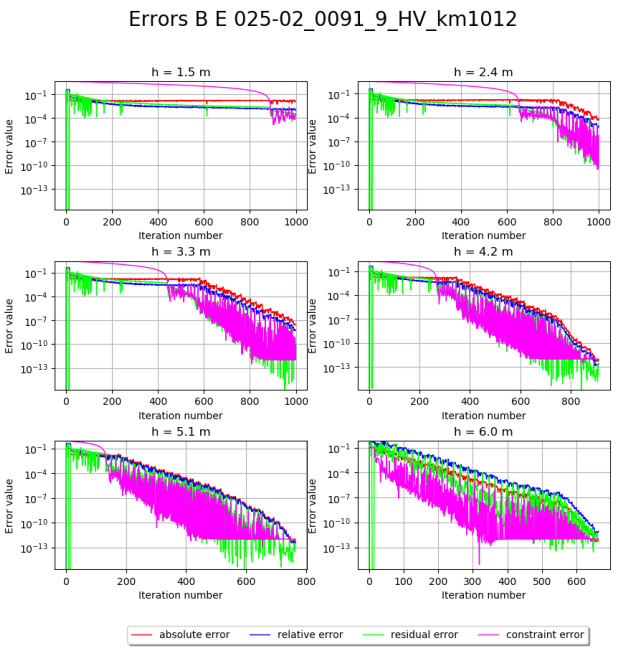

Figure G.49: Error 25-2 0091

G.3.3. 25-02-0242
Fragility curve for each sub mechanism

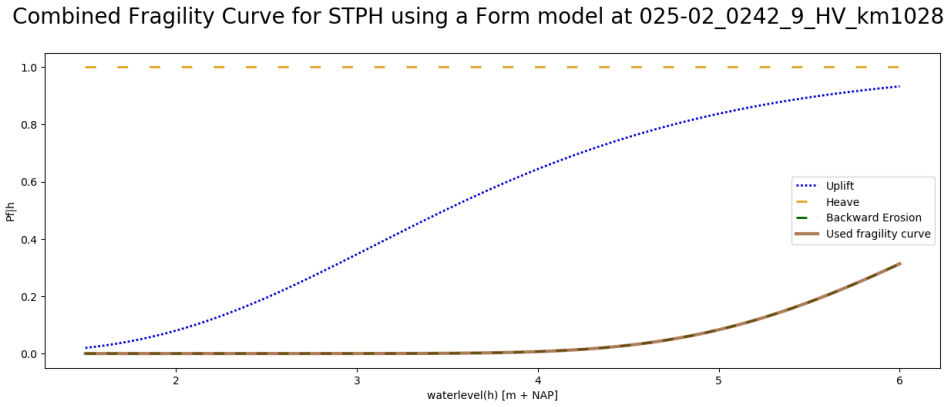

Figure G.50: Combined FC 25-2 0242

Uplift

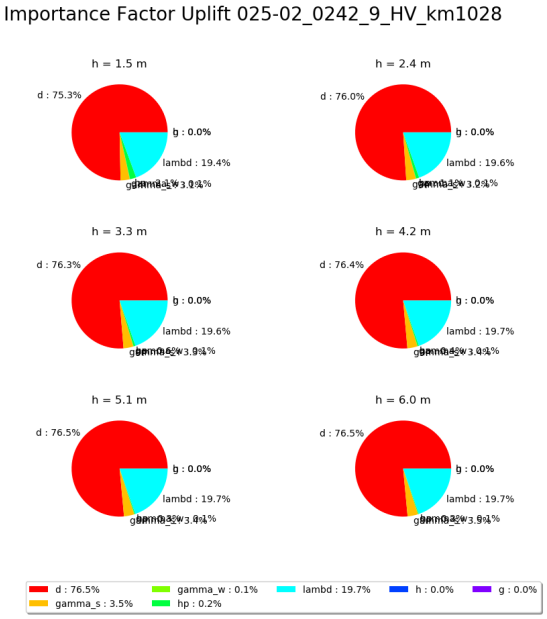

Figure G.51: Importance Factor Uplift 25-2 0242

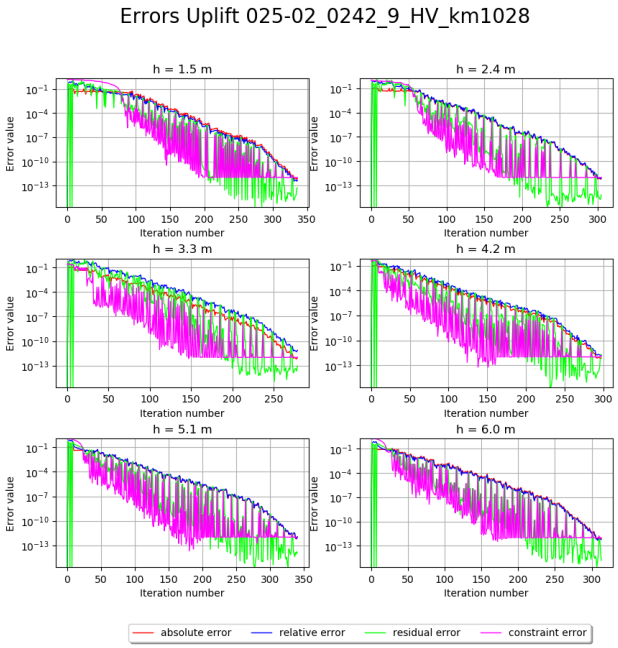

Figure G.52: Error 25-2 0242

Heave

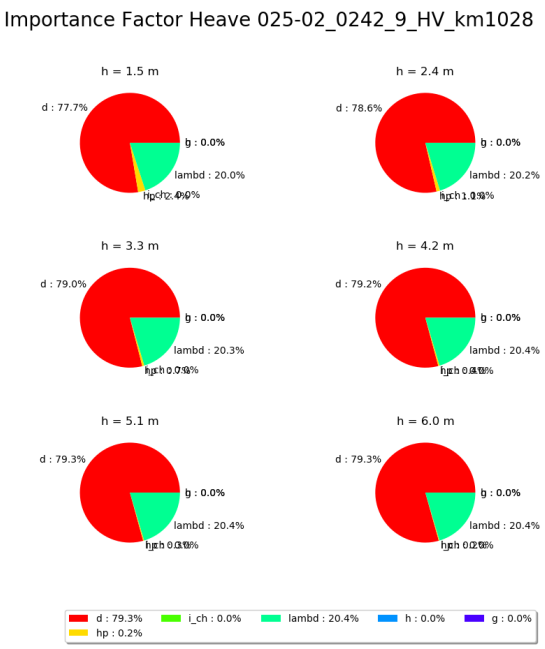

Figure G.53: Importance Factor Heave 25-2 0242

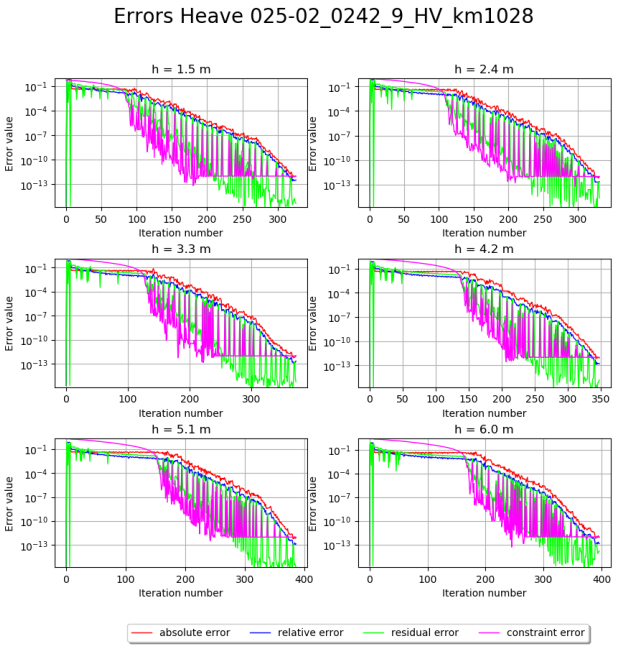

Figure G.54: Error 25-2 0242

Backward Erosion

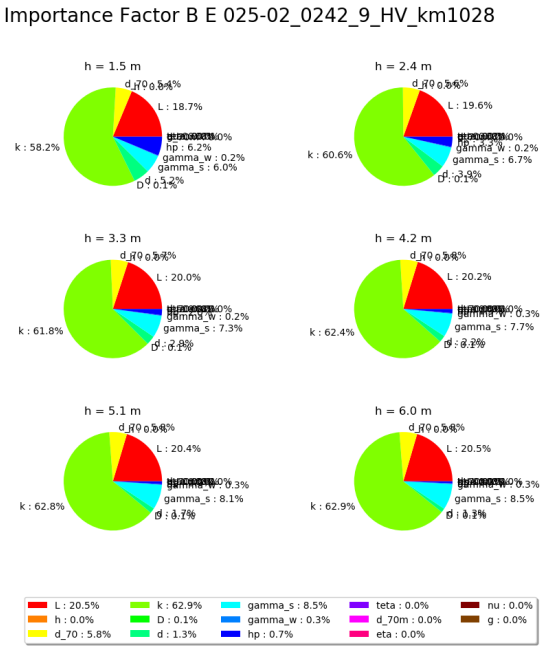

Figure G.55: Importance Factor Backward Erosion 25-2 0242

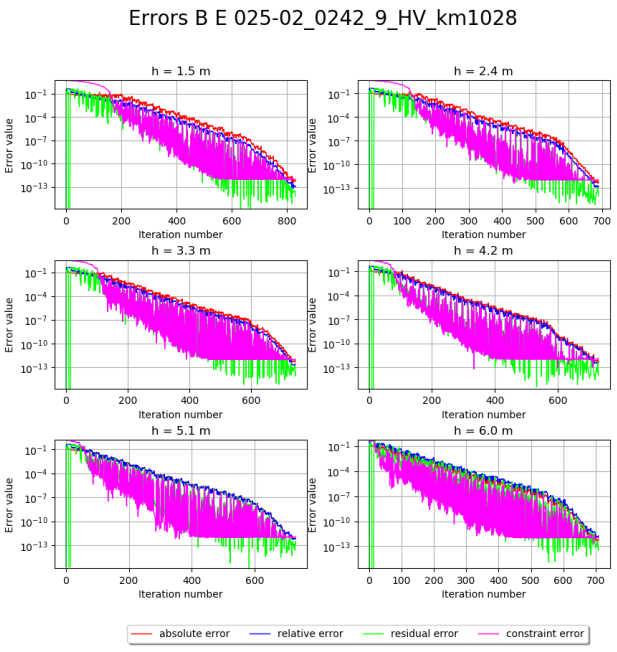

Figure G.56: Error 25-2 0242

G.4. Dike stretch 34-2

G.4.1. 34-02-0011

Fragility curve for each sub mechanism

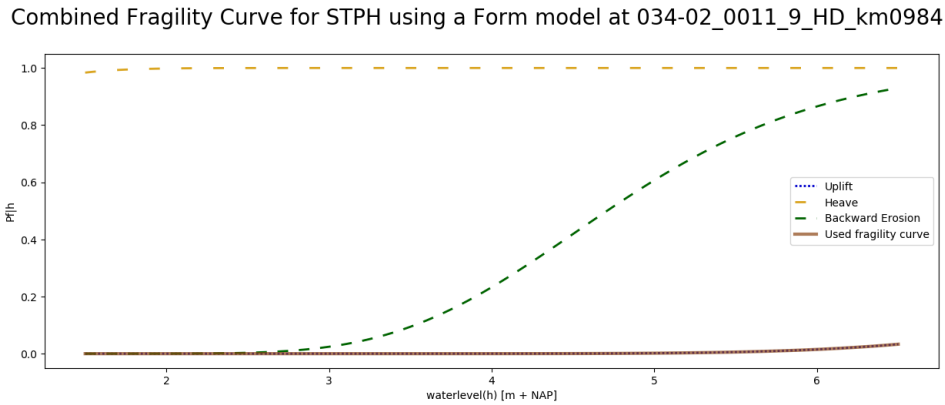

Figure G.57: Combined FC 34-2 0011

Uplift

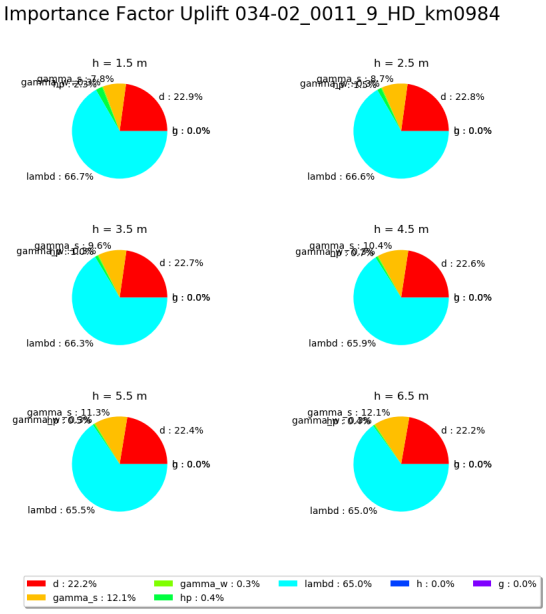

Figure G.58: Importance Factor Uplift 34-2 0011

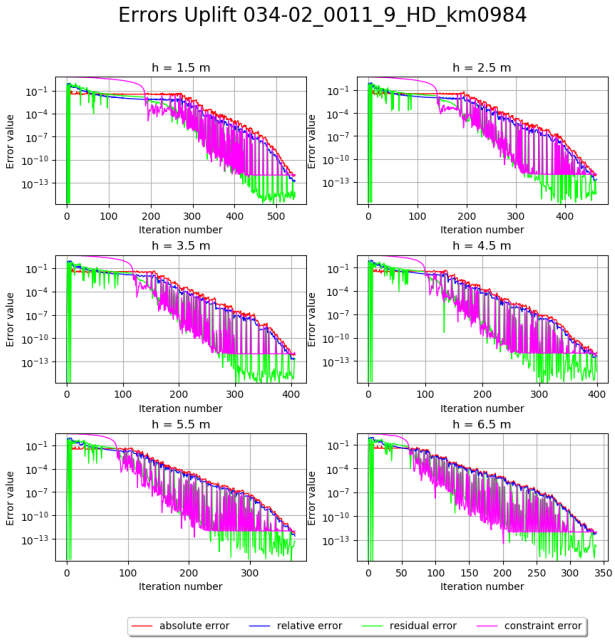

Figure G.59: Error 34-2 0011

Heave

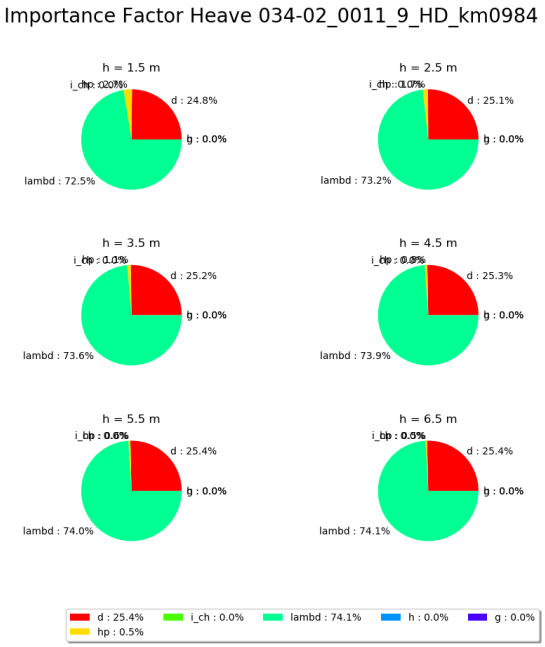

Figure G.60: Importance Factor Heave 34-2 0011

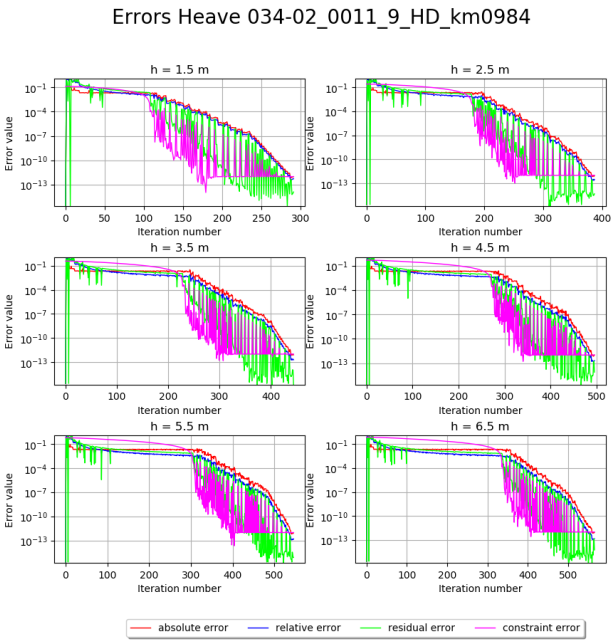

Figure G.61: Error 34-2 0011

Backward Erosion

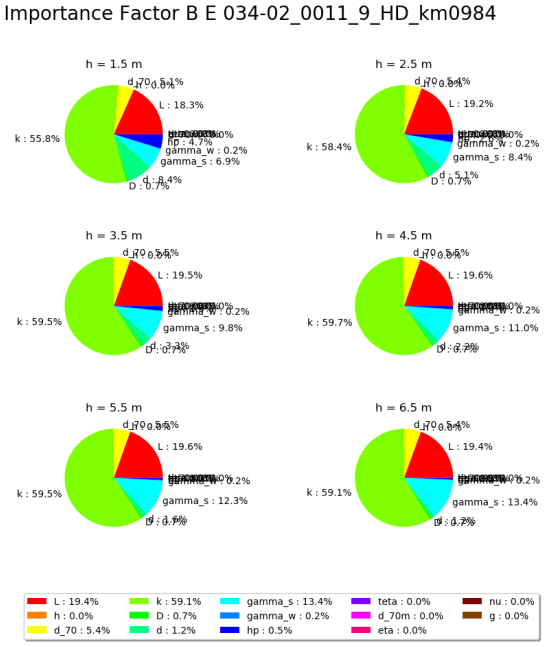

Figure G.62: Importance Factor Backward Erosion 34-2 0011

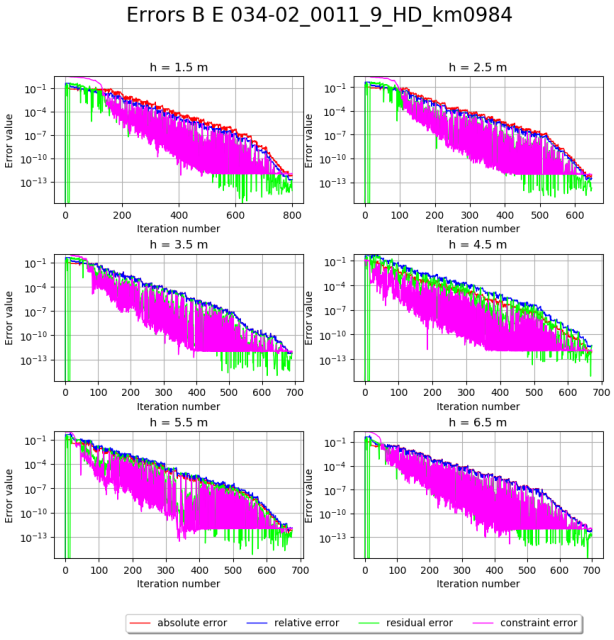

Figure G.63: Error 34-2 0011

G.4.2. 34-02-0130
Fragility curve for each sub mechanism

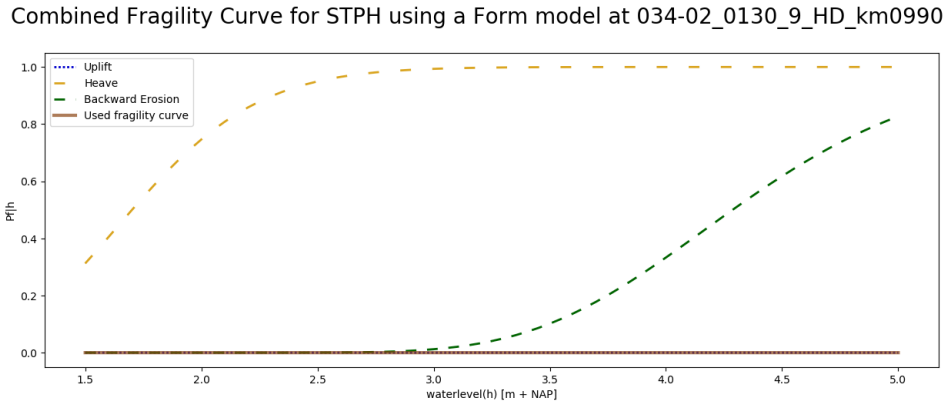

Figure G.64: Combined FC 34-2 0130

Uplift

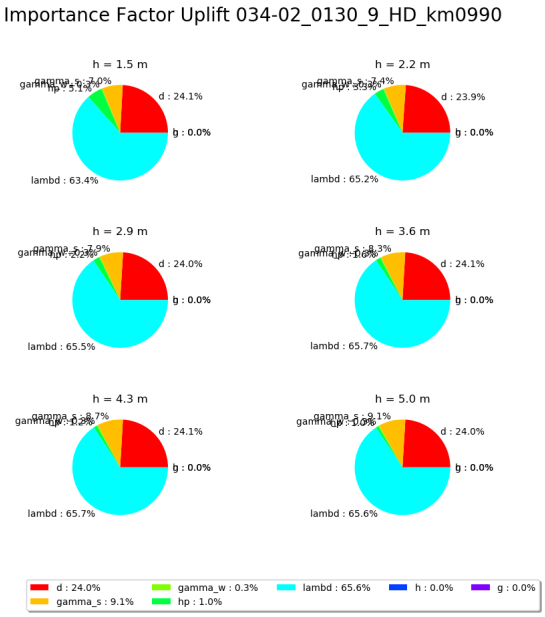

Figure G.65: Importance Factor Uplift 34-2 0130

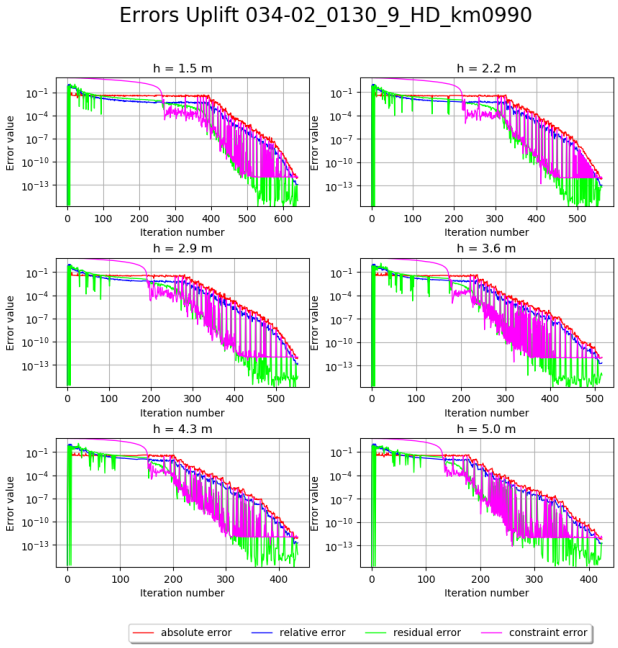

Figure G.66: Error 34-2 0130

Heave

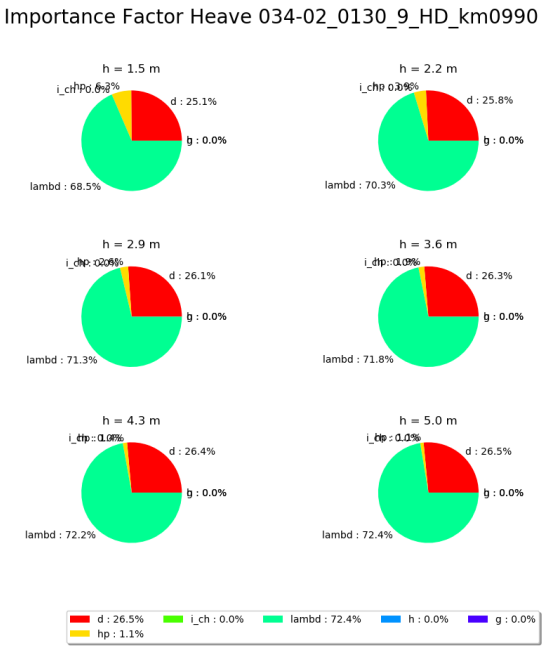

Figure G.67: Importance Factor Heave 34-2 0130

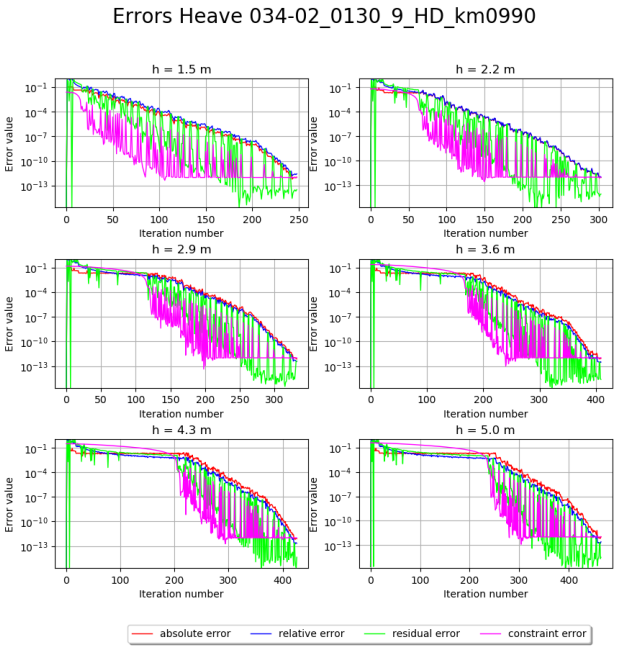

Figure G.68: Error 34-2 0130

Backward Erosion

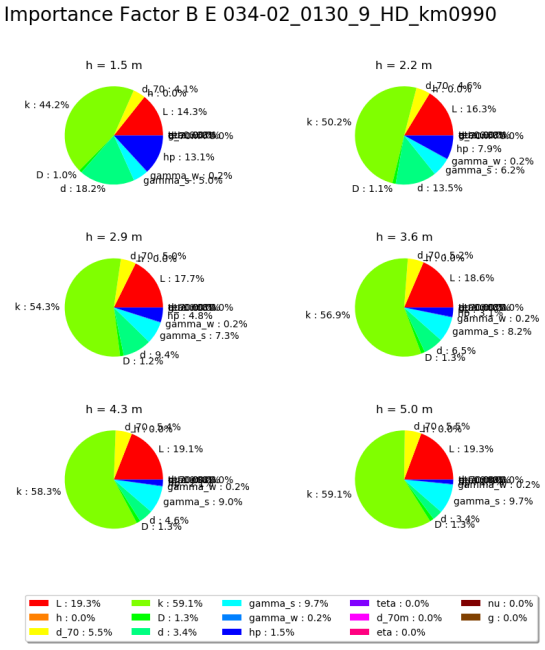

Figure G.69: Importance Factor Backward Erosion 34-2 0130

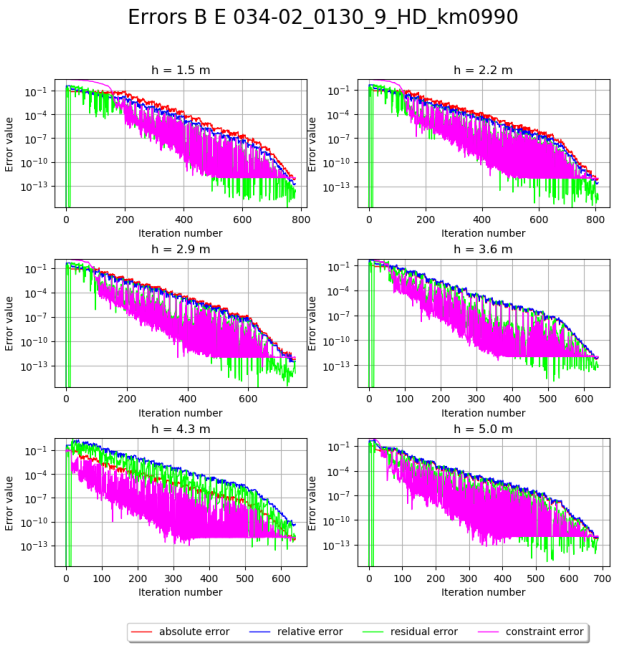

Figure G.70: Error 34-2 0130

G.4.3. 34-02-0190
Fragility curve for each sub mechanism

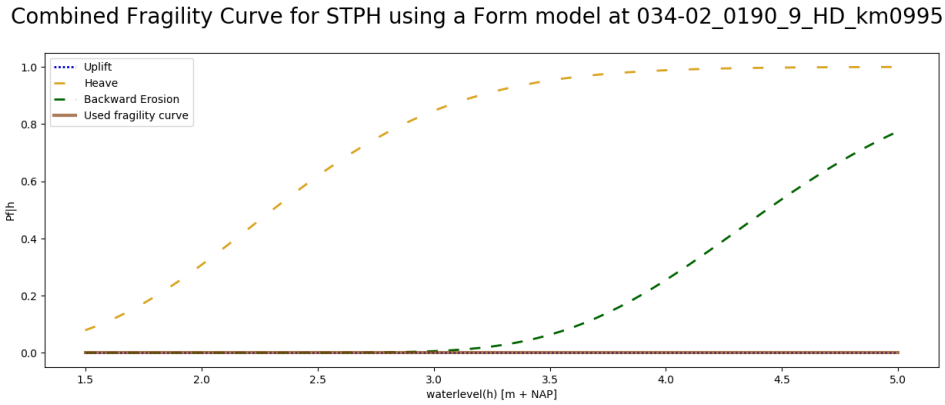

Figure G.71: Combined FC 34-2 0190

Uplift

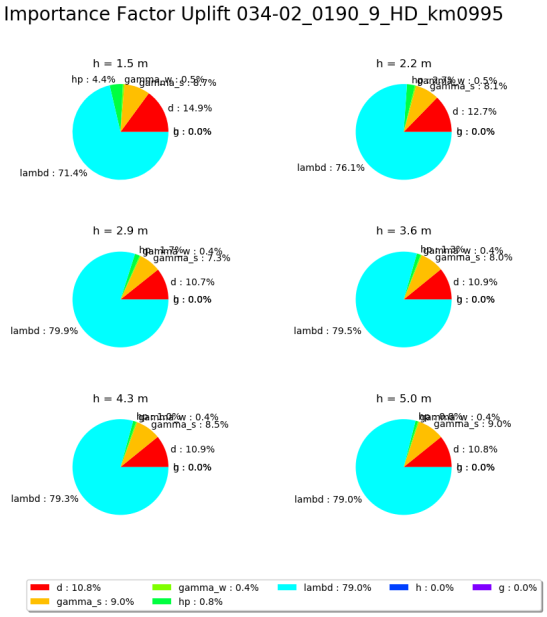

Figure G.72: Importance Factor Uplift 34-2 0190

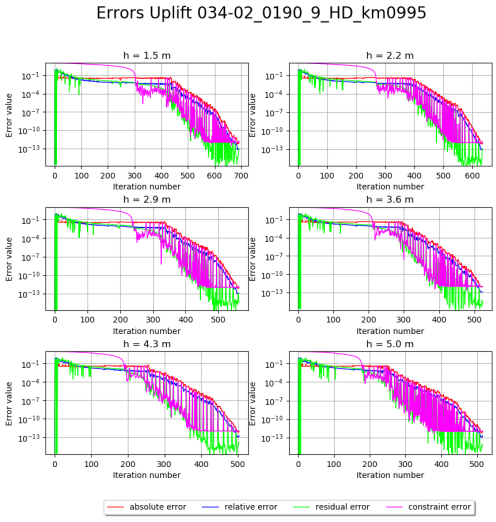

Figure G.73: Error 34-2 0190

Heave

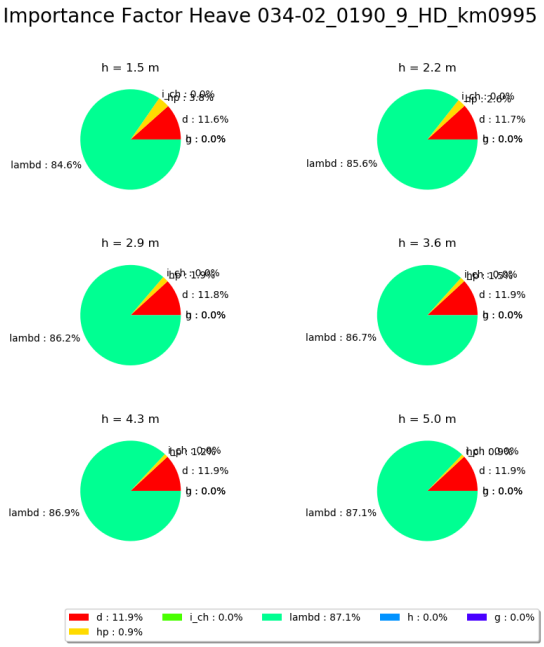

Figure G.74: Importance Factor Heave 34-2 0190

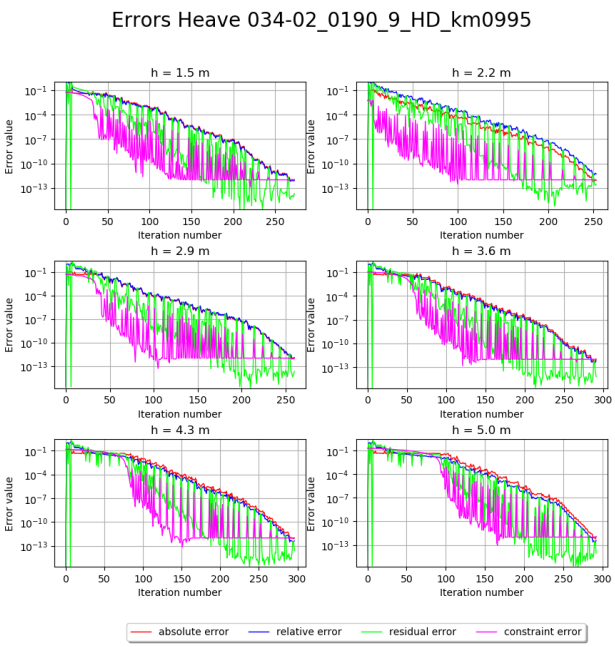

Figure G.75: Error 34-2 0190

Backward Erosion

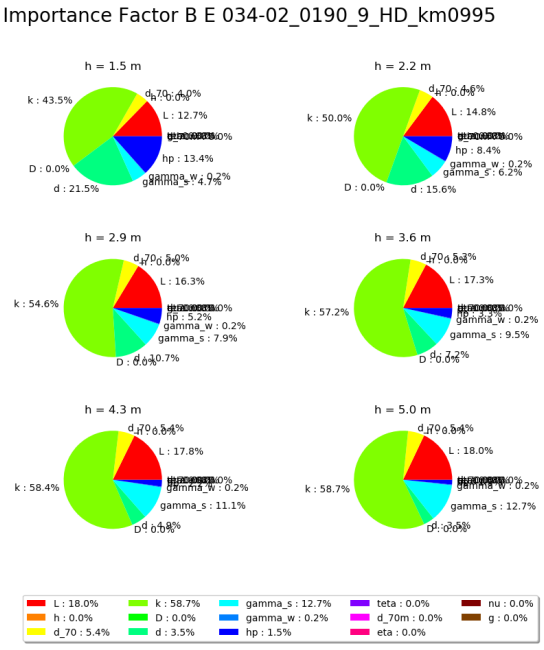

Figure G.76: Importance Factor Backward Erosion 34-2 0190

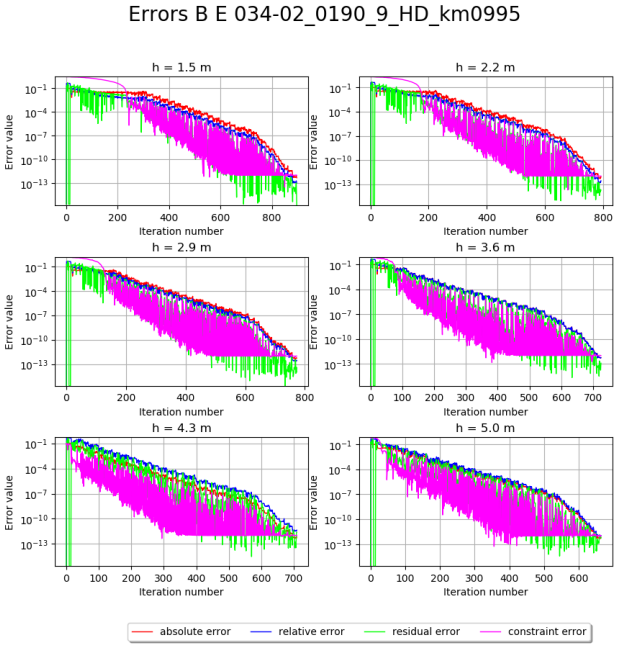

Figure G.77: Error 34-2 0190

H

WBI 2017

H.1. Piping calibration equations

Uplift

$$P_{f;u} = \Phi\left(-1 \cdot \frac{LN\left(\frac{F_u}{0.48} + 0.27 \cdot \beta_{standard}\right)}{0.46}\right) \quad \text{(H.1)}$$

Heave

$$P_{f;u} = \Phi\left(-1 \cdot \frac{LN\left(\frac{F_h}{0.37} + 0.30 \cdot \beta_{standard}\right)}{0.48}\right) \quad \text{(H.2)}$$

Backwards Erosion

$$P_{f;u} = \Phi\left(-1 \cdot \frac{LN\left(\frac{F_u}{1.04} + 0.43 \cdot \beta_{standard}\right)}{0.37}\right) \quad \text{(H.3)}$$

with: $P_{f;u,h,be}$ = Failure probability for each sub-mechanism. Φ = standard normal distribution. $\beta_{standard}$ = Reliability index of the given dike stretch. $F_{u,h,be}$ = the FOS of each sub-mechanism respectively.

H.2. Length effect

$$P_{f,section} = \frac{\omega P_{f,stretch}}{N} \quad \text{(H.4)}$$

$$N = 1 + \frac{\alpha L}{\beta} \quad \text{(H.5)}$$

with: $\alpha = 0.4$ and $\beta = 300m$ for piping

Failure Mechanims

Failure Mechanisms which are included in the software of the WBI [8].

Toetssporen	Code	Groep	ET	GT per vak	GT per traject	Hoofd-stuk	Schematiserings-handleiding
Dijken en dammen							
Macrostabiliteit binnenwaarts	STBI	2	X	X	X	5	Macrostabiliteit
Macrostabiliteit buitenwaarts	STBU	4	X	X		6	Macrostabiliteit
Piping	STPH	2	X	X	X	7	Piping
Microstabiliteit	STMI	4	X	X		8	Microstabiliteit
(*Bekledingen*)							
Golfklappen op asfaltbekleding	AGK	3	X	X		9	Asfaltbekleding
Wateroverdruk bij asfaltbekleding	AWO	4	X			10	Asfaltbekleding
Grasbekleding erosie buitentalud	GEBU	3	X	X		11	Grasbekleding
Grasbekleding afschuiven buitentalud	GABU	4	X	X		12	Grasbekleding
Grasbekleding erosie kruin en binnentalud	GEKB	1		X	X	13	Grasbekleding en Hoogte
Grasbekleding afschuiven binnentalud	GABI	4		X		14	Grasbekleding en Hoogte
Stabiliteit steenzetting	ZST	3		X		15	Steenzetting
Duinwaterkering							
Duinafslag	DA	3		X	X	16	Duinafslag
Kunstwerken							
Hoogte kunstwerk	HTKW	1	X	X	X	17	Hoogte kunstwerk
Betrouwbaarheid sluiting kunstwerk	BSKW	1	X	X	X	18	Betrouwbaarheid sluiting kunstwerk
Piping bij kunstwerk	PKW	2	X	X		19	Piping bij kunstwerk
Sterkte en stabiliteit puntconstructies	STKWp	1		X	X	20	Sterkte en stabiliteit kunstwerk,
Sterkte en stabiliteit langsconstructies	STKWl	4	X			21	puntconstructie
Voorland							
Golfafslag voorland	VLGA	5	X			22	Voorland golfafslag
Afschuiving voorland	VLAF	5	X	X		23	Afschuiving voorland
Zettingsvloeiing voorland	VLZV	5	X	X		24	Zettingsvloeiing
Niet-waterkerende objecten						25	
Bebouwing	NWObe	5	X				
Begroeiing	NWObo	5	X				
Kabels en leidingen	NWOkl	5	X	X			
Overige constructies	NWOoc	5					
Havendammen	HAV	5	X	X		26	Hydraulische condities aan de dijkteen
Technische innovatie	INN	4	X			27	

Figure I.1: All failure mechanisms in the Dutch Formal Assessment [23]

J

Wind directions and distributions

J.1. Wind rose

Figure J.1 shows all the wind directions that are included in Hydra-NL. Depending on which location is calculated. the dominant wind directions are chosen. In most cases those directions are: W, WNW, NW, and NNW. For each step clockwise on the circle the degrees will increase with $22.5°$ from $0°$ at the north.

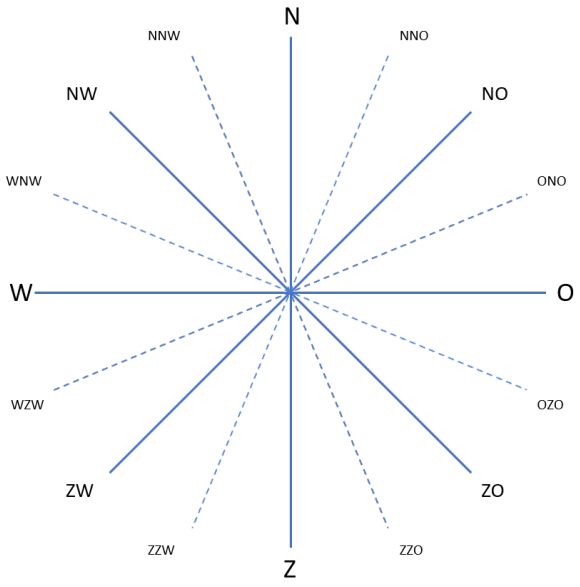

Figure J.1: Wind directions in Hydra-NL

J.2. Wind distribution GEKB calculation

Hydra-NL gives as an output the tables below. For each return period that is provided, such a table is constructed. Below only the wind direction, independent of the Europort Barriers is shown.

Table J.1: Wind directions for reference year 2023 with return period 1/300 years

Reference year	2023
Locatie	034-02_0190_9_HD_km0995 (90634,411565)
Berekeningstype	Waterstand
Waterstand	2.45 (m+NAP)
Terugkeertijd	300 (jaar)
Overschrijdingsfrequentie	3.33E-03 (per jaar)

Windsnelheidspercentielen (m/s) bij gegeven windrichting en onafhankelijk van de keringsituatie

r	NNO	NO	ONO	O	OZO	ZO	ZZO	Z
percentage	0.00%	0.00%	0.00%	0.00%	0.00%	0.00%	0.00%	0.00%
5%	—	—	—	—	—	—	—	—
10%	—	—	—	—	—	—	—	—
25%	—	—	—	—	—	—	—	—
50%	—	—	—	—	—	—	—	—
75%	—	—	—	—	—	—	—	—
90%	—	—	—	—	—	—	—	—
95%	—	—	—	—	—	—	—	—

r	ZZW	ZW	WZW	W	WNW	NW	NNW	N
percentage	0.00%	0.00%	1.40%	13.70%	28.90%	35.00%	18.50%	2.40%
5%	—	—	17.1	15.4	15.6	15.4	15.2	13.2
10%	—	—	18.6	16.5	16.6	16.3	16.3	15.2
25%	—	—	21.1	18.4	18.3	18.1	18.2	18.4
50%	—	—	23.9	21	20.4	20.1	20.4	22.5
75%	—	—	26.9	24.1	22.8	22.2	22.6	26
90%	—	—	29.8	27.1	25.2	24.2	24.6	28.5
95%	—	—	31.8	29	26.8	25.7	25.9	30.4

Table J.2: Wind directions for reference year 2100 with return period 1/300 years

Reference year	2100
Locatie	034-02_0190_9_HD_km0995 (90634,411565)
Berekeningstype	Waterstand
Waterstand	2.79 (m+NAP)
Terugkeertijd	300 (jaar)
Overschrijdingsfrequentie	3.33E-03 (per jaar)

Windsnelheidspercentielen (m/s) bij gegeven windrichting en onafhankelijk van de keringsituatie

r	NNO	NO	ONO	O	OZO	ZO	ZZO	Z
percentage	0.00%	0.00%	0.00%	0.00%	0.00%	0.00%	0.00%	0.00%
5%	—	—	—	—	—	—	—	—
10%	—	—	—	—	—	—	—	—
25%	—	—	—	—	—	—	—	—
50%	—	—	—	—	—	—	—	—
75%	—	—	—	—	—	—	—	—
90%	—	—	—	—	—	—	—	—
95%	—	—	—	—	—	—	—	—

r	ZZW	ZW	WZW	W	WNW	NW	NNW	N
percentage	0.00%	0.20%	4.70%	23.20%	30.90%	26.80%	12.60%	1.60%
5%	—	16.8	15.3	13.7	13.2	13.2	12.9	9.6
10%	—	18.1	16.3	14.4	14.1	14.1	13.8	10.7
25%	—	20.8	18.6	15.9	15.9	15.7	15.5	13.2
50%	—	24.3	21.4	18.3	18	18	17.8	16.8
75%	—	27.9	24.5	21.2	20.6	20.7	20.4	20.4
90%	—	31	27.2	24.3	23.3	23.3	23	23.5
95%	—	32.9	28.9	26.2	25.2	25	24.7	25.3